

Towards Sustainability in Hydrogenation and Hydroformylation Reactions

Cumulative Dissertation

to acquire the academic degree

doctor rerum naturalium (Dr. rer. nat.)

of the Faculty of Mathematics and Natural Sciences

at the University of Rostock

Submitted by Florian Scharnagl, born on 28th of July 1991 in Munich

Rostock, 21.06.2019

Date of defence: 19.11.2019

https://doi.org/10.18453/rosdok_id00002576

The present work was accomplished at the Leibniz Institute for Catalysis e.V. at the University of Rostock, at the chair for Applied Catalysis in the research group of Professor Dr. Matthias Beller during the period from November 2016 to June 2019.

Reviewer 1: Prof. Dr. Dr. h.c. mult. Matthias Beller (Leibniz-Institut für Katalyse e.V.)

Reviewer 2: Prof. Dr. Bas de Bruin (University of Amsterdam)

*“It is not our part to master all the tides of the world,
but to do what is in us for the succour of those years wherein we are set,
uprooting the evil in the fields that we know,
so that those who live after may have clean earth to till.”*

Gandalf
“The Return of the King”
J.R.R. Tolkien
p. 861, 0-618-00224-3

Statement of Authorship

I hereby affirm that I have written the present work by myself without outside assistance. No other resources were utilised than stated. All references as well as verbatim extracts were quoted and all sources of information were specifically acknowledged.

Ich versichere hiermit an Eides statt, dass ich die vorliegende Arbeit selbstständig angefertigt und ohne fremde Hilfe verfasst habe. Dazu habe ich keine außer den von mir angegebenen Hilfsmitteln und Quellen verwendet und die den benutzten Werken inhaltlich und wörtlich entnommenen Stellen habe ich als solche kenntlich gemacht.

Rostock, 20.06.2019

Florian Scharnagl

Acknowledgements - Danksagung

Der erste Dank gilt meinem Doktorvater **Professor Dr. Matthias Beller**. Ich danke Dir für die Aufnahme in deinen Arbeitskreis, für die großartige Unterstützung und für deine schier grenzenlose Kreativität. Die Art, wie du dein umfangreiches Wissen stets verknüpfen kannst und dadurch neue Ideen generierst hat mich sehr beeindruckt. Ich danke Dir auch für die spannenden Forschungsthemen, für die Möglichkeit auf Konferenzen und nach Cardiff zu gehen, für die vielen wissenschaftlichen Gespräche und nicht zuletzt für deine freundliche und immer positive Art. Die letzten drei Jahre haben mich nicht nur wissenschaftlich, sondern auch persönlich weiter gebracht. Danke.

Der zweite Dank gebührt meinem Themenleiter **Dr. Ralf Jackstell**. Mit deiner eigenen Begeisterung für die Katalyse hast du auch uns alle angesteckt. Besonders wenn die Synthese eines neuen Liganden anstand warst du selbst Feuer und Flamme. Auch dein Knowhow bezüglich Autoklaventechnik hat mir sehr weitergeholfen und ich habe viel gelernt. Dein Einsatz für deine Mitarbeiter ist großartig.

Ich möchte auch allen Projektpartnern aus den Projekten „*KataPlasma*“ und „*Metha-Cycle*“ für die gute Zusammenarbeit und dem BMBF (Bundesministerium für Bildung und Forschung), sowie dem BMWi (Bundesministerium für Wirtschaft und Energie) für die Finanzierung danken.

Anschließend möchte ich meinem Büro 1.236 danken. I have to thank **Dr. Francesco “The Mustache” Ferretti**, who assisted me with all daily lab-problems, and who taught me so many things in the lab, due to his experience. He became a true friend. Des Weiteren möchte ich mich bei unserer Laborleiterin **Dr. Anahit Pews-Davtyan** für die gute Arbeitsatmosphäre in den letzten Jahren bedanken. Bei **Maximilian Hertrich** bedanke ich mich für die gute Zusammenarbeit in teils schwierigen projektbezogenen Situationen. **Ricarda Dühren** gilt der Dank nicht nur als beste Abzugs- und Büronachbarin, sondern auch abseits der Arbeit. Ob als Trainingspartnerin im FitX, Ultra-Fan der Rostocker Seawolves, oder als Gastgeberin von WG- und Falafel-Parties: Mit ihr ist stets gut „Erdbeerpflücken“. Auch meinem Bacheloranden und jetzigen HiWi **Gordon Neitzel** möchte ich danken; für die Destillationen, seine fleißige Art und für die unterirdisch schlechten Witze. Ich habe trotzdem gelacht.

I wish to take advantage of this opportunity and thank the whole group “*Organische Großchemikalien*“ for the great atmosphere, the friendliness and the willingness to help each other. It was a pleasure to work with you and I wish every single one of you only the best for you future. I hope that we can stay in contact and hopefully see each other again at some point.

Auch bei der “Mensagruppe” möchte ich mich bedanken. Das tägliche Mittagessen wurde durch mal lustige und häufig politische Themen „erfrischt“. Hierbei möchte ich namentlich auch unseren Gelegenheits-Mitesser **Patrick Piehl** erwähnen. Auch bei **Jacob Schneidewind**, **Moritz Horstmann**, **Berit Umbreit**, **Stefanie Kreft**, **Helge Lange**, **Anna Emmerich**, **Peter Kucmierczyk** und **Florian Fischer** (geb. Weniger) möchte ich mich für die vielen Aktivitäten außerhalb der Arbeit bedanken.

Natürlich möchte ich nicht die Gelegenheit verpassen mich auch bei der gesamten Analytik des LIKATs zu bedanken. NMRs, Massenspektren, Kristallanalysen etc. messen sich nicht von alleine und ohne diese Unterstützung ist Forschung nicht möglich.

Ich möchte mich auch bei meinen Freunden aus meiner Heimat bedanken. Bei meiner Sandkastenfreundin **Anna Wagner**, die ich wohl schon am längsten von allen kenne. Bei **Philipp Wagner**, der mich gleich zweimal in Rostock besucht hat. Bei **Simon Gossert**, der die Schulzeit unvergesslich gemacht hat und zu allen Schandtaten bereit war. Bei **Jana Wichmann**, für Ihre Freundschaft und das Asyl, dass sie mir und meinen Freunden bei allen Besuchen in München gewährt hat (nicht nur zur Wiesn-Zeit). Ihr alle habt mich während meiner gesamten Entwicklung, vom Sandkasten bis heute (und hoffentlich noch viel länger) begleitet und seid die besten Freunde die man sich wünschen kann.

Der größte Dank gilt meiner Familie, die mir das Studium überhaupt erst ermöglicht hat. Ohne euch wäre es niemals zu dieser Arbeit gekommen. Meinen **Eltern** danke ich für die stete Unterstützung und den Rückhalt über all die Jahre. Des Weiteren danke ich meinen Geschwistern **Mirjam** und **Benjamin** für die großartige Kindheit die ich haben durfte. Ihr habt mich geprägt und maßgeblich beeinflusst wer ich heute bin. Danke.

Meiner Freundin **Vanessa Memmel** danke ich für ihre liebe Art, für ihre Unterstützung und für ihre positive Ader. Eine Fernbeziehung ist nicht leicht und funktioniert nur, wenn beide an einem Strang ziehen. Ich bin froh, dass ich dich habe und freue mich auf alles was noch kommen mag.

Vielen lieben Dank!

Abstract

Towards Sustainability in Hydrogenation and Carbonylation Reactions

Florian Scharnagl

Leibniz-Institut für Katalyse e.V. an der Universität Rostock

This thesis deals with the development of novel homogeneous catalysts for the hydrogenation of carbon dioxide and organic carbonates, as well as for the heterogeneous hydrogenation and hydroformylation of olefins. The work focuses on the usage of the inexpensive base-metal cobalt in order to endeavor a replacement of noble-metal based industrial and academic systems. An earlier published system for the cobalt-based hydrogenation of carbon dioxide in the presence of the ligand Triphos was significantly improved by ligand-modification resulting in a 2.5-fold turnover number of the catalyst. Also, the activity of this system in the hydrogenation of organic carbonates was demonstrated for the first time. By applying 2,2,2-trifluoroethanol as fluorinated solvent, a variety of cyclic and acyclic carbonates were hydrogenated to methanol and the corresponding alcohols.

Apart from this, heterogeneous, biomass-derived cobalt-catalysts have been found to be highly active in the hydrogenation of olefins at very mild conditions in water. In addition, easy-to-handle reservoirs of dicobalt octacarbonyl for hydroformylation reactions were obtained by supporting cobalt nanoparticles on inorganic supports. The whole work aims for improved sustainability by replacing noble with base metals and by contributing to the concept of the *“Methanol Economy”*.

Diese Arbeit befasst sich mit der Entwicklung neuartiger Katalysatoren sowohl für die homogene Hydrierung von Kohlendioxid und organischen Carbonaten, als auch für die heterogene Hydrierung und Hydroformylierung von Olefinen. Der Fokus liegt hierbei auf der Anwendung des günstigen, unedlen Metalls Kobalt auf industrielle und akademische Systeme, welche bisher auf Edelmetallen basieren. Die Produktivität eines bekannten, Kobalt- und Triphos-basierten Systems für die homogene Hydrierung von CO₂ wurde durch Modifizierung des Liganden mehr als verdoppelt. Des Weiteren wurde durch den Einsatz des fluorinierten Alkohols 2,2,2-Trifluorethanol die Hydrierung cyclischer und acyclischer Carbonate zu den entsprechenden Alkoholen erstmals mit Kobalt ermöglicht.

Ferner wurden heterogene, aus Biomasse hergestellte Kobalt-Katalysatoren identifiziert, welche eine hohe Aktivität in der Hydrierung von Olefinen bei sehr milden Bedingungen aufweisen. Es wurden auch Co₂(CO)₈-Reservoirs für Hydroformylierungen entwickelt, indem Kobalt-Nanopartikel auf anorganischen Trägermaterialien erzeugt wurden. Die gesamte vorliegende Arbeit strebt eine erhöhte Nachhaltigkeit durch den Ersatz von edlen durch unedle Metalle und durch den Beitrag zum Konzept der *„Methanol Economy“* an.

Table of Contents

| | |
|--|-----|
| Statement of Authorship..... | iv |
| Acknowledgements - Danksagung..... | v |
| Abstract..... | vii |
| List of Abbreviations..... | x |
| 1. Introduction..... | 1 |
| 1.1. Climate Change – Setting the Scene..... | 1 |
| 1.2. A Future Independent from Fossil Fuels – The “Methanol Economy”..... | 2 |
| 1.2.1. The Concept..... | 3 |
| 1.2.2. Utilisation of Methanol..... | 4 |
| 1.3. Methanol from CO ₂ | 6 |
| 1.3.1. Hydrogenation of CO ₂ to Methanol – Theoretical Considerations..... | 7 |
| 1.3.2. Heterogeneous Hydrogenation of CO ₂ | 8 |
| 1.3.3. Homogeneous Hydrogenation of CO ₂ | 9 |
| 1.4. Hydrogenation and Hydroformylation of Olefins..... | 16 |
| 1.4.1. Heterogeneous Olefin-Hydrogenation with Non-Noble Metal Catalysts..... | 16 |
| 1.4.2. Heterogeneous Hydroformylation..... | 20 |
| 2. Objectives of this Work..... | 28 |
| 3. Summary..... | 29 |
| 3.1. Hydrogenation of Olefins Using a Biowaste-Derived Cobalt Catalyst..... | 29 |
| 3.2. Biomolecule-derived supported cobalt nanoparticles for hydrogenation of industrial olefins, natural oils and more in water..... | 32 |
| 3.3. Towards Heterogeneous Cobalt-Catalysed Hydroformylation..... | 34 |
| 3.4. Homogeneous Hydrogenation of CO ₂ to Methanol..... | 37 |
| 3.5. Homogeneous Cobalt-Catalysed Hydrogenation of Carbonates to Methanol and Alcohols..... | 40 |
| 4. References..... | 44 |
| 5. Selected Publications..... | 50 |
| 5.1. Hydrogenation of terminal and internal olefins using a biowaste-derived heterogeneous cobalt catalyst..... | 50 |

| | |
|---|----|
| 5.2. Biomolecule-derived supported cobalt nanoparticles for hydrogenation of industrial olefins, natural oils and more in water | 61 |
| 5.3. Supported Cobalt Nanoparticles for Hydroformylation Reactions | 71 |
| 5.4. Homogeneous catalytic hydrogenation of CO ₂ to methanol – improvements with tailored ligands | 77 |
| 5.5. Additive-Free Cobalt-Catalysed Hydrogenation of Carbonates to Methanol and Alcohols | 84 |
| 6. Appendix | 91 |
| 6.1. List of Publications..... | 91 |
| 6.2. Conference Participation | 92 |
| 6.3. Curriculum Vitae..... | 93 |

List of Abbreviations

| | | | |
|---------------|--|------------------|--|
| 2-MTHF | 2-methyl tetrahydrofuran | MOF | metal-organic framework |
| AAS | atomic absorption spectroscopy | MS | mass spectroscopy |
| acac | acetylacetonate | MSA | methanesulfonic acid |
| BASF | Badische Anilin- und Sodafabrik | MTBC | methane-tetrakis (<i>p</i> -biphenylcarboxylate) |
| BET | Brunauer-Emmett-Teller | MTBE | methyl <i>tert</i> -butyl ether |
| bipy | 2,2'-bipyridine | MTG | methanol to gasoline |
| BMIM | 1- <i>n</i> -butyl-3-methylimidazolium | MTO | methanol to olefin |
| BPa | bisphosphoramidite | <i>n</i> - | normal |
| BTPS | bis(2,2,6,6-tetramethyl-4-piperidyl)sebacate | NHC | <i>N</i> -heterocyclic carbene |
| Bu | butyl | NMP | <i>N</i> -methyl-2-pyrrolidone |
| CCS | carbon capture and storage | NMR | nuclear magnetic resonance |
| CCU | carbon capture and utilisation | NP | nanoparticle |
| COD | 1,5-cyclooctadiene | NTf ₂ | bis(trifluoromethanesulfonyl)imide, N(SO ₂ CF ₃) ₂ |
| cp* | pentamethyl cyclopentadienyl | <i>o</i> - | ortho-substituted |
| DFT | density functional theorem | OAc | acetate |
| dhbp | 4,4'-dihydroxy-2,2'-bipyridine | OES | optical emission spectrometry |
| DIBAL-H | di- <i>iso</i> -butylaluminium hydride | OEt | ethanolate |
| DICP | Dalian Institute for Chemical Physics | OTf | triflate |
| DME | dimethyl ether | <i>p</i> - | para-substituted |
| DMF | dimethylformamide | PEHA | pentaethylene hexamine |
| DMFC | direct methanol fuel cell | Ph | phenyl |
| DMM | dimethoxymethane | phen | 1,10-phenanthroline |
| dppbz | 1,2-bis(diphenylphosphino)benzene | POL | porous organic ligand |
| dppe | 1,2-bis(diphenylphosphino)ethane | ppb | parts per billion |
| dppm | 1,2-bis(diphenylphosphino)methane | ppm | parts per million |
| <i>ee</i> | enantiomeric excess | PVP | polyvinylpyrrolidone |
| EELS | electron energy loss spectroscopy | pz | pyrazol-1-yl |
| EGDMA | ethylene glycol dimethacrylate | QD | quantum dot |
| EMIM | 1-ethyl-3-methylimidazolium | RWGS | reverse water-gas shift reaction |
| ESI | electrospray ionisation | sal | salicylaldimine |
| <i>et al.</i> | et alii, et aliae or et alia | SAP | supported aqueous phase |
| FT-IR | Fourier-transform infrared spectroscopy | SAPO | silicoaluminophosphate |
| HAADF | high-angle annular dark-field imaging | SILP | supported ionic liquid phase |
| HFIP | 1,1,1,3,3,3-hexafluoro isopropanol | SLP | supported liquid phase |
| hmbs | hexamethyldisilazane | STEM | scanning transmission electron microscopy |
| HR | high resolution | syngas | synthesis gas |
| <i>i</i> - | iso | <i>t</i> - | tertiary |
| ICE | internal combustion engine | TEM | transmission electron microscopy |
| ICP | inductively coupled plasma | TFE | 2,2,2-trifluoro ethanol |
| kMC | kinetic Monte Carlo | THF | tetrahydrofuran |
| LPG | liquefied petroleum gas | TMM | trimethylene methane |
| <i>m</i> - | meta-substituted | TOF | turnover frequency |
| Me | methyl | TON | turnover number |

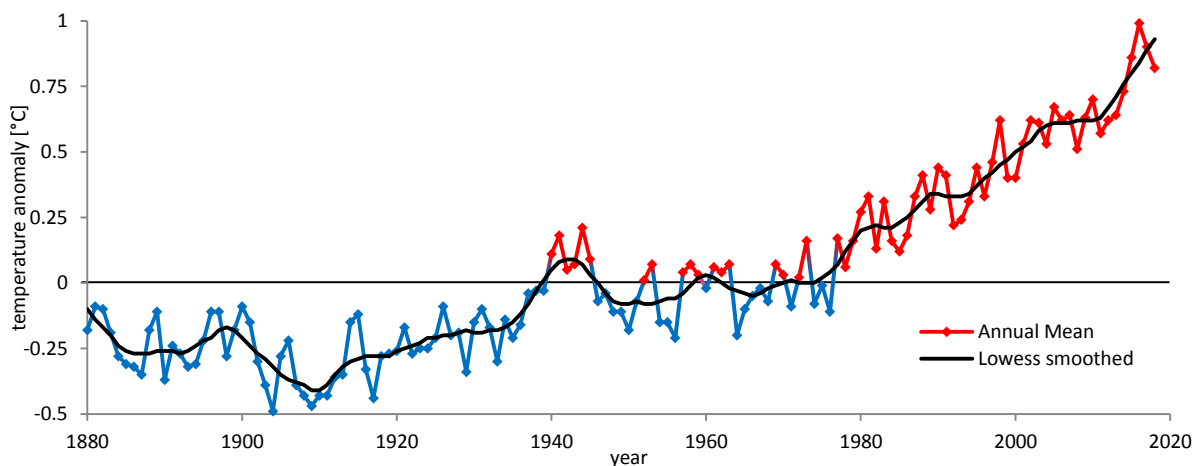
| | | | |
|-----|------------------------|-----|--------------------------|
| TPB | triphenylbenzene | WGS | water-gas shift reaction |
| TPP | triphenylphosphite | XRD | X-ray diffractometry |
| UOP | Universal Oil Products | | |

1. Introduction

1.1. Climate Change – Setting the Scene

“No challenge [...] poses a greater threat to future generations than climate change”, the Ex-President of the United States of America, Barack Obama, once said about global warming in an official announcement in 2015.^[1] The existence of a change in climate is indeed not deniable. This is exemplary depicted in Scheme 1, which shows the plot of annual mean temperatures, as well as their generalization *via* the LOWESS (locally weighted scatterplot smoothing) algorithm from 1880 until 2018. Actually, it is known that changes in climate have occurred even long before the ancestors of *Homo sapiens* appeared for the first time. Therefore, the human impact on the climate has to be considered as superimposed on those caused by natural cycles. Still, the anthropogenic effects on the climate can by far not be neglected; between 1995 and 2006 the planet earth has experienced the eleven warmest years on instrumental record since 1850.^[2] Consequences of this warming are already measurable, too. Since the 1950s, for instance, there has been a decline in the extent of sea-ice during spring and summer in the Arctic of about 20-25%, as well as a prevalent withdrawal of mountain glaciers in the non-polar regions. In addition, the global average sea level increased by 10 to 20 cm throughout the twentieth century. This is especially a danger for low-lying coastal countries, such as The Netherlands, The Maldives and Bangladesh.

Responsible for the rise in global temperature are suspected to be greenhouse gases. Even though these atmospheric gases are important to maintain life-friendly global temperatures, too high amounts of them are detrimental. Already in 1895, Svante Arrhenius calculated that the earth's average surface temperature would be increased by 5-6 °C, if the carbon dioxide level in its atmosphere was doubled due to human activities.^[3] Besides of carbon dioxide (63%), also methane (18%), nitrous oxide (13%) and halogenated compounds (6%) contribute to the increased greenhouse effect, induced by human actions (Scheme 2, left).^[2]

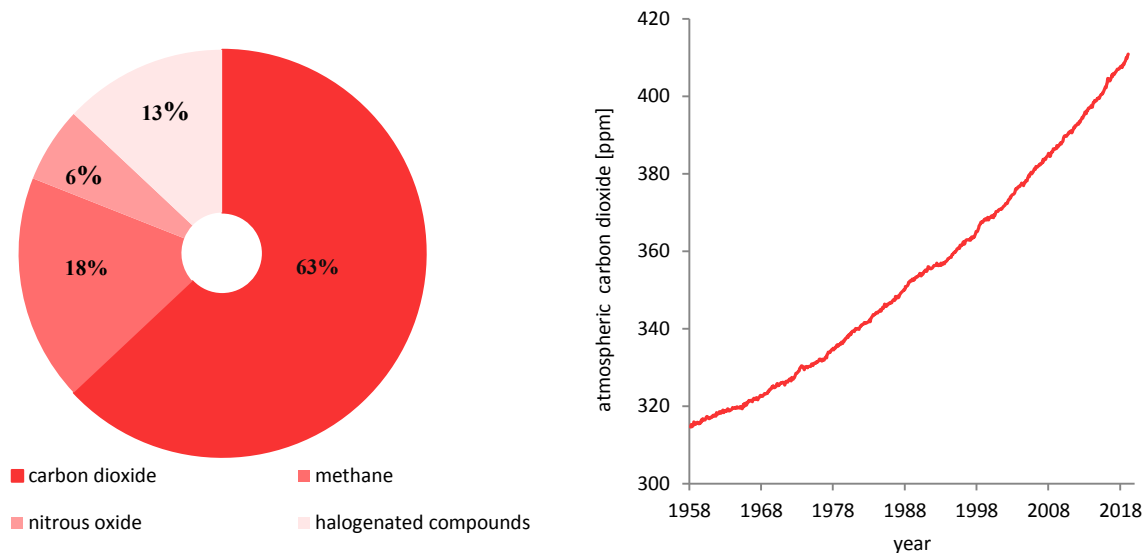


Scheme 1: Plot of the change in global surface temperature relative to 1951-1980 (red/blue) and its generalization via the LOWESS algorithm (black) from 1880 until 2018. Data source: NASA's Goddard Institute for Space Studies (GISS), 25.03.2019.^[4]

Even though methane has the highest absolute influence on the greenhouse effect, the one of carbon dioxide is the greatest relative to its amount, wherefore it is not surprising that it gained the greatest public attention as the “bad guy” in this context. On the right side of Scheme 2 the average, season-corrected atmospheric concentrations of carbon dioxide from March 1958 until February 2019 are

1. Introduction

depicted.^[5] A continuous increase of carbon dioxide during this period can be clearly recognised. In fact, the current concentration of this particular greenhouse gas has not been surpassed in the last 420,000 years, and the present rate of its increase is unmatched since at least 20,000 years. The major impact on the anthropogenic carbon dioxide emissions has the combustion of fossil fuels (32⁹ t CO₂ in 2008), among which coal (13⁹ t) and petroleum (11⁹ t) contribute the most.^[6]



Scheme 2: Left: Relative contributions of carbon dioxide, methane, nitrous oxide and halogenated compounds to the increased greenhouse effect induced by human actions.^[2] Right: Average atmospheric CO₂-level (season corrected), measured by Mauna Loa, Hawaii, from 1958 to 2019. Data source: <https://climate.nasa.gov/>, 25.03.2019.^[5]

An important use of petroleum is the generation of fuels. Interestingly, two percent of the total global carbon dioxide emissions are solely caused by the cars and trucks of the Volkswagen AG.^[7] Even though the automobile-industry-related emission of carbon dioxide is not only restricted to the used fuel, but for example also to the production of the vehicles (including potential batteries for electric cars), this is probably the best point for innovations. In this context, i.e. (pressurised) hydrogen or formic acid in combination with fuel cells, electric cars, and alternative, sustainable fuels, such as methanol, dimethylether and dialkoxymethanes, have been discussed extensively. Currently, however, it seems that the first have prevailed against the others in a long-term perspective in Germany. Due to that reason, the Volkswagen AG, along with other automobile companies, is now investing worth-mentioning amounts of money in the development of electric cars^[8] and their mandatory batteries.^[9]

Not only is petroleum used to produce fuels, but also does it constitute one of the major feedstocks for the chemical industry. As a matter of fact, it is also a limited feedstock, which will only last at most a few more centuries. Due to these reasons, alternative feedstocks are needed in order to become independent of fossil fuel-based resources in a long-term perspective.

1.2. A Future Independent from Fossil Fuels – The “Methanol Economy”

The urge for reducing the carbon dioxide concentration in the earth’s atmosphere is great, and innovative ideas are needed. Clearly, on the one hand the carbon dioxide emissions should be reduced, for instance by optimising the efficiency of existing fossil fuel-consuming processes. In addition, electric energy has to be generated by sustainable methods, such as hydropower, wind, solar, geothermal, tides and biomass power. On the other hand, the existing excess of carbon dioxide in the atmosphere, as well as the further emitted one, should be removed from the atmosphere, and preferably transformed to products of value. There have been several ideas for getting rid of carbon

1. Introduction

dioxide from industrial exhausts. For instance, carbon dioxide could be compressed and stored underground in depleted oil or gas reservoirs, geological formations, or even at the bottom of the sea in liquid phase.^[10] These attempts are called carbon capture and storage (CCS) and obviously would be accompanied by risks. The captured carbon dioxide can volatilize either gradually or spontaneously, whereby the latter case could result in dramatic consequences.

The primary aim of CCS is the reduction or the avoidance of a further increase of carbon dioxide in the atmosphere. However, there are also ideas how to convert carbon dioxide into valuable products, for instance formic acid.^[11] Those attempts are designated as carbon capture and utilisation (CCU). One of the leading concepts is the so-called “*Methanol Economy*” proposed by Asinger^[12] and popularised by Olah.^[13]

1.2.1. The Concept

The increasing global population and standard of living result in high demands for electricity. At the same time, many countries, such as Germany, Switzerland, Denmark, Belgium and Norway, decided to ban the generation of energy from coal, oil, natural gas and nuclear power. Therefore, renewable energy resources will have to take over the supply of electricity progressively in the future.^[14] An even bigger challenge is the storage of excessively generated energy. Especially wind and solar energy, the two most promising renewables, are alternating and highly fluctuating. Storing energy in batteries, compressed air, and pumped hydro is possible; however, the capacities are rather limited. One imaginable approach is the storage of electric energy in chemical bonds, for instance in the form of hydrogen or methane. Storage and transportation of chemicals are easily achievable and particularly for liquids the needed infrastructure is already implemented for fossil fuels. Dihydrogen constitutes the simplest compound, which can be generated from electric energy.^[15] Nowadays, the most advanced way for this is the electrolysis of water, generating molecular hydrogen and oxygen. The produced hydrogen itself is a very clean energy carrier, as its combustion produces energy and water exclusively. Therefore, one could imagine a “*Hydrogen Economy*” in which water is “recycled” to hydrogen.^[16] However, there are several drawbacks for this energy carrier.^[17] Either high pressures (350-700 bar) or liquefaction at -253 °C are required, due to its low volumetric density. Furthermore, it is highly flammable and explosive, and can diffuse through many materials, even metals. Transportation would thus be difficult and the implementation of an adequate infrastructure expensive. Hence, the use of liquid energy carriers is favourable. In this context, methanol combines many advantages, wherefore the Nobel-Laureate George Andrew Olah (1927-2017) popularised the idea to implement a “*Methanol Economy*” (Figure 1).^[13a, 18] Nowadays, this bulk chemical is produced on a huge scale (>90 million tons in 2016)^[19] from fossil-fuel-originating syngas (synthesis gas, generally a mixture of CO, (CO₂) and H₂) in the presence of heterogeneous Cu/ZnO/Al₂O₃ catalysts at 15-90 bar and 190-270 °C.^[20] However, it is also possible to hydrogenate carbon dioxide directly to methanol.^[11, 21] It possesses a high octane rating, which makes it suitable as substitute or additive for gasoline in ICEs (internal combustion engines). In addition, it can be applied in direct methanol fuel cells (DMFCs), which allow for the conversion of chemical energy into electric energy.^[22] Besides, diesel engines may be powered efficiently with methanol after modification.^[23] Methanol can also be converted further to dimethyl ether (DME), which is an easily liquefied gas with a high cetane rating that can substitute diesel fuel and liquefied petroleum gas (LPG) in most cases.^[24] Moreover, gasoline, light olefins and numerous chemicals can be produced from this C1 compound (*vide infra*).

Clearly, for a sustainable economy, methanol has to be synthesised from renewable CO₂-sources in the future. In this regard, the reduction of atmospheric carbon dioxide to methanol is specifically appealing, as it would simultaneously result in a decrease of the greenhouse gas’ concentration in the atmosphere. Even though the current amount of this gas in the earth’s atmosphere is considered as too

1. Introduction

high, it still accounts for only 0.041%. Therefore, efficient methods for its isolation/concentration are needed. This can be achieved by membranes or selective absorption methods.^[25] Also, carbon dioxide can be captured from industrial exhausts directly, avoiding its release in the atmosphere. As will be described below, methanol can be converted to basically all hydrocarbons, which themselves are converted to carbon dioxide and water, ultimately. This means, a closed, carbon-neutral cycle could be realised by this approach and eventually humanity might become completely independent from fossil fuels.

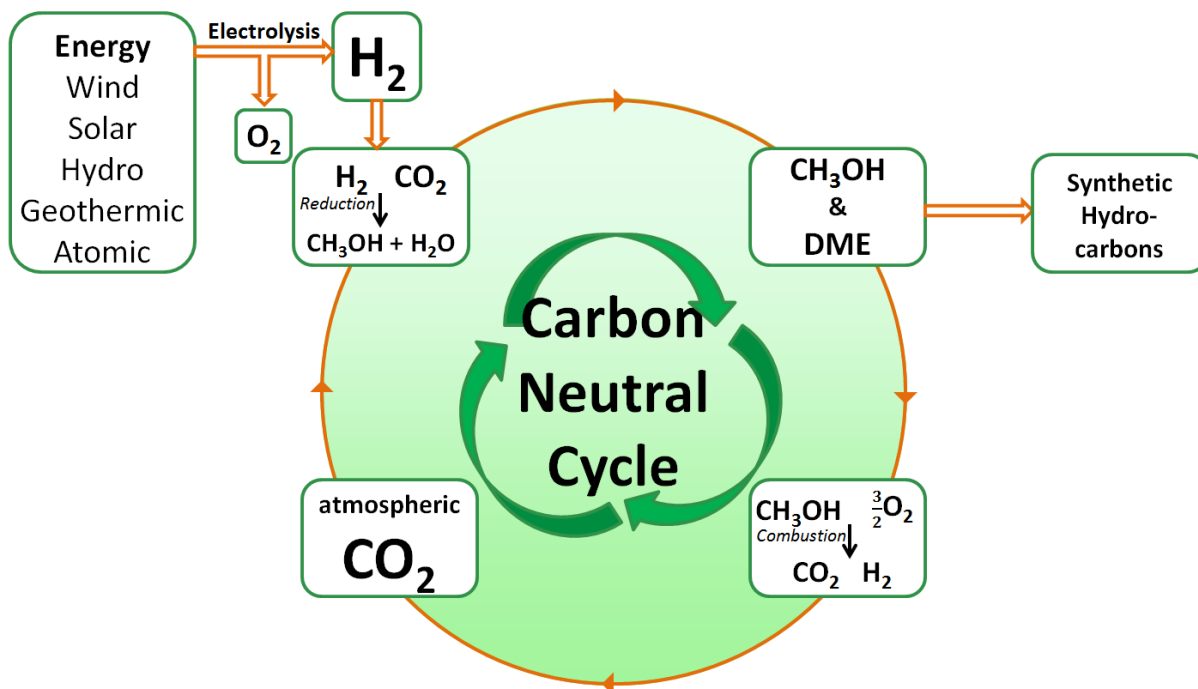


Figure 1: Schematic representation of the "Methanol Economy", as suggested by G. A. Olah.

1.2.2. Utilisation of Methanol

1.2.2.1. Synthesis of Formaldehyde, Acetic Acid and Others

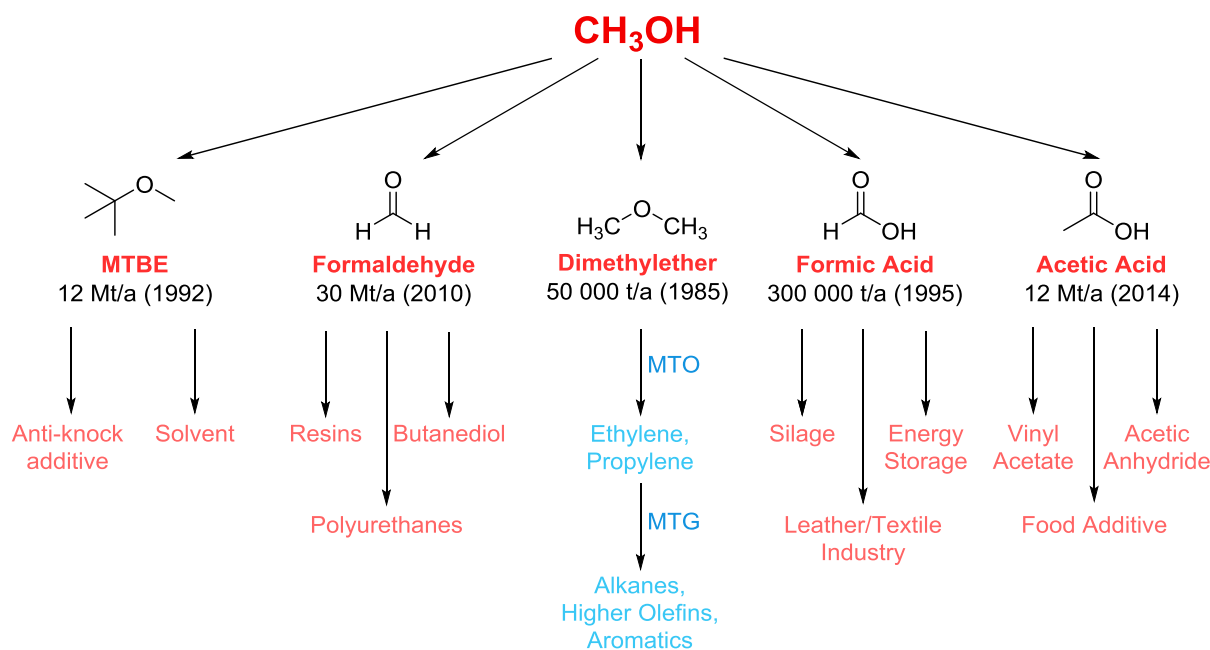
Already today, a number of bulk chemicals are produced from methanol (Scheme 3). For instance, methyl *tert*-butyl ether (MTBE) is synthesised from methanol and isobutene. Besides, also formic acid can be synthesised from methanol, *via* carbonylation to methyl formate and subsequent hydrolysis, yielding in formic acid and methanol, which can be carbonylated again.^[26]

The majority of methanol, however, is oxidised to formaldehyde.^[27] In the so-called BASF-process (BASF: Badische Anilin- und Sodafabrik), silver acts as a catalyst in a mixture of air, steam and methanol, yielding the target molecule almost quantitatively.^[28] Alternatively, reducible metal oxides (molybdenum, iron, and/or vanadium) are used as catalytic material in the so-called *Formox-process*.^[29]

Also acetic acid is accessible from methanol *via* carbonylative procedures and the annual production exceeds 12 million tons. The first commercialisation of such a process was realised by BASF in 1960. $HCo(CO)_4$ was active in this reaction in the presence of iodine at high pressures of 600 atmospheres and a temperature of 230 °C. More selective and nowadays applied routes are the Monsanto and Cativa (BP Chemicals) processes. Analogously to the original cobalt-procedure, both are based on a homogeneously catalysed carbonylative procedure in the presence of iodine. Whereas the Monsanto

1. Introduction

methodology uses a rhodium catalyst, iridium is involved in the Cativa process.^[30] They are both highly efficient, and selective, and the Monsanto-process runs at much milder conditions (30-60 bar, 150-200 °C) compared to that of BASF.



Scheme 3: Currently applied transformations of methanol to other compounds in industry (red), and promising processes for a fossil-fuel independent future (blue).

1.2.2.1. Methanol to Olefins

In a future independent from fossil fuels, another transformation of methanol to organic compounds that might be a key-technology is the so-called Methanol-to-Olefin process (MTO, Scheme 3). This process allows for the synthesis of ethylene and propylene starting from methanol. The importance of the process can be understood considering that no other compound is presently produced in such volumes in the petrochemical industry than those two gases. About 115 million tons of ethylene and 73 million tons of propylene have been produced in 2007.^[18d] They are starting materials for numerous processes, such as polymer synthesis, hydroformylation, hydrogenation, and beyond. Nowadays, they are mostly supplied from steam cracking and fluid catalytic cracking of naphtha and other gas liquids, where they accumulate as side-products.

The synthesis of these light olefins from methanol starts with the condensation of the alcohol to DME (dimethyl ether). Subsequently, the ether is dehydrated further to ethylene and propylene. Efficient materials for this process are for instance synthetic aluminosilicate zeolite (ZSM-5) catalysts.^[31] By using these minerals, the Dalian Institute for Chemical Physics (DICP) finished a 300 t/a MTO fixed bed pilot plant already in 1993. In 2010, the first plant was constructed and started-up, based on DICP's technology. Apart from ZSM-5, also silicoaluminophosphate (SAPO) molecular sieves revealed very high activities for this reaction.^[32] Both zeolites and molecular sieves possess well-defined three-dimensional structures comprising channels and cages of defined sizes, which are typically in the range of 4 Å to 12 Å. Notably, the catalysis itself occurs inside the pores and channels, which results in shape- and size-selectivity. The pore-size of ZSM-5 is 5.5 Å, whereas SAPO-34 has pores of 3.8 Å. This enables high selectivities in the latter case, as larger olefins have lower diffusion-rates, resulting in ethylene and propylene as the main products. Due to the outstanding selectivity of SAPO-34, UOP (Universal Oil Products) announced the construction of a 250,000 t/a plant based on

1. Introduction

this material in cooperation with Norsk Hydro, in 1996.^[33] Remarkably, by changing the operating conditions the ratio of ethylene to propylene can be shifted from 0.77 to 1.33, and therefore this process allows for quick adaption to the current demand. Presently, this process is commercialized in Nigeria with a capacity of 2.5 million tons per year, which is the largest worldwide. Also in other locations, units are under consideration.

Moreover, Lurgi developed a MTO-system, which produces specifically propylene (>70% overall yield).^[13a] Due to that reason it is also called Methanol-to-Propylene (MTP) process. After a demonstration unit in Norway has been successfully tested, this ZSM-5-based system will probably be commercialized in Trinidad and Tobago, as well as in China, with capacities of 450,000 tons per year each. Also Mobil, the pioneer of the MTO-process, implemented their ZSM-5 technology in Germany, which produces 100 barrels per day (approximately 5.8 million liter per year). Already in 1985, Mobil developed and commercialized a process based on ZSM-5 for the conversion of methanol to light olefins, which were oligomerised directly to hydrocarbons in the range of gasoline, wherefore it is also called Methanol-to-Gasoline process (MTG).

1.2.2.2. Methanol to Gasoline

The MTG-process was originally developed in response to the oil crises in 1973 and 1979.^[34] It constituted an alternative route to hydrocarbons, which otherwise have been synthesised by the Fischer-Tropsch-process. ZSM-5 was found to be the most stable and selective material among all zeolites. Analogously to the MTO, the confined space inside the channels and pores of this zeolites results in shape-selective catalysis. The first step involves the dimerization of methanol to DME and the subsequent conversion to light olefins, predominantly ethylene and propylene. Eventually, those unsaturated compounds are transformed into higher olefins, alkanes (C₃-C₆) and aromatic systems (C₆-C₁₀).^[35] By modifying the pore-sizes, heavier products may be obtained; however, C₁₀ usually constitutes the limit for conventional gasoline.

The original plant of Mobil in New Zealand had a capacity of 600,000 tons of gasoline per year and was carried out at 350-400 °C and 20 atm. The as obtained product could be blended with the general gasoline pool without prior distillation or refining. Ironically, only shortly after this plant was started, the oil price fell again to under \$10 in 1986, leading to a cease of the gasoline produced by this plant. However, MTG-processes will probably become important in the future, as oil prices are climbing again and ultimately fossil fuels will be depleted.

1.3. Methanol from CO₂

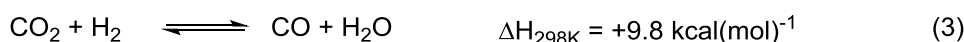
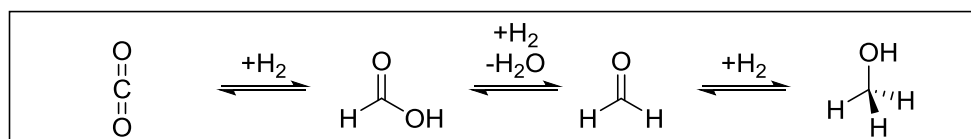
As described above, methanol is at present mainly produced from syngas in the presence of small amounts of carbon dioxide over heterogeneous copper-catalysts ("methanol copper") in amounts exceeding 90 million tons per year - with a rising trend.^[19] Syngas can have varying compositions of hydrogen, carbon monoxide and carbon dioxide, depending on which raw material (any carbonaceous material, i.e. natural gas, coke, petroleum) was chosen to be reformed or partially oxidised. Therefore, this gas-mixture is available on reasonable costs to date; however, in the future it will become more expensive as the raw materials will gradually diminish. Consequently, renewable resources have to be found, which allow for efficient methanol production on big scales. In this context, carbon dioxide is a very encouraging candidate. It was shown that the addition of it to syngas leads to significantly higher methanol yields.^[36] Researchers worldwide are contributing to this topic. Apart from

1. Introduction

electrochemical,^[37] photochemical,^[38] and chemical reduction systems,^[39] the hydrogenation of carbon dioxide with H₂ is of great interest.^[40]

1.3.1. Hydrogenation of CO₂ to Methanol – Theoretical Considerations

The hydrogenation of carbon dioxide to methanol occurs formally *via* the intermediates formic acid/formate and formaldehyde (Scheme 4).^[41] In case of homogeneous systems, it is supposed that the conversion of formic acid to formaldehyde is the most challenging one,^[42] which explains the numerous known catalytic systems for the hydrogenation of carbon dioxide to formic acid.^[11, 43] The reduction of one molecule of carbon dioxide to methanol necessitates three molecules of hydrogen and produced one molecule of water, according to equation (2). This reaction, however, is an equilibrium and occurs simultaneously with the (reverse) water-gas shift reaction (WGS, RWGS) (3), and the hydrogenation of carbon monoxide to methanol (1). Therefore, equation (2) formally is the sum of the other two equations and is of exothermic nature. The same is valid for the hydrogenation of CO to methanol, whereas the RWGS is endothermic. This means, high pressures and low temperatures favour the methanol-producing reaction pathways (principle of Le Chatelier). The WGS is also the reason why the addition of carbon dioxide to syngas is beneficial for the methanol yield. During the hydrogenation of this gas to methanol, water is formed, which can subsequently be converted to hydrogen and carbon dioxide. Afterwards, the latter can be hydrogenated again. This side-pathway improves the carbon balance of the reaction.^[44]



Scheme 4: Thermodynamics for the hydrogenation of carbon dioxide towards methanol (2), and the competing reactions (1) and (3).

Attempts for a proper description of the thermodynamic equilibria of these three reactions have been contributed by Graaf *et al.*^[45] Moreover, they modelled internal mass transport limitations in the synthesis of methanol mathematically^[46] and determined the kinetics of this reaction catalysed by the commercial copper-catalyst.^[47]

Due to practical reasons, methanol synthesis from carbon dioxide is usually carried out at 220 – 270 °C and 50 bar pressure. This results in a thermodynamically limited methanol yield of 35%, which can be improved to about 70% by removing either water or methanol from the reaction and thus shifting the equilibria towards the products.^[48]

In the following, an overview of the literature concerning the hydrogenation of carbon dioxide to methanol will be given. Even though the amount of heterogeneous catalysts for this transformation is by far greater, special focus was set on homogeneous systems.

1. Introduction

1.3.2. Heterogeneous Hydrogenation of CO₂

1.3.2.1. Copper

A large amount of heterogeneous catalysts for the direct hydrogenation of carbon dioxide to methanol is known.^[49] Actually, already today methanol is produced from carbon dioxide in demonstration units, such as the George Olah Plant in Island, which has a capacity of 4000 t/a.^[50] The used catalyst is based on copper in the presence of other metal oxides, as are many of the published systems. For instance, the group of Jinyao Liu reported ultrafine Cu/ZrO₂ catalysts, synthesised by a deposition-precipitation method in 2001.^[51] This particular methodology resulted in materials with a high specific surface area and large pore volumes. Compared to catalysts prepared by impregnation and co-precipitation, increased catalytic activities have been observed at 220 °C to 240 °C. The group of Alexis T. Bell investigated the influence of the zirconia phase on copper catalysts for methanol synthesis one year later.^[52] Therefore, one material was prepared on tetragonal and one on monoclinic zirconia, and the performance of both was examined. This revealed the monoclinic ZrO₂ material to be 4.5 fold more active in the hydrogenation of carbon dioxide at 275 °C and even 7.5 times in the case of carbon monoxide as starting compound. This productivity was improved further by increasing both the surface area of monoclinic ZrO₂ and the ratio of copper to zirconium(II) oxide surface areas. The effect of ZrO₂ doping of a CuZnO catalyst was documented by the group of Yuhan Sun in 2006.^[53] It was observed that the presence of ZrO₂ resulted in a high dispersion of copper, which led to an almost 2-fold catalytic activity compared to the reference un-doped CuZnO. A process for the hydrogenation of carbon dioxide in liquid phase was reported by Tsubaki *et al.*^[54] Copper-based materials were prepared *via* a oxalate-gel precipitation method and a high activity was achieved at 170 °C and 50 bar. Notably, 25.9% of the carbon dioxide was converted with selectivity toward methanol of 72.9%. Dasireddy *et al.* investigated the correlation between pH-value during synthesis, structure and catalytic activity and selectivity of Cu/MgO/Al₂O₃ in a continuous-flow packed-bed reactor.^[55] Alkaline conditions (pH = 8) had beneficial effects on the catalyst's productivity, presumably due to the presence of both CuO and Cu₂O. Heldebrant and co-workers developed a low-temperature hydrogenation system based on Cu/ZnO/Al₂O₃ in condensed phase.^[56] In the presence of NEt₃ and ethanol, carbon dioxide was reduced at 120-170 °C. Apparently, the reaction occurs *via* the intermediates alkyl carbonate, ammonium formate and alkyl ester. Methanol was formed quantitatively at 50 bar CO₂/H₂ (1:2), and only traces of methane and carbon monoxide have been detected in the gas-phase. Very recently, Huš *et al.* demonstrated synergistic effects of bifunctional Cu/Perovskite catalysts *via* DFT-calculations (density functional theorem). Materials of copper on CaTiO₃, SrTiO₃, BaTiO₃ and PbTiO₃ were studied systematically and the results fed into a kMC (kinetic Monte Carlo) setup at conditions, relevant for industry. All of the systems investigated performed better than pure copper, with Cu/PbTiO₃ being the best. An environmentally benign alternative is Cu/SrTiO₃.^[57]

1.3.2.2. Palladium

Besides of copper, also palladium showed activity in the CO₂-hydrogenation to methanol. In 2000, Bonivardi *et al.* demonstrated an impressive promoting effect by the addition of gallium to Pd/SiO₂.^[58] The turnover rate was 500-fold for the Ga-Pd/SiO₂ and the selectivity towards methanol was increased up to 70% (250 °C, 30 bar). This increase in productivity was explained with an interaction between palladium crystallites and reduced gallium species. Iwasa and co-workers investigated the performance of Pd/ZnO in the title reaction at atmospheric pressure.^[59] Upon the reduction conditions, a PdZn alloy is formed and at 170 °C, a higher activity and selectivity was observed than for reference Cu/ZnO. Supporting Pd-ZnO on multi-walled carbon nanotubes also resulted in catalytically active materials.^[60] At 250 °C, a turnover frequency (TOF) of $1.15 \cdot 10^{-2} \text{ s}^{-1}$ was observed by the group of Hong-Bin Zhang. Recently, PdIn intermetallic nanoparticles (NPs) have been examined by García-

1. Introduction

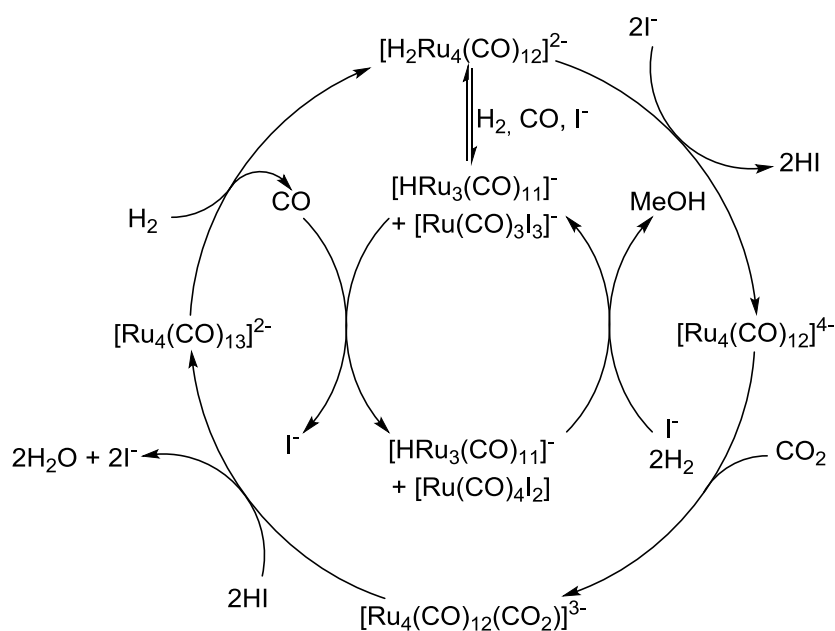
Trenco *et al.*^[61] In the liquid phase, this unsupported material exhibited a 70% higher methanol rate compared to conventional Cu/ZnO/Al₂O₃ at 50 bar (H₂/CO₂ = 3:1) and 210 °C. A selectivity up to >80% was reached, compared to a maximum of 45% for the reference copper-catalyst.

1.3.2.3. Other Metals

In 2015, gold NPs anchored on a CeO_x/TiO₂ interface were reported to be active in the hydrogenation of carbon dioxide to methanol at low pressure (1 bar).^[62] Active centres are generated by the electronic polarisation at the metal-oxide interface of gold NPs, which are stabilised and supported on CeO_x/TiO₂. The absence of CeO_x led to decreased activity and methanol selectivity. Recently, Hongliang Li *et al.* revealed synergistic interactions between neighbouring Pt atoms on MoS₂, which significantly enhance the catalytic activity in the CO₂-hydrogenation by decreasing the activation energy.^[63] Compared to isolated Pt atoms, neighbouring ones go through different reaction pathways. They catalyse the stepwise reduction *via* formic acid, while isolated ones avoid intermediates. The same group investigated the influence of hydroxyl groups on the surface of hydrophilic SiC quantum dots (QDs) on the hydrogenation activity.^[64] These QDs revealed a higher productivity in the methanol production compared to commercial SiC, which was attributed to the surface OH-groups. They activate carbon dioxide by protonating it to form a HCOO*-species as intermediate, and therefore accelerate the catalysis. Finally, also rhenium supported on titania exhibited activity in CO₂-hydrogenation, as was shown very recently by Ken-ichi Shimizu and co-workers.^[65] A maximum turnover number (TON) of 44 and selectivity towards methanol of 82% were achieved at relatively mild conditions (60 bar, 150 °C). The same catalyst was active in the hydrogenation of carboxylic acids and its derivatives, as well as in the N-methylation of amines using CO₂ as the methyl source.^[66]

1.3.3. Homogeneous Hydrogenation of CO₂

Apart from heterogeneous systems for the methanol production from carbon dioxide, there is also a great interest in homogeneous catalysts. Due to their intrinsically higher activity, milder reaction conditions could be applied, making them interesting for delocalised applications. The very first report for a homogeneously catalysed reduction of carbon dioxide to methanol was published by Tominaga in 1993.^[67]



Scheme 5: Schematic mechanism for the hydrogenation of carbon dioxide to methanol with [Ru₃(CO)₁₂], as suggested by Tominaga *et al.*^[68]

1. Introduction

[Ru₃(CO)₁₂] in combination with alkali metal iodides converted the greenhouse gas to a mixture of methanol, methane, ethane and carbon monoxide at harsh conditions (240 °C, 80 bar CO₂/H₂ 1:3) in *N*-methyl-2-pyrrolidone (NMP). By increasing the amount of potassium iodide, the formation of methane and ethane was reduced and methanol became the predominant product with TONs up to 32. In a subsequent mechanistic study this effect was elucidated (Scheme 5).^[68] Under reaction conditions, the metal precursor is quantitatively converted to [Ru(CO)₃I₃]⁻ and [HRu₃(CO)₁₁]⁻, as was observed by FT-IR (Fourier-transform infrared spectroscopy). The latter is further transformed to [H₂Ru₄(CO)₁₂]²⁻, which is the main species in the reaction solution. This step is promoted by the formation of HI in the presence of iodide, yielding in [Ru₄(CO)₁₂]⁴⁻. Subsequent coordination of carbon dioxide to this tetranuclear complex forms the metallocarboxylate species [Ru₄(CO)₁₂(CO₂)]³⁻. The liberation of water assisted by hydrogen iodide results in [Ru₄(CO)₁₃]²⁻. Finally, the dihydride-species is regenerated by replacing one ligated CO with H₂. Carbon monoxide in combination with [Ru(CO)₃I₃]⁻ yields in [Ru(CO)₄I₂], which is then hydrogenated by [HRu₃(CO)₁₁]⁻ to give a formyl complex. Eventually, the latter complex is hydrogenated further to produce methanol. Visibly, iodide plays a role in several steps within the catalytic cycle, which explains its importance for improved methanol selectivities.

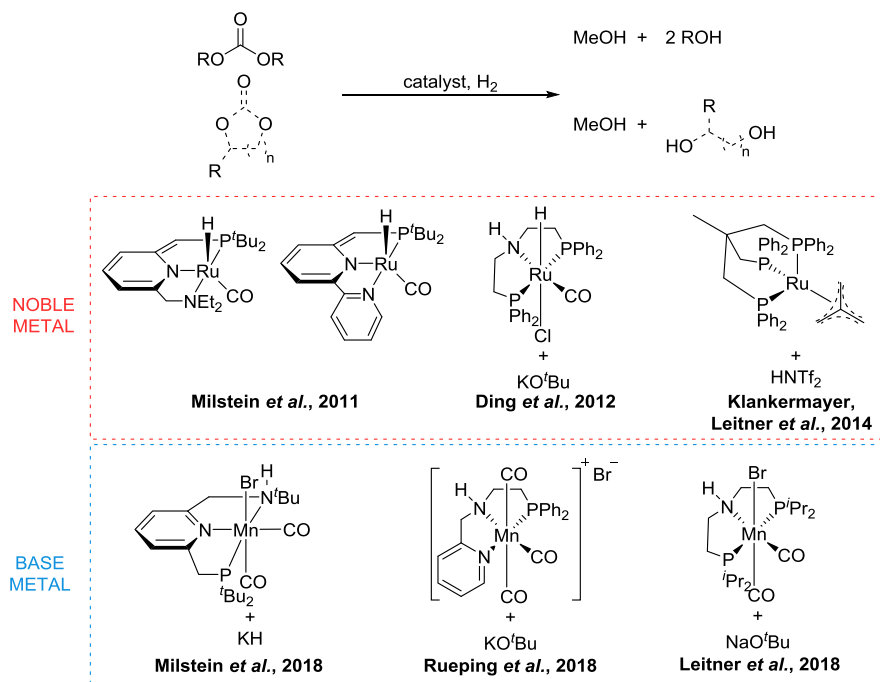
Other metal carbonyls were not active in the hydrogenation of carbon dioxide under conditions optimised for [Ru₃(CO)₁₂]. Rhodium, iridium, tungsten, molybdenum, iron and cobalt have been investigated.

1.3.3.1. Indirect Stepwise Approaches

In the last decade, a number of indirect approaches for the conversion of carbon dioxide to methanol have emerged.^[41a, 69] They all have in common that the gas is first transformed to activated CO₂-derivatives, which subsequently are hydrogenated further to methanol. Such derivatives are for instance carbonates, formates, carbamates, and formamides.^[70] This approach can either occur in a stepwise manner, or the activation of carbon dioxide and the further hydrogenation to methanol happens in a one-pot methodology.

In 2011, the group of Milstein reported the very first catalytic system for the hydrogenation of carbonates and formates to alcohols, as well as carbamates to alcohols and amines (Scheme 6).^[71] Four different PNN ruthenium-pincer complexes were synthesised and tested in the catalytic reactions. TONs up to 4400 have been achieved for dimethyl carbonate as substrate after 14 h in THF at 50 bar hydrogen and 110 °C. Also the unprecedented hydrogenation of urea derivatives to methanol and amines with the same bipy-based PNN ruthenium complex (bipy: 2,2'-bipyridine) has been reported by the same group.^[72] In the following, ruthenium-based NHC-pincer systems (NHC: *N*-heterocyclic carbene) have been studied for the cyclic ethylene carbonate as substrate.^[73] The activity of [Ru(Tripfos)(TMM)] (TMM: trimethylene methane) in the reduction of carboxylic and carbonic acid derivatives, such as carboxylic esters and acids, anhydrides, lactones, as well as secondary amines, has been studied by the groups of Leitner and Klankermayer extensively.^[74] Whereas those compounds have been successfully reduced in additive-free conditions, the highly acidic HNTf₂ was necessary for organic carbonates, primary amides and urea derivatives. Clearly, this system constitutes a highly versatile catalyst for reductions with molecular hydrogen.

1. Introduction

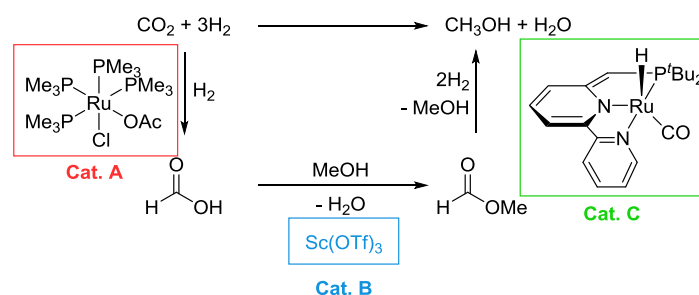


Scheme 6: Selected catalytic systems based on either noble or base metals for the hydrogenation of cyclic and acyclic carbonates to the corresponding alcohols and diols.

The highest TON for the hydrogenation of organic carbonates to alcohols so far has been reported by the group of Kuiling Ding. The commercially available ruthenium-MACHO pincer complex achieved TONs up to 87,000 and TOFs up to 1200 h⁻¹ in the hydrogenation of ethylene carbonate in the presence of KO^tBu as base at 50 bar H₂ and 140 °C.^[75] This substrate is produced within Shell’s “OMEGA” process from ethylene oxide and carbon dioxide, and subsequently converted to ethylene glycol, which regenerates CO₂.^[76] The very first non-noble metal catalysts for the reduction of carbonates to alcohols were reported only recently by the groups of Leitner,^[77] Rueping^[78] and Milstein^[79] basically at the same time. They reported manganese-based pincer complexes for the hydrogenation of organic carbonates under basic conditions. The catalytic systems obtained similar activities at 110-140 °C, 30-50 bar H₂ and loadings of 1-2 mol%.

1.3.3.1. Indirect One-Pot Approaches

Apart from these stepwise methodologies, a number of one-pot processes have been reported. Huff and Sanford demonstrated a cascade catalytic approach for the reduction of carbon dioxide to methanol, which comprised three different catalysts for the different transformations (Scheme 7).^[80]



Scheme 7: Schematic depiction of the cascade catalytic system for the one-pot hydrogenation of carbon dioxide to methanol under acidic conditions, as reported by Melanie S. Sanford.^[80]

[Ru(Cl)(OAc)(PMe₃)₄] (catalyst A) hydrogenates carbon dioxide to formic acid, which is further converted to methyl formate in presence of the Lewis-acid Sc(OTf)₃ (catalyst B) in methanol.

1. Introduction

Eventually Milstein's catalyst (catalyst C) reduces the ester to methanol and water. The reactions were optimized separately and ultimately combined in a simultaneous reduction. A low TON of 2.5 for methanol was achieved after 16 h in one pot at 10 bar CO₂, 30 bar H₂, and 135 °C in CD₃OH. The reason for the low productivity was ascribed to deactivation of catalyst C by Sc(OTf)₃, which explains the accumulation of methyl formate (TON = 34). As a low-tech solution, the catalysts were separated physically by placing catalysts A and B in a vial in the center of the high pressure vessel, while C was located in the outer well of the reactor. This methodology increased the productivity to a TON of 21.

Four years later, the same group developed a tandem procedure for the methanol production from CO₂ under basic conditions.^[81] The system comprises the *in-situ* activation of carbon dioxide with dimethyl amine to form dimethylammonium dimethylcarbamate, and its subsequent hydrogenation to methanol in the presence of a ruthenium pincer catalyst. In the presence of the commercially available complex ruthenium-MACHO-BH (Figure 2), a CO₂ conversion of up to 96% and a methanol TON of 550 were obtained. Importantly, the presence of K₃PO₄ was shown to be crucial, along with a temperature-ramp program, starting with 95 °C for 18 h, followed by 155 °C for 36 h. This is accounted to the competing events of catalyst decomposition and hydrogenation of dimethylammonium dimethylcarbamate at 155 °C. The formation of the intermediate DMF (dimethylformamide) from dimethylammonium dimethylcarbamate occurs already at 95 °C, its further hydrogenation to methanol and water, however, needs higher temperatures. Therefore, DMF accumulates during the first 18 h and is subsequently transformed further at 155 °C.

Unfortunately, the previously described PNN ruthenium-pincer complex (Scheme 6) of Milstein^[71a] for the hydrogenation of carbonates, carbamates and formates (*vide supra*) was not active in the direct hydrogenation of carbon dioxide. However, in a later study the group demonstrated the activity of this catalyst in the hydrogenation of oxazolidinones (i.e. cyclic carbamates).^[82] Based on this catalytic activity a system for the hydrogenation of CO₂ to methanol was developed. First, the gas is captured by 2-aminoalcohols in the presence of catalytic amounts of Cs₂CO₃ to form oxazolidinones at low CO₂-pressures of 1-3 bars. (2-Methylamino)ethanol and valinol (2-amino-3-methyl-1-butanol) captured the carbon dioxide to give the product in 65-70 and 90-95% yields, respectively. The as obtained oxazolidinones have been hydrogenated to methanol with yields up to 92%. When isolation of the intermediate species was omitted, however, the yields decreased to 53%.

In the same year, the groups of George A. Olah and G. K. Surya Prakash reported the capture of carbon dioxide from air and its transformation to methanol by Ru-MACHO-BH.^[83] In their system, the concentrated gas was captured by PEHA (pentaethylene hexamine), and at a total pressure of 75 bar (CO₂:H₂ = 1:3) and 155 °C in THF, a maximum TON of 1060 was achieved after 40 h. After isolation of the produced methanol *via* distillation, the residual catalyst-solution was successfully reused. In this way, four runs were conducted, retaining more than 75% of its initial activity in each run and yielding in a total TON of 1850. For the use of air as CO₂-source, the synthetic gas mixture was bubbled through an H₂O/triglyme mixture containing PEHA and the catalyst. The solvent triglyme was used in order to ease the final distillation of methanol. At 155 °C, a NMR yield of methanol of 79% was achieved after 55 h. Remarkably, this was the first example of methanol synthesis directly from aerobic CO₂. The system was further investigated mechanistically and an improved TON of 9900 after 10 days was achieved, which is the highest reported for homogeneous one-pot hydrogenation of carbon dioxide to date.^[84] Later, the same group reported a recycling strategy for this system.^[85] CO₂ was captured by PEHA in a biphasic 2-MTHF/water system (2-MTHF = 2-methyl tetrahydrofuran) and hydrogenated at 80 bar H₂ to give 95% methanol in the first run. 2-MTHF has a miscibility gap with water, which simplifies the separation of product. In the fourth cycle, 87% of the methanol production and 95% of the catalysts activity were retained. Also a recycling strategy by

1. Introduction

immobilisation of the amine on silica was reported.^[86] In 2017, the group of Karl Gademann demonstrated the use of pyrrolizidines as CO₂ gatherer and the further hydrogenation with the same catalyst, Ru-MACHO-BH, to give methanol with a low TON of 28.^[87]

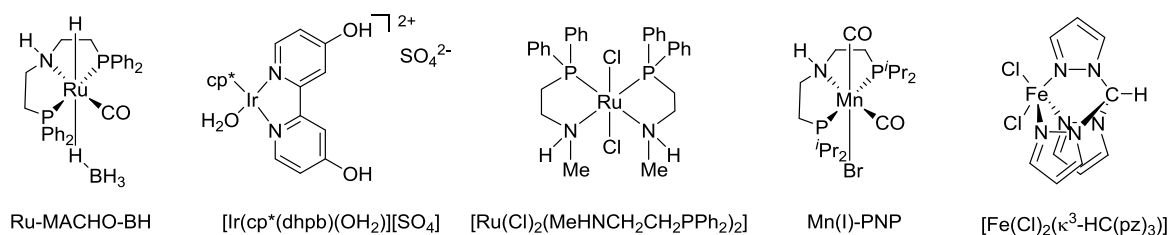


Figure 2: Selection of reported catalysts for the indirect, one-pot hydrogenation of carbon dioxide to methanol.

A different methodology was followed by Himeda, Laurenczy *et al.* in 2016.^[88] Within this approach, CO₂ is hydrogenated to formic acid, which then undergoes a disproportionation to methanol, water and two equivalents of CO₂. The iridium-based complex [Ir(cp*)(dhbp)(OH₂)]²⁺[SO₄²⁻] (cp*: pentamethyl cyclopentadienyl, dhbp = 4,4'-dihydroxy-2,2'-bipyridine, Figure 2) was successfully applied in the hydrogenation of carbon dioxide to formic acid in aqueous conditions. Furthermore, it catalyses the disproportionation of formic acid in the presence of H₂SO₄, yielding in methanol with a selectivity of 96% at a conversion of 98%. One benefit of this approach is that methanol and water do not form azeotropes, which simplifies the following isolation *via* distillation.

One of the highest TONs for an one-pot procedure to date was achieved by Everett and Wass in 2017.^[89] By combining [RuCl₂(MeHNCH₂CH₂PPh₂)₂] (Figure 2) with ⁱPr₂NH, methanol was produced with a TON of 8900 after 20 h, which corresponds to a TOF of 4500 h⁻¹. Relatively low pressures of 10 bar CO₂ and 30 bar H₂, and 100 °C were applied, using toluene as solvent and NaOEt as a base. The amine was added for activating the greenhouse gas as formamide.

All of the above described systems for the consecutive activation and hydrogenation of CO₂ to methanol have been based on noble metals, predominantly ruthenium. The first non-noble metal system was based on manganese and published by G. K. Surya Prakash in 2017.^[90] A PNP Mn-pincer complex (Figure 2) was determined to be active in this reaction. Both the activation of the gas with either morpholine or benzylamine, and the hydrogenation of the formamide to methanol were catalysed by this compound. TONs of up to 36 were obtained.

In the same year, also an iron system was reported for the title reaction.^[91] The group of A. J. L. Pombeiro claimed the iron scorpionate complex [FeCl₂(κ³-HC(pz)₃)] (pz = pyrazol-1-yl, Figure 2) to hydrogenate carbon dioxide to methanol at comparatively very mild conditions of 80 °C and 75 bars with a maximum TON of 2387 (46% yield) after 36 h. Either PEHA or 1,1,3,3-tetramethylguanidine were used as an amine in the absence of any other solvent. Notably, the authors stated that the avoidance of any amine and the use of acetonitrile as solvent were also sufficient, albeit at lower activity. That means, this system can also act in a direct manner (*vide infra*) without pre-activation of carbon dioxide.

1.3.3.2. Direct Approaches

As shown *vide supra*, several systems for the hydrogenation of carbon dioxide-derivatives have been documented, of which some can also convert the gas to those activated species. In contrast, only very few systems for the direct conversion of CO₂ to methanol are known. The very first report was published by the groups of Klankermayer and Leitner in 2012.^[92] The aforementioned [Ru(Triphos)(TMM)] complex for the hydrogenation of divers carboxylic and carbonic acid derivatives also revealed activity in the direct conversion of CO₂ in the presence of one equivalent

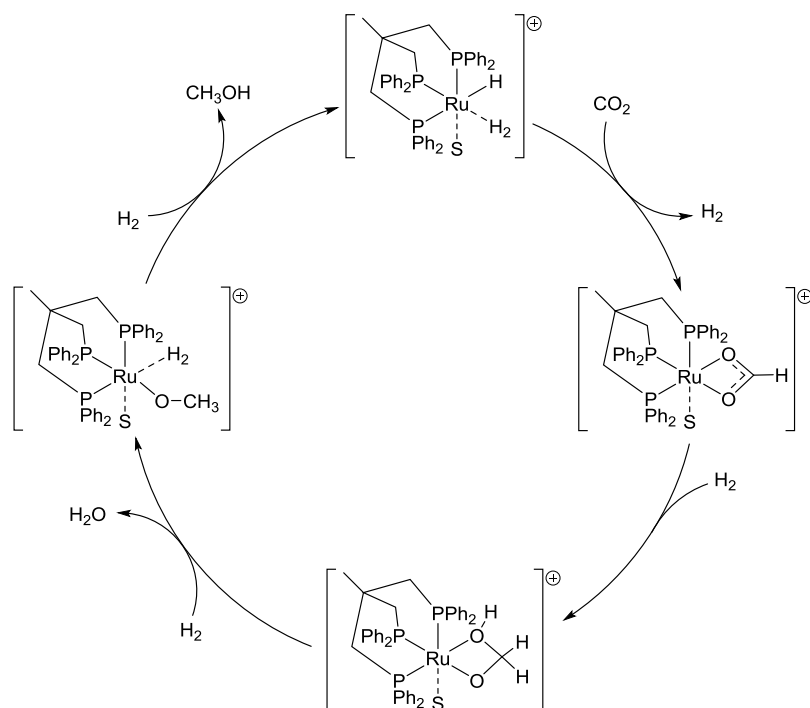
1. Introduction

HNTf₂. A TON of 221 was achieved after 24 h at 140 °C and a total pressure of 80 bar (H₂:CO₂ = 3:1). Also the *in-situ* system comprising of Ru(acac)₃ (acac = acetylacetonate) and Triphos in the presence of the organic acid MSA (methanesulfonic acid) exposed activity in this transformation with a maximum TON of 135 at otherwise same conditions. The reactions were carried out in a mixture of 1.5 mL THF and 10 mmol ethanol (0.58 mL), which was added to tentatively stabilise the formate species (a supposed intermediate) as an ester. The authors proposed the cationic species [Ru(H)(H₂)(S)(Triphos)]⁺ (S = solvent) to be the catalytically active one. Consequently, this would explain the improved activities in the presence of the weakly coordinating counter anion NTf₂⁻, which allows for stabilisation of the cationic complex. In a later study, the mechanism of this system was further elucidated by DFT-calculations.^[93] Notably, this investigation suggested an inner-sphere mechanism, during which a series of hydride transfer and protonolysis steps occur in the coordination sphere of the metal without the cleavage of formic acid or formaldehyde as intermediates. A basic version of the catalytic cycle is depicted in Scheme 8. The formate species [Ru(S)(Triphos)(η²-O₂CH)]⁺ was identified as the resting state under the reaction conditions, which can be produced from numerous stable and readily available catalyst precursors. This was confirmed by testing the acetate complex [Ru(S)(Triphos)(η²-O₂CCH₃)] [NTf₂]⁻ for CO₂ hydrogenation in a high-pressure NMR tube. Using 20 bar CO₂ and 60 bar H₂ at 80 °C for 1.5 h, followed by 140 °C for 1 h led to 60% conversion of the acetate complex to the formate analogous, along with the formation of ethanol from acetate hydrogenation and the production of methanol (TON = 5). Therefore, this complex functions as a molecularly defined precursor for the title reaction.

In addition, the acetate compound catalyses this transformation in the absence of any additive with a TON of 165 and addition of 0.5 equivalents of HNTf₂ did not improve this result. In contrast, [Ru(Triphos)(TMM)] did not show any activity under additive-free conditions. This is consistent with the formation of [Ru(H)(H₂)(S)(Triphos)]⁺ as catalytically active species and initial point for the calculated cycle.

Interestingly, further NMR studies suggested that [Ru(Triphos)(TMM)] in the presence of HNTf₂ (one equivalent) catalyses the hydrogenation of CO₂ even in the absence of ethanol in d₈-THF with a TON of 35 after 1 h at 140 °C. As described *vide supra*, the alcohol was added for stabilising the supposed intermediate formate/formic acid as an ester. Within an inner-sphere mechanism, however, this step is not occurring, which explains the catalytic activity in pure THF, yielding in methanol with a TON of 228 under optimised conditions. By reducing the catalyst loading from 25 μmol to 6.3 μmol, a TON of 442 was achieved. The dimeric compound [Ru₂(Triphos)(m-H)₂] was exposed as possible deactivation pathway. Its formation could be avoided by introducing sterically demanding methoxy-groups in the *para*-position of the ligand.

1. Introduction



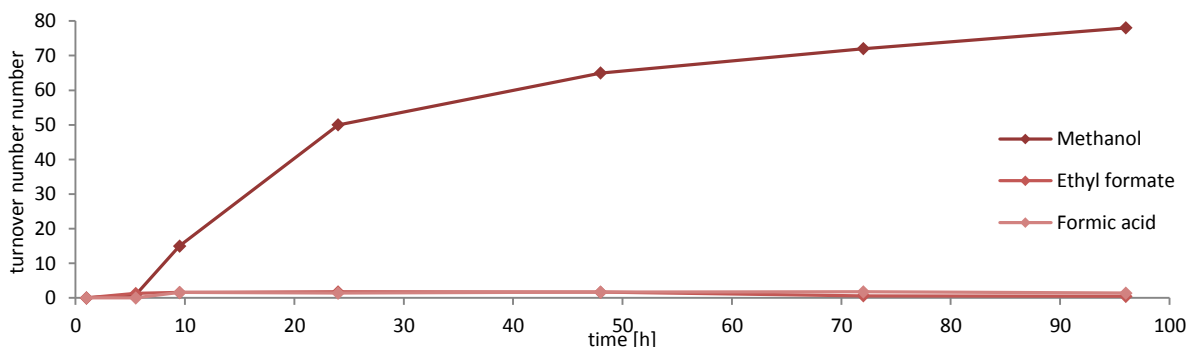
Scheme 8: Simplified catalytic cycle for the hydrogenation of carbon dioxide to methanol using the ruthenium-Triphos system reported by Klankermayer, Leitner and co-workers.^[93]

Furthermore, the authors investigated a possible aqueous biphasic recycling approach for their system. Therefore, the hydrogenation was carried out in 2-MTHF, as this organic solvent has a miscibility gap with water (*vide supra*). Using this solvent led to a slightly decreased TON of 186 after 24 h. For recycling, the hydrogenation was stopped after 16 h and the mixture was extracted with water. Fresh 2-MTHF was added to the catalyst containing organic fraction and the next run was started. By applying this methodology, a total TON of 769 was obtained after four runs.

In 2015, the group of de Bruin used a combination of $\text{Co}(\text{BF}_4)_2 \cdot 6\text{H}_2\text{O}$ and Triphos in the hydrogenation of carboxylic esters and acids to the corresponding alcohols in the absence of additives.^[94] This ground-breaking report in carboxylic acid hydrogenation chemistry led to the successful use of a similar cobalt-based system in the hydrogenation of carbon dioxide to methanol by the group of Beller, two years later.^[95] The use of the same cobalt precursor under additive-free conditions gave only low production of methanol (TON = 3). After screening of several metal salts/complexes and additives, the authors determined $[\text{Co}(\text{acac})_3]$ in combination with two equivalents of triphos and three equivalents of HNTf_2 as the optimised system. In a mixture of THF and ethanol (8:3) at 100 °C and 70 bar pressure, a methanol TON of 50 was determined after 24 h.

In order to shed some light on the system's mechanism, a concentration-time graph of methanol and the potential intermediated ethyl formate and formic acid was plotted. Scheme 9 indeed reveals the formation of those species; however, their concentrations are approximately constant. To determine, whether or not they constitute intermediates, separate hydrogenation experiments under optimised conditions were conducted. Ethyl formate and formic acid were hydrogenated in 66% and 59% yield, respectively, which are relatively low values. Consequently, an accumulation of those compounds would be expected within a stepwise mechanism. Obviously, however, this is not the case, as the concentration-time graph revealed. Therefore, in analogy to the ruthenium-system,^[93] an inner-sphere mechanism was suggested and the formation of formic acid and ethyl formate was attributed to minor reaction pathways.

1. Introduction



Scheme 9: Concentration-time graph of the homogeneous cobalt system for the hydrogenation of carbon dioxide, as reported by the group of Beller.^[95]

In addition, Scheme 9 revealed an induction period of 6-8 h. To elucidate this behaviour, high-pressure NMR and HR-ESI-MS studies were carried out. These investigations suggested $[\text{Co}(\text{Triphos})(\text{L})_n]^{m+}$ to be the catalytically active species. The formation of this cationic complex necessitates the stepwise cleavage of the acetylacetonate ligands, assisted by their protonation *via* the strong acid HNTf_2 . The intermediate species $[\text{Co}(\text{Triphos})(\text{acac})_2]^+$ and $[\text{Co}(\text{Triphos})(\text{acac})]^+$ have been observed by HR-ESI-MS. To further validate this theory, catalyst preformation studies have been conducted. A mixture of $[\text{Co}(\text{acac})_3]$, Triphos and HNTf_2 was heated in THF/EtOH for 2 h at 100 °C. Then, the gases were introduced and after 5.5 h a TON of 8 was detected for methanol. This TON was improved to 12 when 70 bar H_2 was used in the preformation step.

Notably, the group of Klankermayer reported a very similar system to be active in the hydrogenation of carbon dioxide to dimethoxymethane (DMM) in the same year.^[96] The combination of $\text{Co}(\text{BF}_4)_2 \cdot 6\text{H}_2\text{O}$, Triphos and HNTf_2 in a THF/methanol mixture gave a TON of 92 for this product after 22 h at 100 °C. In addition, the selective production of methanol was achieved by replacing methanol with 1,1,1,3,3,3-hexafluoro isopropanol (HFIP) in the solvent mixture. Notably, at just 80 °C a catalyst TON of 131 was found. Also the effect of modified triphos derivatives on the production of DMM was investigated, showing that electron donating methyl groups in *meta*- or *para*- position led to TONs of 120 and 157, respectively.

Apart from those closely-related ruthenium and cobalt triphos-based systems, only the iron-scorpionate complex of Pombeiro revealed activity in the direct hydrogenation of carbon dioxide in acetonitrile ($\text{TON}_{\text{max}} = 1453$, *vide supra*).^[91]

As described above, methanol can be converted to olefins *via* the MTO-process.^[31b] This class of compounds itself constitutes a central feedstock for the chemical industry and is used in a variety of transformations, e.g. hydrogenation to alkanes, hydroformylation to aldehydes and polymerisation to plastics.^[97] In the following, an overview of literature reported base-metal systems for the hydrogenation of olefins, as well as heterogeneous catalysts for their hydroformylation will be given.

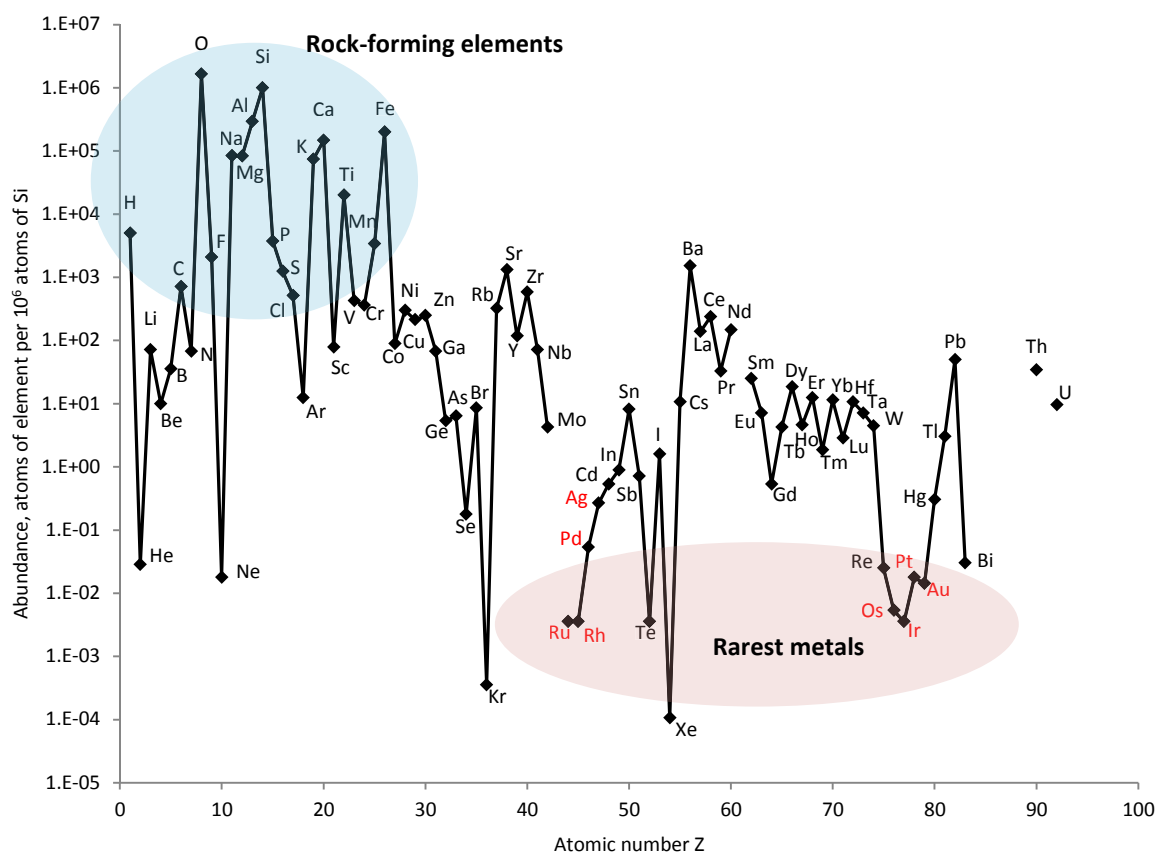
1.4. Hydrogenation and Hydroformylation of Olefins

1.4.1. Heterogeneous Olefin-Hydrogenation with Non-Noble Metal Catalysts

The reduction of olefins to saturated alkanes is of major industrial interest. For instance the hydrogenation of diisobutene to isooctane (2,4,4-trimethylpentane) attracted much attention lately, as this product is an anti-knock additive, which can replace MTBE.^[98] The latter is phased out in parts of the US since 2006, due to environmental concerns. In addition, the catalytic saturation of natural oils to hardened fat is the main process in the production of margarine and is conducted on million metric ton scales.^[99] Also in the pharmaceutical industry the hydrogenation of alkenes is of great

1. Introduction

importance.^[100] The vast majority of industrially applied catalysts are of heterogeneous nature. This is due to an easier separation of the materials compared to molecularly defined complexes. However, most of those methodologies used for the title reaction are based on noble metals, such as platinum and palladium on carbon.^[101] Not only are these elements expensive, but also scarcely available and accompanied by distinct price volatilities. This lack of availability is shown in Scheme 10, where the quantities of atoms of each naturally occurring element per 10^6 atoms of silicon in the earth's crust are plotted. It becomes obvious that a number of industrially used transition metals are among the rarest elements accessible (e.g. rhodium, iridium, palladium and platinum).



Scheme 10: Plot of the abundance of the naturally occurring elements in the earth's crust in atoms per 10^6 silicon atoms. Noble metals are highlighted in red. Data source: CRC Handbook of Chemistry and Physics, Internet Version.^[102]

A cheap and abundant alternative for catalytic hydrogenation reactions is Raney®-nickel, a highly active material, produced by leaching away aluminium from an aluminium-nickel-alloy. It is sold and stored as an aqueous suspension. Due to its high surface area it exhibits a strong reactivity; however, when it becomes too dry, it spontaneously inflames under aerobic conditions, which makes special handling mandatory. Also, the high reducing capability of Raney®-nickel, as well as those of platinum and palladium on carbon, might result in selectivity problems and other functional groups (e.g. nitro, aldehydes, nitriles, etc.) present in the proximity of the olefin might also be hydrogenated.

Due to those reasons, numerous groups worldwide are seeking for base-metal alternatives, either homo-,^[103] or heterogeneous, wherefore the following overview is not comprehensive and only selected recent and particularly interesting reports will be highlighted. For instance, the group of Wenbin Lin reported a range of different metal-organic frameworks (MOFs) for hydrogenation reactions.^[104] In 2014, the zirconium-based MOF with salicylaldimine-derived dicarboxylate bridges was reported to be active in olefin hydrogenations upon post-synthetic metalation with Fe(II) or Co(II)

1. Introduction

(Figure 3).^[105] Once the bridging ligands have been synthesised by multi-step procedures, the frameworks were obtained in the presence of $ZrCl_4$ and metalation occurred by a simple impregnation method. The obtained cobalt- and iron-based MOFs sal-Co-MOF and sal-Fe-MOF were highly active in the title reaction in the presence of $NaBEt_3H$ at room temperature under 40 atm H_2 . The cobalt-based MOF gave TONs up to 25,000 after 18 h (1-octene). Even though iron was generally less active than cobalt, 1-octene was hydrogenated to 1-octane with a TON of 145,000 after eight days. Besides of a small substrate scope, the recyclability of sal-Fe-MOF was investigated. It revealed a constant productivity for nine consecutive runs, after which the yield decreased drastically. The catalyst was regenerated successfully by treating it with $NaBEt_3H$, however, the reaction times had to be increased from 7 to 8 hours.

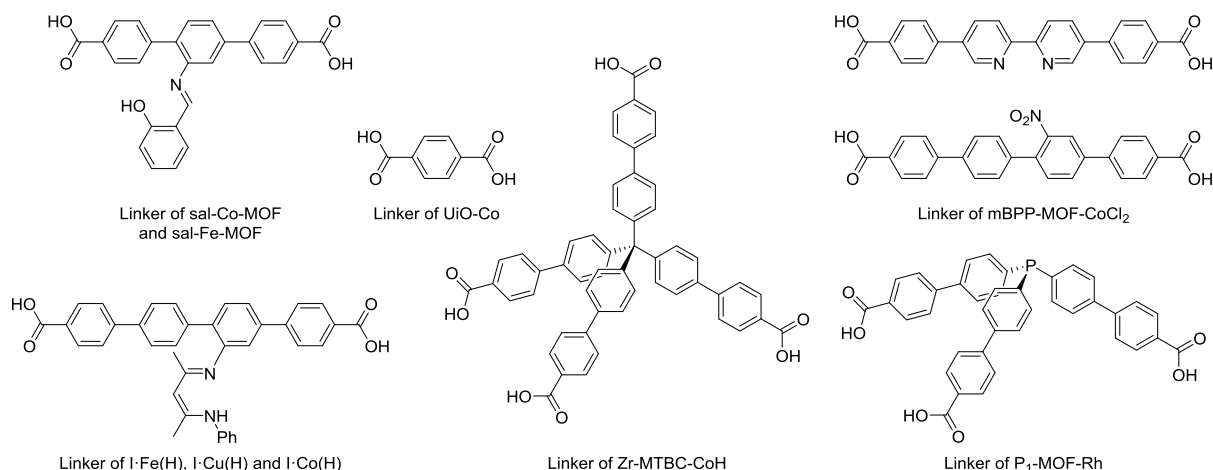


Figure 3: Linker of the MOFs developed by the group of Wenbin Lin for hydrogenation reactions.

Notably, even after 72 hours allyl acetate was not hydrogenated by sal-Co-MOF. Two years later the same group reported another cobalt-based MOF, which was capable of reducing this and also more challenging substrates.^[106] By using the tetrahedral linker methane-tetrakis (*p*-biphenylcarboxylate) (MTBC) in combination with zirconium resulted in the identification of Zr-MTBC-CoCl, which became highly active upon activation with $NaBEt_3H$ yielding in Zr-MTBC-CoH (Figure 3). A range of olefins was hydrogenated towards the corresponding alkane with TONs up to 8000 at 40 bar H_2 and in the presence of $NaBEt_3H$ at 23 °C. Even the tetrasubstituted olefins 2,3-dimethyl-2-butene and 2,3,4-trimethyl-2-pentene have been appropriate substrates, albeit prolonged reaction times (two days) and increased metal loadings were needed. Apart from olefins also imines, carbonyls and heterocycles can be hydrogenated with this catalyst, which might result in selectivity problems. The recyclability was investigated with 1-methylcyclohexene within six runs, during which the yield remained constant.

In the same year, the group reported the UiO-68^[107] based UiO-Co MOF to be active in olefin hydrogenations and C-H activations (borylation and silylation, Figure 3).^[108] In the saturation of 1-octene, a maximum TON of 3,540,000 has been obtained after 66 h. At an increased loading, the transformation was completed after 30 min. Also internal olefins were hydrogenated, albeit long reaction times of up to 72 h were necessary. UiO-Co has the advantage that the linker terephthalic acid is commercially available, which simplifies the synthetic protocol significantly. Also in 2016, the phosphine containing rhodium-metalated MOF P₁-MOF-Rh was reported by the group of Wenbin Lin (Figure 3). Under additive-free conditions, this catalyst was active in the hydrogenation of olefins at loadings as low as $5 \cdot 10^{-4}$ mol%. After 40 hours at room temperature, all investigated substrates were reduced; however, tri- and tetrasubstituted olefins necessitated increased loadings of up to 0.1 mol%.^[109] Notably, comparative reactions with Wilkinson's catalyst $[RhCl(PPh_3)_3]$ revealed no activity under the applied conditions. Alternatively to the phosphine-containing P₁-MOF-Rh, the group

1. Introduction

demonstrated the incorporation of β -diketiminate ligands, better known as NacNac.^[110] The framework was metalated with iron, cobalt or copper, respectively. Subsequently, the catalytic activity of the iron-containing MOF I-Fe(Me) (Figure 3) was demonstrated in the intramolecular C-H amination of terminal azides to give oxazolines. Besides, the copper-based I-Cu(THF) was tested in the amination of cyclohexene with anilines. By using the cobalt-containing I-Co(H), a small selection of terminal and internal olefins were hydrogenated at the same conditions as for the previous systems (40 bar H₂, room temperature, THF). Also, it was used in the hydrogenation of 1-octene for ten consecutive runs, revealing a constant, quantitative yield of n-octane. Finally, a series of MOFs constructed from bipy- and phen-based linkers (phen = 1,10-phenanthroline) were tested for the hydrogenation of olefins.^[111] All four MOFs reported were active in this catalytic transformation. The highest TON of 2,500,000 was reported for the reduction of 1-octene with the novel mBPP-MOF-Co (Figure 3), which is built from the functionalized linker 4,4'-(2,2'-bipyridyl-5,5'-diyl)-dibenzoic acid in combination with the spectating linker 4,4'-bis(carboxyphenyl)-2-nitro-1,1'-biphenyl. Also more challenging substrates have been successfully transformed to the corresponding alkanes using this particular MOF, although with lower TONs.

The group of P. C. Stair reported a catechol-containing porous organic polymer as a support for three-coordinate aluminium sites in 2017.^[112] The polymer was obtained *via* a cobalt-catalysed acetylene trimerization strategy, using a planar diyne and a tetrahedral tetrayne.^[113] Subsequently, the polymer was metalated with either Al^tBu₃ or Al(CH₃)₃. The hydrogenation activity was rather limited; while 1-octene was quantitatively hydrogenated at 75 °C and 14 bar H₂, only 62% of 3,3-dimethyl-1-butene and 10% of the internal 2,3-dimethyl-2-butene were saturated.

Clearly, the use of MOFs or polymers offers interesting possibilities for catalytic applications, however, their syntheses are rather complex, the materials often have to be stored under inert atmosphere, and most of the above mentioned systems necessitate the addition of a strong reducing agent. In this context, the group of J. G. de Vries reported soluble iron NPs as cheap and non-toxic catalysts for the hydrogenation of alkenes and alkynes.^[114] Notably, the synthesis is straightforward and comprises the reduction of FeCl₃ with an excess of commercially available EtMgCl. This methodology provides NPs in the range of 1.5 nm to 4.5 nm with the average size of 2.67 nm. Applying 1 bar H₂ at room temperature yielded in quantitative hydrogenation of norbornene after just 30 min (5 mol% iron). At 20 bar H₂, also other terminal, *cis*-1,2- and 1,1-disubstituted substrates were hydrogenated after 15 h. At an elevated temperature of 100 °C, also cyclic and *trans*-disubstituted olefins were hydrogenated completely. Also the group of J. von Wangelin contributed to this field. In 2017, soluble iron nanostructured catalysts were synthesised with a different methodology and demonstrated to be highly active in olefin and alkyne hydrogenations.^[115] Reduction of Fe(hmnds)₂ (hmnds = hexamethyldisilazane, N(SiMe₃)₂) with DIBAL-H (di-*iso*-butylaluminium hydride) affords planar Fe₄, Fe₆ and Fe₇ nanoclusters with bridging hmnds-ligands in the clusters' peripheries. The latter generate a lipophilic character, resulting in good solubility under the non-polar conditions applied for alkene hydrogenation. Alternatively to the use of Fe(hmnds)₂, the catalyst can also be generated *in-situ* by combining FeCl₂, H-hmnds and *n*-BuLi (normal butyl lithium). At 20 °C and pressures as low as 1 bar excellent yields for a variety of mono-, 1,1 and 1,2 di-, tri- and tetrasubstituted olefins, as well as internal alkynes were obtained. In 2012, the group of A. Moores described the preparation and catalytic application of iron NPs with core-shell morphology.^[116] By reducing FeSO₄ with NaBH₄, a metallic iron core wrapped with an iron-oxide shell was formed. This material was active in the hydrogenation of a small selection of olefins at 80 °C and 40 bars of hydrogen. Furthermore, the group of B. Breit reported ferromagnetic iron NPs supported on graphene as hydrogenation catalyst.^[117] Applying 100 °C and 20 bar H₂ for 24 h resulted in the hydrogenation of uncomplicated olefins to the corresponding alkanes, e.g. styrene, norbornene and 1-octene.

1. Introduction

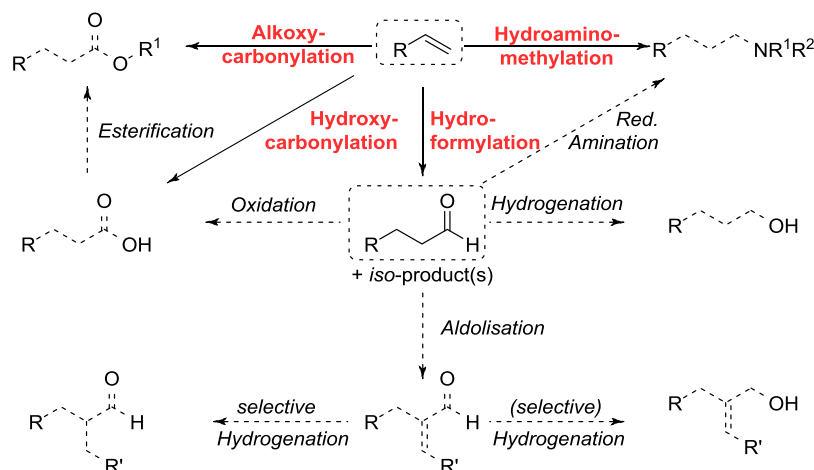
In 2018, the group of von Wangelin expanded the previous iron-based system to cobalt NPs. First, the reduction of CoBr_2 with LiBEt_3H in the presence of olefins yielded in the formation of magnetic, alkene-stabilised NPs.^[118] This catalytic material was highly active in the saturation of a variety of unsaturated carbon-carbon bonds, including the natural products α -pinene and myrcene. In addition to olefins, also carbonyls, imines and quinolines were reduced. Furthermore, an active material was obtained by reducing CoCl_2 with lithium naphthalide in THF.^[119] At pressures between 2 bar to 20 bar and temperatures of 20 °C to 80 °C, a broad scope of olefins, alkynes, imines and quinolines were reduced. Consequently, even at very mild conditions a low functional group tolerance was observed. For this investigation, functional group bearing additives were added to the hydrogenation reaction of α -methyl styrene. Only alcohols, esters, aniline, fluorides and diaryl ethers were tolerated. All the other tested functionalities decreased the yield significantly. Remarkably, the NPs revealed high storage stability over a time-period of up to 35 weeks, and recycling studies revealed a constant yield during ten runs.

In the last years, the selective hydrogenation of α,β -unsaturated compounds using non-noble metal systems got in the focus of research. For instance, Domingos, Philippot *et al.* investigated the performance of nickel NPs in the hydrogenation of this type of substrates.^[120] $\text{Ni}(\text{COD})_2$ (COD = 1,5-cyclooctadiene) was treated with octanoic acid as a stabiliser under hydrogen atmosphere at 70 °C, yielding in a nanosized material, which was subsequently supported on SiO_2 *via* impregnation. The average size of the particles was 5.4 nm and they showed to be active in the hydrogenation of styrene and cyclic substrates, as well as α,β -unsaturated cinnamic acid derivatives including ketones, aldehydes and carboxylic acids and esters with selectivities above 99%. Recyclability was demonstrated in 10 runs during which the product yield dropped slightly. Very recently, the group of Yong Yang reported the synthesis of cobalt NPs in combination with biomass-derived bamboo shoots.^[121] The finely grounded shoots were treated hydrothermally, impregnated with CoCl_2 and then heated at temperatures between 700 °C and 900 °C for two hours. $\text{CoO}_x@\text{NC-800}$ was the most active material in the hydrogenation of chalcone at 20 bar H_2 and 110 °C in water and in the presence of tetrabutyl ammonium iodide. A broad scope of substrates was selectively hydrogenated, revealing a broad functional group tolerance. Notably, some natural/bioactive compounds could be obtained by this procedure, including testosterone and menthone. Interestingly, the material also catalysed the formation of α,β -saturated ketones from aldehydes and ketones with yields up to 93%. Also in 2019, the group of J. G. de Vries documented the use of a molecularly defined cobalt complex ligated by a tridentate NNS ligand for the hydrogenation of α,β -unsaturated compounds in the presence of NaBH_4 and 50 bar H_2 .^[122] Poisoning experiments with PMe_3 (0.15 eq with respect to catalyst) resulted in a complete deactivation of the system, which strongly indicates a heterogeneous nature of the catalyst.

1.4.2. Heterogeneous Hydroformylation

Olefins constitute the feedstock for the most important homogeneously catalysed transformation in industry to date – the hydroformylation.^[123] It comprises the 100% atomically economic addition of one equivalent of H_2 and CO to the $\text{C}=\text{C}$ double bond, resulting in the formation of aldehydes, which subsequently can be further transformed to alcohols, carboxylic acids, esters, and beyond (Scheme 11). Except for ethylene, also the branched Markovnikov product and those stemming from prior isomerisation of the olefin are possible, besides of the linear anti-Markovnikov product.^[124] The hydroformylation was coincidentally discovered by Otto Roehlen, who called it “oxo-process”, in 1938. Whereas cobalt-species were used as catalyst originally, today about 80% of all hydroformylation processes make use of more active rhodium complexes. Clearly, rhodium is among the most precious metals (compare Scheme 10), which makes its recycling mandatory. In fact, a loss of several million euros was estimated by Wiese and Obst for a 400 kt plant, when just 1 ppm rhodium per kilogram of oxo-product is not recycled.^[125]

1. Introduction



Scheme 11: Schematic overview of carbonylative transformations of olefins, as well as further reactions of the obtained products.

Therefore, research groups all over the globe are pressing on finding alternatives to homogeneously Rh-catalysed hydroformylation. For instance, alternative and “cheaper” metals have been investigated, e.g. iridium, ruthenium, palladium, platinum, and even iron.^[126] The generally accepted order of activity of the different metals in the title reaction is $\text{Rh} \gg \text{Co} > \text{Ir}, \text{Ru} > \text{Os} > \text{Pt} > \text{Pd} \gg \text{Fe} > \text{Ni}$. Unfortunately, the more abundant metals iron and nickel are among the least active ones for this transformation. Another approach towards more sustainable processes is the use of heterogeneous catalysts, which potentially allow for an easier recycling of the precious metal. However, a general problem is the catalyst deactivation by leaching of metal from the material’s surface as metal carbonyl species.

1.4.2.1. Immobilisation-Strategies

One methodology for producing heterogeneous catalysts is the immobilisation of known homogeneous systems.^[127] For instance, Peter Wasserscheid and his group pioneered the field of supported ionic liquid phase materials.^[128] This type of immobilised catalytic species was especially tested in hydroformylation and related reactions. In fact, approximately 70% of the reported systems based on either SLPs (supported liquid phases), SAPs (supported aqueous phases), or SILPs (supported ionic liquid phases) deal with this transformation.^[129] In general, those supported liquid phases are generated by dissolution of a homogeneous catalyst in a non-volatile liquid, followed by dispersing on a porous support with a high surface area.^[130] The application of a material of such nature in the gas-phase hydroformylation of propene in continuous mode was reported in 2003.^[131] A rhodium complex with the hydrophilic ligand sulfoxantphos was immobilised with the ionic liquids [BMIM][PF₆] (1-*n*-butyl-3-methylimidazolium hexafluorophosphate) and [BMIM][*n*-C₈H₁₇OSO₃] (1-*n*-butyl-3-methylimidazolium *n*-octylsulfate) on silica (Figure 4, left). By using the former SILP and a ten-fold excess of ligand with respect to metal, a TOF of 37 could be achieved at a high *n*:*iso* ratio of up to 96% within 3-4 h. The halide-free IL led to slightly lower, but still comparable TONs. A strong influence of the ligand/rhodium ratios and pore-filling degrees of the support on the catalytic activities was noticed. In addition, for prolonged reaction times (>24 h) a decrease of both selectivity and activity was observed under all investigated conditions. Later it was demonstrated that pre-treatment of the silica support is beneficial for a long-term stability in [BMIM][*n*-C₈H₁₇OSO₃].^[132] A partially dehydroxylation was achieved by heating the silica at 500 °C for 15 h in the air. In combination with a high ligand to metal ratio of 10, the system retained its initial performance for at least 60 h. The improved stability was ascribed to the irreversible reaction of acidic silanol-groups on the support’s surface with the ligand, wherefore an excess of ligand has to be used to compensate this deactivation. In the following, the stability was demonstrated over a time-period of 200 h.^[133] The support was

1. Introduction

therefore calcined at 450 °C for 24 h before it was loaded with the catalyst containing IL. While the selectivity remained constant, a slight drop of activity was observed during time, as high boiling side products accumulated in the IL. The initial productivity could be regenerated by a simple vacuum-procedure over ten minutes.

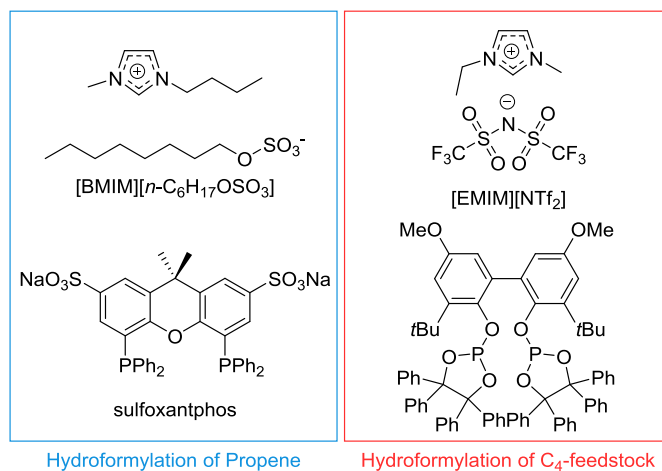


Figure 4: Ligands and ILs for hydroformylation reactions as reported by Wasserscheid and co-workers.^[131, 134]

Besides of propene, also C₄ feedstocks have been investigated. Here, the use of a bulky diphosphate ligand with rhodium and [EMIM][NTf₂] (1-ethyl-3-methylimidazolium bis(trifluoromethanesulfonyl)imide) allowed for selective production of *n*-pentanal from an industrial mixture containing isobutene (43%), 1-butene (26%), *trans*-2-butene (9%), *cis*-2-butene (7%), butanes (15%) and 1,3-butadiene (0.3%) (Figure 4, right).^[134] Clearly, in order to obtain high selectivity the hydroformylation of isobutene had to be omitted and internal butenes had to be isomerised towards terminal ones prior to further transformation. In fact, the system was able to convert the substrate with a rate of 25% and an almost quantitative selectivity for more than 800 h. The TOF was 410 h⁻¹ in average and an accumulated TON of 350,000 were achieved. For this long-term stability a dried olefin feedstock had to be used, as phosphites tend to hydrolyse. Furthermore, the acid scavenger BTPS (Bis(2,2,6,6-tetramethyl-4-piperidyl)sebacate) was added in order to neutralise any phosphoric acid formed by ligand decomposition.

Besides SILP-methodologies, the anchoring of homogeneous rhodium species on polymers was investigated for the title reaction.^[135] In 2015, the group of F.-S. Xiao reported the synthesis of novel rhodium-loaded porous organic ligands (POLs) and demonstrated their high potential in the hydroformylation of 1-octene and 1-dodecene in liquid phase.^[136] The POLs were prepared from the monomers tetravinyl-dppe (dppe = 1,2-bis(diphenylphosphino)ethane), -dppm (dppm = 1,2-bis(diphenylphosphino)methane) and -dppbz (dppbz = 1,2-bis(diphenylphosphino)benzene) *via* free-radical polymerisation yielding in the homo-polymers (Figure 5). Stirring of the white to yellowish solids in toluene led to their swelling, during which the volume was significantly enlarged. Very high BET (Brunauer-Emmett-Teller) surface areas between 846 and 959 m²/g and pore volumes of 0.81 – 1.15 cm³/g have been measured. Therefore, the phosphines are accessible for organometallic complexes, such as [Rh(CO)₂(acac)]. Rh/POL-dppe was highly active in the hydroformylation of 1-octene (96.9% conversion, 99.3% selectivity towards aldehydes, 2.46 *n/iso*) and 1-dodecene (95.5%, 96.2%, 2.45) at a substrate to catalyst ratio of 2000, 90 °C and 20 bar syngas (1:1) for 2.5 h to 3.0 h. The productivity of this material was compared to unmodified and dppe-ligated [Rh(CO)₂(acac)], revealing superior conversion and selectivity of the Rh/POL-dppe. In addition, the reusability of the immobilized catalyst was demonstrated in the hydroformylation of styrene for six runs, during which both the conversion and selectivity remained constant. Furthermore, no rhodium could be detected in

1. Introduction

the solution *via* ICP-OES (inductively coupled plasma – optical emission spectroscopy), which has a detection limit of 10 parts per billion (ppb). A later study of the same group investigated the trivinyl-PPh₃ comprising polymer Rh/POL-PPh₃.^[137] An enhancement of the catalytic activity, selectivity and stability in the hydroformylation of styrene was observed, when the concentration of PPh₃ in the POL was increased.

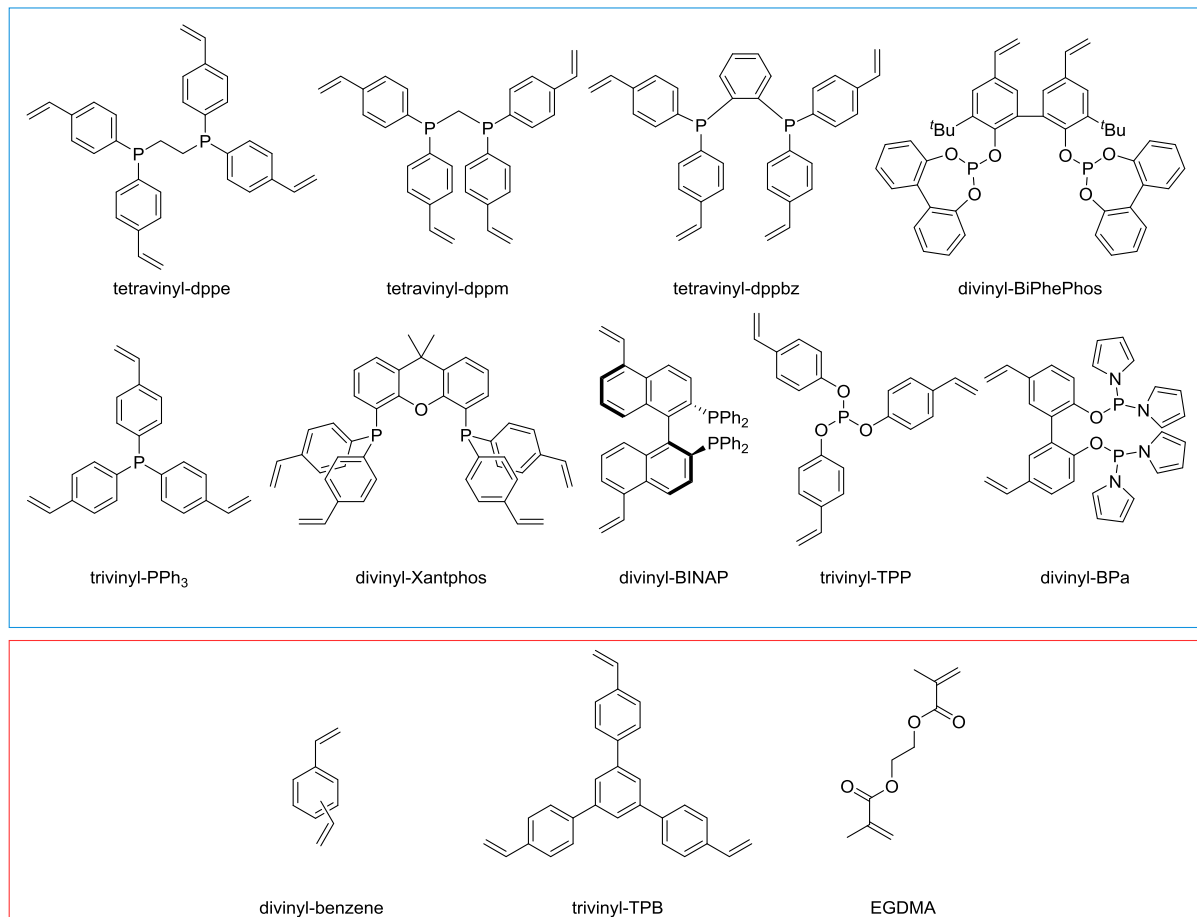


Figure 5: Vinyl-substituted monomers and organic co-monomers for the formation of POLs as reported in the literature.

Also, the group of Y. Ding contributed to this approach. In 2016, co-polymers between divinyl-BiPhePhos and the monomers divinyl-benzene, tetravinyl-dppe, and trivinyl-PPh₃, respectively, were synthesised in different ratios and loaded with rhodium.^[138] BET surface areas of up to 1589 m²/g and pore volumes of 3.82 cm³/g were measured. After promising initial batch-wise hydroformylation of 1-octene in liquid-phase,^[139] the rhodium-loaded POLs were tested in the transformation of propene to butanal in a fixed-bed reactor at 50 bar (propene:CO:H₂ = 1:1:1) and 70 °C for 12 h. The co-polymer with 23 equivalents of trivinyl-PPh₃ and a metal loading of 0.13 wt% was by far the most active POL system with a TOF of 1209 h⁻¹, a selectivity of 93% and an *n/iso* ratio of 24.2. By increasing the amount of BiPhePhos in the polymer, a TOF of 1500 h⁻¹ was achieved. With the former catalytic system, long-time studies were conducted with an industrially relevant time on stream of 1000 h. During the first 200 h, the TOF decreased from 2000 to 800 h⁻¹. However, during the following 800 h it remained constant, as well as the *n/iso* ratio, which is indeed remarkable. HAADF-STEM (high-angle annular dark-field imaging – scanning transmission electron microscopy) revealed rhodium to be dispersed as single atoms both in the fresh and in the used material. In a following study, divinyl-Xantphos was synthesised for the first time, and co-polymers of it with the co-monomers divinyl-benzene, trivinyl-PPh₃, or trivinyl-TPB (trivinyl-triphenylbenzene), respectively, were produced.^[140] After loading of the POLs with rhodium, they were investigated in the hydroformylation of 1-octene.

1. Introduction

The co-polymer with trivinyl-PPh₃ gave the highest conversion of 42% (TOF up to 500 h⁻¹) after 5 h at 100 °C and 10 bar syngas (1:1). Aldehydes were formed with a selectivity of 87% and an *n/iso* ratio of 90:10, which was superior to the other co-polymers. After successful recycling of the catalyst for five runs, the hydroformylation of 1-octene was conducted in a fixed-bed reactor over 400 h. Notably, the catalyst's activity and selectivity remained constant during this period.

Afterwards, the asymmetric hydroformylation to styrene was investigated with BINAP-based POLs.^[141] The combination of divinyl-BINAP with divinyl-benzene, TPB, or ethylene glycol dimethacrylate (EGDMA), respectively, yielded in three POL-systems, which were subsequently loaded with rhodium, again. The highest enantiomeric excesses (*ee*) of up to 58.9% for the *iso*-product were achieved with the commercially available divinyl-benzene as co-monomer at 2 bar syngas (1:1). Interestingly, the homogeneous equivalent of the rhodium BINAP-POL gave an *ee* of just 35.3%. In earlier studies, *ee* of up to 59% have been obtained with BINAP-stabilised rhodium NPs.^[142] In addition, Clark R. Landis reported *ee* values of up to 91% for styrene by applying immobilised bisdiazaphospholanes.^[143] The POL-immobilised catalyst was also used in seven consecutive runs, during which the yield and *ee*-values oscillated between 40% and 60%, while the *n/iso*-ratio dropped slightly. Besides, also the regioselective hydroformylation of 1- and 2-butene to pentanal was investigated by the same group.^[144] A co-polymer consisting of divinyl-BiPhePhos and trivinyl-PPh₃ showed good activity in the conversion of 1-butene with a TOF of 9020 h⁻¹ and a selectivity of pentanals of 93.6% (*n/iso* = 58.6). The transformation of 2-butene was decelerated with a TOF of 301 and the main-product was butane. A C₄ mixture with 60% 1-butene and 20% of *trans*- and *cis*-butene each, was converted selectively to pentanal (TOF = 3674). For 1-butene, also long-time studies were conducted. During 300 h, the catalyst remained active and selective; however, the TOF decreased slowly during this time period. Also the co-polymer of divinyl-BiPhePhos and trivinyl-TPP (triphenylphosphite) showed activity (TOF up to 4957 h⁻¹, *n/iso* up to 40) and stability (100 h time on stream) in the conversion of 1-butene.^[145] Very recently, Xiaofei Jia *et al.* reported the development of the divinyl-functionalised bisphosphoramidite divinyl-BPa.^[146] A rhodium-loaded co-polymer consisting of this novel monomer and trivinyl-PPh₃ gave TONs up to 453,000 in the hydroformylation of 1-hexene, and a *n/iso* ratio of up to 52.8 at 90 °C and 20 bar syngas (1:1). Notably, the material was recycled nine times, revealing its high stability. Both conversion and selectivity remained constant during this procedure. The hydroformylation of 1-octene and 2-octene showcased that also internal olefins can be transformed to the corresponding linear aldehyde, albeit to a lesser extent.

A different approach towards the immobilisation of homogeneous catalysts for hydroformylations was reported by Garcia-Suarez, Godard and co-workers.^[147] A C₁-symmetrical furanose-based diphosphate ligand in combination with rhodium was observed to be active in the homogeneous, asymmetric hydroformylation of norbornene with *ee* values up to 71% with respect to the *exo*-norbornanecarboxaldehyde. Inspired by those results, the ligands were modified with the polycyclic aromatic hydrocarbon pyrene and the corresponding rhodium complexes immobilised onto multi-walled carbon nanotubes, reduced graphene oxide, and carbon beads, respectively. Although recycling of the materials after batch-reactions was not feasible due to metal leaching, under continuous operation in flow mode even higher *ee* values than for the homogeneous catalyst were observed, along with a good stability of the catalysts.

1.4.2.2. Heterogeneous Materials

Apart from immobilisation approaches, also materials consisting of metals supported on inorganic supports have been of interest for the title reaction. In this context, particularly single-atom catalysts (SACs) attracted attention, as mononuclear species are believed to be the active sites in the title reaction.^[148] For instance, Rui Lang *et al.* reported single-atomic rhodium supported on ZnO-

1. Introduction

nanowires with activities comparable to homogeneous Wilkinson's catalyst $[\text{RhCl}(\text{PPh}_3)_3]$ in 2016.^[149] The straightforward synthesis of this material comprises the impregnation of the support with RhCl_3 , followed by ageing and reduction under 20 vol% H_2/He at 450 °C for 30 min. Metal loadings of 0.3%, 0.03% and 0.006%, respectively, were adjusted and the catalysts tested in the hydroformylation of styrene. At 100 °C and 16 bar syngas (1:1), TONs of 7,000 (0.3% Rh), 38,000 (0.03% Rh), and 40,000 (0.006% Rh) were achieved after 12 h with selectivities of 99% for each catalyst. Compared to those results, Wilkinson's catalyst was comparably active (TON = 19,000) and selective (92%). Also other substrates such as α -methylstyrene, 1-octene and propene were hydroformylated with the material containing 0.006% Rh. Also, the catalyst was used in five consecutive runs, throughout which the TON pended from 35,000-40,000 at a constant, almost quantitative selectivity. In the same year, Liangbing Wang, Wenbo Zhang *et al.* reported single rhodium atoms dispersed on cobalt oxide to be highly active in the hydroformylation of propene.^[150] CoO nanosheets were treated with $\text{Na}_3[\text{RhCl}_6]$, which resulted in the replacement of single cobalt atoms with rhodium atoms. With a rhodium-loading of 0.2%, TOFs reached 2065 h^{-1} , which was decreased at higher loadings of 1.0% and 4.8%. Higher metal contents led to the formation of aggregated clusters rather than single atoms. Also, the lowest loading resulted in the highest selectivity of 94.4% for butanal, whereas rhodium NPs gave the *iso*-product to a bigger extend. The most active material was tested in five consecutive runs, maintaining the productivity and selectivity.

Rupflin *et al.* documented a synthetic procedure for the formation of highly crystalline Rh_2P NPs on silica and demonstrated their application as single-site catalysts in ethylene and propylene hydroformylation.^[151] Different materials were prepared by incipient wetness impregnation of SiO_2 with $\text{Rh}(\text{NO}_3)_3$ and phosphoric acid, followed by reduction under hydrogen at varying temperatures between 250 °C and 900 °C. Increased temperatures favoured the formation of NPs, along with an increase of the particle diameters, as was indicated by the diffraction patterns. At 900 °C, the NPs consisting of Rh_2P possessed a high crystallinity, which was shown to be important in order to obtain active, selective and stable catalysts. The material was active in the hydroformylation of ethylene with selectivity toward propionaldehyde of up to 80%. Interestingly, the addition of water led to a complete suppression of ethylene hydrogenation at temperatures below 200 °C. An explanation for this finding might be a selective blocking of reaction sites responsible for hydrogenation by water. Also an accelerated product desorption due to water is possible. In addition it was found that high CO partial pressures are beneficial with respect to selectivity.

Besides of rhodium, Tokunaga and co-workers investigated heterogeneous gold-catalysts for olefin-hydroformylation reactions.^[152] Gold was co-precipitated with cobalt oxide to give $\text{Au}/\text{Co}_3\text{O}_4$. At 130 °C and 40 bar syngas (1:1), 99.5% of 1-hexene has been converted with selectivity toward the aldehyde of 83.9% within 5.5 h. During four consecutive runs, however, the conversion dropped to 60%. In addition, Yunjie Ding reported cobalt supported on carbon for the unusual hydroformylation of ethylene to 3-pentanone and propanal.^[153] The material was obtained by an impregnation method, starting from different cobalt precursors and activated carbon. Notably, the highest selectivity toward the ketone was achieved by starting from either cobalt(II) acetate or nitrate (32.6% and 34.5%, respectively). When the nitrate-derived catalyst was loaded with 0.9 wt% potassium, the conversion of ethylene was increased from 13.8% to 28.5% and the selectivities toward propanal and 3-pentanone changed from 59.9% and 34.5% to 58.3% and 40.2%, respectively. The use of ultrafine cobalt NPs in the hydroformylation of 1-hexene was reported by Yuan Kou and co-workers in 2010.^[154] Particles with an average diameter of just 2.8 nm were produced by a reduction method, starting from cobalt(II) acetate tetrahydrate and sodium borohydride in the presence of the stabilizer PVP (polyvinylpyrrolidone). Afterwards, the precursory NPs were treated with 1-hexene and toluene under 20 bar syngas (1:1) at 100 °C for up to 3 h. The ultrafine particles were obtained by subsequent

1. Introduction

centrifugation. By applying this method, the catalytic activity was increased from a TOF of 121 for the precursory particles up to 149 for the ultrafine ones. Also the selectivity toward aldehydes was improved from 38% to 66%. Poisoning studies with mercury indicated the heterogeneous nature of the system; however, the amount of potentially leached cobalt was not determined.

2. Objectives of this Work

2. Objectives of this Work

The depletion of fossil fuels necessitates the development of alternative technologies and feedstocks in order to maintain today's standards of living. Another major current problem is the storage of electric energy. In this context, methanol may contribute to the solution of both issues. Water can be electrolysed to oxygen and hydrogen by applying (renewable) electricity. The H₂ molecule has a high gravimetric, but a very low volumetric energy density, which makes its compression mandatory. However, it can also be used to hydrogenate the greenhouse gas carbon dioxide to methanol, which can be further converted to a broad scope of base chemicals and therefore constitutes a promising alternative to fossil fuels. This concept is known as "*Methanol Economy*".

One of the objectives of this work was the homogeneously catalysed synthesis of methanol starting from carbon dioxide and hydrogen. This underdeveloped field of research is highly promising for delocalised applications, owing to the relatively mild operating conditions for those systems. A previously published cobalt-based system should be further investigated and optimised to achieve higher TONs. To fulfil the objective it was planned to determine possible deactivation pathways of the system *via* poisoning studies. In addition, the hydrogenation of carbon-dioxide derived organic carbonates should be tested with this cobalt-based system and, if needed, different conditions screened to obtain good activities.

A second objective of this work was the development of heterogeneous base-metal catalysts for the sustainable hydrogenation and hydroformylation of olefins. Both processes are highly important in industry and nowadays catalysed mainly with noble metal complexes (e.g. palladium, platinum, rhodium). In addition, hydroformylation is based on homogeneous catalysts, which makes recycling of the precious metal complicated. Therefore, cobalt-based materials should be synthesised, characterised and tested for the two reactions. Especially the usage of natural products, such as biopolymers, amino acids and nucleobases should be in the focus. In case of the olefin hydrogenation, industrially processes such as fat-hardening should be tested with the newly developed systems. Importantly, the recyclability of those active materials should be showcased by reusing the same sample of catalyst in several consecutive runs. Eventually, the loss of metal during the catalytic reactions should be determined by AAS.

3. Summary

3.1. Hydrogenation of Olefins Using a Biowaste-Derived Cobalt Catalyst

The first reaction of interest was the hydrogenation of olefins using molecular hydrogen. Whereas most industrial processes for this transformation are based either on supported noble metals or pyrophoric Raney-nickel, we sought for a sustainable, low-cost and easy to prepare catalyst. After screening of a variety of cobalt-based materials, Co/Chitosan-700 was found to be highly active and selective in the olefin reduction to alkanes. The catalyst was prepared by simple impregnation of chitosan with $\text{Co}(\text{OAc})_2 \cdot 4\text{H}_2\text{O}$ (OAc: acetate) in a metal to ligand ratio of 1:2, followed by pyrolysis at 700 °C under a flow of argon for 2 h. Chitosan is derived by deacetylation of chitin, which itself is the second most abundant biopolymer, just topped by cellulose, and mainly obtained from crab-shell waste.^[155]

Initial solvent screening for the hydrogenation of the model substrate 1-octene at 40 °C and 10 bar H_2 exposed heptane (Table 1, entries 1 and 2), methanol (entries 5 and 6) and water (entries 13 and 14) as suitable reaction media, as well as 1:1 mixtures of water and heptane or methanol, respectively (entries 9-12). In addition, solvent-free (neat) conditions (entries 15 and 16) gave full conversion and yield already after 6 h. Propylene carbonate (PC, entry 3), acetonitrile (MeCN, entry 4) and tetrahydrofuran (THF, entry 7) were found to decrease the activity of Co@Chitosan-700, probably due to adsorption on the catalyst's surface which competes with the olefin. By plotting the conversions and yields over time, induction periods for water, methanol and neat conditions became obvious (Scheme 12). Even though the catalyst has its highest activity in the absence of any solvent (at least for 1-octene as a substrate), also in the case of both investigated solvents full conversion could be observed in less than 5 h. Notably, metal leaching from the catalyst into solution was negligible for all suitable solvents. The values determined *via* atomic absorption spectroscopy (AAS) were dependent from the reaction medium and did not exceed 0.31 ppm.

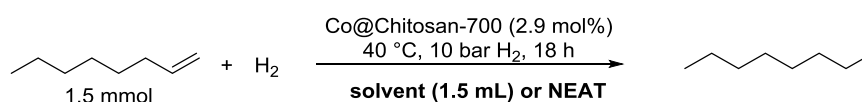
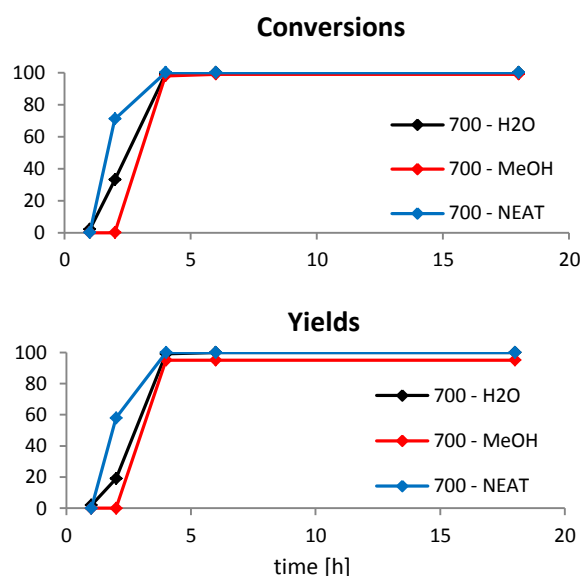


Table 1: Solvent-screening for the olefin hydrogenation with Co@Chitosan-700.

| Entry | Solvent | Conv. [%] ^a | Yield [%] ^a | AAS [ppm] |
|-----------------|--------------------------------|------------------------|------------------------|-----------|
| 1 | Heptane | 98 | 88 | <0.04 |
| 2 ^b | Heptane | 58 | 53 | |
| 3 | PC | 45 | 35 | |
| 4 | MeCN | 10 | 1 | |
| 5 | MeOH | 99 | 95 | 0.31 |
| 6 ^b | MeOH | 99 | 95 | |
| 7 | THF | 13 | 13 | |
| 8 | H ₂ O/PEG (1:1) | 37 | 21 | |
| 9 | H ₂ O/Heptane (1:1) | 99 | 94 | |
| 10 ^b | H ₂ O/Heptane (1:1) | 98 | 93 | |
| 11 | H ₂ O/MeOH (1:1) | 99 | 90 | |
| 12 ^b | H ₂ O/MeOH (1:1) | 98 | 90 | |
| 13 | H ₂ O | >99 | 99 | 0.14 |
| 14 ^b | H ₂ O | 97 | 96 | |
| 15 | Neat | >99 | >99 | <0.04 |
| 16 ^b | Neat | >99 | >99 | |

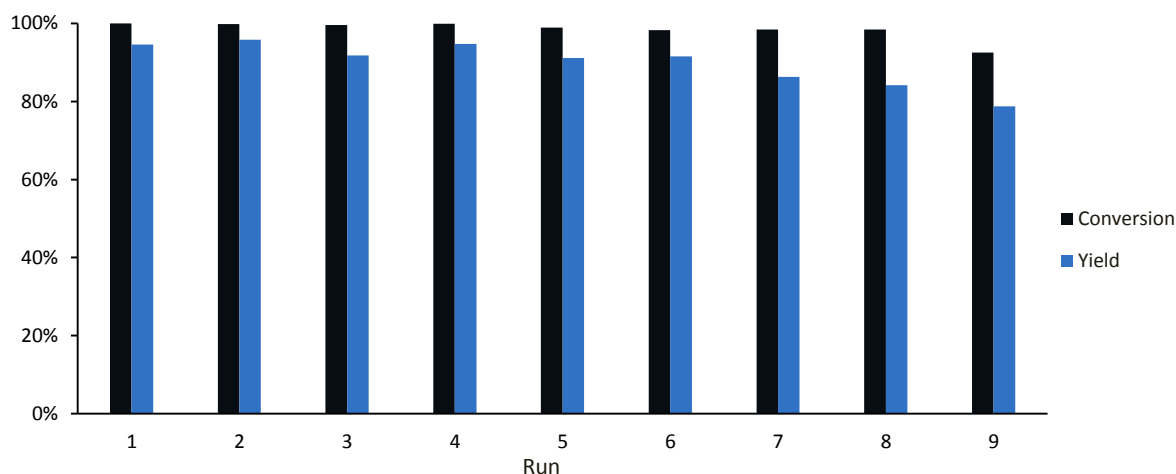
General conditions: 1.5 mmol (237 μL , 168.3 mg) 1-Octene, 2.9 mol% (8.8 mg) catalyst, 1.5 mL solvent, 40 °C, 10 bar H_2 , 18 h. ^a Conversions and yields were determined *via* GC, using hexadecane as internal standard. ^b Reaction conducted for 6 h.



Scheme 12: Conversions and yields for the hydrogenation of 1-octene with Co@Chitosan-700 in different media, plotted over time.

3. Summary

For a sustainable catalytic process, good recyclability of the catalyst is mandatory. This is the main reason, why the chemical industry usually prefers heterogeneous rather than homogeneous catalysts, as they can be recovered *via* simple filtration. For Co@Chitosan-700, this procedure is simplified even further, due to its ferromagnetic behaviour caused by a high cobalt content of almost 30%. In addition, for water as solvent separation of the product can be simply done by extraction. For a demonstration of catalyst's recycling on laboratory scale, after the first catalytic run the material was fixed at the wall of the glass vial by using a small magnet, followed by decanting off the liquids. Then the catalyst was washed three times with acetone and once with water. Eventually a new reaction was started. In this way, nine runs have been carried out for the hydrogenation of 1-octene (Scheme 13).



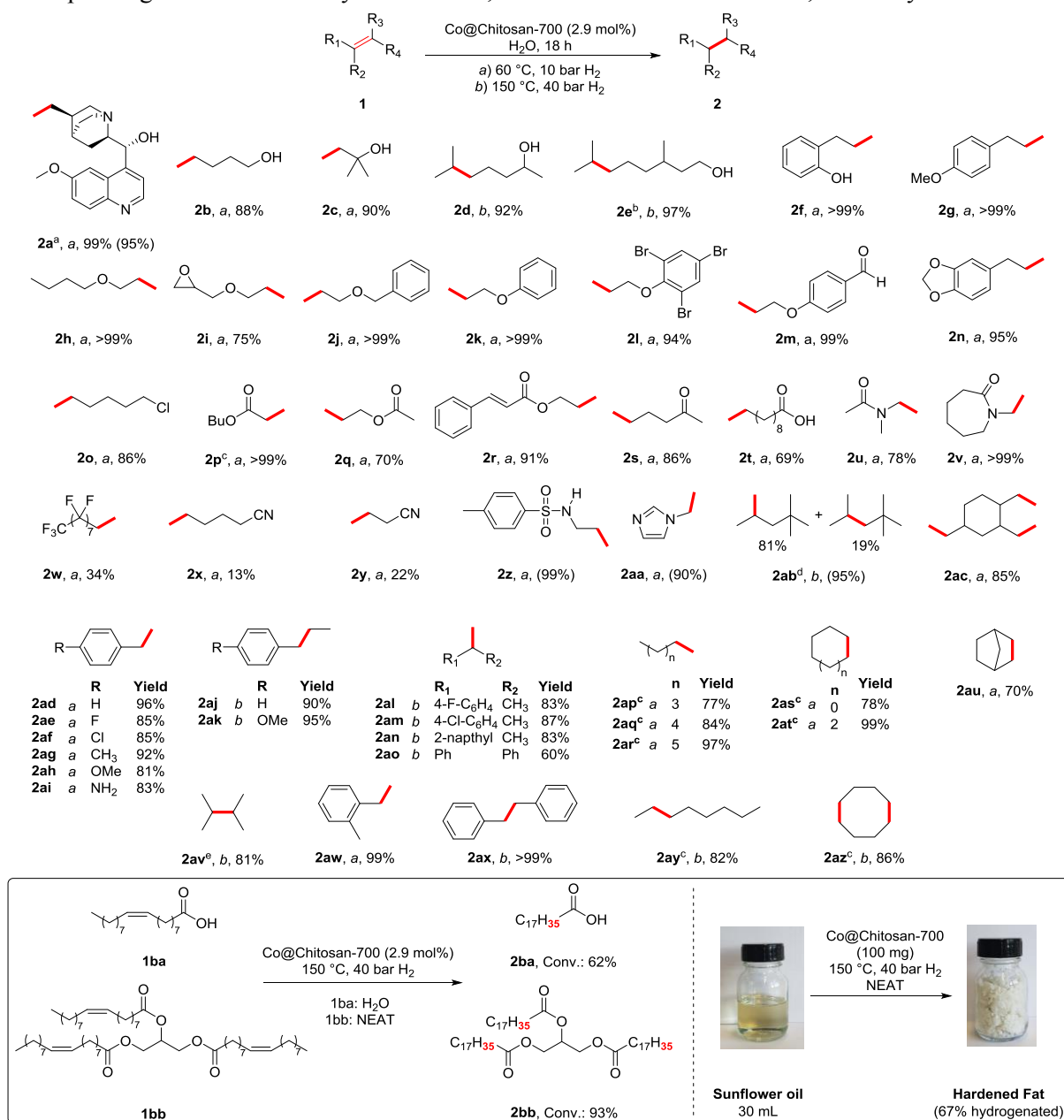
Scheme 13: Recycling of Co@Chitosan-700 in the hydrogenation of 1-octene to n-octane in water.

The productivity of the catalyst was constant for the first six runs, after which a small decrease of yield could be observed. This was accompanied by structural and compositional changes of the material. While the fresh catalyst consisted of metallic cobalt and graphitic carbon, the powder X-ray diffraction (XRD) pattern of the eight times recycled material indicated the formation of Co_3O_4 . This was also observed by electron energy loss spectroscopy (EELS). In addition, both the fresh and the used catalyst were analysed by aberration corrected scanning transmission electron microscopy (STEM). For the unused catalytic material a rather wide range of sizes (roughly 10 nm to 300 nm) was observed. Very small crystallites of cobalt oxide could be detected on the surface of the metallic particles. Furthermore, the presence of nitrogen located in an amorphous carbon phase accompanying the graphitic carbon structures was suggested by EELS. Notably, in the high annular dark-field (HAADF) images bright contrast spots could be observed in and on both carbon structures, which might indicate single cobalt surface atoms; due to their low density on the carbon, however, this could not be confirmed spectroscopically. As a major difference, big structures of cobalt oxide were present in the recycled catalyst. Metallic cobalt, generally covered by graphitic carbon, was still observable.

Besides recyclability and low cost of catalysts, their general applicability and selectivity are important aspects for commercialisation. Therefore, a number of functional groups, industrially important substrates and challenging olefins have been investigated at 60 °C and 10 bar H_2 , or, for internal olefins, at 150 °C and 40 bar H_2 , respectively (Scheme 14). Usually, reactions were carried out in water; however, for water-insoluble substrates methanol was applied (e.g. **1a**). Besides of alcohols (**2a – 2f**), ethers (**2a**, **2g – 2m**, **2ah**, **2ak**), methylenedioxy groups (**2n**), halides (**2l**, **2o**, **2ae**, **2af**, **2al**, **2am**), esters (**2p – 2r**), ketones (**2s**), amides (**2u**, **2v**), sulfonamides (**2z**) and amines (**2ai**), even highly sensible epoxides (**2i**) and aldehydes (**2m**) resisted the reaction conditions and the corresponding alkanes were obtained in good to very good yields. Furthermore, the catalyst revealed high

3. Summary

productivity in the presence of substrates containing an aromatic heterocycle (**1a**, **1aa**). Even though highly fluorinated olefins in general are challenging substrates, **1w** was hydrogenated to the corresponding alkane with 34% yield. Besides, the difficult tetrasubstituted 2,3-dimethyl-2-butene was



Scheme 14: Substrate scope for the olefin hydrogenation using Co@Chitosan-700.

General conditions: 1.5 mmol substrate, 2.9 mol% (8.8 mg) catalyst with respect to Co, 1.5 mL H₂O. Yields were determined *via* ¹H NMR, using mesitylene as internal standard. Isolated yields are given in parentheses. ^a Reaction was conducted in methanol. ^b Yields were determined *via* ¹³C NMR, using mesitylene as internal standard. ^c Yield was determined *via* GC, using hexadecane as internal standard. ^d Reaction was carried out on a 10.0 mL (7.2 g, 64 mmol) scale without additional solvent. Isolated yield is given. ^e Reaction was carried out on a 5.0 mL (3.5 g, 42.1 mmol) scale without solvent.

converted with 81% yield on a 5 mL scale under neat conditions at 150 °C. Notably, by applying mild conditions of 60 °C and 10 bar H₂, the terminal C=C bond of allyl cinnamate was reduced, while the internal one remained intact, giving **2r** selectively in 91%. This means that, by simply operating reactions at mild or harsh conditions, semi- or complete hydrogenation can be achieved. In addition, the industrially important products **2ab** (anti-knock agent, main component of aviation gasoline) and simple unsaturated hydrocarbons (**2ac**, **2ap** – **2at**, **2ay**, **2az**) were obtained in high yields. Eventually, also oleic acid (**1ba**, 62%), its triglyceride triolein (**1bb**, 93%), and sunflower oil were hydrogenated

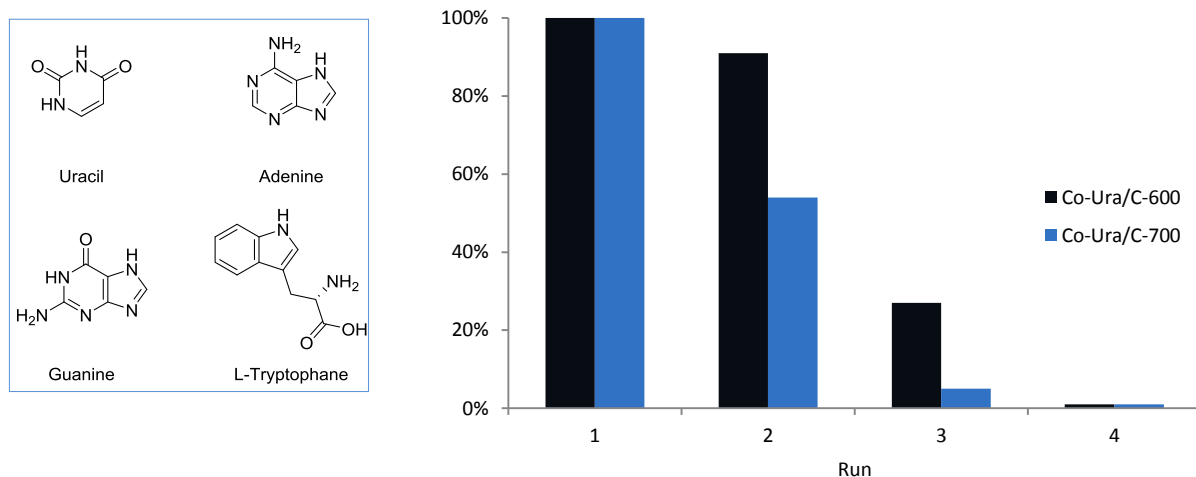
3. Summary

to the saturated fatty acid/ester (67%), as well. Importantly, no metal impurities could be detected *via* AAS in the hardened fat derived by sunflower oil. The moderate yield of stearic acid **1ba** compares well with that of undecanoic acid **2t** and might be explainable by coordination of the acid group to cobalt on the catalysts surface. Even worse effects on the catalytic productivity have nitriles. 5-Hexenenitrile (**1x**), and allyl cyanide (**1y**) just gave 13% and 22% yield of alkane, respectively.

In conclusion, a biowaste derived, versatile and easily prepared catalyst was developed, which enables the additive-free hydrogenation of olefins in water under mild conditions. More than 50 terminal and internal alkenes have been reduced towards the corresponding alkanes, revealing a broad functional group tolerance of the catalytic system. Importantly, recyclability and stability of Co@Chiotsan-700 have been demonstrated during nine consecutive runs. Compared to established heterogeneous catalysts, the present system is highly stable towards air and water for months.

3.2. Biomolecule-derived supported cobalt nanoparticles for hydrogenation of industrial olefins, natural oils and more in water

In a subsequent study, heterogeneous materials were prepared from $\text{Co}(\text{OAc})_2 \cdot 4\text{H}_2\text{O}$ and the biomolecules uracil, guanine, adenine and L-tryptophan. More than 20 materials were prepared by immobilisation of ligated cobalt on either Vulcan XC72R or aluminium oxides, followed by pyrolysis at temperatures between 600 and 1000 °C (*vide supra*). The as prepared materials were tested in the hydrogenation of diisobutene as model substrate. At 60 °C, 30 bar H_2 and 18 h reaction time, the catalysts Co-Ura/C-600 and Co-Ura/C-700 outperformed all the other materials, giving the product isooctane quantitatively. Even at just 40 °C and 10 bar H_2 , 62% and 63% of product were obtained with those two catalysts in water. An increase of pressure to 50 bar restored the quantitative yield. Other solvents than water resulted in inferior yields under otherwise identical conditions.

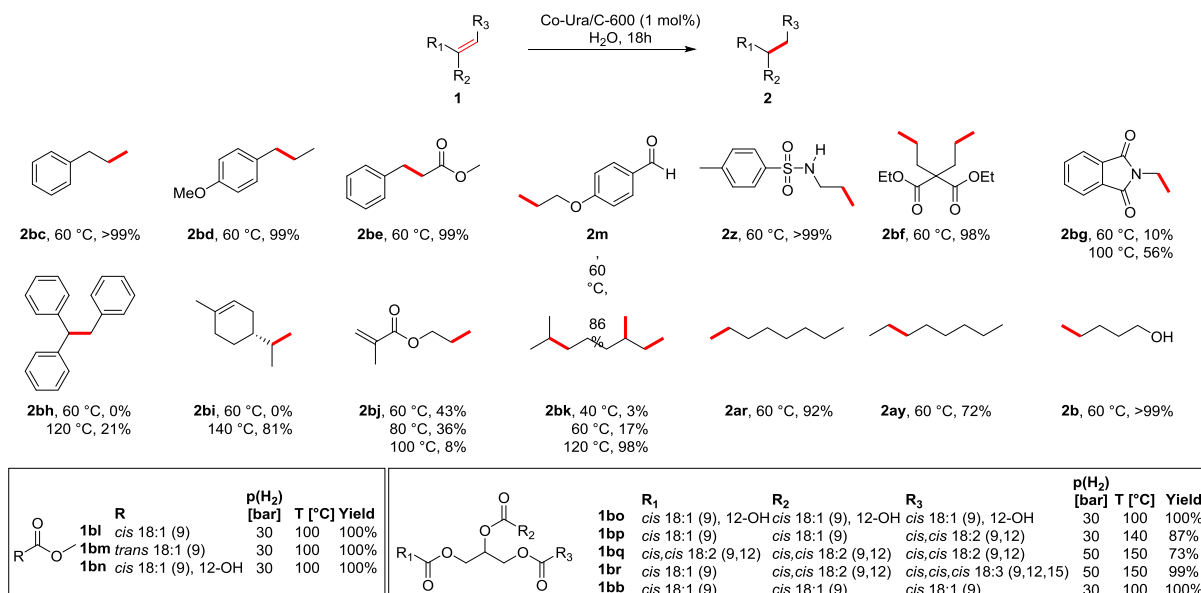


Scheme 15: Left: Molecular structures of the used bio-derived ligands. Right: Recycling studies of Co-Ura/C-600 and Co-Ura/C-700.

With the optimised conditions in hand, recycling studies have been conducted with Co-Ura/C-600 and Co-Ura/C-700. Therefore, the reaction mixtures have been filtered, the materials washed with acetone and then dried under high-vacuum at 60 °C for 4 h. For both materials a drop in catalytic productivity was observed, whereby the decrease was more pronounced for Co-Ura/C-700 (Scheme 15). Interestingly, AAS-analyses of the solutions did not indicate any cobalt-leaching (detection limit 0.04 mg/L). Hence, the decreased productivity might be a result of structural changes of the material. This was investigated by analysing the recycled catalysts and comparing the results with the fresh one. Powder XRD of the fresh materials indicated the formation of Co_3O_4 at a temperature of 500 °C.

3. Summary

Increasing the temperature led to the further reduction to metallic cobalt and at 1000 °C, only Co(0) is present. This was also confirmed by XPS; however, after pyrolysis at 1000 °C, no cobalt could be detected on the surface. STEM measurements of Co-Ura/C-600 indicated the presence of cobalt oxide and metallic cobalt as core-shell structures. Also Co(0) covered by carbon-layers has been identified. XRD of the recycled Co-Ura/C-600 revealed no metallic cobalt, hence either the Co/Co-oxides are transformed into the amorphous state or their crystallite size drops significantly. XPS indicated the formation of either CoO or Co(OH)₂ phases, which was also supported by STEM measurements.



Scheme 16: Substrate scope for the olefin-hydrogenation using Co-Ura/C-600. Following kinetic studies with Co-Ura/C-600 demonstrated that the hydrogenation of diisobutene at 30 bar H₂ and 60 °C is almost complete (96%) after 7 h. Hereby, the 1,1-disubstituted 2,4,4-trimethyl-1-pentene was saturated faster than the trisubstituted 2,4,4-trimethyl-2-pentene, as was expected. Afterwards, this highly active material was tested for other substrates. A variety of functional groups were well tolerated, such as aldehydes, sulfonamides, esters, ethers and alcohols (Scheme 16). An increase of temperature led to polymerisation as competitive reaction pathway in the case of *N*-vinylphtalimide (**1bg**). Even the sterically highly demanding triphenylethylene (**1bh**) could be hydrogenated, albeit to a lesser extend (21%). Notably, also the chemo- and regioselective reduction of the monocyclic terpene R-(+)-limonene towards the semi-hydrogenated product *p*-menthene (**2bi**) was possible. Similarly, the main product for the hydrogenation of **1bj** at 60 °C was the semi-hydrogenated product in allyl-position (43 °C). Elevated temperatures resulted in polymerisations. Also myrcene (**1bk**) can be singly, doubly or triply hydrogenated, and depending on the temperature, mixtures of all possible products could be obtained with conversions between 88-98%. By applying 120 °C, the fully saturated 2,6-dimethyloctane was achieved. Finally, several fatty acid esters and their triglycerides were under investigation for this industrially highly important topic. The esters methyl oleate (**1bl**), methyl elaidate (**1bm**) and methyl ricinoleate (**1bn**) were quantitatively hydrogenated. Also castor oil (main component **1bo**) and triolein (**1bb**) gave the saturated products with yields of 100%. Glycerine tristearate could also be obtained from apricot kernel oil (main component **1bp**), glycerine trilinoleate (**1bq**) or linseed oil (main component **1br**) in high to very high yields. This demonstrates the excellent applicability of Co-Ura/C-600 for such kinds of industrial processes.

3. Summary

In conclusion, the bio-derived Co-Ura/C-600 is a very active hydrogenation catalyst with potential for industrially important processes, such as fat hardening and saturation of diisobutene. Apart from a good functional group tolerance, the selective hydrogenation of a multi-unsaturated compound is feasible.

3.3. Towards Heterogeneous Cobalt-Catalysed Hydroformylation

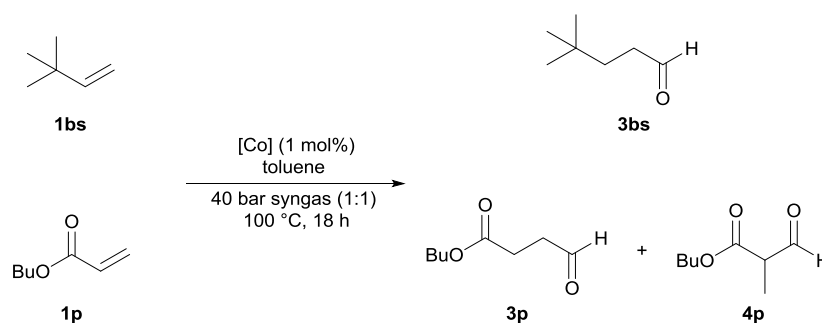
Besides of hydrogenation to alkanes, hydroformylation of olefins is another reaction of tremendous importance for the chemical industry. Therefore, we investigated this interesting, yet challenging topic. At the beginning, a library of about 50 catalysts was synthesised by impregnation of diverse commercially available supports (e.g. carbon, titania, silica, ceria and alumina) with $\text{Co}(\text{OAc})_2 \cdot 4\text{H}_2\text{O}$ ligated by different N-containing organic ligands. Subsequent pyrolysis, in general at 800 °C, gave the materials, which were labelled as Co/Ligand@Support. Besides of 1,10-phenanthroline (phen), also urea, pyridine derivatives and biologically relevant amino acids, nucleobases and the biopolymers chitin and chitosan were used as nitrogen containing ligands. The as prepared materials were tested in the hydroformylation of two model substrates, neohexene (3,3-dimethyl-1-butene) and *n*-butyl acrylate. These substrates were chosen due to the lack of isomerisation problems, and in addition the bulky *tert*-butyl group of neohexene results in a high regioselectivity towards the linear aldehyde. Depicted examples of the catalytic test reactions are shown in Table 2, along with the results of a comparative reaction using the commercially available, homogeneous $\text{Co}_2(\text{CO})_8$ (entry 1).

The hydroformylation of *n*-butyl acrylate with the latter catalyst was observed to be faster than that of neohexene, due to the electronic activation of the double bond by the ester group in *n*-butyl acrylate on the one hand and the steric demand of the *tert*-butyl group in neohexene on the other hand. The same tendency in activity was observed for all phen-based catalysts (entries 2, 4, 6, 8). Conversely, the catalysts prepared with chitosan as ligand revealed a higher activity in the hydroformylation of neohexene (entries 3, 5, 7). This noteworthy finding is in contrast to general expectations. Apparently, both the support and the ligand affect the catalyst's activity. By comparing the performances of materials with same ligand, but different supports, the influence of the latter on the productivity was demonstrated. For both phen- and chitosan-based materials, ceria was the least suitable support in hydroformylation of neohexene. Co/phen@CeO₂ and Co/chitosan@CeO₂ (entries 2 and 3) showed the lowest activity compared to the other materials based on the respective precursor. While the silicon dioxide-supported Co/phen@SiO₂ was slightly more productive in the hydroformylation of neohexene (entry 4), the carbon-based Co/phen@C gave the highest yield of 45% (entry 6), followed by Co/phen@TiO₂ (entry 8). A comparison with the chitosan-based materials revealed a similar activity of Co/chitosan@SiO₂ (46% yield, entry 5) with that of Co/phen@C. The corresponding titania-based material Co/chitosan@TiO₂ was less active (36% yield, entry 7).

While there is no clear trend observed for neohexene hydroformylation, the phen-based materials are more active in the hydroformylation of *n*-butyl acrylate compared to the analogous chitosan derived materials. Among the different supports, cobalt on ceria gave the lowest productivities, again (entries 2 and 3). Actually, neither of the two ceria-supported catalysts has a noteworthy activity. Co/phen@TiO₂ and Co/phen@C have the highest productivity in the hydroformylation of *n*-butyl acrylate (entries 6 and 8). Over 80% yields have been obtained at full conversions in both cases. Co/chitosan@SiO₂ gave the highest conversion (47%) and yield (33%, entry 5) among the chitosan-based materials, followed by Co/chitosan@TiO₂ (Table 1, entry 7).

3. Summary

Table 2: Catalyst screening for the heterogeneously catalysed hydroformylation of olefins.



| Entry | Catalyst (1 mol%) | Conv. 1bs [%] | Yield 3bs [%] | n/iso [%] | Conv. 1p [%] | Yield 3p+4p [%] | n/iso [%] |
|-------|-----------------------------------|-------------------------|-------------------------|--------------|------------------------|---------------------------|--------------|
| 1 | Co ₂ (CO) ₈ | 58 | 51 | >99 | >99 | 92 | 95 |
| 2 | Co/phen@CeO ₂ | 4 | 1 | >99 | 8 | 2 | >99 |
| 3 | Co/chitosan@CeO ₂ | 22 | 17 | >99 | 2 | 2 | >99 |
| 4 | Co/phen@SiO ₂ | 22 | 18 | >99 | 81 | 60 | 95 |
| 5 | Co/chitosan@SiO ₂ | 52 | 46 | >99 | 47 | 33 | 95 |
| 6 | Co/phen@TiO ₂ | 55 | 38 | >99 | >99 | 82 | 95 |
| 7 | Co/chitosan@TiO ₂ | 46 | 36 | >99 | 40 | 31 | 98 |
| 8 | Co/phen@C | 53 | 45 | >99 | >99 | 83 | 98 |

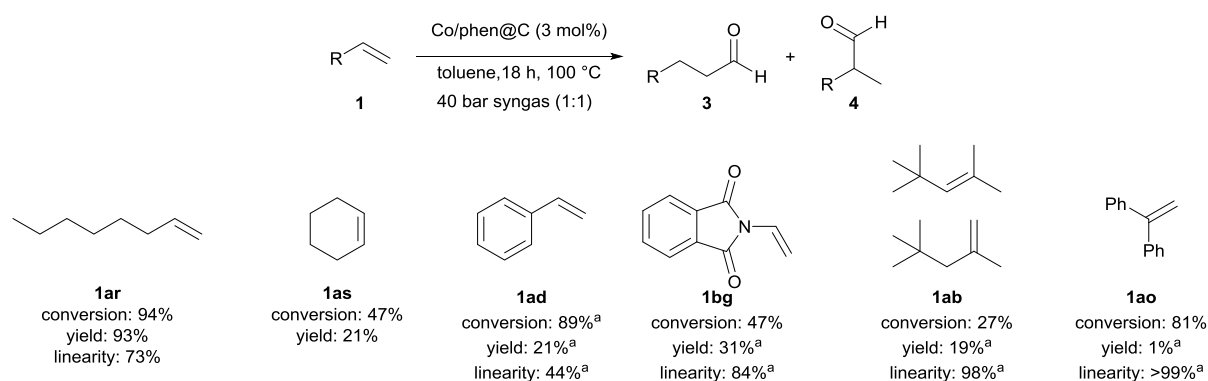
General conditions: neohexene (**1bs**) (193 μ L, 1.5 mmol) or *n*-butyl acrylate (**1p**) (214 μ L, 1.5 mmol), toluene (1.5 mL), 40 bar CO/H₂ (1:1), 100 °C, 18 h. ^a Conversions and yields represent the mean value of three experiments and were determined *via* GC using hexadecane as internal standard. ^b *n/iso* represents the amount of linear product with respect to the total amount of linear and branched aldehyde.

In all reactions the corresponding alkanes were observed as by-products. In the case of *n*-butyl acrylate some by-product originating from a dimerization pathway was also detected.

Furthermore, all other catalysts of the library have been tested. In general, the catalysts based on other ligands than chitosan or phen did not show an enhanced productivity. In addition, the influence of temperature, pressure, and solvent amount in the presence of the most active catalysts have been investigated. A decrease of temperature to 85 °C led to a significant decay of the hydroformylation rate of both olefins. By increasing the temperature to 120 °C or 140 °C, the performances for neohexene were improved.

The general suitability of Co/phen@C for other hydroformylations was investigated in the reactions of 1-octene (**1ar**) and cyclohexene (**1as**) as linear and cyclic aliphatic compounds, styrene (**1ad**) as an aromatic compound, *N*-vinyl phthalimide (**1bg**) and diisobutene (**1ab**) as industrial relevant substrates, and 1,1-diphenyl ethylene (**1ao**) as a sterically hindered one (Scheme 17). Mediocre to good yields for the corresponding aldehydes were observed, excepting the sterically hindered **1ao**, which yielded mostly in the saturated alkane. The same is valid for styrene (**1ad**), for which hydrogenation was the major pathway.

3. Summary



Scheme 17: Substrate scope for the hydroformylation with Co/phen@C.

General conditions: substrate (1.5 mmol), toluene (1.5 mL), 40 bar CO/H₂ (1:1), 100 °C, 18 h. Conversions, yields and n/iso ratios represent the mean value of two experiments and were determined *via* GC using hexadecane as internal standard. ^a determined *via* ¹H NMR using 1,4-dimethoxybenzene as internal standard.

For a better understanding of the observed differences of the catalysts' productivities, concentration-time graphs were plotted, and the amounts of leached cobalt from the materials determined *via* AAS. This has been done for three depicted catalysts, one with a high (Co/phen@TiO₂, Figure 6, red graphs), a medium (Co/chitosan@TiO₂, green graphs) and a low activity (Co/phen@CeO₂, blue graphs) in the hydroformylation of *n*-butyl acrylate. As a comparison, leaching values of Co/phen@C have been identified (purple graph).

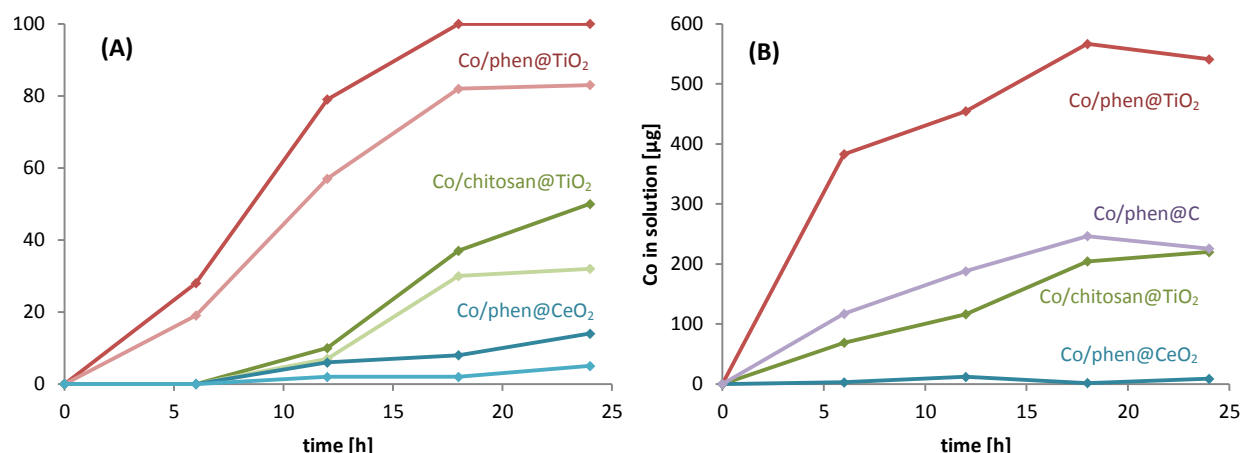


Figure 6: Plotted values of (A) conversions of *n*-butyl acrylate and yields of the corresponding aldehyde, and (B) cobalt in solution due to leaching of Co/phen@TiO₂ (red graphs), Co/chitosan@TiO₂ (green graphs) and Co/phen@CeO₂ (blue graphs), along with leaching values for Co/phen@C (purple graph).

The activity of Co/phen@TiO₂ was initially increasing, accompanied by immediate leaching of metal from the material. After 12 h the performance was decreasing again, due to saturation effects, and full conversion was achieved after 18 h. Co/chitosan@TiO₂ was not active at all until 6 h reaction time. At that point 68.8 µg cobalt has been found in solution, which corresponds to about 6% of the initial metal on the catalyst. Afterwards the conversions and yields, as well as the metal-concentration in solution were continuously increasing. Almost no metal leaching was observed for Co/phen@CeO₂, along with a very low productivity (5% yield after 24 h).

Clearly, there is some correlation between the amount of cobalt in solution and the catalysts' productivity. While Co/phen@CeO₂ leaches only to a little extent, the amount of cobalt deliberated from Co/phen@TiO₂, Co/phen@C and Co/chitosan@TiO₂ is continuously increasing during reaction time, until saturation apparently occurred after 18 hours. Unfortunately, no obvious relationship

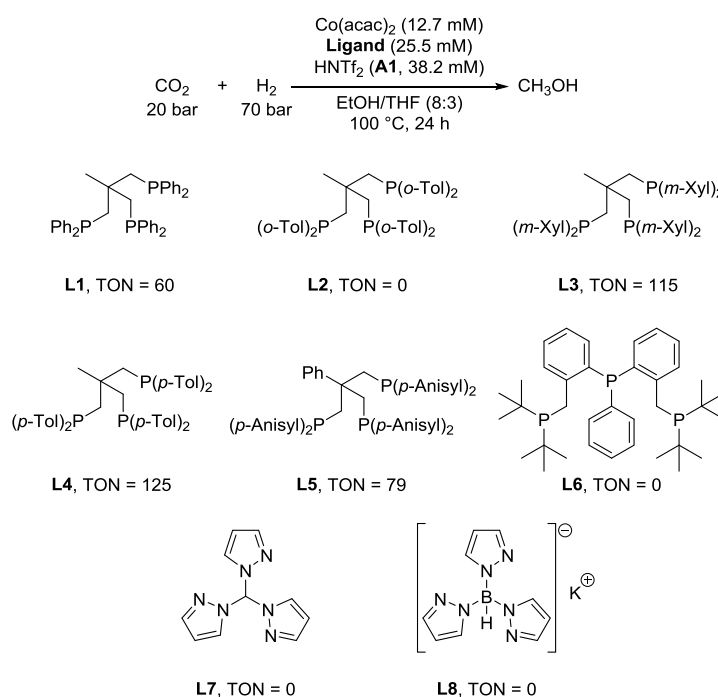
3. Summary

between leaching and productivity could be ascertained for these materials. On the one hand, conversions and yields determined for Co/phen@C and Co/phen@TiO₂ after 18 hours were similar (see Table 2). On the other hand, the amount of metal in solution is twofold higher for Co/phen@TiO₂ than for Co/phen@C. In addition, the leaching values of Co/phen@C and Co/chitosan@TiO₂ are comparable, while the determined yields of **3p** and **4p** of aldehyde after 18 h were 83% and 31%, respectively. These results demonstrate that both precursor and support of the materials affect the metal leaching. Lastly, during recycling-studies of Co/phen@C *via* filtration and washing, a major drop of productivity was observed. Whereas a yield of 58% was obtained in the first run, it dropped to just 8% of aldehyde in the third.

In summary, several cobalt containing materials have been prepared by impregnation and pyrolysis, and their performances were demonstrated in several hydroformylation reactions. The kinetic behaviours and the rates of leaching of the catalysts strongly depend on the supports and *in situ* formed cobalt complexes. These investigations suggest that the presented hydroformylation reactions mainly take place in solution catalysed by leached molecular metal species. Still, active centres on the surface are productive to a limited extent, as well. Overall, the common but toxic Co₂(CO)₈ can possibly be substituted in hydroformylations on lab scale by both Co/phen@TiO₂ and Co/phen@C, as they are air-stable, non-volatile and easy to handle reservoirs for active homogeneous cobalt species.

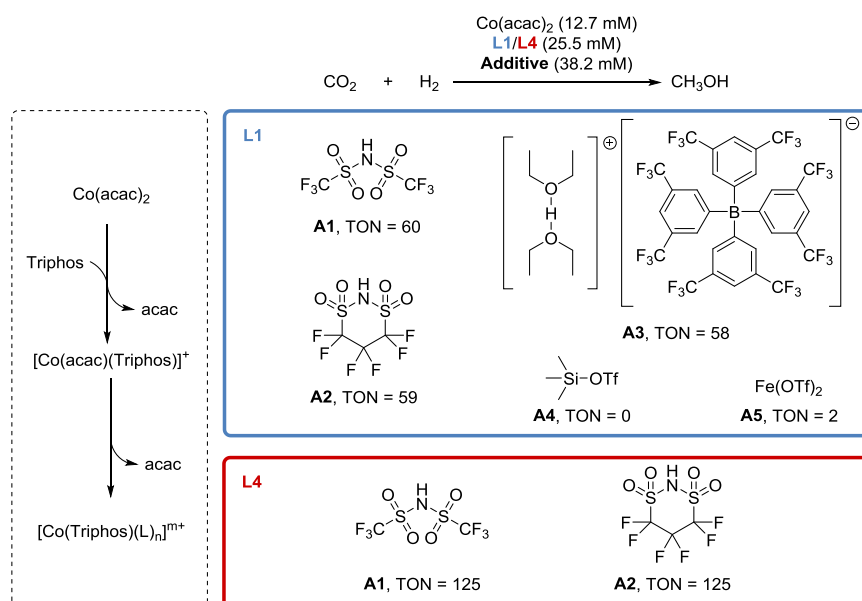
3.4. Homogeneous Hydrogenation of CO₂ to Methanol

In 2017, our group reported a cobalt-Triphos based system for the title reaction. The combination of Co(acac)₃ (acac: acetylacetonate), Triphos (**L1**) and HNTf₂ (**A1**, ratio = 1:2:3) gave a TON of 50 after 24 h at 100 °C and 90 bar pressure (H₂:CO₂ = 3.5:1).^[95] In order to optimise this system further, a small library of ligands was investigated, first (Scheme 18). Instead of Co(acac)₃, the corresponding Co(II) compound was used, as a slightly increased activity was found for freshly sublimed Co(acac)₂, resulting in a TON of 60.



Scheme 18: Investigation of tridentate ligands in the hydrogenation of CO₂ to methanol with cobalt.

3. Summary



Scheme 19: Formation of the suspected catalytic active species (dashed box) and screening of additives for its stabilisation.

Among the investigated ligands, only triphos-based ones showed activity. Those with electron donating methyl groups in *meta*- (**L3**) or *para*-position (**L4**) increased the catalyst's activity to a TON of 115 and 125, respectively. Besides the electronic effect, also a steric effect might play a role; as reported by Klankermayer and Leitner for their ruthenium-based system, one deactivation pathway is the formation of a hydride-bridged ruthenium dimer. By introducing a methoxy-group in *para*-position this dimer-formation was omitted.^[93] Additionally, a methyl-group in ortho-position (**L2**) inhibited the cobalt-system completely, most likely due to steric effects. Interestingly, the *p*-anisyl-substituted Triphos with a phenyl-group in its backbone (**L5**) gave a productivity in-between naked Triphos (**L1**) and **L3/L4**, even though the electron density on the metal is expected to be even higher. By moving from the triphos skeleton to another tridentate phosphine-ligand (**L6**), no methanol was formed. The same is valid for the phosphine-free carbon- (**L7**) and boron-scorpionates (**L8**). Together with the previously investigated ligands, this demonstrates the uniqueness of Triphos in this reaction. No ligand with a different backbone than that of triphos, which was ever investigated for this system gave a methanol TON greater than 2.^[95]

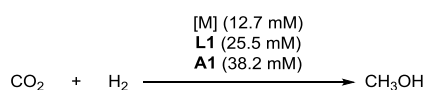


Table 3: Investigation of metal-precursors for the CO₂ hydrogenation to methanol.

| Entry | Metal precursor | TON (MeOH) | Entry | Cobalt precursor | TON (MeOH) |
|-------|-----------------------|------------|-------------------|------------------------------------|------------|
| 1 | Mn(acac) ₂ | 0 | 5 | CoCO ₃ | 43 |
| 2 | Fe(acac) ₃ | traces | 6 | Co ₂ (CO) ₈ | 0 |
| 3 | Ni(acac) ₂ | traces | 7 ^a | Co(NTf ₂) ₂ | 52 |
| 4 | Cu(acac) ₂ | traces | 8 ^b | Co(NTf ₂) ₂ | 45 |
| | | | 9 ^{b,c} | Co(NTf ₂) ₂ | 33 |
| | | | 10 ^{b,d} | Co(NTf ₂) ₂ | 70 |

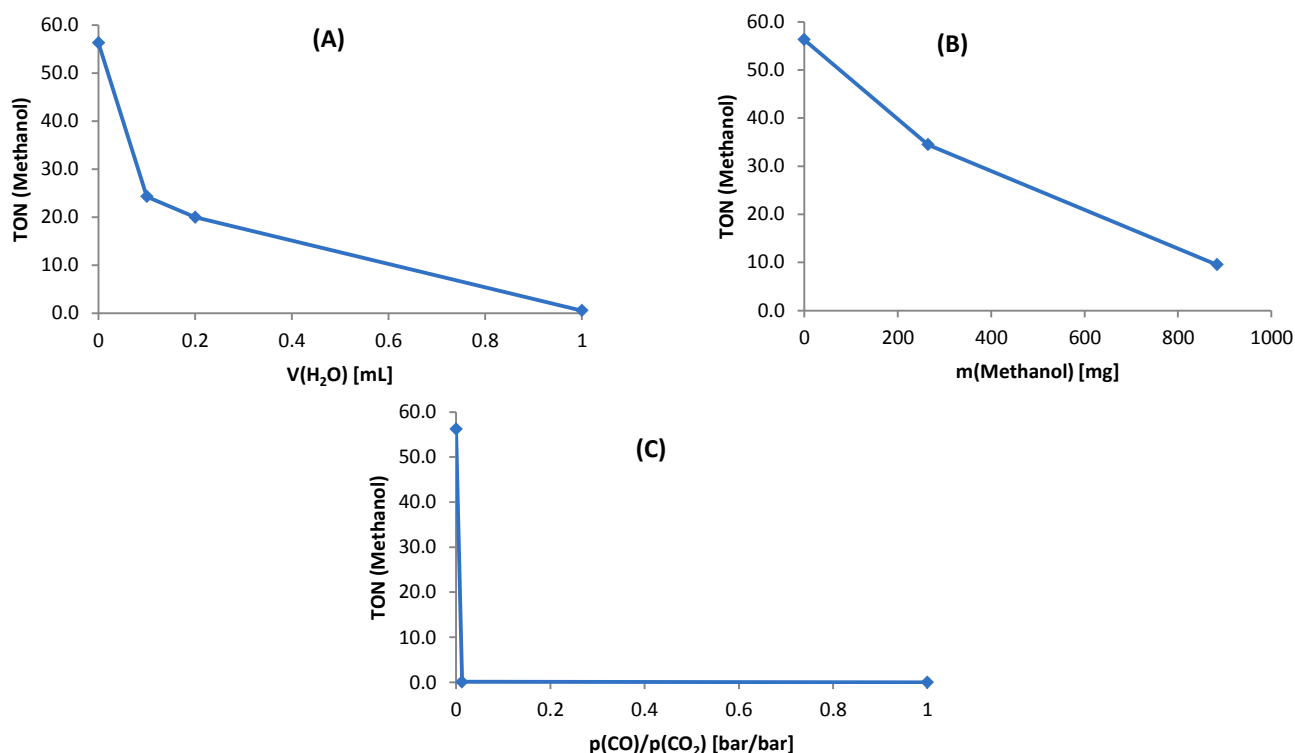
General conditions: [M], ligand, HNTf₂ (1:2:3), THF:EtOH (8:3), 20 bar CO₂, 70 bar H₂, 100 °C, 24 h. Mass of methanol was determined *via* GC using hexadecane as internal standard. TON = n_{product}/n_{catalyst}. ^a 1.0 eq. of **A1** was used. ^b No additive was used. ^c Reaction was carried out at 90 °C. ^d 1.0 eq. of **L1** was used.

Moreover, it was found that the weakly-coordinating anion triflimide plays a key role. It might assist the cleavage of acac ligands from cobalt by their protonation with HNTf₂. Subsequently, Triphos can

3. Summary

coordinate to the free coordination sites of the metal to form a cationic species, which is stabilised by the weakly-coordinating NTf_2 -anion (Scheme 19, dashed box). Additives that are not capable of doing this are not suitable for this system, resulting in no formation of methanol. Consequently, other acidic additives than HNTf_2 with corresponding bases that have a weakly-coordinating behaviour should also be appropriate. Therefore, the effects of the cyclic triflimide **A2** and Brookhart's acid **A3** on the system have been investigated, revealing that both additives result in the same amount of methanol (Scheme 19, blue box). This was also shown during a comparison of **A1** and **A2** using the ligand **L4**, giving a TON of 125 in both cases (Scheme 19, red box). The other investigated additives **A4** and **A5** gave no or very low activity, respectively, as they do not possess weakly-coordinating characteristics.

Next, other $\text{M}(\text{acac})_x$ ($x = 2, 3$) complexes and cobalt precursors have been tested (Table 3). Unfortunately, none of the other metals produced more than traces of methanol. However, while $\text{Co}_2(\text{CO})_8$ neither produces methanol (entry 6), CoCO_3 (TON = 43, entry 5) and $\text{Co}(\text{NTf}_2)_2$ (TON = 52, entry 7) were capable of substituting $\text{Co}(\text{acac})_2$. This can be explained by the strong ligating attributes of carbon monoxide, which hinder the complexation of Triphos. The carbonate ligand, however, is easily cleaved as carbon dioxide in acidic media and triphos can coordinate to form the active cationic species. $\text{Co}(\text{NTf}_2)_2$ is not present as a complex but a salt, and therefore Triphos can coordinate directly. This means that the latter cobalt precursor in principle does not require an acidic additive for the formation of the active complex, which was in fact shown to be the case (TON = 33). The activity could be improved by either using an aged (several weeks), or refluxed (10 min) stock-solution of $\text{Co}(\text{NTf}_2)_2$ and Triphos (1:2) in THF, resulting in TONs of 45 and 46 (entry 8), respectively. Furthermore, a pressure-consumption was detected even after 60 h, which demonstrates the stability of the additive-free system. Notably, it was also active at 90 °C (TON = 33, entry 9), as well as with a ratio of metal to ligand of 1:1 (TON = 70, entry 10).



Scheme 20: Poisoning experiments of the $\text{Co}(\text{acac})_2$ -based system with (A) water, (B) methanol and (C) carbon monoxide.

3. Summary

In addition, poisoning experiments have been carried out for the system based on $\text{Co}(\text{acac})_2$ (Scheme 20). These investigations revealed a product inhibition by water and methanol, along with a drastic effect of even traces of carbon monoxide. 1.0 mL of water reduced the TON to 1 (A), and 1.1 mL of methanol resulted in a TON of 10 (B), which demonstrates the greater poisoning potential of water with respect to methanol. Furthermore, a $\text{CO}:\text{CO}_2$ ratio of 1:80 already was enough to inhibit any product-formation (C).

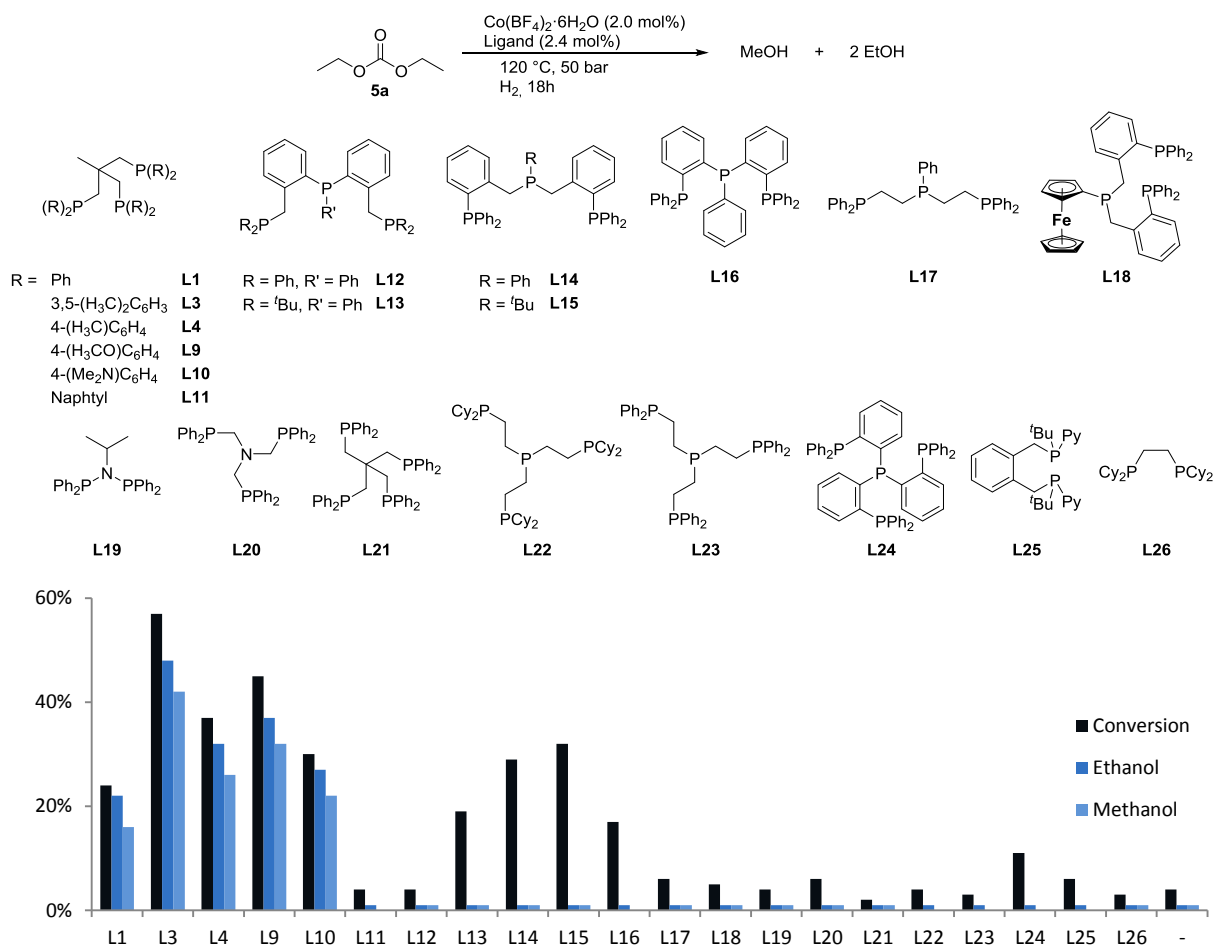
In conclusion, the performance of the cobalt-catalysed reduction of CO_2 to methanol has been optimised further. By modifying naked Triphos, TONs up to 125 were achieved and the substitution of $\text{Co}(\text{acac})_2$ with $\text{Co}(\text{NTf}_2)_2$, led to the development of an additive free system, which is also active after 60 h and at 90 °C. In addition, the function of the additive as a weakly-coordinating anion was highlighted and catalyst poisons were discovered.

3.5. Additive-Free Cobalt-Catalysed Hydrogenation of Carbonates to Methanol and Alcohols

As described in the introduction, the hydrogenation of carbon dioxide derivatives is an alternative approach for the production of methanol starting from the greenhouse gas. Besides the ruthenium pincer and triphos based systems, only very recently the first non-noble metal catalysed systems emerged, all which are manganese-based. This prompted us to investigate the cobalt-triphos system for this reaction. First, different cobalt-precursors have been tested in combination with triphos for the hydrogenation of diethyl carbonate at 120 °C and 50 bar H_2 in THF. Unfortunately, in the presence of 5 mol% of cobalt-species bearing halides, acac, hexafluoro acac, carbonate and acetate, no promising activity could be observed under these conditions. To our delight, both $\text{Co}(\text{NTf}_2)_2$ and $\text{Co}(\text{BF}_4)_2 \cdot 6\text{H}_2\text{O}$ converted 60% and 36% of the substrate, respectively. The selectivity of the former precursor was low (37% ethanol, 13% methanol) and side-products originating from both NTf_2^- -anion and the substrate could be detected *via* GC-MS, though. Fortunately, the selectivity was increased for $\text{Co}(\text{BF}_4)_2 \cdot 6\text{H}_2\text{O}$, giving 31% of ethanol and 25% of methanol at a conversion of 36%. A reduced catalyst loading of 2 mol% and 2.4 mol% ligand yielded in 24% conversion, 22% EtOH and 16% MeOH.

In the following, different ligands have been screened for the model-substrate. As can be seen in Scheme 21, only ligands with the triphos-backbone show activity. Among the Triphos-type ligands, the Xylyl-Triphos **L3** revealed the best performance, followed by Anisyl-Triphos (**L9**) and *p*-Tolyl-Triphos (**L4**). The productivity of Triphos substituted with dimethylamine in *para*-position (**L10**) was slightly better than that of **L1**. The enhanced performance of the catalyst due to ligand modifications seemed to be a result of an increased electron density on the metal and a steric demand *meta*- or *para*-position, which may prevent the formation of catalytically inactive dimeric species.

3. Summary

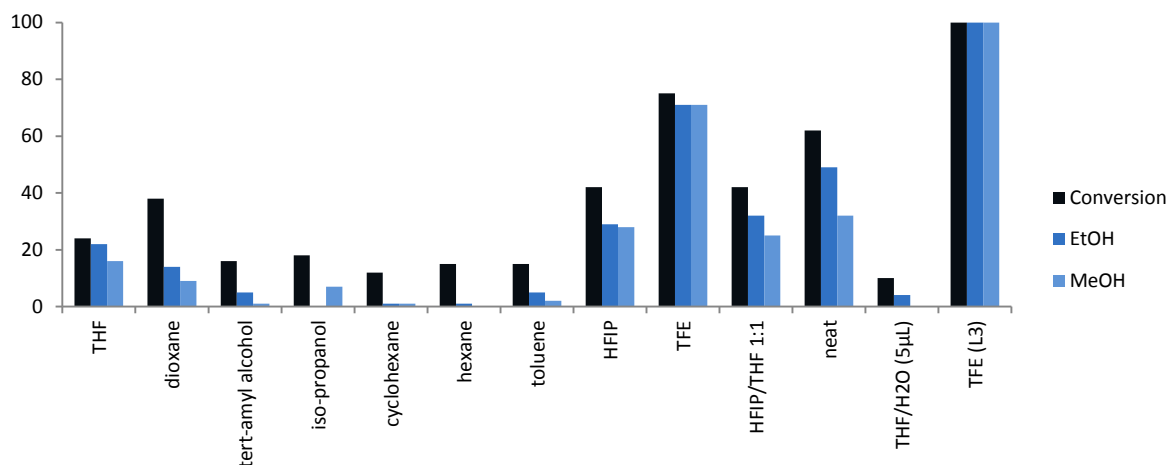


Scheme 21: Ligand-screening for the homogeneous cobalt-catalysed hydrogenation of diethyl carbonate to methanol and ethanol.

General conditions: 1.0 mmol diethyl carbonate, 2 mol% $\text{Co(BF}_4)_2 \cdot 6\text{H}_2\text{O}$, 2.4 mol% ligand, 2 mL THF, 120 °C, 50 bar H_2 , 18 h. Conversions and yields were calculated via GC using hexadecane as internal standard.

In order to further optimise the system, different solvents were tested with the commercially available ligand **L1**. The fluorinated alcohol 2,2,2-trifluoroethanol (TFE) outperformed all the other reaction media, yielding in 71% of both methanol and ethanol (conversion: 75%, Scheme 22). By applying the best ligand **L3**, the substrate was quantitatively converted to the alcohols. Interestingly, TFE gave significantly better results compared to the related solvent HFIP. The best non-fluorinated solvent was THF, however, the addition of only 5 μL (0.28 mmol) distilled water decreased the productivity significantly. The conversion dropped from 24 to 10% and the yield of ethanol from 22% to 4%. Methanol could not be detected by GC anymore, compared to 22% in dry conditions.

3. Summary



Scheme 22: Solvent-Screening for the homogeneous cobalt-catalysed hydrogenation of diethyl carbonate to methanol and ethanol.

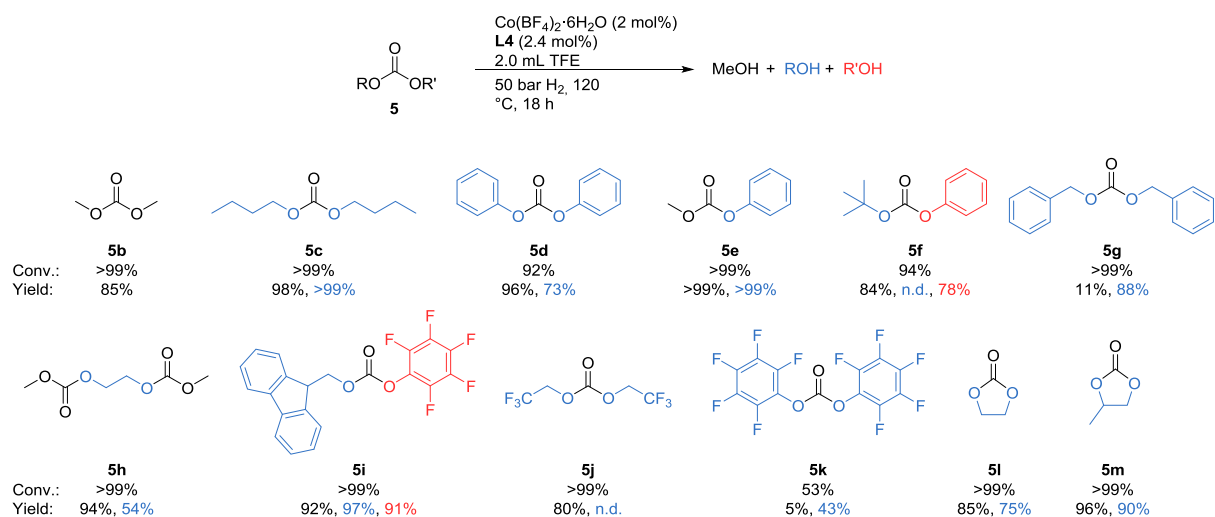
General conditions: 1.0 mmol diethyl carbonate (**5a**), 2.0 mol% $\text{Co}(\text{BF}_4)_2 \cdot 6\text{H}_2\text{O}$, 2.4 mol% **L1** or **L3**, 2 mL solvent, 120 °C, 50 bar H_2 , 18 h. Conversions and yields were calculated via GC using hexadecane as internal standard. The ethanol yield could not be determined in the case of isopropanol as solvent.

With an optimised system in hand, several organic carbonates were investigated to determine the general applicability of the system. To our delight, most of the investigated substrates gave methanol and the corresponding alcohols in high yields (Scheme 23). The acyclic dimethyl carbonate (**5b**) resulted in the formation of three equivalents of methanol (85%). Di-*n*-butyl carbonate (**5c**) was hydrogenated to methanol and butanol in almost quantitative yields. Also the aromatic diphenyl carbonate (**5d**) was effectively converted to phenol and methanol. In addition, asymmetric aromatic/aliphatic carbonates (**5e** and **5f**) yielded the three corresponding alcohols. Unfortunately, dibenzyl carbonate (**5g**) gave only a low methanol yield (11%), even though both the conversion and the yield of benzylic alcohol have been high (>99%/88%). A similar behaviour was observed for the perfluorinated carbonate **5k**, although at a lower conversion. Interestingly, the asymmetric carbonate **5i** yielded in 92% of methanol, along with 97% of 9-fluorenyl methanol and 91% of hexafluoro phenol. Also the fluorinated substrate **5j** gave high yields of methanol. Importantly, also the cyclic carbonates **5l** and **5m** were readily transformed to methanol and the corresponding diols. These carbonates are of particular interest (*vide supra*), as they are commercially produced from carbon dioxide and epoxides or oxetanes.

Finally, the potential intermediates for the hydrogenation of diethyl carbonate have been tested in separate experiments. Therefore, ethyl formate and *para*-formaldehyde have been used as substrates under the optimised conditions of 50 bar H_2 and 120 °C in TFE. After 18 h, ethyl formate was hydrogenated completely and ethanol (>99%) and methanol (86%) were obtained. Also *para*-formaldehyde was converted quantitatively, and the yield of methanol was at comparable 88%. These findings indicate that a step-wise mechanism cannot be excluded. However, also an inner-sphere mechanism, as was proposed for the direct CO_2 -hydrogenation, is possible.

In conclusion, a homogeneous cobalt catalyst for the hydrogenation of organic carbonates to methanol and the corresponding alcohols was developed for the first time. The use of a fluorinated alcohol (TFE) and a modified Triphos-derivative (**L3**) were found to be key-factors for a good performance.

3. Summary



Scheme 23: Substrate scope for the homogeneous cobalt-catalysed hydrogenation of cyclic and acyclic organic carbonates to methanol and the corresponding alcohols.

General conditions: 1.0 mmol carbonate (**5**), 2.0 mol% $\text{Co}(\text{BF}_4)_2 \cdot 6\text{H}_2\text{O}$, 2.4 mol% **L3**, 2 mL TFE, 120 °C, 50 bar H_2 , 18 h. Conversions and yields were calculated via GC using hexadecane as internal standard. n.d.: was not determined due to overlap of product-peak and TFE-peak in GC chromatogram.

4. References

- [1] 2015, *Remarks by the President in State of the Union*, The White House - Office of the Press Secretary, <https://obamawhitehouse.archives.gov/the-press-office/2015/01/20/remarks-president-state-union-address-january-20-2015>, accessed on 28.03.2019
- [2] S. Salomon, D. Qin, M. Manning, Z. Chen, M. Marquis, K. B. Averyt, M. Tignor, H. L. Miller, *Climate Change 2007: The Physical Science Basis. Contribution of Working Group I to the Fourth Assessment Report of the Intergovernmental Panel on Climate Change*, Cambridge University Press, Cambridge, UK, **2007**.
- [3] S. Arrhenius, *Lond. Edinb. Dublin Phil Mag. J. Sci. (5th ser.)* **1896**, *41*, 237-276.
- [4] NASA/GISS, 2019, *Global Land-Temperature Index*, <https://climate.nasa.gov/vital-signs/global-temperature/>, accessed on 25.03.2019
- [5] NASA, 2019, <https://climate.nasa.gov/vital-signs/carbon-dioxide/>, accessed on 25.03.2019
- [6] T. A. Boden, G. Marland, R. J. Andres, 2010, *Global, Regional, and National Fossil-Fuel CO₂ Emissions*, Carbon Dioxide Information Analysis Center, Oak Ridge Laboratory, U.S. Department of Energy, Oak Ridge, Tenn., USA., https://cdiac.ess-dive.lbl.gov/trends/emis/tre_glob.html, accessed on 27.03.2019
- [7] M. Seiwert, 2019, *VW weltweit für zwei Prozent der CO₂-Emissionen verantwortlich*, Wirtschaftswoche, <https://www.wiwo.de/unternehmen/auto/volkswagen-konzern-vw-weltweit-fuer-zwei-prozent-der-co2-emissionen-verantwortlich/24155948.html>, accessed on 12.05.2019
- [8] 2019, *Volkswagen to manufacture electric cars on three continents*, Volkswagen AG, <https://www.volkswagenag.com/en/news/stories/2019/01/volkswagen-to-manufacture-electric-cars-on-three-continents.html>, accessed on 27.03.2019
- [9] 2019, *Volkswagen invests in US start-up Forge Nano*, Volkswagen AG, https://www.volkswagenag.com/en/news/2019/01/Volkswagen_invests_in_US_start-up_Forge_Nano.html, accessed on 27.03.2019
- [10] R. Socolow, *Sci. Am.* **2005**, *293*, 49-55.
- [11] K. Sordakis, C. Tang, L. K. Vogt, H. Junge, P. J. Dyson, M. Beller, G. Laurenczy, *Chem. Rev.* **2018**, *118*, 372-433.
- [12] F. Asinger, *Methanol, Chemie- und Energierohstoff*, Akademie-Verlag, Berlin, **1987**.
- [13] a) G. A. Olah, A. Goepfert, G. K. S. Prakash, *Beyond Oil and Gas: The Methanol Economy*, 2nd ed., Wiley-VCH, Weinheim, **2009**; b) G. A. Olah, *Catal. Lett.* **2004**, *93*, 1-2.
- [14] R. Schlögl, *Angew. Chem. Int. Ed.* **2011**, *50*, 6424-6426.
- [15] S. Dunn, *Int. J. Hydrogen Energy* **2002**, *27*, 235-264.
- [16] a) J. Rifkin, *The Hydrogen Economy: The Creation of the Worldwide Energy Web and the Redistribution of Power on Earth*, J.P. Tarcher/Putnam, **2002**; b) G. W. Crabtree, M. S. Dresselhaus, M. V. Buchanan, *Phys. Today* **2004**, *57*, 39-44.
- [17] U. Bossel, *Proceedings of the IEEE* **2006**, *94*, 1826-1837.
- [18] a) *Methanol as an Energy Carrier, Vol. 55*, Forschungszentrum Jülich GmbH, Jülich, **2019**; b) A. Goepfert, M. Czaun, J.-P. Jones, G. K. Surya Prakash, G. A. Olah, *Chem. Soc. Rev.* **2014**, *43*, 7995-8048; c) G. A. Olah, G. K. S. Prakash, A. Goepfert, *J. Am. Chem. Soc.* **2011**, *133*, 12881-12898; d) G. A. Olah, A. Goepfert, G. K. S. Prakash, *J. Org. Chem.* **2009**, *74*, 487-498; e) G. A. Olah, *Angew. Chem. Int. Ed.* **2005**, *44*, 2636-2639.
- [19] K. A. Ali, A. Z. Abdullah, A. R. Mohamed, *Renew. Sust. Energ. Rev.* **2015**, *44*, 508-518.
- [20] a) M. Behrens, F. Studt, I. Kasatkin, S. Kühl, M. Hävecker, F. Abild-Pedersen, S. Zander, F. Girgsdies, P. Kurr, B.-L. Knief, M. Tovar, R. W. Fischer, J. K. Nørskov, R. Schlögl, *Science* **2012**, *336*, 893-897; b) S. K. Wilkinson, L. G. A. van de Water, B. Miller, M. J. H. Simmons, E. H. Stitt, M. J. Watson, *J. Catal.* **2016**, *337*, 208-220; c) K. C. Waugh, *Catal. Today* **1992**, *15*, 51-75.
- [21] a) M. Behrens, *Angew. Chem. Int. Ed.* **2014**, *53*, 12022-12024; b) J. Artz, T. E. Müller, K. Thenert, J. Kleinekorte, R. Meys, A. Sternberg, A. Bardow, W. Leitner, *Chem. Rev.* **2018**, *118*, 434-504; c) G. Fiorani, W. Guo, A. W. Kleij, *Green Chem.* **2015**, *17*, 1375-1389; d) A. W. Kleij, *Adv. Synth. Catal.* **2019**, *361*, 221-222.

4. References

- [22] a) K. M. McGrath, G. K. S. Prakash, G. A. Olah, *Direct methanol fuel cells*, Vol. 10, **2004**; b) S. Wasmus, A. Küver, *J. Electroanal. Chem.* **1999**, 461, 14-31; c) X. Zhao, M. Yin, L. Ma, L. Liang, C. Liu, J. Liao, T. Lu, W. Xing, *Energ. Environ. Sci.* **2011**, 4, 2736-2753; d) S. S. Munjewar, S. B. Thombre, R. K. Mallick, *Renew. Sust. Energ. Rev.* **2017**, 67, 1087-1104; e) N. K. Shrivastava, T. A. L. Harris Direct Methanol Fuel Cells, in *Encyclopedia of Sustainable Technologies* (Ed.: M. A. Abraham), Elsevier, Oxford, pp. 343-357, **2017**.
- [23] a) L. Bromberg, D. R. Cohn, *Alcohol Fueled Heavy Duty Vehicles Using Clean, High Efficiency Engines*, Massachusetts Institute of Technology report PSFC/JA-09-31, Cambridge, **2009**; b) L. Bromberg, D. R. Cohn, *Heavy Duty Vehicles Using Clean, High Efficiency Alcohol Engines*, Massachusetts Institute of Technology report PSFC/JA-10-43, Cambridge, **2010**.
- [24] a) T. A. Semelsberger, R. L. Borup, H. L. Greene, *J. Power Sources* **2006**, 156, 497-511; b) C. Arcoumanis, C. Bae, R. Crookes, E. Kinoshita, *Fuel* **2008**, 87, 1014-1030; c) J. Burger, E. Ströfer, H. Hasse, *Chem. Eng. Res. Des.* **2013**, 91, 2648-2662; d) J. Burger, M. Siegert, E. Ströfer, H. Hasse, *Fuel* **2010**, 89, 3315-3319; e) B. Lump, D. Rothe, C. Pastötter, R. Lämmermann, E. Jacob, *MTZ worldwide eMagazine* **2011**, 72, 34-38.
- [25] a) S. Zeng, X. Zhang, L. Bai, X. Zhang, H. Wang, J. Wang, D. Bao, M. Li, X. Liu, S. Zhang, *Chem. Rev.* **2017**, 117, 9625-9673; b) A. Alonso, J. Moral-Vico, A. Abo Markeb, M. Busquets-Fité, D. Komilis, V. Puentes, A. Sánchez, X. Font, *Sci. Total Environ.* **2017**, 595, 51-62; c) E. S. Sanz-Pérez, C. R. Murdock, S. A. Didas, C. W. Jones, *Chem. Rev.* **2016**, 116, 11840-11876; d) S. A. Didas, S. Choi, W. Chaikittisilp, C. W. Jones, *Acc. Chem. Res.* **2015**, 48, 2680-2687; e) S. Choi, J. H. Drese, C. W. Jones, *ChemSusChem* **2009**, 2, 796-854; f) C. M. White, B. R. Strazisar, E. J. Granite, J. S. Hoffman, H. W. Pennline, *J. Air Waste Manage.* **2003**, 53, 645-715.
- [26] W. Leitner, *Angew. Chem. Int. Ed.* **1995**, 34, 2207-2221.
- [27] S. Kowatsch Formaldehyde, in *Phenolic Resins: A Century of Progress* (Ed.: L. Pilato), Springer Berlin Heidelberg, Berlin, Heidelberg, pp. 25-40, **2010**.
- [28] a) G. J. Millar, M. Collins, *Ind. Eng. Chem. Res.* **2017**, 56, 9247-9265; b) M. Bahmanpour Ali, A. Hoadley, A. Tanksale, in *Rev. Chem. Eng., Vol. 30*, **2014**, p. 583; c) G. J. Millar, M. L. Nelson, P. J. R. Uwins, *J. Catal.* **1997**, 169, 143-156.
- [29] a) M. Rellán-Piñero, N. López, *ChemSusChem* **2015**, 8, 2231-2239; b) C. Brookes, P. P. Wells, G. Cibir, N. Dimitratos, W. Jones, D. J. Morgan, M. Bowker, *ACS Catal.* **2014**, 4, 243-250.
- [30] A. Haynes Acetic Acid Synthesis by Catalytic Carbonylation of Methanol, in *Catalytic Carbonylation Reactions* (Ed.: M. Beller), Springer Berlin Heidelberg, Berlin, Heidelberg, pp. 179-205, **2006**.
- [31] a) J. F. Haw, W. Song, D. M. Marcus, J. B. Nicholas, *Acc. Chem. Res.* **2003**, 36, 317-326; b) P. Tian, Y. Wei, M. Ye, Z. Liu, *ACS Catal.* **2015**, 5, 1922-1938.
- [32] J. Zhong, J. Han, Y. Wei, P. Tian, X. Guo, C. Song, Z. Liu, *Catal. Sci. Technol.* **2017**, 7, 4905-4923.
- [33] M. Stöcker, J. Weitkamp (eds), *Micropor. Mesopor. Mater.* **1999**, 29, 1-218.
- [34] C. D. Chang, *Catal. Rev.* **1983**, 25, 1-118.
- [35] a) U. Olsbye, S. Svelle, M. Bjørgen, P. Beato, T. V. W. Janssens, F. Joensen, S. Bordiga, K. P. Lillerud, *Angew. Chem. Int. Ed.* **2012**, 51, 5810-5831; b) I. Yarulina, A. D. Chowdhury, F. Meirer, B. M. Weckhuysen, J. Gascon, *Nat. Catal.* **2018**, 1, 398-411.
- [36] M. Aresta, A. Dibenedetto, *Dalton Trans.* **2007**, 2975-2992.
- [37] a) C. D. Windle, R. N. Perutz, *Coord. Chem. Rev.* **2012**, 256, 2562-2570; b) H. Takeda, C. Cometto, O. Ishitani, M. Robert, *ACS Catal.* **2017**, 7, 70-88; c) J.-P. Jones, G. K. S. Prakash, G. A. Olah, *Isr. J. Chem.* **2014**, 54, 1451-1466; d) Y. Yang, S. Ajmal, X. Zheng, L. Zhang, *Sustain. Energy Fuels* **2018**, 2, 510-537.
- [38] a) S. N. Habisreutinger, L. Schmidt-Mende, J. K. Stolarczyk, *Angew. Chem. Int. Ed.* **2013**, 52, 7372-7408; b) Y. Ma, X. Wang, Y. Jia, X. Chen, H. Han, C. Li, *Chem. Rev.* **2014**, 114, 9987-10043; c) X. Chang, T. Wang, J. Gong, *Energ. Environ. Sci.* **2016**, 9, 2177-2196; d) C. Peng, G. Reid, H. Wang, P. Hu, *J. Chem. Phys.* **2017**, 147, 030901; e) Y. Sohn, W. Huang, F. Taghipour, *Appl. Surf. Sci.* **2017**, 396, 1696-1711; f) X. Li, J. Yu, M. Jaroniec, X. Chen,

4. References

- Chem. Rev.* **2019**, *119*, 3962-4179; g) T. Di, B. Zhu, B. Cheng, J. Yu, J. Xu, *J. Catal.* **2017**, *352*, 532-541.
- [39] a) R. Obert, B. C. Dave, *J. Am. Chem. Soc.* **1999**, *121*, 12192-12193; b) S. N. Riduan, Y. Zhang, J. Y. Ying, *Angew. Chem. Int. Ed.* **2009**, *48*, 3322-3325; c) G. Ménard, D. W. Stephan, *J. Am. Chem. Soc.* **2010**, *132*, 1796-1797; d) M. J. Sgro, D. W. Stephan, *Angew. Chem.* **2012**, *124*, 11505-11507; e) M.-A. Courtemanche, M.-A. Légaré, L. Maron, F.-G. Fontaine, *J. Am. Chem. Soc.* **2013**, *135*, 9326-9329; f) Z. Lu, T. J. Williams, *ACS Catal.* **2016**, *6*, 6670-6673.
- [40] a) W.-H. Wang, Y. Himeda, J. T. Muckerman, G. F. Manbeck, E. Fujita, *Chem. Rev.* **2015**, *115*, 12936-12973; b) R. K. Singh, R. Singh, D. Sivakumar, S. Kondaveeti, T. Kim, J. Li, B. H. Sung, B.-K. Cho, D. R. Kim, S. C. Kim, V. C. Kalia, Y.-H. P. J. Zhang, H. Zhao, Y. C. Kang, J.-K. Lee, *ACS Catal.* **2018**, 11085-11093; c) G. Leonzio, *J. CO2 Util.* **2018**, *27*, 326-354; d) W.-H. Wang, Y. Himeda, J. T. Muckerman, G. F. Manbeck, E. Fujita, *Chem. Rev.* **2015**, *115*, 12936-12973.
- [41] a) Y.-N. Li, R. Ma, L.-N. He, Z.-F. Diao, *Catal. Sci. Technol.* **2014**, *4*, 1498-1512; b) M. F. Hertrich, M. Beller Metal-Catalysed Hydrogenation of CO₂ into Methanol, in *Organometallics for Green Catalysis* (Eds.: P. H. Dixneuf, J. F. Soulé), Springer, **2018**.
- [42] H. Ge, X. Chen, X. Yang, *Chem. - Eur. J.* **2017**, *23*, 8850-8856.
- [43] a) D. A. Bulushev, J. R. H. Ross, *Catal. Rev.* **2018**, *60*, 566-593; b) C. Federsel, R. Jackstell, M. Beller, *Angew. Chem. Int. Ed.* **2010**, *49*, 6254-6257; c) J. Klankermayer, S. Wesselbaum, K. Beydoun, W. Leitner, *Angew. Chem. Int. Ed.* **2016**, *55*, 7296-7343.
- [44] S. G. Jadhav, P. D. Vaidya, B. M. Bhanage, J. B. Joshi, *Chem. Eng. Res. Des.* **2014**, *92*, 2557-2567.
- [45] a) G. H. Graaf, P. J. J. M. Sijtsema, E. J. Stamhuis, G. E. H. Joosten, *Chem. Eng. Sci.* **1986**, *41*, 2883-2890; b) G. H. Graaf, J. G. M. Winkelman, *Ind. Eng. Chem. Res.* **2016**, *55*, 5854-5864.
- [46] B. J. Lommerts, G. H. Graaf, A. A. C. M. Beenackers, *Chem. Eng. Sci.* **2000**, *55*, 5589-5598.
- [47] G. H. Graaf, E. J. Stamhuis, A. A. C. M. Beenackers, *Chem. Eng. Sci.* **1988**, *43*, 3185-3195.
- [48] a) A. Zachopoulos, E. Heracleous, *J. CO2 Util.* **2017**, *21*, 360-367; b) K. Stangeland, H. Li, Z. Yu, *Ind. Eng. Chem. Res.* **2018**, *57*, 4081-4094.
- [49] A. Álvarez, A. Bansode, A. Urakawa, A. V. Bavykina, T. A. Wezendonk, M. Makkee, J. Gascon, F. Kapteijn, *Chem. Rev.* **2017**, *117*, 9804-9838.
- [50] <http://www.carbonrecycling.is/george-olah>, accessed on 17.05.2019
- [51] J. Liu, J. Shi, D. He, Q. Zhang, X. Wu, Y. Liang, Q. Zhu, *Appl. Catal., A* **2001**, *218*, 113-119.
- [52] K. T. Jung, A. T. Bell, *Catal. Lett.* **2002**, *80*, 63-68.
- [53] C. Yang, Z. Ma, N. Zhao, W. Wei, T. Hu, Y. Sun, *Catal. Today* **2006**, *115*, 222-227.
- [54] L. Yong, Z. Yi, W. Tiejun, T. Noritatsu, *Chem. Lett.* **2007**, *36*, 1182-1183.
- [55] V. D. B. C. Dasireddy, S. Š. Neja, L. Blaž, *J. CO2 Util.* **2018**, *28*, 189-199.
- [56] J. Kothandaraman, R. A. Dagle, V. L. Dagle, S. D. Davidson, E. D. Walter, S. D. Burton, D. W. Hoyt, D. J. Heldebrant, *Catal. Sci. Technol.* **2018**, *8*, 5098-5103.
- [57] M. Huš, D. Kopač, B. Likozar, *ACS Catal.* **2019**, *9*, 105-116.
- [58] A. L. Bonivardi, D. L. Chiavassa, C. A. Querini, M. A. Baltanás Enhancement of the catalytic performance to methanol synthesis from CO₂/H₂ by gallium addition to palladium/silica catalysts, in *Stud. Surf. Sci. Catal., Vol. 130* (Eds.: A. Corma, F. V. Melo, S. Mendioroz, J. L. G. Fierro), Elsevier, pp. 3747-3752, **2000**.
- [59] N. Iwasa, H. Suzuki, M. Terashita, M. Arai, N. Takezawa, *Catal. Lett.* **2004**, *96*, 75-78.
- [60] X.-L. Liang, X. Dong, G.-D. Lin, H.-B. Zhang, *Applied Catalysis B: Environmental* **2009**, *88*, 315-322.
- [61] A. García-Trenco, A. Regoutz, E. R. White, D. J. Payne, M. S. P. Shaffer, C. K. Williams, *Applied Catalysis B: Environmental* **2018**, *220*, 9-18.
- [62] X. Yang, S. Kattel, S. D. Senanayake, J. A. Boscoboinik, X. Nie, J. Graciani, J. A. Rodriguez, P. Liu, D. J. Stacchiola, J. G. Chen, *J. Am. Chem. Soc.* **2015**, *137*, 10104-10107.
- [63] H. Li, L. Wang, Y. Dai, Z. Pu, Z. Lao, Y. Chen, M. Wang, X. Zheng, J. Zhu, W. Zhang, R. Si, C. Ma, J. Zeng, *Nat. Nanotechnol.* **2018**, *13*, 411-417.
- [64] Y. Peng, L. Wang, Q. Luo, Y. Cao, Y. Dai, Z. Li, H. Li, X. Zheng, W. Yan, J. Yang, J. Zeng, *Chem* **2018**, *4*, 613-625.
- [65] K. W. Ting, T. Toyao, S. M. A. H. Siddiki, K.-i. Shimizu, *ACS Catal.* **2019**, *9*, 3685-3693.

4. References

- [66] a) T. Toyao, S. M. A. H. Siddiki, A. S. Touchy, W. Onodera, K. Kon, Y. Morita, T. Kamachi, K. Yoshizawa, K. i. Shimizu, *Chem. Eur. J.* **2017**, *23*, 1001-1006; b) T. Toyao, S. M. A. H. Siddiki, Y. Morita, T. Kamachi, A. S. Touchy, W. Onodera, K. Kon, S. Furukawa, H. Ariga, K. Asakura, K. Yoshizawa, K.-i. Shimizu, *Chem. Eur. J.* **2017**, *23*, 14848-14859.
- [67] K.-i. Tominaga, Y. Sasaki, M. Kawai, T. Watanabe, M. Saito, *J. Chem. Soc., Chem. Commun.* **1993**, 629-631.
- [68] T. Ken-ichi, S. Yoshiyuki, W. Taiki, S. Masahiro, *Bull. Chem. Soc. Jpn.* **1995**, *68*, 2837-2842.
- [69] a) X.-L. Du, Z. Jiang, D. S. Su, J.-Q. Wang, *ChemSusChem* **2016**, *9*, 322-332; b) E. Alberico, M. Nielsen, *Chem. Commun.* **2015**, *51*, 6714-6725; c) J. Choudhury, *ChemCatChem* **2012**, *4*, 609-611; d) S. Kar, J. Kothandaraman, A. Goepfert, G. K. Surya Prakash, *J. CO2 Util.* **2018**, *23*, 212-218.
- [70] Q. Liu, L. Wu, R. Jackstell, M. Beller, *Nat. Commun.* **2015**, *6*, 5933.
- [71] a) E. Balaraman, C. Gunanathan, J. Zhang, L. J. W. Shimon, D. Milstein, *Nat. Chem.* **2011**, *3*, 609-614; b) F. Hasanayn, A. Baroudi, A. A. Bengali, A. S. Goldman, *Organometallics* **2013**, *32*, 6969-6985; c) Y. Li, K. Junge, M. Beller, *ChemCatChem* **2013**, *5*, 1072-1074; d) P. H. Dixneuf, *Nat. Chem.* **2011**, *3*, 578.
- [72] E. Balaraman, Y. Ben-David, D. Milstein, *Angew. Chem. Int. Ed.* **2011**, *50*, 11702-11705.
- [73] X. Wu, L. Ji, Y. Ji, E. H. M. Elageed, G. Gao, *Catal. Commun.* **2016**, *85*, 57-60.
- [74] a) T. vom Stein, M. Meuresch, D. Limper, M. Schmitz, M. Hölscher, J. Coetzee, D. J. Cole-Hamilton, J. Klankermayer, W. Leitner, *J. Am. Chem. Soc.* **2014**, *136*, 13217-13225; b) F. M. A. Geilen, B. Engendahl, M. Hölscher, J. Klankermayer, W. Leitner, *J. Am. Chem. Soc.* **2011**, *133*, 14349-14358.
- [75] a) Z. Han, L. Rong, J. Wu, L. Zhang, Z. Wang, K. Ding, *Angew. Chem. Int. Ed.* **2012**, *51*, 13041-13045; b) Z. Han, L. Rong, J. Wu, L. Zhang, Z. Wang, K. Ding, *Angew. Chem.* **2012**, *124*, 13218-13222.
- [76] a) M. Cokoja, C. Bruckmeier, B. Rieger, W. A. Herrmann, F. E. Kühn, *Angew. Chem. Int. Ed.* **2011**, *50*, 8510-8537; b) J. Ma, N. Sun, X. Zhang, N. Zhao, F. Xiao, W. Wei, Y. Sun, *Catal. Today* **2009**, *148*, 221-231; c) H. J. v. Milligen, P. Veenstra, *Int. Pat.*, WO2009071654A1, **2008**.
- [77] A. Kaithal, M. Hölscher, W. Leitner, *Angew. Chem.* **2018**, *130*, 13637-13641.
- [78] V. Zubar, Y. Lebedev, L. M. Azofra, L. Cavallo, O. El-Sepelgy, M. Rueping, *Angew. Chem. Int. Ed.* **2018**, *57*, 13439-13443.
- [79] A. Kumar, T. Janes, N. A. Espinosa-Jalapa, D. Milstein, *Angew. Chem. Int. Ed.* **2018**, *57*, 12076-12080.
- [80] C. A. Huff, M. S. Sanford, *J. Am. Chem. Soc.* **2011**, *133*, 18122-18125.
- [81] N. M. Rezayee, C. A. Huff, M. S. Sanford, *J. Am. Chem. Soc.* **2015**, *137*, 1028-1031.
- [82] J. R. Khusnutdinova, J. A. Garg, D. Milstein, *ACS Catal.* **2015**, *5*, 2416-2422.
- [83] J. Kothandaraman, A. Goepfert, M. Czaun, G. A. Olah, G. K. S. Prakash, *J. Am. Chem. Soc.* **2016**, *138*, 778-781.
- [84] S. Kar, R. Sen, J. Kothandaraman, A. Goepfert, R. Chowdhury, S. B. Munoz, R. Haiges, G. K. S. Prakash, *J. Am. Chem. Soc.* **2019**, *141*, 3160-3170.
- [85] S. Kar, R. Sen, A. Goepfert, G. K. S. Prakash, *J. Am. Chem. Soc.* **2018**, *140*, 1580-1583.
- [86] S. Kar, A. Goepfert, S. G. Prakash, *ChemSusChem* **2019**, doi: 10.1002/cssc.201900324.
- [87] J. M. Hanusch, I. Kerschgens, F. Huber, M. Neuburger, K. Gademann, *Chem. Commun.* **2018**, *55*, 949-952.
- [88] a) K. S. Sordakis, G. Laurency, Y. Himeda, H. Kawanami, A. Tsurusaki, M. Iguchi, *Int. Pat.*, WO2017093782A1, **2017**; b) K. Sordakis, A. Tsurusaki, M. Iguchi, H. Kawanami, Y. Himeda, G. Laurency, *Chem. Eur. J.* **2016**, *22*, 15605-15608.
- [89] D. Wass, M. Everett, *Chem. Commun.* **2017**, *53*, 9502-9504.
- [90] a) S. Kar, A. Goepfert, J. Kothandaraman, G. K. S. Prakash, *ACS Catal.* **2017**, *7*, 6347-6351; b) S. C. Mandal, K. S. Rawat, S. Nandi, B. Pathak, *Catal. Sci. Technol.* **2019**, *9*, 1867-1878.
- [91] A. P. C. Ribeiro, L. M. D. R. S. Martins, A. J. L. Pombeiro, *Green Chem.* **2017**, *19*, 4811-4815.
- [92] S. Wesselbaum, T. vom Stein, J. Klankermayer, W. Leitner, *Angew. Chem. Int. Ed.* **2012**, *51*, 7499-7502.

4. References

- [93] S. Wesselbaum, V. Moha, M. Meuresch, S. Brosinski, K. M. Thenert, J. Kothe, T. v. Stein, U. Englert, M. Holscher, J. Klankermayer, W. Leitner, *Chem. Sci.* **2015**, *6*, 693-704.
- [94] T. J. Korstanje, J. Ivar van der Vlugt, C. J. Elsevier, B. de Bruin, *Science* **2015**, *350*, 298-302.
- [95] J. Schneidewind, R. Adam, W. Baumann, R. Jackstell, M. Beller, *Angew. Chem. Int. Ed.* **2017**, *56*, 1890-1893.
- [96] B. G. Schieweck, J. Klankermayer, *Angew. Chem. Int. Ed.* **2017**, *56*, 10854-10857.
- [97] H.-U. Blaser, F. Spindler, M. Thommen Industrial Applications, in *The Handbook of Homogeneous Hydrogenation* (Eds.: J. G. De Vries, C. J. Elsevier), Wiley-VCH, Weinheim, pp. 1279-1324, **2008**.
- [98] B. M. Goortani, A. Gaurav, A. Deshpande, F. T. T. Ng, G. L. Rempel, *Ind. Eng. Chem. Res.* **2015**, *54*, 3570-3581.
- [99] G. R. List, J. W. King, *Hydrogenation of Fats and Oils: Theory and Practice*, 2 ed., AOCS Press, Urbana, Illinois, **2015**.
- [100] B. Chen, U. Dingerdissen, J. G. E. Krauter, H. G. J. Lansink Rotgerink, K. Möbus, D. J. Ostgard, P. Panster, T. H. Riermeier, S. Seebald, T. Tacke, H. Trauthwein, *Appl. Catal., A* **2005**, *280*, 17-46.
- [101] J. G. d. Vries, C. J. Elsevier, *Handbook of Homogeneous Hydrogenation*, Wiley-VCH, Weinheim, Germany, **2007**.
- [102] Abundance of Elements in the Earth's Crust and in the Sea., in *CRC Handbook of Chemistry and Physics, Internet Version* (Ed.: D. R. Lide), CRC Press, Boca Raton, FL, **2005**.
- [103] a) P. J. Chirik, *Acc. Chem. Res.* **2015**, *48*, 1687-1695; b) S. C. Bart, E. Lobkovsky, P. J. Chirik, *J. Am. Chem. Soc.* **2004**, *126*, 13794-13807; c) M. R. Friedfeld, G. W. Margulieux, B. A. Schaefer, P. J. Chirik, *J. Am. Chem. Soc.* **2014**, *136*, 13178-13181; d) N. G. Léonard, P. J. Chirik, *ACS Catal.* **2018**, *8*, 342-348; e) M. R. Friedfeld, H. Zhong, R. T. Ruck, M. Shevlin, P. J. Chirik, *Science* **2018**, *360*, 888-893; f) I. Bauer, H.-J. Knölker, *Chem. Rev.* **2015**, *115*, 3170-3387; g) I. M. Angulo, S. M. Lok, V. F. Quiroga Norambuena, M. Lutz, A. L. Spek, E. Bouwman, *J. Mol. Catal. A: Chem.* **2002**, *187*, 55-67; h) T. J. Mooibroek, E. C. M. Wenker, W. Smit, I. Mutikainen, M. Lutz, E. Bouwman, *Inorg. Chem.* **2013**, *52*, 8190-8201.
- [104] T. Drake, P. Ji, W. Lin, *Acc. Chem. Res.* **2018**.
- [105] K. Manna, T. Zhang, M. Carboni, C. W. Abney, W. Lin, *J. Am. Chem. Soc.* **2014**, *136*, 13182-13185.
- [106] P. Ji, K. Manna, Z. Lin, A. Urban, F. X. Greene, G. Lan, W. Lin, *J. Am. Chem. Soc.* **2016**, *138*, 12234-12242.
- [107] J. H. Cavka, S. Jakobsen, U. Olsbye, N. Guillou, C. Lamberti, S. Bordiga, K. P. Lillerud, *J. Am. Chem. Soc.* **2008**, *130*, 13850-13851.
- [108] K. Manna, P. Ji, Z. Lin, F. X. Greene, A. Urban, N. C. Thacker, W. Lin, *Nat. Commun.* **2016**, *7*, 12610.
- [109] T. Sawano, Z. Lin, D. Boures, B. An, C. Wang, W. Lin, *J. Am. Chem. Soc.* **2016**, *138*, 9783-9786.
- [110] N. C. Thacker, Z. Lin, T. Zhang, J. C. Gilhula, C. W. Abney, W. Lin, *J. Am. Chem. Soc.* **2016**, *138*, 3501-3509.
- [111] T. Zhang, K. Manna, W. Lin, *J. Am. Chem. Soc.* **2016**, *138*, 3241-3249.
- [112] J. Camacho-Bunquin, M. Ferrandon, U. Das, F. Dogan, C. Liu, C. Larsen, A. E. Platero-Prats, L. A. Curtiss, A. S. Hock, J. T. Miller, S. T. Nguyen, C. L. Marshall, M. Delferro, P. C. Stair, *ACS Catal.* **2017**, *7*, 689-694.
- [113] M. H. Weston, O. K. Farha, B. G. Hauser, J. T. Hupp, S. T. Nguyen, *Chem. Mater.* **2012**, *24*, 1292-1296.
- [114] a) P.-H. Phua, L. Lefort, J. A. F. Boogers, M. Tristany, J. G. de Vries, *Chem. Commun.* **2009**, 3747-3749; b) C. Rangheard, C. de Julián Fernández, P.-H. Phua, J. Hoorn, L. Lefort, J. G. de Vries, *Dalton Trans.* **2010**, *39*, 8464-8471.
- [115] T. N. Gieshoff, U. Chakraborty, M. Villa, A. Jacobi von Wangelin, *Angew. Chem. Int. Ed.* **2017**, *56*, 3585-3589.
- [116] R. Hudson, A. Rivière, C. M. Cirtiu, K. L. Luska, A. Moores, *Chem. Commun.* **2012**, *48*, 3360-3362.
- [117] M. Stein, J. Wieland, P. Steurer, F. Tölle, R. Mülhaupt, B. Breit, *Adv. Synth. Catal.* **2011**, *353*, 523-527.

4. References

- [118] S. Sandl, F. Schwarzhuber, S. Pöllath, J. Zweck, A. Jacobi von Wangelin, *Chem. Eur. J.* **2018**, *24*, 3403-3407.
- [119] P. Büschelberger, E. Reyes-Rodriguez, C. Schöttle, J. Treptow, C. Feldmann, A. Jacobi von Wangelin, R. Wolf, *Catal. Sci. Technol.* **2018**, *8*, 2648-2653.
- [120] L. Zaramello, B. L. Albuquerque, J. B. Domingos, K. Philippot, *Dalton Trans.* **2017**, *46*, 5082-5090.
- [121] T. Song, Z. Ma, Y. Yang, *ChemCatChem* **2019**, *11*, 1313-1319.
- [122] P. Puylaert, A. Dell'Acqua, F. El Ouahabi, A. Spannenberg, T. Roisnel, L. Lefort, S. Hinze, S. Tin, J. G. de Vries, *Catal. Sci. Technol.* **2019**, *9*, 61-64.
- [123] a) R. Franke, D. Selent, A. Börner, *Chem. Rev.* **2012**, *112*, 5675-5732; b) A. Börner, R. Franke, *Hydroformylation: Fundamentals, Processes, and Applications in Organic Synthesis*, Wiley-VCH, Weinheim, **2016**.
- [124] I. P. Beletskaya, V. G. Nenajdenko, *Angew. Chem. Int. Ed.* **2019**, *58*, 4778-4789.
- [125] K.-D. Wiese, D. Obst Catalytic Carbonylation Reactions, in *Catalytic Carbonylation Reactions* (Ed.: M. Beller), Springer, Berlin-Heidelberg, pp. 1-33, **2006**.
- [126] a) J. Pospech, I. Fleischer, R. Franke, S. Buchholz, M. Beller, *Angew. Chem. Int. Ed.* **2013**, *52*, 2852-2872; b) S. Pandey, K. V. Raj, D. R. Shinde, K. Vanka, V. Kashyap, S. Kurungot, C. P. Vinod, S. H. Chikkali, *J. Am. Chem. Soc.* **2018**, *140*, 4430-4439.
- [127] A. C. B. Neves, M. J. F. Calvete, T. M. V. D. Pinho e Melo, M. M. Pereira, *Eur. J. Org. Chem.* **2012**, *2012*, 6309-6320.
- [128] A. Riisager, R. Fehrmann, M. Haumann, P. Wasserscheid, *Eur. J. Inorg. Chem.* **2006**, *2006*, 695-706.
- [129] a) Z. Fengyu, F. Shin-ichiro, A. Masahiko, *Curr. Org. Chem.* **2006**, *10*, 1681-1695; b) M. Haumann, A. Riisager, *Chem. Rev.* **2008**, *108*, 1474-1497.
- [130] J. M. Marinkovic, A. Riisager, R. Franke, P. Wasserscheid, M. Haumann, *Ind. Eng. Chem. Res.* **2019**, *58*, 2409-2420.
- [131] A. Riisager, P. Wasserscheid, R. van Hal, R. Fehrmann, *J. Catal.* **2003**, *219*, 452-455.
- [132] A. Riisager, R. Fehrmann, S. Flicker, R. van Hal, M. Haumann, P. Wasserscheid, *Angew. Chem. Int. Ed.* **2005**, *44*, 815-819.
- [133] A. Riisager, R. Fehrmann, M. Haumann, B. S. K. Gorle, P. Wasserscheid, *Ind. Eng. Chem. Res.* **2005**, *44*, 9853-9859.
- [134] a) M. Jakuttis, A. Schönweiz, S. Werner, R. Franke, K. D. Wiese, M. Haumann, P. Wasserscheid, *Angew. Chem. Int. Ed.* **2011**, *50*, 4492-4495; b) S. Walter, H. Spohr, R. Franke, W. Hieringer, P. Wasserscheid, M. Haumann, *ACS Catal.* **2016**, 1035-1044.
- [135] C. Li, W. Wang, L. Yan, Y. Ding, *Front. Chem. Sci. Eng.* **2018**, *12*, 113-123.
- [136] Q. Sun, Z. Dai, X. Liu, N. Sheng, F. Deng, X. Meng, F.-S. Xiao, *J. Am. Chem. Soc.* **2015**, *137*, 5204-5209.
- [137] Q. Sun, Z. Dai, X. Meng, F.-S. Xiao, *Catal. Today* **2017**, *298*, 40-45.
- [138] C. Li, L. Yan, L. Lu, K. Xiong, W. Wang, M. Jiang, J. Liu, X. Song, Z. Zhan, Z. Jiang, Y. Ding, *Green Chem.* **2016**, *18*, 2995-3005.
- [139] C. Li, K. Xiong, L. Yan, M. Jiang, X. Song, T. Wang, X. Chen, Z. Zhan, Y. Ding, *Catal. Sci. Technol.* **2016**, *6*, 2143-2149.
- [140] C. Li, K. Sun, W. Wang, L. Yan, X. Sun, Y. Wang, K. Xiong, Z. Zhan, Z. Jiang, Y. Ding, *J. Catal.* **2017**, *353*, 123-132.
- [141] T. Wang, W. Wang, Y. Lyu, K. Xiong, C. Li, H. Zhang, Z. Zhan, Z. Jiang, Y. Ding, *Chin. J. Catal.* **2017**, *38*, 691-698.
- [142] D. Han, X. Li, H. Zhang, Z. Liu, G. Hu, C. Li, *J. Mol. Catal. A: Chem.* **2008**, *283*, 15-22.
- [143] T. T. Adint, C. R. Landis, *J. Am. Chem. Soc.* **2014**, *136*, 7943-7953.
- [144] Y. Wang, L. Yan, C. Li, M. Jiang, W. Wang, Y. Ding, *Appl. Catal., A* **2018**, *551*, 98-105.
- [145] Y. Wang, L. Yan, C. Li, M. Jiang, Z. Zhao, G. Hou, Y. Ding, *J. Catal.* **2018**, *368*, 197-206.
- [146] X. Jia, Z. Liang, J. Chen, J. Lv, K. Zhang, M. Gao, L. Zong, C. Xie, *Org. Lett.* **2019**, *21*, 2147-2150.
- [147] A. Cunillera, C. Blanco, A. Gual, J. M. Marinkovic, E. J. Garcia-Suarez, A. Riisager, C. Claver, A. Ruiz, C. Godard, *ChemCatChem* **2019**, *11*, 2195-2205.
- [148] a) F. Chen, X. Jiang, L. Zhang, R. Lang, B. Qiao, *Chin. J. Catal.* **2018**, *39*, 893-898; b) L. Liu, A. Corma, *Chem. Rev.* **2018**, *118*, 4981-5079.

5. Selected Publications

- [149] R. Lang, T. Li, D. Matsumura, S. Miao, Y. Ren, Y.-T. Cui, Y. Tan, B. Qiao, L. Li, A. Wang, X. Wang, T. Zhang, *Angew. Chem. Int. Ed.* **2016**, 16054-16058.
- [150] L. Wang, W. Zhang, S. Wang, Z. Gao, Z. Luo, X. Wang, R. Zeng, A. Li, H. Li, M. Wang, X. Zheng, J. Zhu, W. Zhang, C. Ma, R. Si, J. Zeng, *Nat. Commun.* **2016**, 7, 14036.
- [151] L. Alvarado Rupflin, J. Mormul, M. Lejkowski, S. Titlbach, R. Papp, R. Gläser, M. Dimitrakopoulou, X. Huang, A. Trunschke, M. G. Willinger, R. Schlögl, F. Rosowski, S. A. Schunk, *ACS Catal.* **2017**, 7, 3584-3590.
- [152] L. Xiaohao, H. Masatake, T. Makoto, *Chem. Lett.* **2008**, 37, 1290-1291.
- [153] X. Song, Y. Ding, W. Chen, W. Dong, Y. Pei, J. Zang, L. Yan, Y. Lu, *Appl. Catal., A* **2013**, 452, 155-162.
- [154] Z. Cai, H. Wang, C. Xiao, M. Zhong, D. Ma, Y. Kou, *J. Mol. Catal. A: Chem.* **2010**, 330, 94-98.
- [155] N. Yan, X. Chen, *Nature* **2015**, 524, 155-157.

5. Selected Publications

5.1. Hydrogenation of terminal and internal olefins using a biowaste-derived heterogeneous cobalt catalyst

F. K. Scharnagl, M. F. Hertrich, F. Ferretti, C. Kreyenschulte, H. Lund, R. Jackstell, M. Beller, *Sci. Adv.* **2018**, 4, eaau1248

From *Sci. Adv.* **2018**, 4, eaau1248. © The Authors, some rights reserved; exclusive licensee American Association for the Advancement of Science. Distributed under a Creative Commons Attribution NonCommercial License 4.0 (CC BY-NC) <http://creativecommons.org/licenses/by-nc/4.0/>

Contribution: F.K.S. initially found the high activity of Co@Chitosan-700 and optimised the system. Furthermore, he screened most of the substrates, recycled the catalyst and discussed the characterisation of the material with the analytical department. Eventually, he prepared the manuscript together with M.B. The overall contribution is about 75%.

CHEMISTRY

Hydrogenation of terminal and internal olefins using a biowaste-derived heterogeneous cobalt catalyst

Florian Korbinian Scharnagl, Maximilian Franz Hertrich, Francesco Ferretti, Carsten Kreyenschulte, Henrik Lund, Ralf Jackstell, Matthias Beller*

Hydrogenation of olefins is achieved using biowaste-derived cobalt chitosan catalysts. Characterization of the optimal Co@Chitosan-700 by STEM (scanning transmission electron microscopy), EELS (electron energy loss spectroscopy), PXRD (powder x-ray diffraction), and elemental analysis revealed the formation of a distinctive magnetic composite material with high metallic Co content. The general performance of this catalyst is demonstrated in the hydrogenation of 50 olefins including terminal, internal, and functionalized derivatives, as well as renewables. Using this nonnoble metal composite, hydrogenation of terminal C=C double bonds occurs under very mild and benign conditions (water or methanol, 40° to 60°C). The utility of Co@Chitosan-700 is showcased for efficient hydrogenation of the industrially relevant examples diisobutene, fatty acids, and their triglycerides. Because of the magnetic behavior of this material and water as solvent, product separation and recycling of the catalyst are straightforward.

INTRODUCTION

Olefins constitute a central feedstock for the chemical industry and represent major platform molecules for the development of basic synthetic methodologies. Among the different reactions of alkenes, catalytic hydrogenations continue to attract significant interest from both academic and industrial researchers (1, 2). Today, they are of crucial importance for all kinds of products spanning from pharmaceuticals to food, specialty chemicals, commodity chemicals, and agrochemicals (3). More specifically, in the petrochemical industry, hydrogenation of diisobutene to isooctane (2,4,4-trimethylpentane) is of current interest, as it substitutes one of the largest organic chemicals methyl tert-butyl ether (MTBE), which has been phased out as an antiknock additive in the United States since 2006 (4).

With respect to nutrition and food additives, natural oils are hydrogenated to harden them and to obtain better processable and storable fats on million metric ton scales (5). Moreover, catalytic hydrogenations play a role in the synthesis of vitamins such as biotin (6), a vitamin K₃ derivative, and β-carotene, a precursor of vitamin A.

In the pharmaceutical industry selective hydrogenations of C=C double bonds are applied in the production of sertraline (antidepressant), betamethasone (glucocorticoid), and dihydroergotamine (antimigraine agent) (2). Most of the hydrogenation processes *vide supra* are based either on noble metal catalysts containing Pd and Pt or on less expensive but difficult to handle and pyrophoric Raney-Ni. Because of these disadvantages in recent years, a strong interest in catalysts using Earth-abundant base metals developed in research groups worldwide. Obviously, their main advantage in comparison with noble metals is the stable price, which makes calculations for industry more certain. However, motivations to substitute them are beyond costs. Because of their reactivity, noble metal catalysts sometimes have selectivity problems, which can be improved by poisoning (Lindlar catalyst).

Nevertheless, relatively few organometallic complexes consisting of first-row transition metals have been reported for the hydrogenation

of olefins. In this respect, apart from Fe (7–10) and Ni (11–14), Co (9, 15, 16) also offers interesting possibilities. For instance, the group of Chirik investigated Co complexes for the asymmetric hydrogenation of alkenes (17, 18). Furthermore, a bis(arylimidazol-2-ylidene)pyridine cobalt methyl complex revealed activity for the hydrogenation of unactivated and even sterically hindered alkenes, such as 2,3-dimethyl-2-butene, at comparably mild conditions (19). In addition, cobalt complexes with bidentate phosphine ligands proved to be sufficient for hydrogenation of internal and endocyclic trisubstituted alkenes through hydroxyl group activation (20). However, a downside of all these sophisticated molecular-defined catalysts is their sensitivity toward oxygen and water, as well as their general stability. Notably, although the metals in these systems are inexpensive, the ligands are precious.

Hence, the development of more stable and reusable heterogeneous cobalt catalysts offers a more attractive and practical option for selective hydrogenations. In this context, Lin and co-workers reported metal-organic framework (MOF)-based iron and cobalt catalysts for the hydrogenation of olefins at room temperature. Furthermore, imines, carbonyls, and heterocycles were hydrogenated successfully (21). Unfortunately, these materials were only active in the presence of 10 equivalent (equiv.) (with respect to metal) of NaBEt₃H (22–24). In addition, the synthesis of these MOFs is rather complicated.

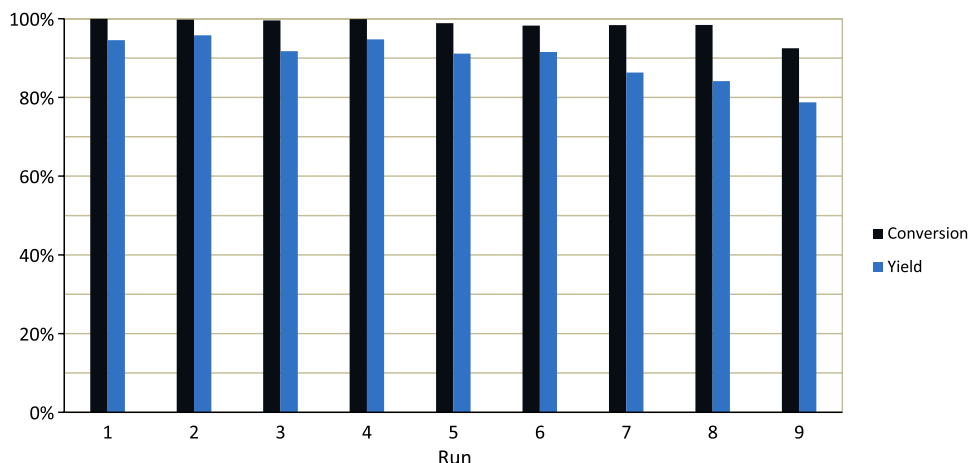
Our group (25–27) and others (28–30) have shown that simple pyrolysis of molecular-defined cobalt complexes, impregnated on inert supports, leads to materials with activity/selectivity profiles similar to homogeneous catalysts. Most recently, it was shown that the pyrolysis of a defined MOF gave a highly active reductive amination catalyst showing a broad substrate scope (31).

An ideal, industrially relevant catalyst should make use not only of base metals but also of inexpensive and renewable ligands/supports. In this context, we introduced the crab shell-derived biopolymer chitosan for catalyst preparation, both in hydrodehalogenations of alkyl and (hetero)aryl halides (32), as well as the selective hydrogenation of nitroarenes (33). Chitosan is derived by deacetylation of chitin, which represents a biowaste on a million metric ton scale (34). Despite the availability, cheap price, and known coordination to a

Copyright © 2018
The Authors, some
rights reserved;
exclusive licensee
American Association
for the Advancement
of Science. No claim to
original U.S. Government
Works. Distributed
under a Creative
Commons Attribution
NonCommercial
License 4.0 (CC BY-NC).

Leibniz-Institut für Katalyse e.V. an der Universität Rostock, Albert-Einstein Straße 29a, D-18059 Rostock, Germany.

*Corresponding author. Email: matthias.beller@catalysis.de



Scheme 1. Recycling of Co@Chitosan-700 in the hydrogenation of 1-octene. General conditions: 1.5 mmol 1-octene, 1.5 ml of H₂O, 2.9 mol % of Co@Chitosan-700, 60°C, 10 bar H₂, 18 hours.

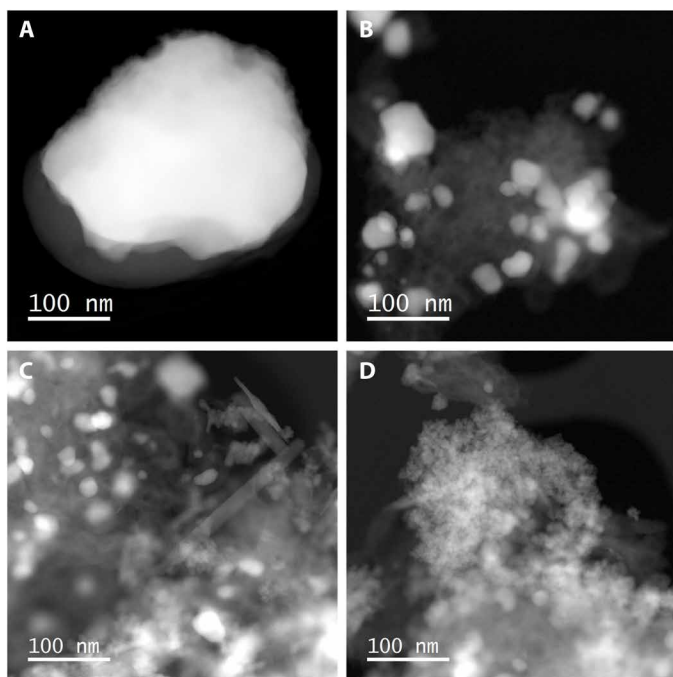


Fig. 1. Characterization of fresh and recycled Co@Chitosan-700 by HAADF-STEM. Images of fresh (A and B) and nine times-used (C and D) Co@Chitosan-700 catalyst, giving an overview on the general morphology.

variety of metals (35, 36) of this biopolymer, its use in heterogeneous catalysis still is narrow (37, 38). In addition, an efficient catalyst recycling is important especially for bulk chemical applications. In this respect, magnetic nanostructured materials might offer innovative potential (39).

RESULTS

At the start of our investigations, around 25 different cobalt catalysts were synthesized by thermal treatment of cobalt(II) acetate and chitosan. Typically, these materials were prepared by stirring different ratios of Co(OAc)₂·4H₂O and chitosan in ethanol at 65°C for 18 hours. Afterward, the solvent was removed and the residue

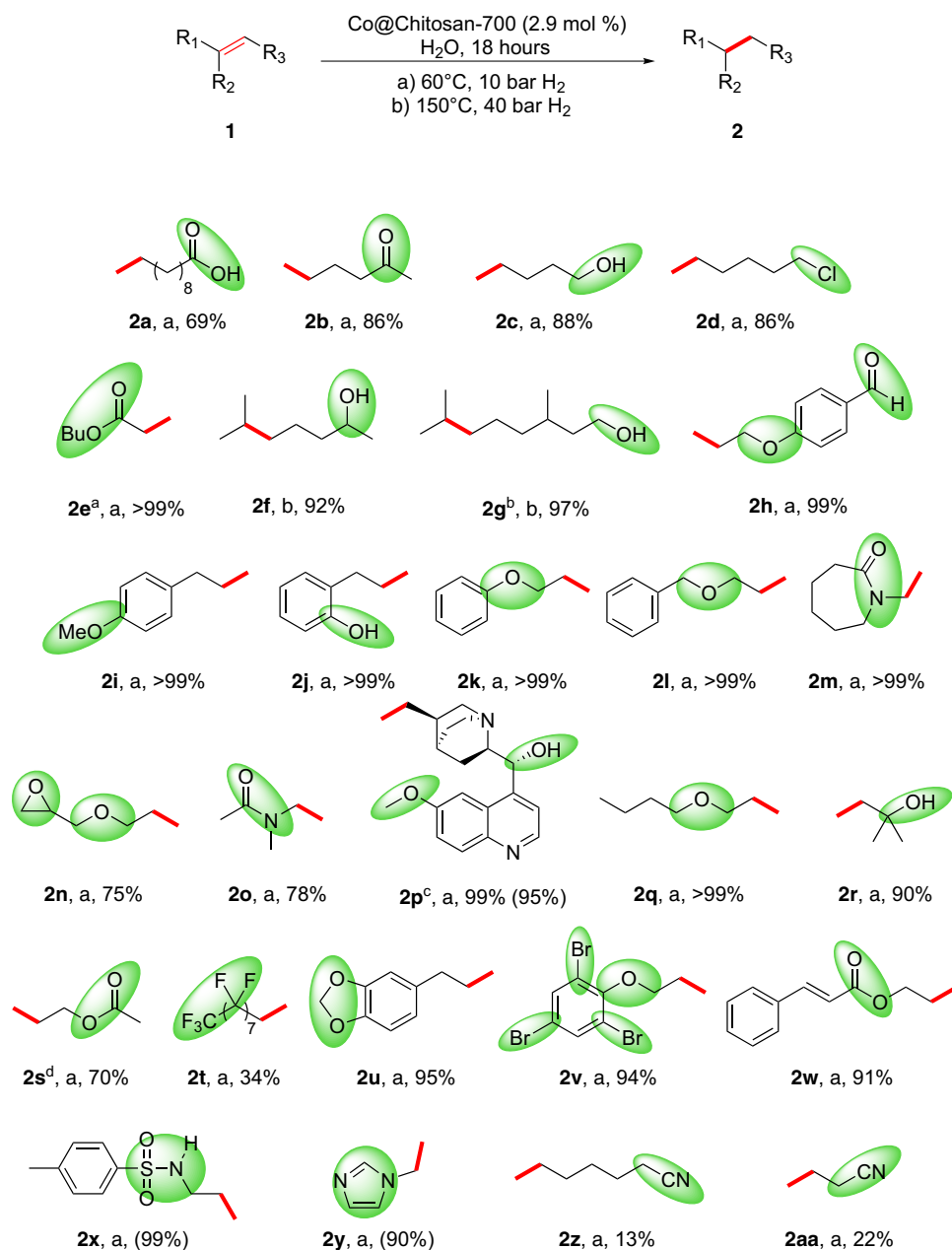
was dried overnight at 65°C by applying high vacuum. The resulting samples were ground in an agate mortar, pyrolyzed in between 700° and 1000°C, and ground again.

As a benchmark catalytic test, the hydrogenation of 1-octene was investigated under mild conditions (40°C). Among all the prepared materials, Co@Chitosan-700 (cobalt/chitosan ratio of 1:2; pyrolysis temperature: 700°C) resulted in the most active catalyst for this hydrogenation (table S1). As shown in table S2, this system is active in the presence of several solvents at 40°C and 10 bar hydrogen without any other additives. Near-quantitative conversion and best yields (>88%) were obtained in heptane, methanol, and water (table S2, entries 1, 5, and 13). Other solvents such as propylene carbonate (PC), acetonitrile (MeCN), and tetrahydrofuran (THF) were not suitable for this system, most likely due to a preferential adsorption on the catalyst's surface with respect to the olefin (table S2, entries 3, 4, and 7).

In general, for industrial applications, neat conditions are desirable. Gratifyingly, excellent conversion and product yield were obtained without any solvent present (table S2, entries 15 and 16). To illustrate the activities of the catalyst Co@Chitosan-700 in water, MeOH, and under neat conditions, we plotted a conversion-time graph for the best reaction media (scheme S1).

These investigations revealed that neat conditions seem to be most suitable for this system (60% yield after 2 hours), while in the case of water and methanol, significantly lower yields (19% and traces of *n*-octane, respectively) were observed. Nevertheless, for several applications, the use of a solvent is advantageous: For example, improved heat exchange is desirable for exothermic hydrogenations. Moreover, for the synthesis of fine chemicals, the required substrate amount can be minimized. Hence, the recyclability of this catalyst was investigated under aqueous conditions (40).

In general, the reusability of a given material is an important aspect of heterogeneous catalysis. For this purpose, such catalysts are typically separated by filtration. In contrast, Co@Chitosan-700 can be simply magnetically separated due to the high metal content (see Supplementary Materials). After washing the catalyst three times with acetone and once with water, new substrate and solvent were added. No significant drop of the activity of the catalyst was noticed for hydrogenation of 1-octene (1.5-mmol scale) for six runs (Scheme 1). After that, a slight deactivation is observed. It should be mentioned that in each decanting procedure, a small amount of catalyst was

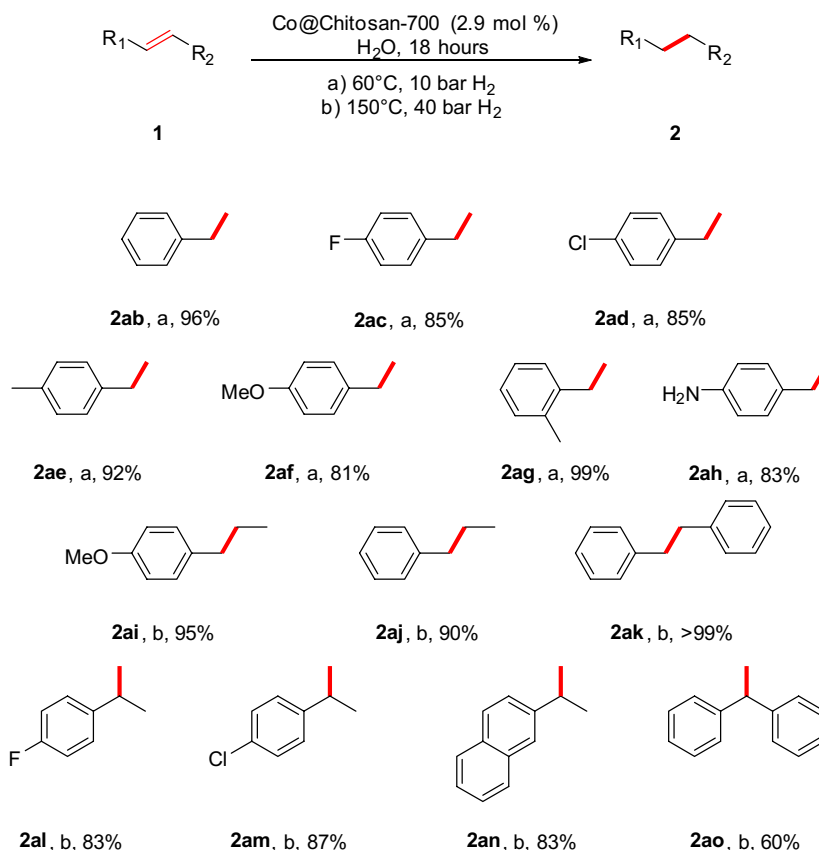


Scheme 2. Olefin hydrogenation with Co@Chitosan-700: Investigation of functional group tolerance. General conditions: 1.5 mmol substrate, 2.9 mol % (8.8 mg) of catalyst with respect to Co, 1.5 of ml H_2O . Yields were determined via ^1H NMR using mesitylene as internal standard. Isolated yields are given in parentheses. ^aYield was determined via gas chromatography (GC) using hexadecane as internal standard. ^bYields were determined via ^{13}C NMR using mesitylene as internal standard. ^cReaction was conducted in methanol. ^dReaction was conducted neat.

lost, which explains the decrease in activity. Atomic absorption spectroscopy (AAS) experiments revealed extremely low cobalt leaching of 0.055% [0.14 parts per million (ppm); 0.053% of the initial cobalt was found in the aqueous and 0.002% in the product phase].

Elemental analysis (EA) of the fresh catalyst revealed high cobalt content of 29.31%, which is the reason for the magnetic behavior of the material. The nitrogen content is relatively low with 2.53%, whereas carbon is dominant with 58.94%. To get more insight into the catalyst structure, we conducted powder x-ray diffraction (XRD) and scanning transmission electron microscopy (STEM) analyses.

XRD was measured to gain knowledge about the cobalt and carbon phases present in the composite materials. After pyrolysis at 700°C (Co@Chitosan-700), the cubic phase of metallic cobalt and graphitic carbon was indexed (fig. S9) from the received powder pattern. In contrast to related known cobalt catalysts (32, 33), no crystalline cobalt oxides (Co_3O_4 or CoO) were observed. Aberration-corrected STEM analysis was conducted from the fresh catalyst, as well as from the eight-times-recycled one. Before use, the catalytic material consisted mainly of metallic cobalt particles with graphitic carbon attached to the surface and with a rather wide range of sizes



Scheme 3. Olefin hydrogenation with Co@Chitosan-700: Investigation of aromatic mono- and disubstituted substrates. General conditions: 1.5 mmol substrate, 2.9 mol % (8.8 mg) of catalyst with respect to Co, 1.5 ml of H₂O. Yields were determined via ¹H NMR using mesitylene as internal standard.

(roughly 10 to 300 nm observed; Fig. 1, A and B, and figs. S2 to S4). Cobalt oxide could be found as some very small crystallites on the surface of the metallic particles, which is in contrast to previous systems, in which cobalt was mostly present as oxides, rather than metallic (32, 33). In addition, electron energy loss spectroscopy (EELS) suggests the presence of nitrogen located in an amorphous carbon phase accompanying the graphitic carbon structures. In/on both carbon structures, bright contrast spots could be observed in the high-angle annular dark-field (HAADF) images. These might be a hint for single cobalt surface atoms; however, this could not be ensured spectroscopically because of their low density on the carbon. The small cobalt oxide particles might consist of CoO; however, the noisy oxygen K-edge in the energy loss spectrum of the small Co oxide crystallites makes comparison to literature data (41) difficult (figs. S4 and S8).

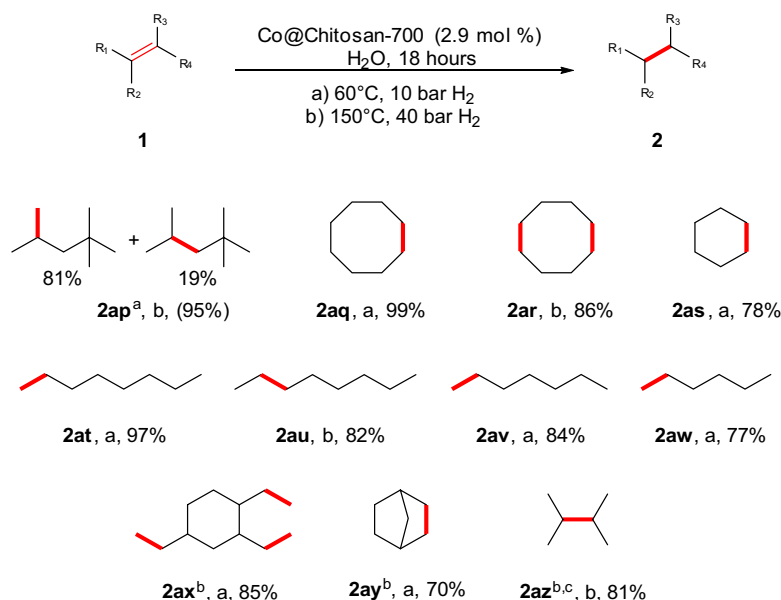
The recycled catalyst consisted in part of metallic cobalt, generally covered by graphitic carbon, but as a major difference, also big structures of cobalt oxide were present (Fig. 1, C and D, and figs. S5 to S7). Here, the fine structure of the oxygen K-edge of the EELS data (fig. S6) compares well with Co₃O₄ data from the literature (41). Also, an amorphous carbon structure containing nitrogen is still present. These data are in good accordance with the results of XRD from the recycled catalyst, which indicate the formation of Co₃O₄ (fig. S10).

To demonstrate the general utility of Co@Chitosan-700, we performed catalytic hydrogenations of >25 functionalized olefins. The following substrate scope was carried out in water to reduce the

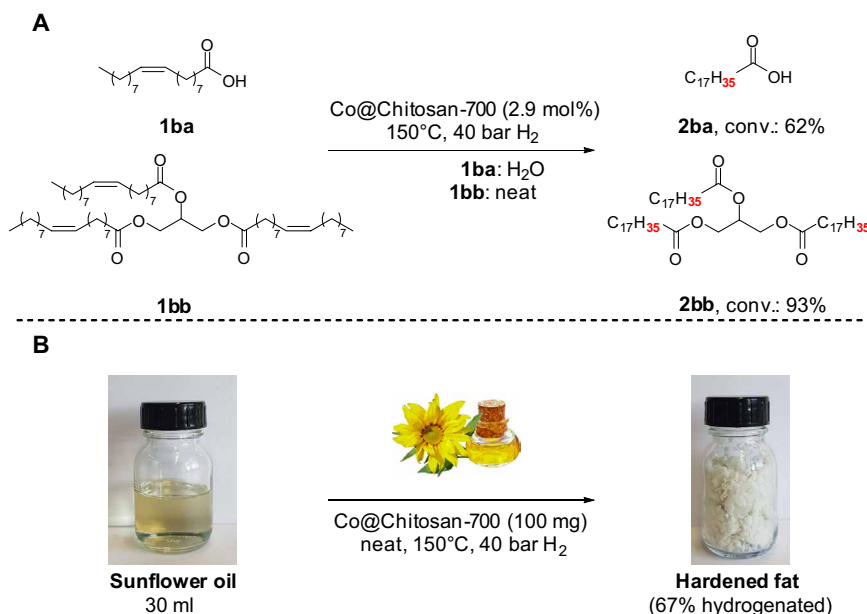
amounts of catalyst and substrate. As shown in Scheme 2, the system tolerates well several functional groups, that is, carboxylic acids (2a), alcohols (2c, 2f, 2g, 2j, 2p, and 2r), halides including bromides (2d and 2v), esters (2e, 2s, and 2w), ethers (2h, 2i, 2k, 2l, 2n, 2p, 2q, and 2v), amides (2m and 2o), methylenedioxy groups (2u), sulfonamides (2x), and coordinating heterocycles (2p and 2y). Nitriles give lower yields (2z and 2aa), possibly due to a competitive coordination of the nitrile group, which partially deactivates the catalyst. This is in accordance with the results obtained using acetonitrile as the solvent (vide supra). Our catalyst allows for selective olefin hydrogenation even in the presence of sensitive ketones (2b), aldehydes (2h), and epoxides (2n). In recent years, there is an increasing interest in fluorinated building blocks (42, 43). However, apparently simple hydrogenation of perfluoroalkenes is rather challenging (44). Nevertheless, a highly fluorinated substrate (2t) was hydrogenated under these mild conditions, albeit to a lesser extent.

Furthermore, the rather complex natural compound quinine was successfully converted to dihydroquinine 2p in excellent isolated yield. In the past, these dihydrocinchona alkaloid derivatives have been used as organocatalysts and ligands in asymmetric catalysis (45, 46). Notably, because of solubility problems, in this case, methanol was chosen as solvent. The same strategy was used for the hydrogenation of solid 2,4,6-tribromophenyl allyl ether 1v to give 2v in 95% yield.

Apart from terminal olefins, which react easily (10 bar H₂, 60°C), internal ones also can be hydrogenated. For example, trisubstituted



Scheme 4. Olefin hydrogenation with Co@Chitosan-700: Investigation of industrially relevant unsaturated hydrocarbons. General conditions: 1.5 mmol substrate, 2.9 mol % (8.8 mg) of catalyst with respect to Co, 1.5 ml of H₂O. Yields were determined via GC using hexadecane as internal standard. ^aReaction was carried out on a 10-ml scale (7.2 g, 64 mmol) without additional solvent. Isolated yield is given. ^bYields were determined via ¹H NMR using mesitylene as internal standard. ^cReaction was carried out on a 5-ml scale (3.5 g, 42.1 mmol) without solvent.



Scheme 5. Hydrogenation of fatty acids and esters. Hydrogenation of (A) oleic acid and its triglyceride triolein and (B) sunflower oil. General conditions: (A) 1.5 mmol substrate, 2.9 mol % (8.8 mg) of catalyst with respect to Co, 0.5 ml of solvent if used, 150°C, 40 bar H₂, 18 hours; (B) 30 ml (25.68 g) of substrate, 100 mg of catalyst, 150°C, 40 bar H₂, 19 hours. Conversions were determined via ¹H NMR using mesitylene as internal standard. Photo Credit: Florian K. Scharnagl, Leibniz-Institut für Katalyse e.V. an der Universität Rostock.

double bonds (**2f** and **2g**) were reduced at 150°C and 40 bar H₂ in 97 and 92% yield, respectively. Obviously, this opens the possibility of selective hydrogenation of an easily accessible double bond in the presence of a less reactive one (47), as was shown for the formation of **2w**. At 60°C, the terminal double bond was selectively hydrogenated, while the internal was not.

As another important class of unsaturated compounds, several aromatic olefins were investigated (Scheme 3). Again, both terminal and internal olefins were effectively converted to the saturated al-

kanes in high yields. Styrene (**2ab**) and derivatives with either electron withdrawing (**2ac**, **2ad**) or electron donating groups (**2ae**–**2ah**), respectively, were converted to the corresponding ethylbenzenes in 81 to 99%. It is noteworthy that primary amines (**2ah**) also were tolerated by the system.

Next, apart from terminal olefins, also 1,2- and 1,1-disubstituted substrates (**2ai**–**2ak** and **2al**–**2ao**, respectively) were investigated. The yields for the latter were, in general, lower than those for 1,2-disubstituted olefins, indicating a reduced catalytic activity. For

instance, *trans*-stilbene was quantitatively hydrogenated to **2ak**, whereas the 1,1-disubstituted diphenylethylene gave 60% yield of **2ao**.

An exemplary industrial application for hydrogenation catalysts is the saturation of diisobutene. Since the ban of MTBE as an anti-knock additive in gasoline in the United States in 2006, isooctane (2,4,4-trimethylpentane) represents an attractive alternative in the petrochemical industry because of its high octane number, aliphatic character, and low vapor pressure (4). Furthermore, it is the primary component of aviation gasoline. It is produced via dimerization of isobutene to diisobutene, a mixture of two isomers, followed by hydrogenation. Many of the known catalysts for this latter reaction are based on noble metals, that is, Pd (48) and Pt (49). In addition, also Ni (50) and scarcely Co (51) gained some attention. Hence, we investigated the performance of Co@Chitosan-700 in the hydrogenation of diisobutene. As can be seen in Scheme 4, this novel material is able to fully hydrogenate diisobutene to give **2ap** on a 10-ml scale. With a metal loading of only 0.08 mole percent (mol %), the desired product was obtained in 95% yield after 5 hours. Using 0.4 mol % of catalyst, the reaction was finished within ~1 hour, which makes Co@Chitosan-700 an interesting candidate in the petrochemical industry.

Similarly, several other nonfunctionalized, aliphatic, unsaturated hydrocarbons were converted well, including terminal (**2at**, **2av**, **2aw**, and **2ax**), internal cyclic (**2aq**, **2ar**, **2as**, and **2ay**), and internal acyclic substrates (**2au**). Notably, even the tetrasubstituted olefin 2,3-dimethyl-2-butene was hydrogenated to **2az** under neat conditions on a 5-ml scale. The reaction was conducted directly in a 25-ml stainless steel autoclave with mechanical stirring to achieve proper mixing. Commonly, such olefins are challenging substrates for hydrogenation (52).

Hydrogenation experiments using 1-octene with D₂ in H₂O and with H₂ in D₂O, respectively, showed that H₂ and D₂ are the hydrogen sources in each case, and not H₂O or D₂O (see Supplementary Materials). Internal octene derivatives were observed when D₂ was used, whereas for H₂ in H₂O or D₂O, respectively, only *n*-octane and traces of 1-octene were detected. This indicates a large kinetic isotope effect of the hydrogenation step, which makes isomerization more likely.

Besides the synthesis of isooctane, the hydrogenation of vegetable oils is another important industrial process, for instance, in the production of margarine (vide supra) (5). These oils consist mainly of triglycerides of fatty acids, which can be either saturated, mono, or multiple unsaturated. In general, a higher degree of saturation increases the melting point of the acids and triglycerides. By altering the degree of hydrogenation, the melting point can be adjusted and tailored for applications. Therefore, we investigated the behavior of Co@Chitosan-700 in the hydrogenation of oleic acid [**1ba**, (9*Z*)-octadec-9-enoic acid] and its triglyceride triolein (**1bb**) (Scheme 5A).

Both substrates were hydrogenated to the corresponding products stearic acid (**2ba**) and tristearin (**2bb**) in good to very good yields. Tristearin is generally recognized as safe (GRAS) food additive (53). It has many applications, for instance, as hardening agent in the manufacture of soap and candles. The fact that the degree of hydrogenation is lower for oleic acid than for triolein might be due to coordination of the acid functionality to cobalt on the catalyst surface. This would be consistent with the yield for the carboxylic acid **2a** (Scheme 2), which was comparable (69%). Furthermore, in the case of **2ba**, the reaction solution became slightly

pinkish, indicating complexation of cobalt. This was not the case for the triglyceride.

As another application, the hydrogenation of sunflower oil was investigated on a 30-ml scale under neat conditions using 100 mg of catalyst. The oil consists mainly of triglycerides of unsaturated fatty acids (89%), which are oleic acid (monounsaturated, 30%) and linoleic acid (double unsaturated, 59%) (54). To our delight, hydrogenation leads to a white solid, and ¹H NMR revealed a conversion of 67% (Scheme 5B).

For the food industry, it is crucial that the product does not contain significant amounts of metal. Determination of the cobalt content of the product via AAS revealed no metal contamination. This analysis was carried out three times, and in each case, the amount of cobalt was below the detection limit of 0.04 ppm.

CONCLUSION

In conclusion, we have developed a versatile, biowaste-derived, and easily prepared catalyst, which permits olefin hydrogenation in water under mild conditions and does not require any additives. A variety of more than 50 terminal and internal alkenes were hydrogenated with broad functional group tolerance. In the presence of Co@Chitosan-700, industrially important processes can be successfully carried out, that is, hydrogenation of diisobutene and fatty acids and their esters, including sunflower oil. Recycling studies demonstrated the simplicity of reusing the catalyst, as well as its stability during several consecutive runs. Compared to established metallic nanoparticles, the present system is highly stable toward air and water for months. Hence, we believe that the here reported material is one of the most promising nonnoble metal-based heterogeneous catalysts for olefin hydrogenations including industrial applications.

MATERIALS AND METHODS

Unsupported catalysts—Preparation

Unsupported catalysts were prepared by stirring Co(OAc)₂·4H₂O (1.00 g, 4.01 mmol, 1.0 equiv.) and chitosan (1.29 g, 8.03 mmol, 2.0 equiv.) in 80 ml of ethanol at 65°C for 18 hours. Afterward, the solvent was removed at the rotary evaporator and the residue was dried overnight at 65°C by applying high vacuum. The dried sample was ground in an agate mortar, pyrolyzed at temperatures between 700° and 1000°C, and ground again in an agate mortar. The catalysts were stored in glass vials in air without special protection. The catalysts were labeled as Co@Chitosan-temperature (for example, Co@Chitosan-700).

Supported catalysts—Preparation

One gram of supported catalyst was prepared by stirring Co(OAc)₂·4H₂O (126.8 mg, 0.51 mmol, 1.0 equiv.) and chitosan (164.4 mg, 1.02 mmol, 2.0 equiv.) in 80 ml of ethanol at 65°C for 18 hours. Afterward, inorganic support (708.8 mg) was added and the mixture was stirred for 2 hours. The solvent was removed at the rotary evaporator and the residue was dried overnight at 65°C by applying high vacuum. The dried sample was ground in an agate mortar, pyrolyzed at temperatures between 700° and 1000°C, and ground again in an agate mortar. The catalyst was stored in glass vials in the air without special protection. The catalysts were labeled as Co/Chitosan@support-temperature (for example, Co/Chitosan@BN-1000).

General catalytic procedure

A 4-ml screw cap vial was charged with catalyst (8.8 mg, 2.9 mol %), substrate (1.5 mmol), 1.5 ml of solvent, and a glass-coated stirring bar. The vial was closed by polytetrafluoroethylene (PTFE)/white rubber septum (Wheaton 13 mm Septa) and phenolic cap and connected with atmosphere with a needle. The vial was fixed in an alloy plate and put into a Parr 4560 series autoclave (300 ml). At room temperature, the autoclave was flushed with H₂ three times and H₂ was charged at the required pressure. The autoclave was placed in an aluminum block on a heating plate equipped with magnetic stirring. The reaction was heated for 18 hours. Afterward, the autoclave was cooled in an ice bath and the pressure was carefully released. For GC analysis, hexadecane (32 μ l) was added into the reaction mixture as an internal standard. The mixture was diluted with ethyl acetate, stirred properly, and the organic fraction was analyzed by GC. For ¹H and ¹³C NMR, instead of hexadecane, mesitylene (20 μ l) was added into the reaction mixture as an internal standard, and 2 ml of CDCl₃ was added. After proper stirring, the organic fraction was filtered through a 0.2- μ m PTFE syringe filter, and both NMR and GC were measured. The obtained NMR spectra were compared with the ones reported in the literature.

Isolation of products was done by extraction with dichloromethane (DCM) or ether, followed by filtration through a 0.2- μ m PTFE syringe filter. 1,1-Diphenylethane (**2ao**) was purified by column chromatography over silica using hexane as an eluent.

Upscale procedure for diisobutene

A 25-ml stainless steel autoclave with mechanical stirrer was loaded with 50 mg of catalyst and 10 ml (7.0584 g, 62.9 mmol) of substrate, which was dried over Na and freshly distilled. The autoclave was closed and flushed with H₂ three times. H₂ (40 bar) was charged, and the autoclave was heated to 150°C with an aluminum block and stirred properly. When the pressure dropped to around 5 bar, it was readjusted to 40 bar. After the denoted reaction time, the autoclave was cooled with an ice bath and the pressure was carefully released. The mixture was filtered through a filter paper into a round bottom flask (6.843 g, 59.9 mmol, 95%). Mesitylene was added as internal standard, and ¹H NMR was measured.

Upscale procedure for 2,3-dimethyl-2-butene

A 25-ml stainless steel autoclave with mechanical stirrer was loaded with 2.9 mol % of catalyst (245.2 mg) and 5 ml (3.5 g, 42.1 mmol) of substrate, which was filtered over a plug of basic Al₂O₃ prior to the reaction. The autoclave was closed and flushed with H₂ three times. H₂ (40 bar) was charged, and the autoclave was heated to 150°C with an aluminum block and stirred properly. After 18 hours, the autoclave was cooled with an ice bath and the pressure was carefully released. The mixture was filtered through a 0.2- μ m PTFE syringe filter. Mesitylene was added as internal standard, and ¹H NMR was measured.

Upscale procedure for sunflower oil

A 100-ml stainless steel autoclave with mechanical stirrer was loaded with 100 mg of catalyst and 30 ml of sunflower oil. The autoclave was closed and flushed with H₂ three times. H₂ (40 bar) was charged, and the autoclave was heated to 150°C with a heating system and stirred properly. After 19 hours, the autoclave was cooled with an ice bath and the pressure was carefully released. The solid was taken up in DCM and sucked with a PTFE tube into a big round bottom

flask. It was dissolved in DCM completely and filtered off the catalyst with a PTFE tube, wrapped with filter paper. The volatiles were removed in vacuo, and the remaining oil became solid at room temperature. For further drying, it was heated and melted with an oil bath (bath temperature, 65°C) and connected to high vacuum for several hours. The degree of hydrogenation was determined by measuring ¹H NMR with mesitylene as internal standard. From both the product and the starting material, the mol % of double bonds was calculated with mesitylene as internal standard, and the amounts before and after the reaction were compared and the conversion was calculated with respect to that difference.

Procedure for hydrogenation of 1-octene with D₂

A 25-ml stainless steel autoclave with mechanical stirrer was loaded with 2.9 mol % of catalyst (46.6 mg), closed, and set under argon carefully. In a flow of argon, 8.0 mmol 1-octene and 12 ml of H₂O were added. The autoclave was connected to a D₂ bottle, and the connection was put under argon. Then, 10 bar D₂ was introduced into the reactor, and the autoclave was heated to 60°C with an aluminum block and stirred properly. After 18 hours, the autoclave was cooled with an ice bath and the pressure was carefully released. The organic phase was diluted with ethyl acetate, filtered through a 0.2- μ m PTFE syringe filter, and GC-mass spectrometry (MS) was measured.

Recycling procedure

A 4-ml screw-cap vial was charged with Co@Chitosan-700 (8.8 mg, 2.9 mol %), 1-octene (1.5 mmol, 168.3 mg, 237 μ l), 1.5 ml of H₂O, and a glass-coated stirring bar. The vial was closed by a PTFE/white rubber septum (Wheaton 13 mm Septa) and phenolic cap and connected with atmosphere with a needle. The vial was fixed in an alloy plate and put into a Parr 4560 series autoclave (300 ml). At room temperature, the autoclave was flushed with H₂ three times, and 10 bar H₂ was charged. The autoclave was placed in an aluminum block on a heating plate equipped with magnetic stirring. The reaction was heated at 60°C for 18 hours. Afterward, the autoclave was cooled with an ice bath, and the pressure was carefully released. For GC analysis, hexadecane (32 μ l) was added into the reaction mixture as an internal standard. The mixture was diluted with ethyl acetate, stirred properly, and the organic fraction was analyzed by GC. Then, a magnet was placed at the outer wall of the vial, in a way that as much catalyst as possible was attracted by it. The liquids were decanted off, and the catalyst was washed with acetone three times and once with deionized water. Then, new substrate was added, along with 1.5 ml of H₂O, and the vial was closed by a new PTFE/white rubber septum (Wheaton 13 mm Septa) and phenolic cap and connected with atmosphere with a fresh needle. The next reaction was started analogously to the first one.

SUPPLEMENTARY MATERIALS

Supplementary material for this article is available at <http://advances.sciencemag.org/cgi/content/full/4/9/eaau1248/DC1>

Table S1. Screening of different supports, substrates, solvents, conditions, and temperatures of pyrolysis.

Table S2. Solvent screening for the hydrogenation of 1-octene.

Table S3. Content of C, H, N, and Co before and after pyrolysis.

Table S4. Leached metal content in different reaction media detected by AAS.

Scheme S1. Plot of conversions (top) and yields (bottom) against time in different solvent conditions of Co@Chitosan-700.

Fig. S1. Recycling of Co@Chitosan-700.

Fig. S2. High-resolution (HR)-STEM images of Co@Chitosan-700.

Fig. S3. EELS and energy-dispersive x-ray spectroscopy (EDXS) elemental distributions of carbon, nitrogen, oxygen and cobalt, along with the overlay put onto the annular dark-field (ADF) survey image of Co@Chitosan-700.

Fig. S4. ADF survey image, EELS, and EDX spectra of fresh Co@Chitosan-700.

Fig. S5. HR-STEM images of nine-times-used Co@Chitosan-700.

Fig. S6. ADF survey image, EELS, and EDX spectra of recycled Co@Chitosan-700.

Fig. S7. EELS and EDXS elemental maps of carbon, oxygen, and cobalt, and the overlay on the corresponding ADF survey image of nine-times-used Co@Chitosan-700.

Fig. S8. Comparison of O-K edge from Co oxide particles of fresh and nine-times-used Co@Chitosan-700 showing the difference in edge fine structure.

Fig. S9. Powder pattern of fresh Co@Chitosan-700.

Fig. S10. Powder pattern of nine-times-used Co@Chitosan-700.

REFERENCES AND NOTES

- H.-U. Blaser, F. Spindler, M. Thommen, *The Handbook of Homogeneous Hydrogenation*, J. G. De Vries, C. J. Elsevier, Eds. (Wiley-VCH, 2008), chap. 37.
- B. Chen, U. Dingerdissen, J. G. E. Krauter, H. G. J. Lansink Rotgerink, K. Möbus, D. J. Ostgard, P. Panster, T. H. Riermeier, S. Seebald, T. Tacke, H. Trauthwein, New developments in hydrogenation catalysis particularly in synthesis of fine and intermediate chemicals. *Appl. Catal. A* **280**, 17–46 (2005).
- L. A. Saudan, Hydrogenation processes in the synthesis of perfumery ingredients. *Acc. Chem. Res.* **40**, 1309–1319 (2007).
- B. M. Goortani, A. Gaurav, A. Deshpande, F. T. T. Ng, G. L. Rempel, Production of Isooctane from Isobutene: Energy Integration and Carbon Dioxide Abatement via Catalytic Distillation. *Ind. Eng. Chem. Res.* **54**, 3570–3581 (2015).
- G. R. List, J. W. King, *Hydrogenation of Fats and Oils: Theory and Practice* (AOCS Press, ed. 2, 2015).
- S. Lavielle, S. Bory, B. Moreau, M. J. Luche, A. Marquet, A total synthesis of biotin based on the stereoselective alkylation of sulfoxides. *J. Am. Chem. Soc.* **100**, 1558–1563 (1978).
- I. Bauer, H.-J. Knölker, Iron Catalysis in Organic Synthesis. *Chem. Rev.* **115**, 3170–3387 (2015).
- S. C. Bart, E. Lobkovsky, P. J. Chirik, Preparation and molecular and electronic structures of iron(0) dinitrogen and silane complexes and their application to catalytic hydrogenation and hydrosilylation. *J. Am. Chem. Soc.* **126**, 13794–13807 (2004).
- P. J. Chirik, Iron- and cobalt-catalyzed alkene hydrogenation: Catalysis with both redox-active and strong field ligands. *Acc. Chem. Res.* **48**, 1687–1695 (2015).
- M. Villa, D. Miesel, A. Hildebrandt, F. Ragaini, D. Schaarschmidt, A. J. v. Wangelin, Synthesis and catalysis of redox-active Bis(imino)acenaphthene (BIAN) iron complexes. *ChemCatChem* **9**, 3203–3209 (2017).
- N. G. Léonard, P. J. Chirik, Air-Stable α -diimine nickel precatalysts for the hydrogenation of hindered, unactivated alkenes. *ACS Catal.* **8**, 342–348 (2018).
- T. J. Mooibroek, E. C. M. Wenker, W. Smit, I. Mutikainen, M. Lutz, E. Bouwman, Homogeneous hydrogenation and isomerization of 1-octene catalyzed by nickel(II) complexes with bidentate diarylphosphane ligands. *Inorg. Chem.* **52**, 8190–8201 (2013).
- I. M. Angulo, A. M. Kluwer, E. Bouwman, Fast and selective homogeneous hydrogenation with nickel(II) phosphane catalysts. *Chem. Commun.* **10**, 2689–2690 (1998).
- Y. Wang, A. Kostenko, S. Yao, M. Driess, Divalent silicon-assisted activation of dihydrogen in a bis(N-heterocyclic silylene)xanthene nickel(0) complex for efficient catalytic hydrogenation of olefins. *J. Am. Chem. Soc.* **139**, 13499–13506 (2017).
- K. Tokmic, C. R. Markus, L. Zhu, A. R. Fout, Well-defined cobalt(I) dihydrogen catalyst: Experimental evidence for a Co(I)/Co(III) redox process in Olefin hydrogenation. *J. Am. Chem. Soc.* **138**, 11907–11913 (2016).
- P. Büschelberger, D. Gärtner, E. Reyes-Rodríguez, F. Kreyenschmidt, K. Koszinowski, A. J. von Wangelin, R. Wolf, Alkene Metalates as Hydrogenation Catalysts. *Chemistry* **23**, 3139–3151 (2017).
- S. Monfette, Z. R. Turner, S. P. Semproni, P. J. Chirik, Enantiopure C1-symmetric bis(imino)pyridine cobalt complexes for asymmetric alkene hydrogenation. *J. Am. Chem. Soc.* **134**, 4561–4564 (2012).
- M. R. Friedfeld, M. Shevlin, J. M. Hoyt, S. W. Kraska, M. T. Tudge, P. J. Chirik, Cobalt precursors for high-throughput discovery of base metal asymmetric alkene hydrogenation catalysts. *Science* **342**, 1076–1080 (2013).
- R. P. Yu, J. M. Darmon, C. Milsmann, G. W. Margulieux, S. C. E. Stieber, S. DeBeer, P. J. Chirik, Catalytic hydrogenation activity and electronic structure determination of bis(arylimidazol-2-ylidene)pyridine cobalt alkyl and hydride complexes. *J. Am. Chem. Soc.* **135**, 13168–13184 (2013).
- M. R. Friedfeld, G. W. Margulieux, B. A. Schaefer, P. J. Chirik, Bis(phosphine)cobalt dialkyl complexes for directed catalytic alkene hydrogenation. *J. Am. Chem. Soc.* **136**, 13178–13181 (2014).
- P. Ji, K. Manna, Z. Lin, A. Urban, F. X. Greene, G. Lan, W. Lin, Single-site cobalt catalysts at new $Zr_6(\mu_2-O)_8(\mu_2-OH)_4$ metal-organic framework nodes for highly active hydrogenation of alkenes, imines, carbonyls, and heterocycles. *J. Am. Chem. Soc.* **138**, 12234–12242 (2016).
- N. C. Thacker, Z. Lin, T. Zhang, J. C. Gilhula, C. W. Abney, W. Lin, Robust and porous β -diketiminate-functionalized metal-organic frameworks for earth-abundant-metal-catalyzed C–H amination and hydrogenation. *J. Am. Chem. Soc.* **138**, 3501–3509 (2016).
- T. Zhang, K. Manna, W. Lin, Metal-organic frameworks stabilize solution-inaccessible cobalt catalysts for highly efficient broad-scope organic transformations. *J. Am. Chem. Soc.* **138**, 3241–3249 (2016).
- K. Manna, P. Ji, Z. Lin, F. X. Greene, A. Urban, N. C. Thacker, W. Lin, Chemoselective single-site Earth-abundant metal catalysts at metal-organic framework nodes. *Nat. Commun.* **7**, 12610 (2016).
- R. V. Jagadeesh, A.-E. Surkus, H. Junge, M.-M. Pohl, J. Radnik, J. Rabeah, H. Huan, V. Schünemann, A. Brückner, M. Beller, Nanoscale Fe_2O_3 -based catalysts for selective hydrogenation of nitroarenes to anilines. *Science* **342**, 1073–1076 (2013).
- F. A. Westerhaus, R. V. Jagadeesh, G. Wienhöfer, M.-M. Pohl, J. Radnik, A.-E. Surkus, J. Rabeah, K. Junge, H. Junge, M. Nielsen, A. Brückner, M. Beller, Heterogenized cobalt oxide catalysts for nitroarene reduction by pyrolysis of molecularly defined complexes. *Nat. Chem.* **5**, 537–543 (2013).
- D. Formenti, F. Ferretti, C. Topf, A.-E. Surkus, M.-M. Pohl, J. Radnik, M. Schneider, K. Junge, M. Beller, F. Ragaini, Co-based heterogeneous catalysts from well-defined α -diimine complexes: Discussing the role of nitrogen. *J. Catal.* **351**, 79–89 (2017).
- W. Liu, L. Zhang, W. Yan, X. Liu, X. Yang, S. Miao, W. Wang, A. Wang, T. Zhang, Single-atom dispersed Co–N–C catalyst: Structure identification and performance for hydrogenative coupling of nitroarenes. *Chem. Sci.* **7**, 5758–5764 (2016).
- L. Liu, P. Concepción, A. Corma, Non-noble metal catalysts for hydrogenation: A facile method for preparing Co nanoparticles covered with thin layered carbon. *J. Catal.* **340**, 1–9 (2016).
- Z. Wei, Y. Chen, J. Wang, D. Su, M. Tang, S. Mao, Y. Wang, Cobalt encapsulated in N-doped graphene layers: An efficient and stable catalyst for hydrogenation of quinoline compounds. *ACS Catal.* **6**, 5816–5822 (2016).
- R. V. Jagadeesh, K. Murugesan, A. S. Alshammari, H. Neumann, M.-M. Pohl, J. Radnik, M. Beller, MOF-derived cobalt nanoparticles catalyze a general synthesis of amines. *Science* **358**, 326–332 (2017).
- B. Sahoo, A.-E. Surkus, M.-M. Pohl, J. Radnik, M. Schneider, S. Bachmann, M. Scalone, K. Junge, M. Beller, Development of biomass-derived non-noble metal catalysts for selective hydrodehalogenation of alkyl and (hetero)aryl halides. *Angew. Chem. Int. Ed.* **56**, 11242–11247 (2017).
- B. Sahoo, D. Formenti, C. Topf, S. Bachmann, M. Scalone, K. Junge, M. Beller, Biomass-derived catalysts for selective hydrogenation of nitroarenes. *ChemSusChem* **10**, 3035–3039 (2017).
- N. Yan, X. Chen, Sustainability: Don't waste seafood waste. *Nature* **524**, 155–157 (2015).
- E. Guibal, Interactions of metal ions with chitosan-based sorbents: A review. *Sep. Purif. Technol.* **38**, 43–74 (2004).
- E. Taboada, G. Cabrera, R. Jimenez, G. Cardenas, A kinetic study of the thermal degradation of chitosan-metal complexes. *J. Appl. Polym. Sci.* **114**, 2043–2052 (2009).
- E. Guibal, Heterogeneous catalysis on chitosan-based materials: A review. *Prog. Polym. Sci.* **30**, 71–109 (2005).
- A. Primo, P. Atienzar, E. Sanchez, J. M. Delgado, H. Garcia, From biomass wastes to large-area, high-quality, N-doped graphene: Catalyst-free carbonization of chitosan coatings on arbitrary substrates. *Chem. Commun.* **48**, 9254–9256 (2012).
- K. Zhu, Y. Ju, J. Xu, Z. Yang, S. Gao, Y. Hou, Magnetic nanomaterials: Chemical design, synthesis, and potential applications. *Acc. Chem. Res.* **51**, 404–413 (2018).
- B. H. Lipshutz, F. Gallou, S. Handa, Evolution of solvents in organic chemistry. *ACS Sustainable Chem. Eng.* **4**, 5838–5849 (2016).
- Z. Zhang, Surface effects in the energy loss near edge structure of different cobalt oxides. *Ultramicroscopy* **107**, 598–603 (2007).
- D. O'Hagan, Fluorine in health care: Organofluorine containing blockbuster drugs. *J. Fluorine Chem.* **131**, 1071–1081 (2010).
- K. Müller, C. Faeh, F. Diederich, Fluorine in pharmaceuticals: Looking beyond intuition. *Science* **317**, 1881–1886 (2007).
- Y. Carcenac, M. Tordeux, C. Wakselman, P. Diter, Convenient synthesis of fluorinated alkanes and cycloalkanes by hydrogenation of perfluoroalkylalkenes under ultrasound irradiation. *J. Fluorine Chem.* **126**, 1347–1355 (2005).
- E. N. Jacobsen, I. Marko, W. S. Mungall, G. Schroeder, K. B. Sharpless, Asymmetric dihydroxylation via ligand-accelerated catalysis. *J. Am. Chem. Soc.* **110**, 1968–1970 (1988).
- S.-K. Tian, Y. Chen, J. Hang, L. Tang, P. McDaid, L. Deng, Asymmetric organic catalysis with modified cinchona alkaloids. *Acc. Chem. Res.* **37**, 621–631 (2004).
- M. Miyazaki, S. Furukawa, T. Komatsu, Regio- and chemoselective hydrogenation of dienes to monoenes governed by a well-structured bimetallic surface. *J. Am. Chem. Soc.* **139**, 18231–18239 (2017).

48. S. Talwalkar, S. Thotla, K. Sundmacher, S. Mahajani, Simultaneous hydrogenation and isomerization of diisobutylenes over pd-doped ion-exchange resin catalyst. *Ind. Eng. Chem. Res.* **48**, 10857–10863 (2009).
49. M. S. Lylykangas, P. A. Rautanen, A. O. I. Krause, Hydrogenation and deactivation kinetics in the liquid-phase hydrogenation of isooctenes on Pt/Al₂O₃. *Ind. Eng. Chem. Res.* **43**, 1641–1648 (2004).
50. M. S. Lylykangas, P. A. Rautanen, A. O. I. Krause, Liquid-phase hydrogenation kinetics of isooctenes on Ni/Al₂O₃. *AIChE J.* **49**, 1508–1515 (2003).
51. M. S. Lylykangas, P. A. Rautanen, A. Krause, Liquid-phase hydrogenation kinetics of isooctenes on Co/SiO₂. *Appl. Catal. A* **259**, 73–81 (2004).
52. S. Kraft, K. Ryan, R. B. Kargbo, Recent advances in asymmetric hydrogenation of tetrasubstituted olefins. *J. Am. Chem. Soc.* **139**, 11630–11641 (2017).
53. <https://www.fda.gov/>, checked on 19.03.2018
54. B. P. Commission, *British Pharmacopoeia 2005* (Stationery Office, 2005).

Acknowledgments: We thank the analytical department of the Leibniz-Institute for Catalysis, Rostock, and A.-E. Surkus for the fruitful discussions. **Funding:** We acknowledge the support from the Federal Ministry of Education and Research (BMBF project: KataPlasma, FKZ: 03XP0060) and the State of Mecklenburg-West Pomerania. **Author**

contributions: M.B., F.K.S., and M.F.H. planned the project. F.K.S. and M.F.H. developed and prepared the catalysts, and conducted preliminary test reactions. F.K.S. optimized the system. F.K.S. and F.F. performed the substrate scope and upscaling investigations. F.K.S., F.F., M.F.H., and M.B. wrote the paper. C.K. performed the transmission electron microscopy (TEM) measurements and analysis. H.L. performed the XRD measurements and analysis. R.J. assisted with technical support concerning high-pressure apparatus. **Competing interests:** The authors declare that they have no competing interests. **Data and materials availability:** All data needed to evaluate the conclusions in the paper are present in the paper and/or the Supplementary Materials. Additional data related to this paper may be requested from the authors.

Submitted 9 May 2018

Accepted 10 August 2018

Published 21 September 2018

10.1126/sciadv.aau1248

Citation: F. K. Scharnagl, M. F. Hertrich, F. Ferretti, C. Kreyenschulte, H. Lund, R. Jackstell, M. Beller, Hydrogenation of terminal and internal olefins using a biowaste-derived heterogeneous cobalt catalyst. *Sci. Adv.* **4**, eaau1248 (2018).

Hydrogenation of terminal and internal olefins using a biowaste-derived heterogeneous cobalt catalyst

Florian Korbinian Scharnagl, Maximilian Franz Hertrich, Francesco Ferretti, Carsten Kreyenschulte, Henrik Lund, Ralf Jackstell and Matthias Beller

Sci Adv 4 (9), eaau1248.
DOI: 10.1126/sciadv.aau1248

ARTICLE TOOLS

<http://advances.sciencemag.org/content/4/9/eaau1248>

SUPPLEMENTARY MATERIALS

<http://advances.sciencemag.org/content/suppl/2018/09/17/4.9.eaau1248.DC1>

REFERENCES

This article cites 50 articles, 4 of which you can access for free
<http://advances.sciencemag.org/content/4/9/eaau1248#BIBL>

PERMISSIONS

<http://www.sciencemag.org/help/reprints-and-permissions>

Use of this article is subject to the [Terms of Service](#)

Science Advances (ISSN 2375-2548) is published by the American Association for the Advancement of Science, 1200 New York Avenue NW, Washington, DC 20005. 2017 © The Authors, some rights reserved; exclusive licensee American Association for the Advancement of Science. No claim to original U.S. Government Works. The title *Science Advances* is a registered trademark of AAAS.

5. Selected Publications

5.2. Biomolecule-derived supported cobalt nanoparticles for hydrogenation of industrial olefins, natural oils and more in water

A. Pews-Davtyan, F. K. Scharnagl, M. F. Hertrich, C. R. Kreyenschulte, S. Bartling, H. Lund, R. Jackstell, M. Beller, *Green Chem.* **2019**, *21*, 5104-5112.

Reproduced from *Green Chem.* **2019**, *21*, 5104-5112 with permission from the Royal Society of Chemistry.

Contribution: F.K.S. contributed to the test-reactions of the catalysts and assisted A.P.-D. to optimise the system. The overall contribution is about 15%.



Cite this: *Green Chem.*, 2019, **21**, 5104

Biomolecule-derived supported cobalt nanoparticles for hydrogenation of industrial olefins, natural oils and more in water†

Anahit Pews-Davtyan, Florian Korbinian Scharnagl, Maximilian Franz Hertrich, Carsten Kreyenschulte, Stephan Bartling, Henrik Lund, Ralf Jackstell and Matthias Beller*

Catalytic hydrogenation of olefins using noble metal catalysts or pyrophoric RANEY® nickel is of high importance in the chemical industry. From the point of view of green and sustainable chemistry, design and development of Earth-abundant, less toxic, and more environmentally friendly catalysts are highly desirable. Herein, we report the convenient preparation of active cobalt catalysts and their application in hydrogenations of a wide range of terminal and internal carbon–carbon double bonds in water under mild conditions. Catalysts are prepared on multi-gram scale by pyrolysis of cobalt acetate and uracil, guanine, adenine or L-tryptophan. The most active material Co-Ura/C-600 showed good productivity in industrially relevant hydrogenation of diisobutene to isooctane and in natural oil hardening.

Received 17th April 2019,
Accepted 13th August 2019

DOI: 10.1039/c9gc01276a

rsc.li/greenchem

Introduction

Catalytic hydrogenation of olefins is one of the central synthetic methods in chemistry and intensively used in the petrochemical, pharmaceutical, agrochemical, fine chemical and food industries.^{1,2} Typically, these reductions are accomplished by using molecular hydrogen in the presence of sensitive RANEY® nickel or heterogeneous precious metal catalysts, predominantly based on palladium, rhodium, iridium, or ruthenium. Their limited availability, price, and sometimes toxicity created enormous interest in alternative technologies and catalysts.^{3,4} In this respect, design and development of Earth-abundant 3d-metal based hydrogenation catalysts are highly desirable. Among the different 3d metals, especially cobalt showed promising potential to be a good alternative to the noble metals regarding activity and generality. Therefore in the past decade, the development of efficient homogeneous^{5,6} and heterogeneous⁷ cobalt based catalysts^{8–10} has gained attention.¹¹ Exemplarily, efficient homogeneous complexes for directed or asymmetric olefin hydrogenation were synthesized by Chirik and co-workers.^{12–14} In addition, in recent years the groups of von Wangelin,^{15–18} Yang,^{9,10} and Lin^{19–21} reported notable advancements. Complementary to such molecularly

defined systems, more stable and practical heterogeneous cobalt catalysts have attracted considerable attention. For example, the synthesis of olefin-stabilized Co nanoparticles¹⁸ and solid Zr-MTBC-CoH catalysts²⁰ has been reported for catalytic hydrogenations of alkenes, imines, carbonyls, nitroarenes, and heterocycles.^{9,16,22}

During the last decade, our group also developed novel cobalt-based homogeneous²³ and heterogeneous^{24–30} catalysts. In this regard, herein, we report the convenient preparation of novel heterogeneous catalysts *via* pyrolysis of cobalt acetate with biological N-containing ligands on different supports (carbon and aluminium oxides). N-Ligands were chosen from commercially available and relatively cheap amino acid tryptophan (Trp) and purine or pyrimidine nucleobases guanine (Gua), adenine (Ade) and uracil (Ura). To the best of our knowledge to date these nitrogen-rich ligands (Fig. 1) have not been used in the preparation of cobalt heterogeneous catalysts.³¹ Similarly, cobalt homogeneous complexes with nucleobases, *e.g.* uracil or modified uracil, have rarely been prepared before and have not been used in catalysis.^{32–34} For the first time, the

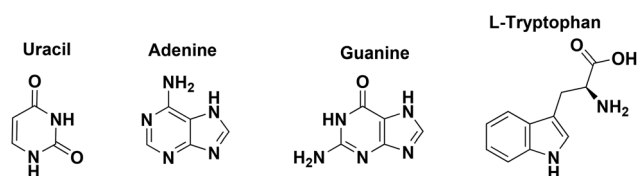


Fig. 1 N-Containing biological ligands used for catalyst preparation.

Leibniz-Institut für Katalyse e.V. an der Universität Rostock, Albert-Einstein-Straße 29a, D-18059 Rostock, Germany. E-mail: matthias.beller@catalysis.de

† Electronic supplementary information (ESI) available: General experimental procedures, characterisation data and NMR spectra. See DOI: 10.1039/c9gc01276a

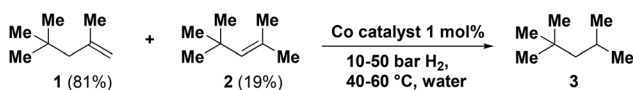
catalytic activity of such materials is demonstrated in hydrogenations of a wide range of substrates. Advantageously, reactions can be performed in water without using any additives.^{35,36}

Results and discussion

We initiated our study on the development of new hydrogenation catalysts with the preparation of more than 20 potentially active cobalt catalysts.

All the materials were prepared in a straightforward manner on multi-gram scale starting from commercially available cobalt(II) acetate, the corresponding N-ligands (Fig. 1), and Vulcan XC72R or aluminium oxides as inorganic supports (see Experimental: catalyst preparation, ESI†). Then, the obtained cobalt pre-catalysts with a 3 wt% metal content were subjected to pyrolysis at 500, 600, 700, 800 or 1000 °C for 2 h under argon and are denoted as Co-ligand/support- $T_{\text{pyrolysis}}$ (additionally (a) or (b) was used, if the Al_2O_3 support was acidic or basic, respectively; dry – if non pyrolyzed; air – if pyrolyzed under static air, ESI†). The catalytic performance of all materials was evaluated in the industrially relevant diisobutene hydrogenation as a model reaction (Scheme 1).

Diisobutene is formed by dimerization of isobutene and is generally available as an equilibrium mixture (~4:1) of its isomers, namely terminal olefin **1** (2,4,4-trimethylpent-1-ene) and its internal isomer **2** (2,4,4-trimethylpent-2-ene). In recent years, there has been increasing interest in the hydrogenation of diisobutene for the preparation of isooctane **3** (2,2,4-trimethylpentane) as an alternative anti-knock gasoline additive.³⁷ Due to environmental concerns of existing products, *e.g.* methyl *tert*-butyl ether (MTBE), the petrochemical industry is seeking more environmentally friendly octane booster compounds. In this respect, isooctane is one of the leading candidates because of its high octane number and economically attractive production using existing infrastructure. In fact, this process was successfully implemented in a world-scale plant (Fortum's NEXOCTANE technology).³⁸



Scheme 1 Diisobutene (mixture of isomers **1** + **2**) hydrogenation to isooctane **3**.

Diisobutene hydrogenation to isooctane **3** has been reported in the past mainly with noble-metal catalysts, such as Pd^{39,40} and Pt.⁴¹ Besides, studies on kinetics of diisobutene hydrogenation were performed by Lylykangas *et al.* using commercial nickel–alumina $\text{Ni}/\text{Al}_2\text{O}_3$ ⁴² and Co/SiO_2 ⁴³ catalysts. Other cobalt catalysts have scarcely been studied in this hydrogenation process, although there is an increasing interest in cobalt-catalysed hydrogenation.²³ As an example, in 2018, we reported the hydrogenation of different olefins including diisobutene in the presence of biowaste-derived cobalt chitosan cat-

alysts. However, comparably harsh conditions (150 °C, 40 bar hydrogen) were necessary for the latter reaction.³⁰ To identify more active and improved cobalt catalysts, our newly prepared materials and commercial ones were screened in the model reaction (Scheme 1) under mild conditions in water as a green solvent (Table 1; ESI – Table S1†). More specifically, the experiments were performed in high pressure equipment in parallel vials, using 1.5 mmol diisobutene and 1 mol% of catalyst in 1.5 ml of water at 60 °C and under 30 bar of molecular hydrogen pressure for 18 h. As shown in Table 1, commercial catalysts (Table 1, entries 1 and 2), non-pyrolyzed materials (Table 1, entries 3 and 10) and cobalt samples prepared without biological ligands (Table 1, entries 4 and 11) were completely inactive, indicating the crucial role of ligands and importance of pyrolysis conditions in the formation of the catalytically active cobalt species. Among the pyrolyzed materials, adenine (Ade), guanine (Gua) and tryptophan (Trp) based cobalt catalysts demonstrated low or moderate catalytic activity (Table 1, entries 14–20). To our delight, uracil (Ura) based and Vulcan supported catalysts were more active. Furthermore, at 600 and 700 °C, pyrolyzed materials turned out to be excellent catalysts for diisobutene (**1** + **2**) hydrogenation ensuring quantitative conversions and excellent yields of isooctane **3** even with 0.5 mol% catalyst under very mild conditions (Table 1, entries 6 and 7).

Table 1 Hydrogenation of diisobutene (Scheme 1) in water with different supported and biomolecule ligated cobalt catalysts^a

| Entry | Catalyst | Conversion 1 + 2 ^b [%] | Yield 3 ^b [%] |
|-------|---|---|---------------------------------|
| 1 | Co_3O_4 | 0 | 0 |
| 2 | CoO_4W | 2 | Traces |
| 3 | Co-Ura/C-dry | 0 | 0 |
| 4 | Co/C-600 | 5 | 0 |
| 5 | Co-Ura/C-500 | 65 | 65 |
| 6 | Co-Ura/C-600 | 100 (100 ^c) | >99 (>99 ^c) |
| 7 | Co-Ura/C-700 | 100 | >99 |
| 8 | Co-Ura/C-800 | 96 | 94 |
| 9 | Co-Ura/C-1000 | 37 | 35 |
| 10 | Co-Ura/ Al_2O_3 (b)-dry | 4 | 0 |
| 11 | Co/ Al_2O_3 (b)-800 | 8 | 0 |
| 12 | Co-Ura/ Al_2O_3 (b)-700 | 2 | Traces |
| 13 | Co-Ura/ Al_2O_3 (b)-800 | 6 | 5 |
| 14 | Co-Trp/C-700 | 3 | 2 |
| 15 | Co-Trp/ Al_2O_3 (a)-700 | 33 | 31 |
| 16 | Co-Trp/ Al_2O_3 (b)-700 | 40 | 38 |
| 17 | Co-Trp/ Al_2O_3 (b)-800 | 64 | 62 |
| 18 | Co-Ade/C-700 | 18 | 17 |
| 19 | Co-Ade/ Al_2O_3 (a)-800 | 34 | 25 |
| 20 | Co-Gua/C-700 | 10 | 0 |

^a Reaction conditions: 1.5 mmol substrate, 1.5 ml water, 1 mol% catalyst, 30 bar H_2 , 60 °C, 18 h. ^b Yields were determined *via* GC, using hexadecane as the internal standard. ^c 0.5 mol% catalyst was used.

Having the first efficient catalysts in hand, we investigated the influence of critical reaction parameters for this transformation (Scheme 1; Table 2; ESI – Table S2†). Interestingly, testing various solvents showed that the active catalyst is effective in water even at 40 °C and 10 bars of molecular hydrogen (Table 2, entries 8 and 9). Other tested solvents gave

Table 2 Hydrogenation of diisobutene (1 + 2) in water with Co-Ura/C (Scheme 1), and reaction optimization^a

| Entry | Catalyst | <i>p</i> (H ₂) [bar] | Conversion 1 + 2 ^b [%] | Yield 3 ^b [%] |
|-------|--------------|----------------------------------|-----------------------------------|--------------------------|
| 1 | Co-Ura/C-600 | 50 | 100 | >99 |
| 2 | Co-Ura/C-700 | 50 | 100 | >99 |
| 3 | Co-Ura/C-800 | 50 | 83 | 82 |
| 4 | Co-Ura/C-600 | 30 | 99 (90 ^c) | 99 (90 ^c) |
| 5 | Co-Ura/C-700 | 30 | 98 (90 ^c) | 98 (90 ^c) |
| 6 | Co-Ura/C-600 | 20 | 98 | 97 |
| 7 | Co-Ura/C-700 | 20 | 98 | 97 |
| 8 | Co-Ura/C-600 | 10 | 64 | 63 |
| 9 | Co-Ura/C-700 | 10 | 63 | 62 |

^a Reaction conditions: 1.5 mmol substrate, 1.5 ml water, 1 mol% catalyst, 10–50 bar H₂, 40 °C, 18 h. ^b Yields were determined *via* GC, using hexadecane as the internal standard. ^c 0.5 mol% catalyst was used.

inferior results under identical conditions (ESI – Table S2†). Some of these solvents (propylene carbonate, acetonitrile or methanol) are even inactive at higher reaction temperature, which might be due to their adsorption/coordination behaviour on the catalyst surface (ESI – Table S2†). Consequently, all further experiments were performed in water. From the three most active catalysts (Table 1, entries 6–8) tested at 40 °C and 50 bar hydrogen, Co-Ura/C-800 still showed very good activity (Table 2, entry 3).

Furthermore, variations of hydrogen pressure and the catalyst amount (Table 2, entries 4 and 5) revealed Co-Ura/C-600 and Co-Ura/C-700 as the best catalytic systems with similar performances. As is evident from Table 2, both catalysts ensure excellent yields of the desired hydrogenation product 3 even at 40 °C/20 bar hydrogen pressure (Table 2, entries 6 and 7) and function equally throughout all experiments. Next, both Co-Ura/C-600 and Co-Ura/C-700 were used in diisobutene hydrogenation under standard reaction conditions (1.5 mmol substrate, 1 mol% catalyst, 60 °C, 30 bar hydrogen, 1.5 mL water and 18 h) for four consecutive runs (Fig. 2, ESI – Table S5†).

After each run the catalyst was separated by filtration and thoroughly washed with acetone to remove traces of hexadecane (internal standard) and the product or substrate. The separated catalysts were dried at 60 °C under high vacuum for 4 h,

before being used in the next run. As shown in Fig. 2, in the second run Co-Ura/C-600 still showed >90% of the previous productivity, while that of Co-Ura/C-700 dropped down to 54%. However, during the third run a significant decrease of activity was observed for both materials, while in the fourth run the catalysts were almost inactive. To determine the reasons for this loss of activity, leaching tests were performed. Thus, the reaction mixtures were filtered, all volatile components were removed and the residues were dissolved in *aqua regia*.

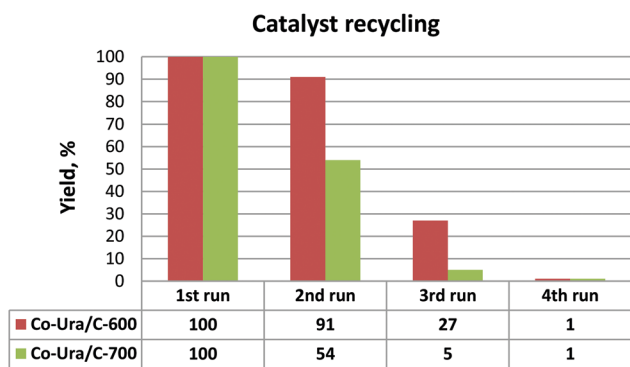
The cobalt contents of the obtained aqueous solutions were determined *via* Atomic Absorption Spectroscopy (AAS), which confirmed that they were below the detection limit of 0.04 mg L⁻¹. Consequently, the observed productivity loss cannot be an effect of cobalt leaching.

Subsequently, for characterization of the active catalysts and their deactivation mechanism, detailed analyses of both fresh and recycled catalysts were performed by means of powder X-ray diffraction (XRD), X-ray photoelectron spectroscopy (XPS) and transmission electron microscopy (TEM) (ESI – S10†).

The samples obtained after pyrolysis at different temperatures were investigated by powder X-ray diffraction in the first step. As seen from the diffraction pattern, Co₃O₄ is obtained as the main crystalline phase if a 500 °C temperature is applied in the synthesis procedure. If the pyrolysis temperature is further increased to 700 °C the Co-oxide is further reduced to metallic cobalt (cubic, ESI – Fig. S10B†). When the synthesis is performed at 1000 °C, the oxide seems to be fully reduced to cobalt. However, due to the low catalyst loading and broad overlapping diffraction peaks the presence of CoO or Co-carbide species cannot be ruled out from the diffraction data.

The XPS analysis of catalysts pyrolyzed at 500, 600, and 700 °C shows very similar results in their C 1s, N 1s and Co 2p spectra as well as in the quantitative analysis of the surface composition (ESI – S10C† for a quantification table). The C 1s spectra display strong peaks of carbon–carbon bonds (ESI – Fig. S10C-2†). In the N 1s region binding energies characteristic of pyridinic and pyrrolic nitrogen can be found in all spectra (ESI – Fig. S10C-4†). With increasing pyrolysis temperature an increasing oxygen concentration can be observed. When 1000 °C was used no cobalt and nitrogen could be detected at the surface of the catalyst while for carbon distinct C–O bonds could be found (ESI – Fig. S10C-2†). The Co 2p spectra for the fresh catalysts and pyrolysis temperatures up to 700 °C are quite similar and show two main features at 779.8 eV and 797 eV corresponding to Co 2p_{3/2} and Co 2p_{1/2}, which are characteristic of Co₃O₄ (Fig. 4 for Co-Ura/C-600 and ESI – Fig. S10C-3†).⁴⁴

Analytical scanning transmission electron microscopy (STEM) was used to characterize the morphology of Co-Ura/C-600. The general overview confirms different types of structures, comprising Co oxide, Co metal and core–shell type particles with the Co metal at the core surrounded by a Co oxide shell (Fig. 3a, ESI – S10D-1†). Co metal surfaces not surrounded by its oxide are usually covered by several layers of carbon (Fig. 3b, ESI – S10D†).

**Fig. 2** Recycling tests of Co-Ura/C-600 and Co-Ura/C-700 catalysts by hydrogenation of diisobutene in water.

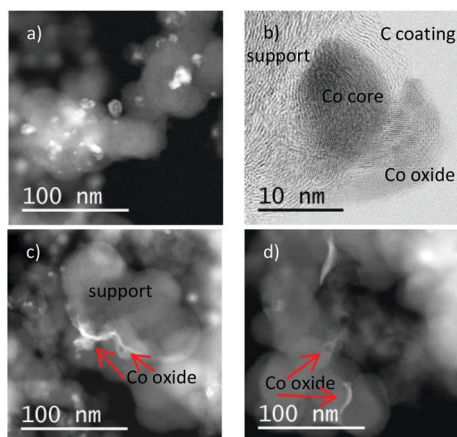


Fig. 3 High angle annular dark field (HAADF) STEM image (a) showing the general morphology of fresh Co-Ura/C-600 and an annular bright field (ABF) STEM image (b) highlighting a Co metal core partially covered by carbon and Co oxide of the same sample. HAADF-STEM image of a one time used Co-Ura/C-600rec1 sample (c) shows formation of a Co oxide type structure growing around C-support particles. HAADF-STEM image of catalyst Co-Ura/C-600rec4 recovered four times (d) emphasizes further evolution of the new Co oxide phase.

To gain insights into the deactivation of the Co-Ura/C-600 catalyst the recycled material was studied by XRD, XPS and TEM after its fourth usage. X-ray diffraction reveals that no crystalline Co species can be found. This either indicates that the Co/Co-oxides are transformed into an amorphous state or their crystallite size drops significantly. After recycling of the catalyst Co-Ura/600 pronounced changes are observed in the XPS spectra of Co 2p indicating a change in the oxidation state of cobalt (see Fig. 4). The Co 2p signal is shifted to slightly higher binding energies and a new satellite feature around 803 eV becomes visible, indicating the formation of CoO or Co(OH)₂ phases⁴⁴ with each recycling step. Only minor changes can be observed in the C 1s (ESI – Fig. S10C-2[†]) and N 1s (ESI – Fig. S10C-4[†]) spectra after each cycle.

STEM measurements of recovered catalysts Co-Ura/C-600rec1 and rec 4 further support the XRD and XPS results as the morphology of Co phases changes during the reaction. After recovering once used Co-Ura/C-600rec1 a veil like structure attached to the surface of Vulcan support particles could be identified (Fig. 3c). Electron energy loss spectroscopy of these structures indicates a Co–oxygen bond (ESI – D-2[†]) although a content of hydrogen is also possible. However, it is not possible to verify the hydrogen content by this method. The four times recovered catalyst Co-Ura/C-600rec4 shows further evolution of the veil type structure at the cost of other Co metal or Co oxide particles (Fig. 3d; ESI – S10D-3[†]).

Next, kinetic investigations on diisobutene hydrogenation were performed under our standard conditions. The hydrogenation of diisobutene (**1** + **2**) to isooctane **3** was stopped after 1 h, 2 h, 4 h, 7 h and 18 h reaction times and the reaction mixture was analysed by GC (Fig. 5). As expected, terminal olefin **1** is more reactive than the internal one **2** and after 4 h

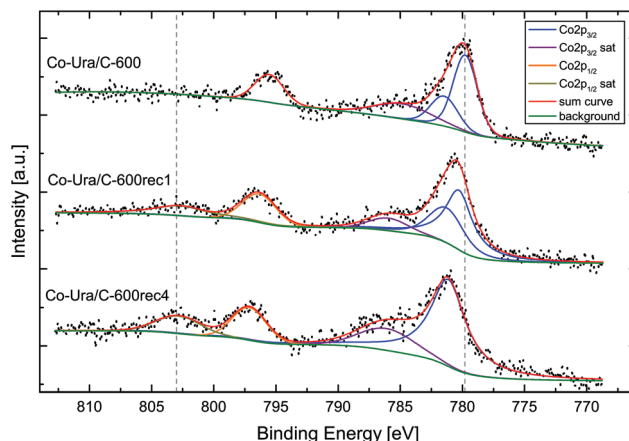


Fig. 4 Co 2p XPS spectra of fresh Co-Ura/C-600, and recycled Co-Ura/C-600rec1 and Co-Ura/C-600rec4 from top to bottom, respectively. The dashed lines at 779.8 eV and 803 eV mark pronounced changes in the spectra from predominantly Co₃O₄ in the fresh catalyst to CoO or Co(OH)₂ in the catalyst recycled four times.

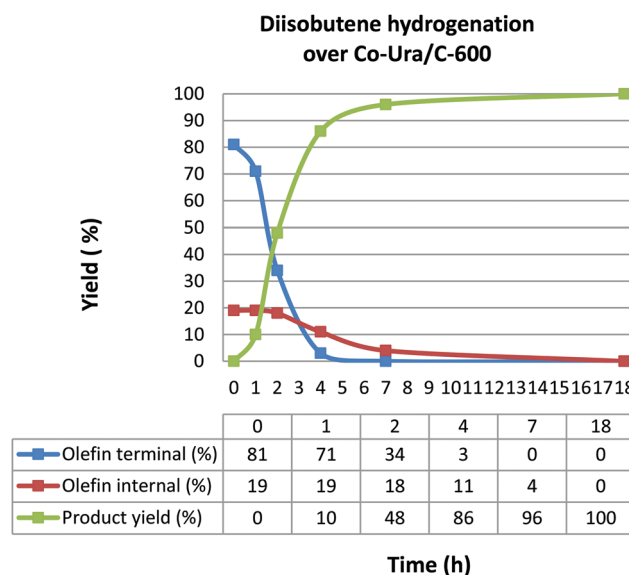


Fig. 5 Reaction profile for the hydrogenation of diisobutene over Co-Ura/C-600 at 30 bar H₂, 60 °C, 1–18 h.

both substrates reached 96% and 42% conversion, respectively. After 7 h, the reaction mixture consisted of 96% of desired product isooctane **3** along with 4% of remaining internal olefin **2**.

To explore the scope and limitations of our catalyst Co-Ura/C-600, it was applied in the hydrogenation of 15 diverse olefins including various functional groups. The results shown in Table 3 demonstrate excellent catalytic activity of this material often leading to full conversion and quantitative yield under mild conditions in water (Table 3, entries 1–4, 6, and 11). A number of functional groups such as alcohol, amine, nitrile, ether, ester, aldehyde, and sulfonamide groups are well tolerated.

Table 3 Co-Ura/C-600 catalyzed hydrogenations in water: substrate scope^a

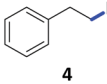
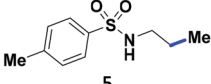
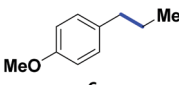
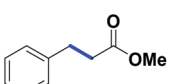
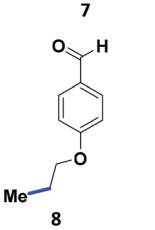
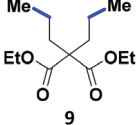
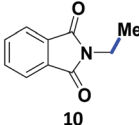
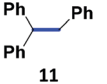
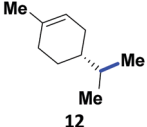
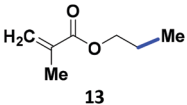
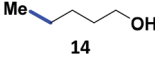
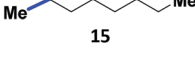
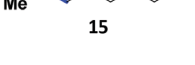
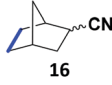
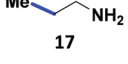
| Entry | Products | T (°C) | Conversion ^b (%) | Yield ^b (%) |
|-------|---|-----------------|-----------------------------|------------------------|
| 1 |  | 60 | 100 | >99 |
| 2 |  | 60 | 100 | >99 |
| 3 |  | 60 | 100 | >99 |
| 4 |  | 60 | 99 | 99 |
| 5 |  | 60 | 96 | 86 |
| 6 |  | 60 | 100 | 98 |
| 7 |  | 60 100 | 16 100 | 10 56 |
| 8 |  | 60 120 | 0 21 | 0 21 |
| 9 |  | 60 140 | 0 99 | 0 81 |
| 10 |  | 60 80 100 | 52 52 80 | 43 36 8 |
| 11 |  | 60 | 100 | >99 |
| 12 |  | 60 | 100 | 92 |
| 13 |  | 60 | 83 | 72 |

Table 3 (Contd.)

| Entry | Products | T (°C) | Conversion ^b (%) | Yield ^b (%) |
|-------|--|--------|-----------------------------|------------------------|
| 14 |  | 60 | 50 | 48 |
| 15 |  | 60 | 98 | 98 |

^a Reaction conditions: 1.5 mmol substrate, 1 mol% catalyst, 30 bar H₂, 1.5 ml water, 18 h. ^b Yields were determined *via* GC or NMR, using hexadecane or mesitylene, respectively, as the internal standard. Bonds in blue indicate sites of double bond hydrogenation.

In the case of vinylphthalimide (2-vinylisoindoline-1,3-dione), hydrogenation led to low conversion under standard conditions (Table 3, entry 7). However, increasing the temperature to 100 °C ensured 56% yield of product **10** due to partial polymerization of the substrate. Even the highly hindered double bond in triphenylethylene could be hydrogenated to give product **11**, albeit elevated temperature was required for this hydrogenation (Table 3, entry 8).

The hydrogenation of substrates with multiple double bonds is a demanding task, which is of interest in the valorisation of natural terpenes. Thus, we were pleased to find that our best catalyst was able to ensure high regio- and chemoselectivity in the hydrogenation of monocyclic terpene *R*-(+)-limonene ((*R*)-1-methyl-4-(prop-1-en-2-yl)cyclohex-1-ene) (Table 3, entry 9), which is the main component of essential oils from the rinds of citrus fruits. Both limonene and its mono-hydrogenation product *p*-menthene **12** ((*R*)-4-isopropyl-1-methylcyclohex-1-ene) are valuable products and widely used in cosmetics and in the fragrance industry⁴⁵ as well as in the synthesis of fine and bulk chemicals, *e.g.* aviation biofuel.⁴⁶ Notably, selective hydrogenation of *R*-(+)-limonene to (+)-*p*-1-menthene has recently been reported by Leitner⁴⁷ using commercially available noble metal catalysts Pt/C and Pt/Al₂O₃, as well as by Feldmann, von Wangelin¹⁸ and Wolf¹⁶ using unsupported cobalt nanoparticles.

The Co-Ura/C-600 catalyst performed preferred reduction of the external double bond against the internal one to yield partially hydrogenated versatile product (+)-*p*-1-menthene **12** in 81% yield (Table 3, entry 9). In addition, a tiny amount (~6%) of fully hydrogenated product *p*-menthane (mixture of isomers) was also formed. Similarly, selective hydrogenation of allyl methacrylate was achieved, which occurred preferably at the allylic double bond to form product **13** as a single product. At higher temperature mainly polymerization of the substrate/product was observed, which demonstrates the importance of running such hydrogenations at lower temperature (Table 3, entry 10).

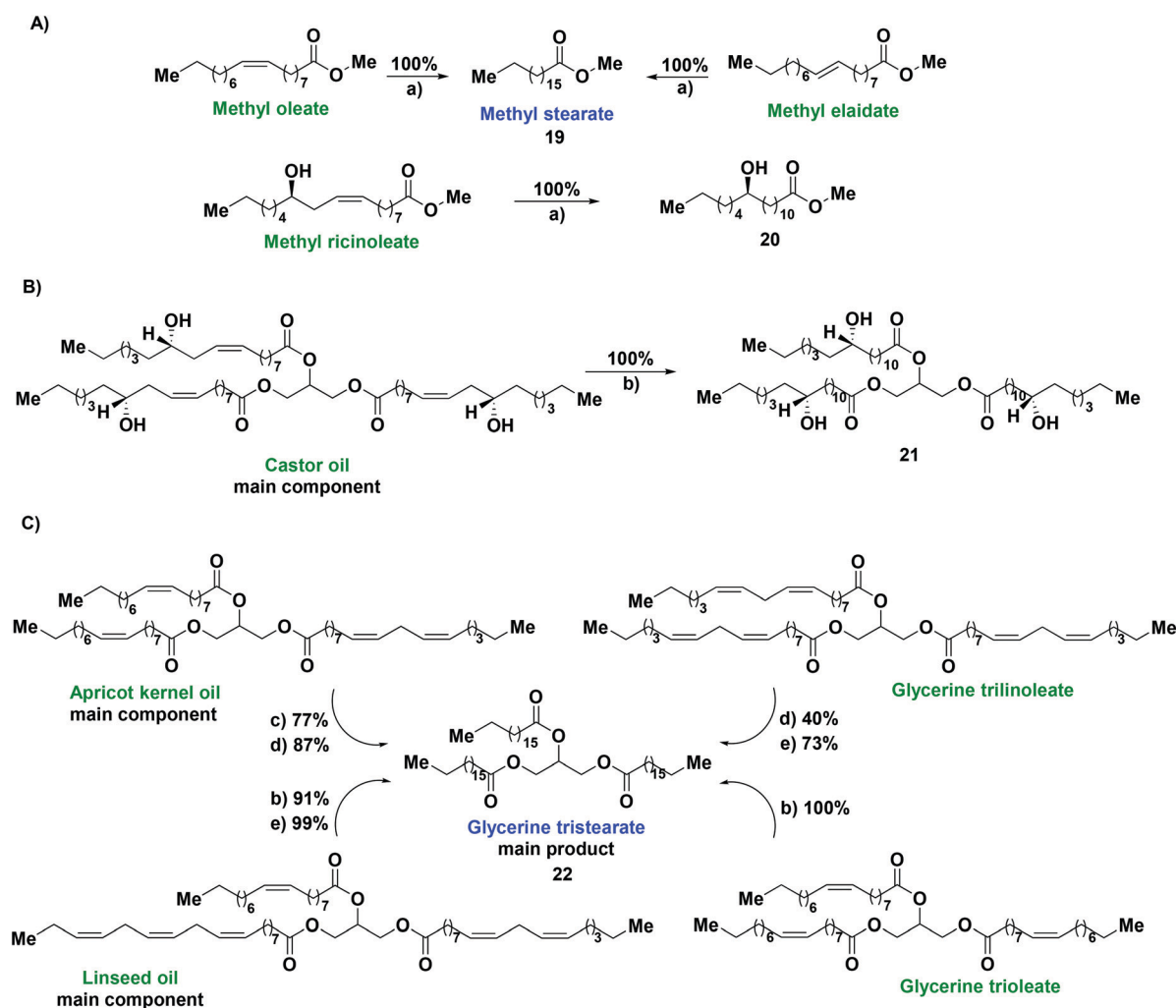
An example of another relevant hydrogenation is the selective reduction of myrcene (7-methyl-3-methyleneocta-1,6-diene) (Table 4). Myrcene is an important natural monoterpene and represents a substantial component of the essential

Table 4 Co-Ura/C-600 catalyzed hydrogenations in water: substrate scope – natural monoterpenes^a

| Entry | Substrate | Products | | | | Yields of 18a–d and total ^b (%) |
|-------|----------------------|----------|-----|-----|-----|--|
| | | 18a | 18b | 18c | 18d | |
| 1 | Myrcene T (°C) 40 | 20 | 18 | 49 | 3 | 90 |
| 2 | 60 | 0 | 10 | 61 | 17 | 88 |
| 3 | 120 | 0 | 0 | 0 | 98 | 98 |

^a Reaction conditions: 1.5 mmol substrate, 1 mol% catalyst, 1.5 ml water, 30 bar H₂, 18 h. ^b Yields were determined *via* NMR, using mesitylene as the internal standard. Bonds in blue indicate sites of double bond hydrogenation.

oils of several plants including wild thyme, lemon grass, mango, cannabis, parsley, cardamom, hops and more.⁴⁸ Structurally, this triene consists of two isoprene units like other monoterpenes. Myrcene and its hydrogenation products are highly valued as raw materials for the preparation of pharmaceuticals, and flavour and fragrance chemicals such as menthol, citronellal and nerol.^{49–51} In this respect, selective hydrogenation of myrcene is of commercial importance, since the obtained products are potential precursors for further functionalized oxygenated derivatives. However, since myrcene contains three different carbon–carbon double bonds, the selective hydrogenation is highly challenging. Previous studies on myrcene hydrogenation made use of precious metal catalysts,⁵² such as Pd/SiO₂,⁵³ palladium nanoparticles,⁵⁴ or chiral phosphine complexes of rhodium and ruthenium.⁵⁵ Furthermore, also unsupported cobalt(0) nanoparticles were applied for the non-selective, complete hydrogenation.¹⁶

**Scheme 2** Co-Ura/C-600 catalyzed hydrogenations in water: substrate scope – natural oils and fatty acid derivatives.^{a,b}

^a Reaction conditions: a) 1.5 mmol substrate, 1 mol% catalyst, 1.5 ml water, 30 bar H₂, 100 °C, 18 h; b) 300 mg substrate, 30 mg catalyst, 1.5 ml water, 30 bar H₂, 100 °C, 18 h; c) similar to b) at 120 °C; d) similar to b) at 140 °C; and e) similar to b) at 150 °C, 50 bar H₂. ^b Conversions and yields were determined *via* NMR, using mesitylene as the internal standard.

In contrast, the Co-Ura/C-600 catalyst showed excellent activity and good selectivity towards mono-, di- or full hydrogenation of myrcene leading to isolated dienes, internal alkenes or branched alkanes depending on the reaction temperature (Table 4). Thus, at 40 °C high regioselectivity toward mono- and dihydrogenated products **18a–c** was observed with a very good combined selectivity of 90%. Product distribution showed that the selectivity to **18c** was 49% which is the highest value and dienes **18a** and **18b** were formed roughly in the same proportion (18–20% each). The alkyl-substituted double bond remained almost intact. Then, at 60 °C predominantly the dihydrogenated product **18c** was formed in 61% yield along with diene **18b** (10%) and internal alkane **18d** (17%). Increasing the reaction temperature to 120 °C led exclusively to the complete hydrogenation product **18d** in an excellent 98% yield. This full hydrogenation of myrcene to 2,6-dimethyloctane **18d** can be considered as a renewable route to synthesize fuel additives.⁵⁶

Finally, we were attracted by the highly important hydrogenation of vegetable oils, fatty acid esters and their triglycerides under our mild conditions. Oils still constitute one of the most important renewable raw materials of the chemical industry. Their hardening over catalytic hydrogenation is a fundamental industrial bulk scale process for the production of important chemicals, such as stabilizers and surfactants, environmentally friendly industrial fluids and lubricants or eatable fats, such as margarine.^{57–59} Since biodiesel (commonly fatty acid methyl esters) and oil based bio-paraffins are non-toxic, biodegradable renewable alternatives to fossil based fuel, their feedstock diversification has become an important topic for scientists in industry and academia.⁶⁰ In this context, also the potential of apricot kernel,⁶¹ linseed or castor⁶² oils was explored, besides their use as important components in cosmetic preparations or pharmaceutical formulations.

The following industrially relevant substrates were explored: fatty acid methyl esters (Scheme 2A); triglyceride glycerine trioleate and trilinoleate (Scheme 2C) as well as natural apricot kernel, linseed and castor oils (Scheme 2B and C; ESI – Fig. S4, Table S6†). As is evident from Scheme 2, Co-Ura/C-600 turned out to be a very good catalyst for hydrogenation of fatty acid derivatives applied in our study. Hence, methyl oleate and its isomer methyl elaidate were hydrogenated at 100 °C to the corresponding methyl stearate **19** and methyl ricinoleate to produce **20** quantitatively (Scheme 2A). Moreover, methyl oleate and methyl ricinoleate were hydrogenated already at 60 °C with almost 90% yield, whereas methyl elaidate conversion was 55% (Scheme 2A; ESI – Table S6†). Additionally, hydrogenation of glycerine trioleate led to glycerine tristearate **22** in 88% yield at 60 °C (ESI – Table S6†) and to excellent quantitative yield at 100 °C. In the case of multiply unsaturated glycerine trilinoleate, the hydrogenation degree increased with temperature and conversion (Scheme 2C).

To our delight, natural vegetable oils also were hydrogenated smoothly. Their main component triglycerides are shown in Scheme 2 and their detailed composition and NMR spectra are available in the ESI in the S9 section.† Hence, refined castor

oil was easily hydrogenated and converted to the white solid product **21** almost quantitatively (Scheme 2B). Finally, hydrogenation of apricot kernel oil was performed both at 120 °C and 150 °C with 77% and 87% conversion, respectively, as determined by ¹H NMR (ESI – S9†). Here, the main product glycerine tristearate **22** was obtained as a waxy, white solid. Moreover, the hydrogenation degree of linseed oil was very high at 150 °C and the conversion to product **22** was almost complete.

Conclusions

Novel heterogeneous cobalt catalysts were prepared by impregnation of inorganic supports with cobalt salts in the presence of 4 different bioorganic ligands (tryptophan (Trp), guanine (Gua), adenine (Ade), and uracil (Ura)) and subsequent pyrolysis. Among the resulting materials, specifically Co-Ura/C-600 showed excellent catalytic activity for hydrogenation of diverse substrates, such as industrially relevant olefins (diisobutene), natural oils, fatty acid derivatives and monoterpenes in water, without any additives. Broad functional group tolerance and often high selectivity towards hydrogenation of terminal olefins have been shown. The easy preparation of the Co-Ura/C-600 catalyst in multi-gram scale, no need for special handling, long shelf life, and high air- and water-stability, makes it an attractive alternative to presently used homogeneous and noble metal based catalysts.

Experimental

General preparation of Co-Ura/C catalysts (3 wt% cobalt-based, uracil ligated and Vulcan supported)

In a 500 mL two-neck round bottomed flask, equipped with a reflux condenser and a magnetic stir bar, Co(OAc)₂·4H₂O (762.2 mg, 3.06 mmol, 1.0 equiv.) and ligand uracil (692.9 mg, 6.12 mmol, 2.0 equiv.) were dissolved in ethanol (360 mL). The flask was immersed in an oil bath and heated at 70 °C. After 30 min, 4.77 g of Vulcan powder was added to the reaction mixture and the resulting heterogeneous mixture was heated for 4 h at 80 °C. The solvent was removed using a rotary evaporator and the residue was dried overnight at 65 °C under high-vacuum. The dried sample was ground in an agate mortar to a fine powder (5.9 g), from which a 0.5 g portion was transferred to a ceramic crucible and pyrolyzed at temperatures between 500 and 1000 °C (the oven was evacuated to ca. 5 mbar and then flushed with argon three times, and the heating rate was 25 °C per minute and held at pyrolysis temperature for 2 h under an argon atmosphere). The pyrolyzed catalysts were ground again in an agate mortar, and stored in glass vials in air, without special protection. The catalysts were labelled as Co-ligand/support-temperature (e.g. Co-Ura/C-600).

General procedures for hydrogenation reactions

A 4 mL screw-cap vial was charged with a catalyst (30 mg, ~1 mol%), a substrate (1.5 mmol), 1.5 mL of deionized water

(or screened solvent) and a Teflon-coated stirring bar. The vial was closed with a phenolic cap with a PTFE/white rubber septum (Wheaton 13 mm septa) and for the connection to the atmosphere the septum was punctured with a syringe needle. The vial was fixed in an alloy plate and then transferred into a Parr 4560 series autoclave (300 mL). At room temperature, the autoclave was flushed with hydrogen three times before it was pressurized at the required hydrogen pressure. The autoclave was placed into an aluminum block on a heating plate and heated up to required temperature. The heating was continued for 18 h under intensive stirring (1000 rpm). Afterwards, the autoclave was cooled in an ice bath to room temperature, the hydrogen was discharged and the vials containing reaction products were removed. In the case of GC analysis, to the crude reaction mixture an internal standard *n*-hexadecane (100 μ L) was added, the mixture was diluted with ethyl acetate and a GC sample was analyzed. For ^1H and ^{13}C NMR analyses, mesitylene (20 μ L) was taken as the internal standard. To the reaction mixture 2 mL CDCl_3 was added and the organic phase was subjected to NMR and GC analyses, after filtration through a 0.2 μm PTFE syringe filter. The obtained chromatograms and NMR spectra were compared with the reported ones.

Catalyst recycling procedure

The reaction was performed according to the general procedure using the Co-Ura/C-600 or Co-Ura/C-700 catalyst (30 mg, ~ 1 mol%) and diisobutene (169 mg, 1.5 mmol) in 1.5 mL of deionized water. After 18 h, to the crude reaction mixture the internal standard *n*-hexadecane (100 μ L) was added, the reaction mixture was diluted with ethyl acetate and a sample was analyzed by gas chromatography. Reported GC yields are the average of at least three runs. Afterwards, the reaction mixture was filtered off and the obtained catalyst was washed with 10–15 mL acetone. The recycled catalyst was then dried at 60 $^\circ\text{C}$ under high vacuum for 4 h before using for the next run.

Conflicts of interest

There are no conflicts to declare.

Acknowledgements

This work has been supported by the State of Mecklenburg – Western Pomerania, the BMBF (Grant No. 03XP0060, KataPlasma). We thank Dr C. Fischer, S. Buchholz, S. Schareina, A. Lehmann, and K. Schubert for their excellent technical and analytical support (all from LIKAT). We also thank Reinhard Eckelt for performing BET measurements and Dr Angela Koeckritz for fruitful discussions on heterogeneous catalysts.

Notes and references

1 S. Nishimura, *Handbook of Heterogeneous Catalytic Hydrogenation for Organic Synthesis*, Wiley-VCH, New York, 2001.

- J. G. de Vries and C. J. Elsevier, *The Handbook of Homogeneous Hydrogenation*, Wiley-VCH, Weinheim, 2007, vol. 1–3.
- P. J. Chirik, *Acc. Chem. Res.*, 2015, **48**, 1687–1695.
- G. A. Filonenko, R. van Putten, E. J. M. Hensen and E. A. Pidko, *Chem. Soc. Rev.*, 2018, **47**, 1459–1483.
- K. Tokmic, C. R. Markus, L. Zhu and A. R. Fout, *J. Am. Chem. Soc.*, 2016, **138**, 11907–11913.
- C. S. G. Seo and R. H. Morris, *Organometallics*, 2019, **38**, 47–65.
- L. Liu and A. Corma, *Chem. Rev.*, 2018, **118**, 4981–5079.
- Z. Wei, Y. Chen, J. Wang, D. Su, M. Tang, S. Mao and Y. Wang, *ACS Catal.*, 2016, **6**, 5816–5822.
- T. Song, P. Ren, Y. Duan, Z. Wang, X. Chen and Y. Yang, *Green Chem.*, 2018, **20**, 4629–4637.
- T. Song, Z. Ma and Y. Yang, *ChemCatChem*, 2019, **11**, 1313–1319.
- W. Ai, R. Zhong, X. Liu and Q. Liu, *Chem. Rev.*, 2019, **119**, 2876–2953.
- M. R. Friedfeld, G. W. Margulieux, B. A. Schaefer and P. J. Chirik, *J. Am. Chem. Soc.*, 2014, **136**, 13178–13181.
- M. R. Friedfeld, M. Shevlin, J. M. Hoyt, S. W. Krska, M. T. Tudge and P. J. Chirik, *Science*, 2013, **342**, 1076–1080.
- M. R. Friedfeld, H. Zhong, R. T. Ruck, M. Shevlin and P. J. Chirik, *Science*, 2018, **360**, 888–893.
- P. Büschelberger, D. Gärtner, E. Reyes-Rodriguez, F. Kreyenschmidt, K. Koszinowski, A. J. v. Wangelin and R. Wolf, *Chem. – Eur. J.*, 2017, **23**, 3139–3151.
- P. Büschelberger, E. Reyes-Rodriguez, C. Schöttle, J. Treptow, C. Feldmann, A. Jacobi von Wangelin and R. Wolf, *Catal. Sci. Technol.*, 2018, **8**, 2648–2653.
- D. Gärtner, A. Welther, B. R. Rad, R. Wolf and A. Jacobi von Wangelin, *Angew. Chem., Int. Ed.*, 2014, **53**, 3722–3726.
- S. Sandl, F. Schwarzhuber, S. Pöllath, J. Zweck and A. J. v. Wangelin, *Chem. – Eur. J.*, 2018, **24**, 3403–3407.
- P. Ji, K. Manna, Z. Lin, X. Feng, A. Urban, Y. Song and W. Lin, *J. Am. Chem. Soc.*, 2017, **139**, 7004–7011.
- P. Ji, K. Manna, Z. Lin, A. Urban, F. X. Greene, G. Lan and W. Lin, *J. Am. Chem. Soc.*, 2016, **138**, 12234–12242.
- K. Manna, P. Ji, Z. Lin, F. X. Greene, A. Urban, N. C. Thacker and W. Lin, *Nat. Commun.*, 2016, **7**, 12610.
- T. Schwob and R. Kempe, *Angew. Chem., Int. Ed.*, 2016, **55**, 15175–15179.
- W. Liu, B. Sahoo, K. Junge and M. Beller, *Acc. Chem. Res.*, 2018, **51**, 1858–1869.
- M. F. Hertrich, F. K. Scharnagl, A. Pews-Davtyan, C. R. Kreyenschulte, H. Lund, S. Bartling, R. Jackstell and M. Beller, *Chem. – Eur. J.*, 2019, **25**, 5534–5538.
- F. A. Westerhaus, R. V. Jagadeesh, G. Wienhofer, M. M. Pohl, J. Radnik, A. E. Surkus, J. Rabeah, K. Junge, H. Junge, M. Nielsen, A. Bruckner and M. Beller, *Nat. Chem.*, 2013, **5**, 537–543.
- F. Chen, W. Li, B. Sahoo, C. Kreyenschulte, G. Agostini, H. Lund, K. Junge and M. Beller, *Angew. Chem., Int. Ed.*, 2018, **57**, 14488–14492.

- 27 D. Formenti, F. Ferretti, C. Topf, A.-E. Surkus, M.-M. Pohl, J. Radnik, M. Schneider, K. Junge, M. Beller and F. Ragaini, *J. Catal.*, 2017, **351**, 79–89.
- 28 R. V. Jagadeesh, K. Murugesan, A. S. Alshammari, H. Neumann, M.-M. Pohl, J. Radnik and M. Beller, *Science*, 2017, **358**, 326–332.
- 29 R. Ferraccioli, D. Borovika, A.-E. Surkus, C. Kreyenschulte, C. Topf and M. Beller, *Catal. Sci. Technol.*, 2018, **8**, 499–507.
- 30 F. K. Scharnagl, M. F. Hertrich, F. Ferretti, C. Kreyenschulte, H. Lund, R. Jackstell and M. Beller, *Sci. Adv.*, 2018, **4**, eaau1248.
- 31 J. R. Lusty, P. Wearden and V. Moreno, *CRC handbook of nucleobase complexes: Transition metal complexes of naturally occurring nucleobases and their derivatives*, 2017.
- 32 A. R. Sarkar and P. Ghosh, *Inorg. Chim. Acta*, 1983, **78**, L39–L41.
- 33 M. Gupta and M. N. Srivastava, *Synth. React. Inorg. Met.-Org. Chem.*, 1996, **26**, 305–320.
- 34 K. Hassanein, F. Zamora, O. Castillo and P. Amo-Ochoa, *Inorg. Chim. Acta*, 2016, **452**, 251–257.
- 35 X. Wu and J. Xiao, in *Metal-Catalyzed Reactions in Water*, ed. P. H. Dixneuf and V. Cadierno, Wiley-VCH, Weinheim, 2013, pp. 173–242.
- 36 C. J. Clarke, W.-C. Tu, O. Levers, A. Bröhl and J. P. Hallett, *Chem. Rev.*, 2018, **118**, 747–800.
- 37 B. M. Goortani, A. Gaurav, A. Deshpande, F. T. T. Ng and G. L. Rempel, *Ind. Eng. Chem. Res.*, 2015, **54**, 3570–3581.
- 38 R. S. Kamath, Z. Qi, K. Sundmacher, P. Aghalayam and S. M. Mahajani, *Ind. Eng. Chem. Res.*, 2006, **45**, 1575–1582.
- 39 S. Talwalkar, S. Thotla, K. Sundmacher and S. Mahajani, *Ind. Eng. Chem. Res.*, 2009, **48**, 10857–10863.
- 40 A. Sarkar, D. Seth, F. T. T. Ng and G. L. Rempel, *AIChE J.*, 2006, **52**, 1142–1156.
- 41 M. S. Lylykangas, P. A. Rautanen and A. O. I. Krause, *Ind. Eng. Chem. Res.*, 2004, **43**, 1641–1648.
- 42 M. S. Lylykangas, P. A. Rautanen and A. O. I. Krause, *AIChE J.*, 2003, **49**, 1508–1515.
- 43 M. S. Lylykangas, P. A. Rautanen and A. Krause, *Appl. Catal., A*, 2004, **259**, 73–81.
- 44 M. C. Biesinger, B. P. Payne, A. P. Grosvenor, L. W. M. Lau, A. R. Gerson and R. S. C. Smart, *Appl. Surf. Sci.*, 2011, **257**, 2717.
- 45 E. Singer and B. Holscher, US20130090390A1, 2013.
- 46 M. A. Fraga, L. E. P. Borges and F. R. Goncalves, WO2012012856A1, 2012.
- 47 G. Rubulotta, K. L. Luska, C. A. Urbina-Blanco, T. Eifert, R. Palkovits, E. A. Quadrelli, C. Thieuleux and W. Leitner, *ACS Sustainable Chem. Eng.*, 2017, **5**, 3762–3767.
- 48 A. Behr and L. Johnen, *ChemSusChem*, 2009, **2**, 1072–1095.
- 49 S. Akutagawa, T. Sakaguchi and H. Kumobayashi, *Dev. Food Sci.*, 1988, **18**, 761–765.
- 50 M. Emura and K. Matsumura, *Aroma Res.*, 2012, **13**, 313–318.
- 51 J. B. Woell, US5017726A, 1991.
- 52 M. G. Speziali, F. C. C. Moura, P. A. Robles-Dutenhefner, M. H. Araujo, E. V. Gusevskaya and E. N. dos Santos, *J. Mol. Catal. A: Chem.*, 2005, **239**, 10–14.
- 53 P. A. Robles-Dutenhefner, M. G. Speziali, E. M. B. Sousa, E. N. dos Santos and E. V. Gusevskaya, *Appl. Catal., A*, 2005, **295**, 52–58.
- 54 T.-A. Chen and Y.-S. Shon, *Catal. Sci. Technol.*, 2017, **7**, 4823–4829.
- 55 C. Margarita, W. Rabten and P. G. Andersson, *Chemistry*, 2018, **24**, 8022–8028.
- 56 N. I. Tracy, D. Chen, D. W. Crunkleton and G. L. Price, *Fuel*, 2009, **88**, 2238–2240.
- 57 J. W. Veldsink, M. J. Bouma, N. H. Schoon and A. A. C. M. Beenackers, *Catal. Rev.: Sci. Eng.*, 1997, **39**, 253–318.
- 58 G. R. List and J. W. King, *Hydrogenation of Fats and Oils: Theory and Practice*, AOCS Press, Urbana, Illinois, 2 edn, 2015.
- 59 J. O. Metzger and U. Bornscheuer, *Appl. Microbiol. Biotechnol.*, 2006, **71**, 13–22.
- 60 J. Hancsók, T. Kasza, S. Kovács, P. Solymosi and A. Holló, *J. Cleaner Prod.*, 2012, **34**, 76–81.
- 61 V. S. Gurau and S. S. Sandhu, *J. Sci. Ind. Res.*, 2018, **77**, 345–348.
- 62 W. Li, B. Ni, Q. Guan, L. He, F. Ye and X. Cui, WO2017020401A1, 2017.

5.3. Supported Cobalt Nanoparticles for Hydroformylation Reactions

M. F. Hertrich,* F. K. Scharnagl,* A. Pews-Davtyan, C. R. Kreyenschulte, H. Lund, S. Bartling, R. Jackstell, M. Beller, *Chem. Eur. J.* **2019**, *25*, 5534-5538

* These authors contributed equally to this work.

DOI: 10.1002/chem.201806282

© 2019 Wiley-VCH Verlag GmbH & Co. KGaA, Weinheim

Contributions: F.K.S. developed the chitosan-derived catalysts and tested them in the hydroformylation reaction. Also he discussed the characterisation of the material with the analytical department and conducted leaching studies. Eventually, he prepared the manuscript together with M.F.H. and M.B. The overall contribution is about 40%.

Heterogeneous Catalysis

Supported Cobalt Nanoparticles for Hydroformylation Reactions

Maximilian Franz Hertrich⁺, Florian Korbinian Scharnagl⁺, Anahit Pews-Davtyan, Carsten Robert Kreyenschulte, Henrik Lund, Stephan Bartling, Ralf Jackstell, and Matthias Beller^{*[a]}

Abstract: Hydroformylation of olefins has been studied in the presence of specific heterogeneous cobalt nanoparticles. The catalytic materials were prepared by pyrolysis of pre-formed cobalt complexes deposited onto different inorganic supports. Atomic absorption spectroscopy (AAS) measurements indicated a correlation of catalyst activity and cobalt

leaching as well as a strong influence of the heterogeneous support on the productivity. These new, low-cost, easy-to-handle catalysts can substitute more toxic, unstable and volatile cobalt carbonyl complexes for hydroformylations on a laboratory scale.

Introduction

The hydroformylation of olefins constitutes the most important homogeneously catalysed methodology with respect to the production scale.^[1,2] The resulting aldehydes are easily transformed into esters, alcohols, carboxylic acids, and aliphatic amines, which are widely used as intermediates for plasticizers, solvents, detergents and fine chemicals. In industry, to date only cobalt- and rhodium-based homogeneous catalysts have been applied, even though alternative metals continue to attract significant attention.^[3] Since the 1970s, for lower olefins (<C₅) cobalt carbonyl complexes have been replaced by phosphine- or phosphite-modified rhodium systems, which possess superior activity and selectivity.^[4,5] Alternatively, cobalt catalysts are mainly applied for the conversion of mid- and long-chained olefins to alcohols due to their inherent high hydrogenation activity.

Notably, for both cases costs for metal/ligands or recycling are decisive. Hence, there is a growing interest to develop more economic technologies, which allow for quantitative catalyst recycling.^[6] In this respect, many research groups investigated both heterogeneous and immobilised homogeneous catalysts for the title reaction, mainly using rhodium,^[7–14] but also cobalt systems^[15–17] as well as other metals.^[18–23] The main problem of all these catalysts is the leaching of active metal species from the support in the presence of CO. Furthermore,

both activity and selectivity of heterogenised catalysts are in general lower compared to their homogeneous counterparts.

To overcome these limitations, immobilisation of metal complexes, for instance, was introduced with supported ionic liquid-phase (SILPs) systems.^[24–28] Other methods attempted to build a bridge between homogeneous and heterogeneous catalysis by the formation of dispersed single metal atom catalysts (SACs)^[29–31] or small nanoparticles (NPs).^[32,33]

In the past years, our group has developed several nano-scale catalysts, especially based on N-doped carbon-supported cobalt and iron species. Those catalysts are easily prepared by pyrolysis of a carbon source, such as Vulcan XC 72R, impregnated with in situ ligated Co^[34,35] and Fe,^[36,37] respectively. Similar materials containing nanoparticles supported on inorganic carriers^[38] and biomass-derived catalysts were also studied.^[39–41] Based on these works, here we described the synthesis of cobalt-containing materials and studied their catalytic performance in hydroformylation reactions.

Results and Discussion

Preparation of and structural trends for the materials

Initially, we prepared around 50 materials based on a general procedure developed by our group.^[34] For this purpose, different commercially available supports (e.g., carbon, titania, silica, ceria, alumina) were impregnated with cobalt(II) acetate in the presence of different N-containing organic ligands (2 equiv). Subsequent pyrolysis, in general at 800 °C, led to a library of catalysts named Co/Ligand@Support. Detailed descriptions of the preparation method, thermogravimetric analyses for the two mainly used ligands as well as for the preparation of Co/phen@C, the analytical methodologies, and the characterisation of selected materials are given in the Supporting Information.

[a] M. F. Hertrich,⁺ F. K. Scharnagl,⁺ Dr. A. Pews-Davtyan, Dr. C. R. Kreyenschulte, Dr. H. Lund, Dr. S. Bartling, Dr. R. Jackstell, Prof. M. Beller
Leibniz-Institut für Katalyse e.V. an der Universität Rostock
Albert-Einstein-Straße 29a, 18059 Rostock (Germany)
E-mail: matthias.beller@catalysis.de

[*] These authors contributed equally to this work.

Supporting information and the ORCID identification number(s) for the author(s) of this article can be found under:
<https://doi.org/10.1002/chem.201806282>.

The general compositions of selected catalysts were studied by powder X-ray diffraction (XRD) experiments and elementary analysis (EA), whereas the surface structures for some supported nanoparticles were characterised in more detail by X-ray photoelectron spectroscopy (XPS) or transmission electron microscopy (TEM). All supported cobalt nanoparticles are either core-shell structured with a cobalt core and a closed cobalt oxide shell or a pure cobalt oxide or metallic cobalt phase, respectively. In some cases, graphene layers covering big particles were observed. Remarkably, no clear correlation between cobalt content or oxidation state of the cobalt species at the surface and catalytic activity of the materials could be ascertained.

As ligands, inexpensive compounds such as urea, typical pyridine derivatives, but also biologically relevant nucleobases, amino acids, and even biopolymers (chitosan and chitin)^[42] were used. Notably, chitosan is produced through deacetylation of chitin, simply obtained from shrimp or crab shells.^[43–45] It is known to form stable complexes with metal ions^[46,47] and it was found to be an excellent precursor for N-doped graphene.^[48,49] Previously, both chitosan- and phenanthroline-based materials exhibited good performance in catalytic hydrogenation reactions,^[39–41] thus, we focused especially on these systems.

Catalytic activity

We started to explore the activity of the cobalt catalysts in two hydroformylation reactions (Table 1). Neohexene (*tert*-butyl ethylene) and *n*-butyl acrylate were chosen as model sub-

strates. In the first case, the hydroformylation was expected to yield regioselectivity the linear aldehyde **2** as the product due to the steric demand of the *tert*-butyl group.

As an example of an electronically activated olefin, *n*-butyl acrylate was selected to study the *n/iso* selectivity. In both cases unwanted isomerization reactions cannot take place. We decided to perform the reaction under a pressure of 40 bar syngas (CO/H₂ = 1:1) at 100 °C for 18 hours. To compare the activity of our systems with the “corresponding” homogeneous one, we carried out experiments also with dicobalt octacarbonyl as the pre-catalyst (Table 1, entry 1).

In general, the conversion of *n*-butyl acrylate in hydroformylation should be faster than the conversion of neohexene. Indeed, when dicobalt octacarbonyl was used as pre-catalyst this prediction was confirmed (Table 1, entry 1). The reason for that is the steric demand of the *tert*-butyl group in neohexene, on the one hand, and the electronic activation of the double bond by the ester group in *n*-butyl acrylate, on the other hand. Following this trend, all catalysts based on the phenanthroline precursor were less active in neohexene hydroformylation than for the reaction of *n*-butyl acrylate (Table 1, entries 2, 4, 6, 8). Conversely, the catalysts prepared with the chitosan precursor showed the opposite behaviour (Table 1, entries 3, 5, 7). This finding is remarkable and contrary to general expectations. Obviously, the support of the catalyst as well as the ligand has an important influence on the activity.

As a general trend for the hydroformylation of neohexene, we found that the ceria-supported catalysts Co/phen@CeO₂ and Co/chitosan@CeO₂ (Table 1, entries 2, 3) showed the lowest activity compared to the other materials based on the respective precursor. The phenanthroline-derived catalyst supported on silicon dioxide Co/phen@SiO₂ was slightly more productive in neohexene hydroformylation (Table 1, entry 4). Best activity for the phenanthroline-based materials was reached with Co/phen@C, followed by Co/phen@TiO₂ (Table 1, entries 6, 8). However, the conversion rates for that type of catalysts were not higher than 55% (Table 1, entry 6) and product yields did not exceed 45% (Table 1, entry 8). Comparing materials resulting from the pyrolysis of chitosan, we found that the silicon dioxide support led to the best performance (52% conversion and 46% yield; Table 1, entry 5), comparable to that of Co/phen@C. The corresponding material based on titania Co/chitosan@TiO₂ was less active (Table 1, entry 7).

Although the phenanthroline-based catalysts are more active in the hydroformylation of *n*-butyl acrylate compared to the corresponding chitosan derived materials, there is no clear trend observed for neohexene hydroformylation. Among the different supports, cobalt on ceria gave the lowest conversions and yields (Table 1, entries 2, 3). In fact, the two ceria-supported catalysts are almost inactive. Most suitable for catalysing *n*-butyl acrylate hydroformylation are Co/phen@TiO₂ and Co/phen@C (Table 1, entries 6, 8). Both showed full conversion of *n*-butyl acrylate and over 80% yield. In the case of the chitosan catalysts, Co/Chitosan@SiO₂ gave the highest conversion rate (47%) and a yield of 33% (Table 1, entry 5), followed by the titania-supported Co/chitosan@TiO₂ (Table 1, entry 7). As by-products, we observed in all reactions the corresponding al-

Table 1. Hydroformylation of neohexene and *n*-butyl acrylate catalysed by cobalt nanoparticles on different supports.

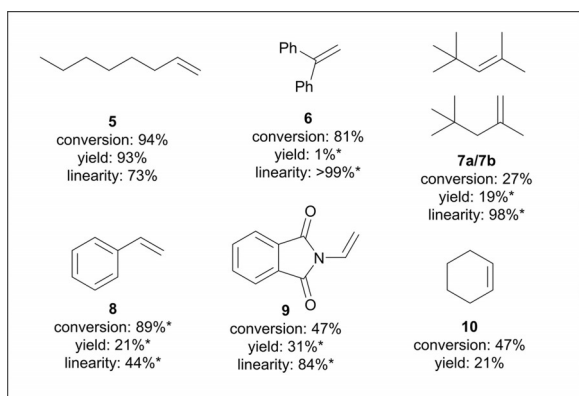
| Entry | Catalyst | Conv. 1 [%] | Yield 2 [%] | Conv. 3 [%] ^[a] | Yield 4 a + 4 b [%] ^[a] | Linearity 4 a, 4 b [%] ^[b] |
|-------|-----------------------------------|-----------------------|-----------------------|--------------------------------------|--|---|
| | | | | | | |
| 1 | Co ₂ (CO) ₈ | 58 | 51 | > 99 | 92 | 95 |
| 2 | Co/phen@CeO ₂ | 4 | 1 | 8 | 2 | > 99 |
| 3 | Co/chitosan@CeO ₂ | 22 | 17 | 2 | 2 | > 99 |
| 4 | Co/phen@SiO ₂ | 22 | 18 | 81 | 60 | 95 |
| 5 | Co/chitosan@SiO ₂ | 52 | 46 | 47 | 33 | 95 |
| 6 | Co/phen@TiO ₂ | 55 | 38 | > 99 | 82 | 95 |
| 7 | Co/chitosan@TiO ₂ | 46 | 36 | 40 | 31 | 98 |
| 8 | Co/phen@C | 53 | 45 | > 99 | 83 | 96 |

Standard reaction conditions: neohexene (**1**) (193 μL, 1.5 mmol) or *n*-butyl acrylate (**3**) (214 μL, 1.5 mmol), catalyst (29.5 mg), toluene (1.5 mL), 40 bar CO/H₂ (1:1), 100 °C, 18 h. [a] Conversions and yields represent the mean value of three experiments and were calculated by GC using hexadecane as internal standard. [b] Linearity represents the amount of **4 a** with respect to the total amount of linear and branched aldehyde (**4 a + 4 b**).

kanes. In the case of *n*-butyl acrylate, we could also detect some dimerisation by-product.

In addition, we tested all catalysts of our library. In general, the catalysts based on other ligands than chitosan or phenanthroline did not show an improved activity. Furthermore, the reaction conditions were varied to study the influence of temperature, pressure, and solvent amount in the presence of the most active catalysts. An overview of these experiments is given in the Supporting Information (Table S3). At 85 °C the rate of hydroformylation of both olefins was significantly declined. The performance for hydroformylation of neohexene could be improved by increasing the reaction temperature to 120 or 140 °C, respectively. Solvent concentration had only a minor influence on the catalysis, however, under neat conditions the selectivity was rather low. By using butyl acrylate, the reaction was also scaled up by a factor of 10 leading to similar results (see Supporting Information, Experimental Methods).

To prove the general suitability of Co/phen@C for other hydroformylations, we investigated reactions of 1-octene (**5**) and cyclohexene (**10**) as linear and cyclic aliphatic compounds, styrene (**8**) as an aromatic compound, *N*-vinyl phthalimid (**9**) and diisobutene (**7**) as industrial relevant substrates, and 1,1-diphenyl ethylene (**6**) as a sterically hindered one. The results of this substrate scope are summarised in Scheme 1.



Scheme 1. Standard reaction conditions: substrate (1.5 mmol), catalyst (29.5 mg), toluene (1.5 mL), 40 bar CO/H₂ (1:1), 100 °C, 18 h. Conversion of **5**–**10**, the yielded products and the linearity represent the mean value of two experiments and were calculated by GC using hexadecane as the internal standard (*) or calculated by ¹H NMR measurements by using 1,4-dimethoxybenzene as the internal standard.

Except for the sterically hindered **6**, we observed mediocre-to-good yields for the generated aldehydes. The hydrogenation of the olefins to the corresponding alkanes is a competitive pathway in some cases. In fact, for **6** and **8** 1,1-diphenyl ethane and ethyl benzene were detected as major products.

Kinetic behaviour and leaching

For a better understanding of the activity of the catalytic materials, we investigated the kinetic behaviour of our systems as well as the metal leaching of the catalysts for hydroformylation

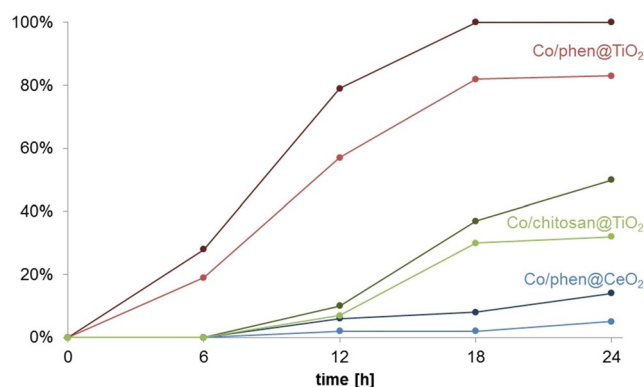


Figure 1. Conversion rates (dark colours) and yields (bright colours) for hydroformylation of *n*-butyl acrylate after a certain reaction time with three different catalysts. Standard reaction conditions: *n*-butyl acrylate (1.5 mmol), catalyst (29.5 mg), toluene (1.5 mL), 40 bar CO/H₂ (1:1), 100 °C. Conversions and yields were calculated by GC using hexadecane as internal standard. Key: dark-red/red graphs represent conversion/yield with catalyst Co/phen@TiO₂, dark-green/green graphs represent conversion/yield with catalyst Co/chitosan@TiO₂, and dark-blue/blue graphs represent conversion/yield with catalyst Co/phen@CeO₂.

of *n*-butyl acrylate under the standard conditions. Therefore, we determined the conversion rates and yields after different reaction times from hours up to 24 hours. The results of these experiments are summarised in Figure 1. We chose three catalysts—one with low (Co/phen@CeO₂, blue graphs), one with moderate (Co/chitosan@TiO₂, green graphs) and one with high productivity (Co/phen@TiO₂, red graphs). For Co/phen@TiO₂ we saw a growing activity until the twelfth hour of the reaction. After that point the activity declined due to saturation effects. Actually, after 18 hours the substrate was completely converted, and the yield of aldehydes remained stable at a level of about 85%. In contrast, for the two least productive catalysts Co/phen@CeO₂ and Co/chitosan@TiO₂, we found out that there is an induction period of at least 6 hours in which the systems are not active. Even after 12 hours, the conversion rates and yields are not higher than 10% for both materials.

Although the activity of Co/chitosan@TiO₂ and the yield and conversions were rising after this induction period, the productivity of the catalysts decreased again after 18 hours and no higher yields than 32% were detected after 24 hours reaction time. Co/phen@CeO₂ showed a slightly different behaviour: for the whole investigated period, there seemed to be the same activity after the induction period. However, the overall productivity of Co/phen@CeO₂ was very low (5% yield after 24 h).

It is well known in the literature that heterogeneous metal catalysts are leaching under typical conditions of hydroformylation. In those cases, the active species—usually a metal carbonyl—is formed in situ.^[50–53] Considering that the reaction solutions were normally coloured after stopping the reaction, we presumed that this colour originated from leached cobalt carbonyl species. Indeed, recycling of the catalyst Co/phen@C by filtration and washing resulted in a significant drop of the productivity. For example, only 8% product yield was detected after the third run compared to 58% after the first cycle (see Supporting Information, Table S4).

Consequently, we decided to study the amount of cobalt in the reaction solutions after stopping the hydroformylation at certain times (6, 12, 18, and 24 hours). For this purpose, the reaction mixtures were filtered immediately after opening the reactor. All volatile components were removed, and the residues were dissolved in aqua regia. Afterwards, the cobalt content of these aqueous solutions was determined by atomic absorption spectroscopy (AAS). The results of this analysis for Co/phen@TiO₂ (red graph), Co/phen@C (orange graph), Co/chitosan@TiO₂ (green graph) and Co/phen@CeO₂ (blue graph) are shown in Figure 2.

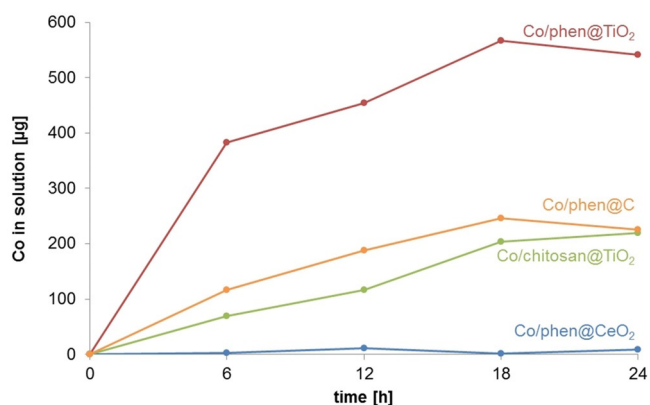


Figure 2. Amount of leached cobalt after a certain time with four different catalysts. Standard reaction conditions: *n*-butyl acrylate (1.5 mmol), catalyst (29.5 mg), toluene (1.5 mL), 40 bar CO/H₂ (1:1), 100 °C. Cobalt mass was calculated based on AAS analysis of the fused reaction solutions. Key: the red graph represents cobalt in solution with catalyst Co/phen@TiO₂, the orange graph represents cobalt in solution with catalyst Co/phen@C, the green graph represents cobalt in solution with catalyst Co/chitosan@TiO₂, and blue graph represents cobalt in solution with catalyst Co/phen@CeO₂.

Obviously, the amount of cobalt in solution correlates to some degree with the productivity of the catalysts. Independent of the reaction time, the leaching of Co/phen@CeO₂ remains on a low level as well as the activity of this catalyst. The amount of cobalt deliberated from the other investigated catalysts Co/phen@TiO₂, Co/phen@C and Co/chitosan@TiO₂ is increasing with the reaction time and seemed to be saturated after 18 hours. For these three materials no clear correlation between leaching and productivity could be ascertained. On the one hand, Co/phen@C and Co/phen@TiO₂ showed almost same results for conversion and yield after 18 hours (see Table 1). In contrast to that, the amount of leached cobalt is two-fold higher for Co/phen@TiO₂ as for Co/phen@C. On the other hand, the detected values for cobalt in solution for the reaction with Co/phen@C and Co/chitosan@TiO₂ are at the same level, whereas the activity of both materials for hydroformylation differs not proportionally. Interestingly, there is no correlation between cobalt content at the surface and amount of leached cobalt, as well (see Supporting Information).

These results demonstrate that both precursor and support of the catalyst have an influence on metal leaching. Notably, adding the commercial support material silica or titania to the active homogeneous catalyst, resulted in a strong decline of

the catalyst activity, whereas addition of carbon or ceria did not show any influence on the performance (see Supporting Information, Table S4).

Conclusions

In summary, we prepared several Co-containing materials by pyrolysis and demonstrated their performance in several hydroformylation reactions. The kinetic behaviour and the rate of leaching of the catalysts depend strongly on the support and the in situ generated cobalt complex. As a result of these investigations, we assume that the presented hydroformylation reactions take place mainly in solution. Nevertheless, active centres on the surface are also productive to a limited extent. In general, both Co/phen@TiO₂ and Co/phen@C represent stable, non-volatile, and easy-to-handle reservoirs for active homogeneous cobalt species, and thus can conveniently substitute the common but toxic dicobalt octacarbonyl complex in hydroformylations on a small scale. Further investigations to find more stable heterogeneous catalysts for hydroformylation are ongoing in our group.

Experimental Section

Catalytic experiments

Typically, the catalytic experiments were carried out in 4 mL glass vials. The vials were filled with 1.5 mL toluene, 193 µL neohexene (1.5 mmol) or 214 µL *n*-butyl acrylate, 29.5 mg of the catalyst (corresponding to 1 mol% of Co), and a glass-coated stirring bar and closed with a septum cap. To allow gas exchange, a needle was pierced through the septum. The vials were placed on a steel plate in a 300 mL steel autoclave. The closed reactor was washed three times with syngas and filled with 40 bar syngas (H₂/CO = 1:1). The reaction was performed for 18 hours at 100 °C while stirring (700 to 800 rpm) the reaction mixtures. After stopping the reaction by cooling the autoclave, the gas was released. The vials were moved out of the autoclave and hexadecane as the standard was added to the reaction solution. After diluting with acetone, ethyl acetate, or toluene the grey-to-black suspension was filtered through a syringe filter. Yields and conversion rates were calculated by GC analysis with hexadecane as the internal standard.

Proof of leaching

To prove the leaching, the filtered reaction solution (hydroformylation of *n*-butyl acrylate) was transferred into a pressure tube. All volatile components of the solution were removed under reduced pressure and 6 mL of aqua regia (HNO₃/HCl = 1:3) were added to the residue. The pale-yellow mixture was heated up to 140 °C for 4 hours in the closed pressure tube. The resulting red-brownish solution was cooled down to room temperature and then diluted with 6 mL of water. After that, air was funnelled through the solution to remove all nitrogen oxides, the solution was filled with water up to 25 mL and was analysed by AAS.

Kinetic experiments

For the kinetic experiments, the reaction protocol was the same as for the catalytic experiments. The reaction time was decreased to 6

or 12 hours or increased to 24 h, respectively. The workup and the analytic procedure were the same as described before.

Acknowledgements

This work was part of the KataPlasma project (MatResources program) funded by the German Federal Ministry of Education and Research (BMBF). NoNaCat program and the federal state of Mecklenburg Western Pomerania are gratefully acknowledged for financial funding. We thank Dr. Annette-Enrica Surkus for fruitful discussions and her useful advice for the preparation of heterogeneous catalysts. Dr. Giovanni Agostini is acknowledged for the XPS measurements. We thank Alexander Wotzka for conducting TGA measurements. The support of the analytical department of the LIKAT and the University of Rostock especially for the elementary analysis is acknowledged.

Conflict of interest

The authors declare no conflict of interest.

Keywords: aldehydes · carbonylation · cobalt · heterogeneous catalysis · hydroformylation · leaching

- [1] R. Franke, D. Selent, A. Börner, *Chem. Rev.* **2012**, *112*, 5675–5732.
- [2] A. Börner, R. Franke, *Hydroformylation: Fundamentals, Processes, and Applications in Organic Synthesis*, Wiley-VCH, Weinheim, **2016**.
- [3] J. Pospech, I. Fleischer, R. Franke, S. Buchholz, M. Beller, *Angew. Chem. Int. Ed.* **2013**, *52*, 2852–2872; *Angew. Chem.* **2013**, *125*, 2922–2944.
- [4] R. Tudor, M. Ashley, *Platinum Met. Rev.* **2007**, *51*, 116.
- [5] K.-D. Wiese, D. Obst in *Catalytic Carbonylation Reactions* (Ed.: M. Beller), Springer, Heidelberg, **2006**, pp. 1–33.
- [6] F. Hebrard, P. Kalck, *Chem. Rev.* **2009**, *109*, 4272–4282.
- [7] L. Alvarado Rupflin, J. Mormul, M. Lejkowski, S. Titlbach, R. Papp, R. Gläser, M. Dimitrakopoulou, X. Huang, A. Trunschke, M. G. Willinger, R. Schlögl, F. Rosowski, S. A. Schunk, *ACS Catal.* **2017**, *7*, 3584–3590.
- [8] C. Li, L. Yan, L. Lu, K. Xiong, W. Wang, M. Jiang, J. Liu, X. Song, Z. Zhan, Z. Jiang, Y. Ding, *Green Chem.* **2016**, *18*, 2995–3005.
- [9] R. Lang, T. Li, D. Matsumura, S. Miao, Y. Ren, Y.-T. Cui, Y. Tan, B. Qiao, L. Li, A. Wang, X. Wang, T. Zhang, *Angew. Chem. Int. Ed.* **2016**, *55*, 16054–16058; *Angew. Chem.* **2016**, *128*, 16288–16292.
- [10] Q. Sun, Z. Dai, X. Liu, N. Sheng, F. Deng, X. Meng, F.-S. Xiao, *J. Am. Chem. Soc.* **2015**, *137*, 5204–5209.
- [11] T. T. Adint, C. R. Landis, *J. Am. Chem. Soc.* **2014**, *136*, 7943–7953.
- [12] M. Jakuttis, A. Schönweiz, S. Werner, R. Franke, K. D. Wiese, M. Haumann, P. Wasserscheid, *Angew. Chem. Int. Ed.* **2011**, *50*, 4492–4495; *Angew. Chem.* **2011**, *123*, 4584–4588.
- [13] C. Li, W. Wang, L. Yan, Y. Ding, *Front. Chem. Sci. Eng.* **2018**, *12*, 113–123.
- [14] D. Gorbunov, D. Safronova, Y. Kardasheva, A. Maximov, E. Rosenberg, E. Karakhanov, *ACS Appl. Mater. Interfaces* **2018**, *10*, 26566–26575.
- [15] X. Song, Y. Ding, W. Chen, W. Dong, Y. Pei, J. Zang, L. Yan, Y. Lu, *Appl. Mech. Mater.* **2013**, *477–478*, 155–159.
- [16] Z. Cai, H. Wang, C. Xiao, M. Zhong, D. Ma, Y. Kou, *J. Mol. Catal. A* **2010**, *330*, 94–98.
- [17] Y. Zhang, K. Nagasaka, X. Qiu, N. Tsubaki, *Catal. Today* **2005**, *104*, 48–54.
- [18] G. Parrinello, J. K. Stille, *J. Am. Chem. Soc.* **1987**, *109*, 7122–7127.
- [19] J. Su, C. Xie, C. Chen, Y. Yu, G. Kennedy, G. A. Somorjai, P. Yang, *J. Am. Chem. Soc.* **2016**, *138*, 11568–11574.
- [20] D. G. Hanna, S. Shylesh, P. A. Parada, A. T. Bell, *J. Catal.* **2014**, *311*, 52–58.
- [21] L. Oresmaa, M. A. Moreno, M. Jakonen, S. Suvanto, M. Haukka, *Appl. Catal. A* **2009**, *353*, 113–116.
- [22] A. E. Marteel, T. T. Tack, S. Bektesevic, J. A. Davies, M. R. Mason, M. A. Abraham, *Environ. Sci. Technol.* **2003**, *37*, 5424–5431.
- [23] L. Alvila, J. Pursiainen, J. Kiviaho, T. A. Pakkanen, O. Krause, *J. Mol. Catal.* **1994**, *91*, 335–342.
- [24] M. Haumann, A. Riisager, *Chem. Rev.* **2008**, *108*, 1474–1497.
- [25] A. Riisager, R. Fehrmann, M. Haumann, P. Wasserscheid, *Eur. J. Inorg. Chem.* **2006**, 695–706.
- [26] A. Riisager, P. Wasserscheid, R. van Hal, R. Fehrmann, *J. Catal.* **2003**, *219*, 452–455.
- [27] A. Riisager, R. Fehrmann, S. Flicker, R. van Hal, M. Haumann, P. Wasserscheid, *Angew. Chem. Int. Ed.* **2005**, *44*, 815–819; *Angew. Chem.* **2005**, *117*, 826–830.
- [28] C. Van Doorslaer, J. Wahlen, P. Mertens, K. Binnemans, D. De Vos, *Dalton Trans.* **2010**, *39*, 8377–8390.
- [29] J. Liu, *ACS Catal.* **2017**, *7*, 34–59.
- [30] X.-F. Yang, A. Wang, B. Qiao, J. Li, J. Liu, T. Zhang, *Acc. Chem. Res.* **2013**, *46*, 1740–1748.
- [31] X. Cui, K. Junge, X. Dai, C. Kreyenschulte, M.-M. Pohl, S. Wohlrab, F. Shi, A. Brückner, M. Beller, *ACS Cent. Sci.* **2017**, *3*, 580–585.
- [32] D. Astruc, F. Lu, J. R. Aranzas, *Angew. Chem. Int. Ed.* **2005**, *44*, 7852–7872; *Angew. Chem.* **2005**, *117*, 8062–8083.
- [33] L. Liu, A. Corma, *Chem. Rev.* **2018**, *118*, 4981–5079.
- [34] F. A. Westerhaus, R. V. Jagadeesh, G. Wienhöfer, M.-M. Pohl, J. Radnik, A.-E. Surkus, J. Rabeah, K. Junge, H. Junge, M. Nielsen, A. Brückner, M. Beller, *Nat. Chem.* **2013**, *5*, 537–543.
- [35] D. Formenti, C. Topf, K. Junge, F. Ragaini, M. Beller, *Catal. Sci. Technol.* **2016**, *6*, 4473–4477.
- [36] R. V. Jagadeesh, A.-E. Surkus, H. Junge, M.-M. Pohl, J. Radnik, J. Rabeah, H. Huan, V. Schünemann, A. Brückner, M. Beller, *Science* **2013**, *342*, 1073–1076.
- [37] M. Lefèvre, E. Proietti, F. Jaouen, J.-P. Dodelet, *Science* **2009**, *324*, 71–74.
- [38] F. Chen, C. Kreyenschulte, J. Radnik, H. Lund, A.-E. Surkus, K. Junge, M. Beller, *ACS Catal.* **2017**, *7*, 1526–1532.
- [39] F. K. Scharnagl, M. F. Hertrich, F. Ferretti, C. Kreyenschulte, H. Lund, R. Jackstell, M. Beller, *Sci. Adv.* **2018**, *4*, eaau1248.
- [40] B. Sahoo, A.-E. Surkus, M.-M. Pohl, J. Radnik, M. Schneider, S. Bachmann, M. Scalone, K. Junge, M. Beller, *Angew. Chem. Int. Ed.* **2017**, *56*, 11242–11247; *Angew. Chem.* **2017**, *129*, 11394–11399.
- [41] B. Sahoo, D. Formenti, C. Topf, S. Bachmann, M. Scalone, K. Junge, M. Beller, *ChemSusChem* **2017**, *10*, 3035–3039.
- [42] T. X. Wu, G. Z. Wang, X. Zhang, C. Chen, Y. X. Zhang, H. J. Zhao, *Chem. Commun.* **2015**, *51*, 1334–1337.
- [43] K. Kurita, *Mar. Biotechnol.* **2006**, *8*, 203.
- [44] X. Chen, H. Yang, N. Yan, *Chem. Eur. J.* **2016**, *22*, 13402–13421.
- [45] N. Yan, X. Chen, *Nature* **2015**, *524*, 155–157.
- [46] E. Guibal, *Sep. Purif. Technol.* **2004**, *38*, 43–74.
- [47] E. Taboada, G. Cabrera, R. Jimenez, G. Cardenas, *J. Appl. Polym. Sci.* **2009**, *114*, 2043–2052.
- [48] A. Primo, P. Atienzar, E. Sanchez, J. M. Delgado, H. Garcia, *Chem. Commun.* **2012**, *48*, 9254–9256.
- [49] L. Zhao, N. Baccile, S. Gross, Y. Zhang, W. Wei, Y. Sun, M. Antonietti, M.-M. Titirici, *Carbon* **2010**, *48*, 3778–3787.
- [50] D. F. Taylor, B. E. Hanson, M. E. Davis, *Inorg. Chim. Acta* **1987**, *128*, 55–60.
- [51] M. Lenarda, L. Storaro, R. Ganzerla, *J. Mol. Catal. A* **1996**, *111*, 203–237.
- [52] J. A. Díaz-Auñón, M. C. Román-Martínez, C. Salinas-Martínez de Lecea, *J. Mol. Catal. A* **2001**, *170*, 81–93.
- [53] M. C. Román-Martínez, J. A. Díaz-Auñón, C. Salinas-Martínez de Lecea, H. Alper, *J. Mol. Catal. A* **2004**, *213*, 177–182.

Manuscript received: December 19, 2018

Accepted manuscript online: February 19, 2019

Version of record online: March 19, 2019

5.4. Homogeneous catalytic hydrogenation of CO₂ to methanol – improvements with tailored ligands

F. K. Scharnagl,* M. F. Hertrich,* G. Neitzel, R. Jackstell, M. Beller, *Adv. Synth. Catal.* **2019**, *361*, 374-379

* These authors contributed equally to this work.

DOI: 10.1002/adsc.201801314

© 2019 Wiley-VCH Verlag GmbH & Co. KGaA, Weinheim

Contributions: F.K.S. synthesised the modified Triphos-ligands and tested them in the catalytic reaction, along with other ligands. Also he tested additional additives and cobalt-precursors. The overall contribution is about 40%.

Homogeneous Catalytic Hydrogenation of CO₂ to Methanol – Improvements with Tailored Ligands

Florian Korbinian Scharnagl,^{+a} Maximilian Franz Hertrich,^{+a} Gordon Neitzel,^a Ralf Jackstell,^a and Matthias Beller^{a,*}

^a Leibniz-Institut für Katalyse e.V. an der Universität Rostock, Albert-Einstein-Straße 29A, 18059 Rostock, Germany
E-mail: matthias.beller@catalysis.de

⁺ These authors contribute equally to this work.

Manuscript received: September 28, 2018; Revised manuscript received: November 9, 2018;
Version of record online: December 11, 2018



Supporting information for this article is available on the WWW under <https://doi.org/10.1002/adsc.201801314>

Abstract: Improved molecularly-defined cobalt catalysts for the hydrogenation of carbon dioxide to methanol have been developed. A key factor for increased productivity (up to twofold compared to previous state-of-the-art-system) is the specific nature of substituents on the triphos ligand. In addition, the effect of metal precursors, and variations of additives have been investigated.

Keywords: carbon dioxide; methanol; homogeneous catalysis; triphos; hydrogenation

Introduction

The hydrogenation of mixtures of carbon monoxide, carbon dioxide and hydrogen to methanol is one of the most important catalytic processes in the area of industrial bulk chemicals.^[1] In fact, there was an annual demand of more than 90 million tons in 2016.^[2] In addition to current applications, methanol is considered as potential energy carrier, within the concept of “methanol economy”, which has been proposed by Asinger^[3] and Olah.^[4] In this vision, either methanol or its derivative dimethylether is used for fuel cells or engines, respectively.^[5]

Today, the present route to methanol uses synthesis gas as main feedstock, which is transformed with water to carbon dioxide *in situ*. The majority of these processes make use of Cu/ZnO/Al₂O₃ catalyst systems at 190–270 °C and 15–90 bar pressure.^[6] In recent years, an increasing interest exists for methanol production directly by carbon dioxide hydrogenation.^[7] As an example, besides pilot applications, the so-called “George Olah CO₂ to Renewable Methanol

Plant” exists in Iceland with a capacity of about 4’000 tons per year.^[8] Obviously, the particular conditions for low cost energy are crucial for this demonstration unit. For the future a sustainable methanol production on a larger scale necessitates hydrogenation of (captured) CO₂ with H₂, which in turn comes from electrolysis of water.^[5b,9] Advantageously, such a concept offers the possibility for a decentralized supply of methanol from CO₂.

Although several heterogeneous materials are known for the direct conversion of CO₂ to methanol, similar homogeneous approaches with organometallic complexes are still at an early stage.^[10] The majority of these molecularly-defined systems work under basic conditions. For instance, basic pre-activation of CO₂ with amines and subsequent hydrogenation of the intermediate to methanol in a second step was demonstrated by the groups of Milstein,^[11] Sanford,^[12] Olah/Prakash,^[1b,13] and Wass,^[14] as well as Martins and Pombeiro.^[15]

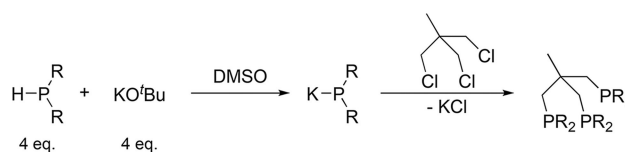
On the other hand, only few systems are known for direct CO₂ hydrogenation to methanol, which requires acidic conditions. As a step in this direction, Huff and Sanford reported a Ru-based cascade catalysis process, which involves three different catalysts at once.^[16] In this system, CO₂ was hydrogenated to formic acid, which was subsequently esterified in the presence of acid. Eventually, the ester was hydrogenated to methanol with an overall TON of 2.5. Furthermore, the CO₂ reduction to methanol at ambient, aqueous, acidic conditions was enabled by a disproportionation strategy. The groups of Himeda and Laurency reported Ir-based, sulfuric acid co-catalysed transformation of CO₂ to formic acid, followed by complete and selective decomposition to methanol by regenerating CO₂, again.^[17]

However, all these systems involve either pre-activation of CO₂ or multiple catalysts for the formation of methanol. For a direct process, the tridentate phosphorous-ligand triphos (1,1,1-tris(diphenylphosphinomethyl)ethane) plays a crucial role. First, the groups of Klankermayer and Leitner expanded their previously published studies on the hydrogenation of carboxylic acids with a system based on this very ligand and ruthenium to the hydrogenation of CO₂.^[18] Here, methanol was formed in the presence of HNTf₂ (bis(trifluoromethane) sulfimide) at 140 °C, 20 bar CO₂ and 60 bar H₂ with a TON of up to 221.^[19] The TON was later doubled to 442 by reducing the catalyst loading by half, along with an extensive mechanistic investigation *via* NMR, MS and computational studies.^[20] The group of de Bruin transferred this concept to cobalt, which was able to hydrogenate carboxylic esters and acids with high conversion at 100 °C.^[21] In continuation of this work, the first homogeneous, base-metal catalyst for the direct methanol production from CO₂ was reported by our group in 2017.^[22] The combination of triphos and Co(acac)₃ with HNTf₂ as an additive in a solvent mixture of THF/ethanol gave methanol with a TON of 50. The presence of ethanol was found to be important for this system, even though ethyl formate seems not to be an intermediate in this reaction. Here, we report an improved cobalt catalyst system which allows for the synthesis of methanol at low temperature (90–100 °C) with improved turnover numbers and demonstrates the possibility to run such a process without additives.

Results and Discussion

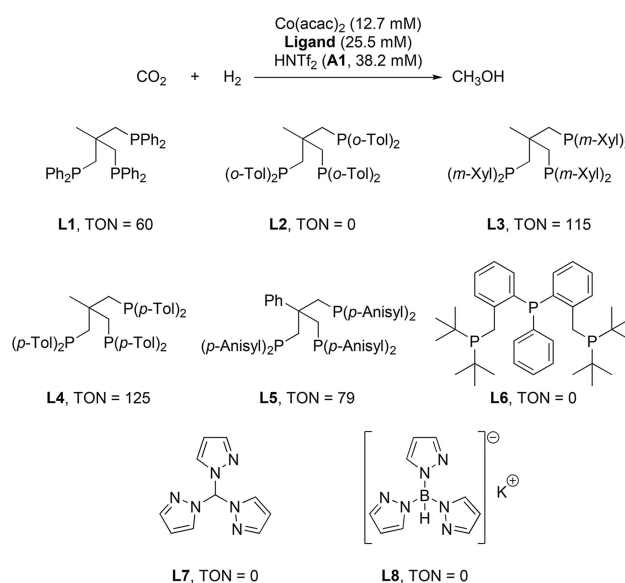
Basically all the known homogeneous catalysts for direct CO₂ to methanol conversion make use of the ligand triphos or its derivatives. In this respect, modifications of the ligand skeleton, but also variation of the phosphorus substituents are of general interest.^[23] Already in 1994, Huttner and co-workers developed a convenient methodology for the preparation of aryl-modified triphos derivatives.^[24] Starting from secondary phosphines and threefold chloro-substituted neopentane (1,1,1-tris(chloromethyl)ethane) in presence of potassium hydroxide a simple metathesis reaction in DMSO gave the corresponding tripod ligand, water and potassium chloride as products. Based on a slightly modified procedure (Scheme 1),^[25] we have recently reported the preparation of a small library of such ligands.^[23]

Hence, ligands **L1–L6** were tested for the CO₂-hydrogenation to methanol in the presence of cobalt salts and HNTf₂ as an additive. Using sublimed Co(acac)₂ together with the parent ligand **L1** gave a slightly more active catalyst system (TON: 60) than Co(acac)₃ (TON: 50). As shown in Scheme 2, using



Scheme 1. General synthesis of triphos-derivatives.

the *ortho*-substituted derivative **L2** instead of **L1** inhibited the reaction completely. This indicates the strong influence of sterically demanding groups, which likely disturb the coordination of the P-atom to the metal centre. On the other hand, methyl-substitution on the aryl substituents in *meta*- or *para*-position improved the TONs (**L3**, **L4**) by a factor of two with respect to unmodified triphos.^[26] This might have two reasons; first the electron density on phosphorus is significantly increased. Therefore, also the metal centre is electron-rich, which accelerates the H₂-activation. In addition, a substitution in *meta*- or *para*-position might prevent the formation of a μ₂-dihydro-bridged Co-dimer. The generation of an analogous Ru-dimer was determined as deactivation pathway in the system reported by Klankermayer and Leitner.^[20,25] Unexpectedly, the stronger electron-donating methoxy-group in *para*-position (**L5**) gave a lower TON of 79.



Scheme 2. Investigation of ligands in the homogeneous hydrogenation of CO₂ to methanol with cobalt. Reaction conditions: Co(acac)₂, ligand, HNTf₂ (1:2:3), THF:EtOH (8:3), 20 bar CO₂, 70 bar H₂, 100 °C, 24 h. Mass of methanol was determined *via* GC using hexadecane as internal standard. TON = n_{product}/n_{catalyst}.

The resulting free coordination sites of cobalt can rapidly be occupied by triphos. The conjugated base of the additive acts as weakly coordinating anion and stabilises the cationic species. In the case of CoCO_3 , carbon dioxide is released in strong acidic media and again cobalt can be ligated and form a cationic species. $\text{Co}(\text{NTf}_2)_2$ does not need an additive, as Tf_2N^- is weakly coordinating and triphos can therefore easily coordinate to cobalt to give $[\text{Co}(\text{Triphos})(\text{L})_n]^{m+}$, again.

Previously, it was shown that the activity of the cobalt-based system decreases during time.^[22a] For this reason, studies on the deactivation of the catalyst in the presence of potential poisons have been conducted (Scheme 4). It was found that both products of the

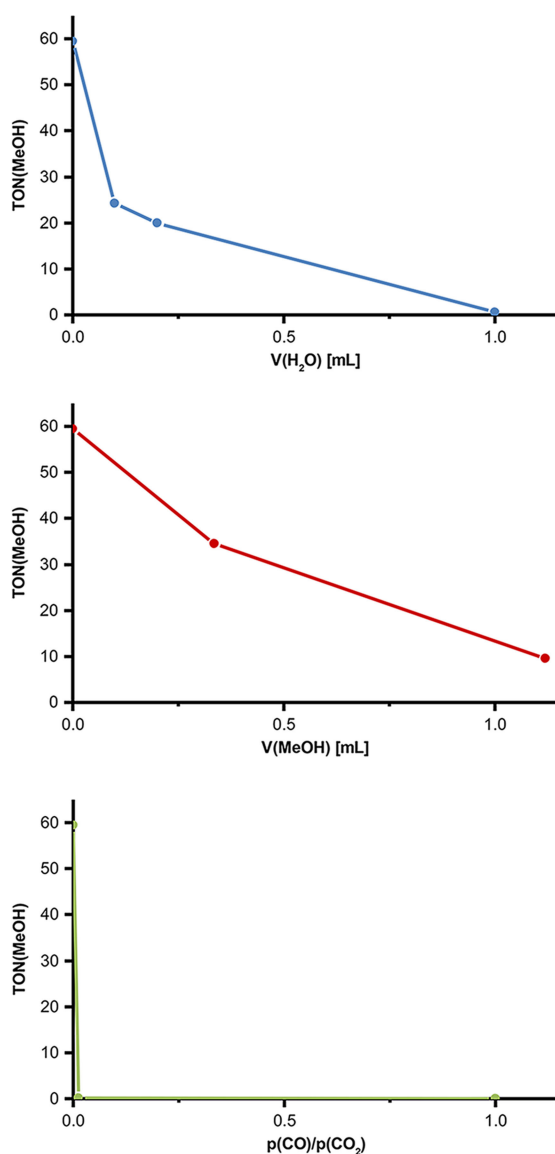
reaction, water and methanol, inhibit the catalyst system. With increasing amounts of them, the TON for the production of methanol decreased to a TON of 10 (1.1 ml MeOH) or 1 (1 ml of water), respectively. Hence, we tried to remove the *in situ* produced water by addition of triethyl orthoester. Unfortunately, with a TON of 52 the catalyst performance could not be improved. Besides of product-inhibition, a major poisoning effect has carbon monoxide. Even traces of CO ($\text{CO}_2:\text{CO}=80:1$) quenched the reaction completely and no methanol was detected. Hence, it is clear that catalyst improvements in the future need to take these points into account, for instance by removing the products from the product phase.

Conclusion

In conclusion, the performance of the cobalt-catalysed reduction of CO_2 to methanol has been improved. Using modified triphos ligands led to higher TON up to 125 and by replacing $\text{Co}(\text{acac})_2$ with $\text{Co}(\text{NTf}_2)_2$, an additive free system was developed, which is also active below 100°C . Apart, the role of the additive as a weakly coordinating anion was highlighted and catalyst deactivation pathways were identified. For further optimisations, CO-, methanol- and water-resistant catalyst systems have to be developed. Currently, further mechanistic investigations are ongoing in our laboratory, which should shed more light on this interesting topic.

Experimental Section

All chemicals were purchased from commercial sources and were used as received without additional purification, if not stated otherwise. Gases were purchased by *Linde*. All experiments were carried out under argon atmosphere by using a glovebox or standard Schlenk-techniques, unless stated otherwise. Solvents were stored over molecular sieves 4 Å. THF was dried over sodium and benzophenone. Ethanol was dried over magnesium. The ligands **L2**,^[28] **L3**,^[25] **L4**,^[25] **L5**^[23] and **L6**^[29] were synthesised according to reported procedures. Catalytic experiments were conducted in high pressure Parr autoclaves and stirred either mechanically, or with a cross-shaped stirring bar. ^1H , ^{31}P and ^{13}C NMR spectra were recorded on Bruker AV-300, Bruker Fourier 300 or Bruker AV-400 spectrometers. Chemical shifts (δ) are reported in ppm downfield of tetramethylsilane. The NMR chemical shifts are reported relative to the centre of solvent resonance [CD_2Cl_2 : 5.32 (^1H), 53.8 (^{13}C), CDCl_3 : 7.26 (^1H), 77.0 (^{13}C)]. Gas chromatography analysis was performed on an *Agilent* HP-6890 chromatograph with a FID detector and an *Agilent* HP Ultra 1 column (19091A-105, 50 m, 0.20 mm i.d., 0.33 μm film thickness, 100% dimethylpolysiloxane) using hydrogen as carrier gas.



Scheme 4. Investigations on the deactivation of the catalyst in the presence of potential poisons: water (blue), methanol (red) and CO (green).

Synthesis of Brookhart's Acid

According to a modified literature procedure of Brookhart *et al.*^[30] 1.14 mmol (1012.6 mg) Na[BAR^F₄] were dissolved in 14 mL Et₂O at -78 °C. To the pale yellow solution, 4.57 mL of a 1 M solution of HCl in Et₂O were added. A white solid precipitated out and after 2 h stirring, the cold suspension was filtered. The filtrate was concentrated to give a white solid in a pale yellow liquid. The mixture was stored overnight and then the mother liquor was removed with a syringe. The white product was dried in high vacuum (801 mg, 69%)

General Procedure for the Hydrogenation of CO₂

Experiments in a 100 mL Autoclave

0.14 mmol of metal-precursor and 0.28 mmol ligand were weighed in a Schlenk-tube inside the glovebox. In a separate Schlenk-tube were weighed in 0.42 mmol of additive, if used, inside the glovebox. Outside, the metal-precursor and the ligand were dissolved in 8 mL THF. The additive was dissolved in 3 mL ethanol. The solutions were combined and stirred for further 5–10 minutes. A 100 mL (Hastelloy® C) autoclave was sealed, and evacuated and purged with argon for three times. If a stainless-steel autoclave was used, the reaction was carried out in a glass insert. Afterwards, the catalyst-solution was injected. The autoclave was loaded with 20 bar CO₂ at room temperature, followed by 70 bar H₂. It was heated by an aluminium-block for 24 h. Finally, it was cooled with an ice-bath to quench the reaction. 100 µL hexadecane were added as internal standard and after proper stirring of the solution it was analysed by GC.

Experiments in a 25 mL Autoclave

0.035 mmol of metal-precursor and 0.07 mmol ligand were weighed in a Schlenk-tube inside the glovebox. In a separate Schlenk-tube were weighed in 0.105 mmol of additive, if used, inside the glovebox. Outside, the metal-precursor and the ligand were dissolved in 2 mL THF. The additive was dissolved in 0.75 mL ethanol. The solutions were combined and stirred for further 5–10 minutes. A 25 mL Hastelloy® C autoclave was sealed, and evacuated and purged with argon for three times. Afterwards, the catalyst-solution was injected. The autoclave was loaded with 20 bar CO₂ at room temperature, followed by 70 bar H₂. It was heated by an aluminium-block for 24 h. Finally, it was cooled with an ice-bath to quench the reaction. 20 µL hexadecane were added as internal standard and after proper stirring of the solution it was analysed by GC.

Experiments with a Stock-Solution

0.7 mmol (433.46 mg, 1.0 eq) Co(NTf₂)₂ and 1.4 mmol (874.54 mg, 2.0 eq) L1 were weighed in a 100 mL Schlenk-flask inside the glovebox. Outside, 40 mL THF were added and the reddish solution was refluxed for 10 minutes, during which the colour changed to dark red/brownish (see SI). Alternatively, the fresh stock-solution was stored at room-temperature for several days, during which the same colour-

change took place. For the catalytic testing, 8 mL of the stock-solution was injected in the autoclave under argon, followed by 3 mL ethanol. The autoclave was loaded with 20 bar CO₂ at room temperature, followed by 70 bar H₂. It was heated by an aluminium-block for 24 h. Finally, it was cooled with an ice-bath to quench the reaction. 100 µL hexadecane were added as internal standard and after proper stirring of the solution it was analysed by GC.

Deactivation Studies for the CO₂ Hydrogenation

Inhibition with Water or Methanol

The catalyst-solution was prepared as usual, but the indicated amounts of water or methanol, respectively, were added additionally. The reaction was then carried out and worked up as stated above.

Poisoning with CO

The catalyst-solution was prepared as usual and injected in the autoclave. For a 1:1 mixture of CO₂ and CO, the autoclave was first loaded with 10 bar CO, followed by 10 bar CO₂. Afterwards H₂ was introduced and the reaction was then carried out and worked up as stated above. For a poisoning with 1.25 vol% CO, the autoclave was first loaded with 1 atm of CO. Then, CO₂ was loaded to a total pressure of 40 bars at room temperature. The pressure was released to 10 bar, and CO₂ was loaded to a total pressure of 20 bars. Afterwards, a total pressure of 90 bar was adjusted with H₂ and the reaction was carried out and worked up as stated above.

Acknowledgements

Financial support from the state of Mecklenburg-West Pomerania, the Federal Ministry of Education and Research (BMBF), the Danish National Research Foundation CA-DIAC (Carbon Dioxide Activation Centre), and MethaCycle Project from the Federal Ministry for Economic Affairs and Energy (BMWi) is gratefully acknowledged. We also thank Dr. Weiping Liu (LIKAT) for providing L5, and Veronica Papa, Jacob Schneidewind (both LIKAT) and Prof. Jiwoong Lee (University of Copenhagen) for helpful discussions. We thank the analytical department of LIKAT for conducting measurements.

References

- [1] a) M. Behrens, F. Studt, I. Kasatkin, S. Kuhl, M. Havecker, F. Abild-Pedersen, S. Zander, F. Girgsdies, P. Kurr, B. L. Kniep, M. Tovar, R. W. Fischer, J. K. Nørskov, R. Schlögl, *Science* **2012**, *336*, 893–897; b) J. Kothandaraman, A. Goepfert, M. Czaun, G. A. Olah, G. K. S. Prakash, *J. Am. Chem. Soc.* **2016**, *138*, 778–781.
- [2] K. A. Ali, A. Z. Abdullah, A. R. Mohamed, *Renew. Sustain. Energy Rev.* **2015**, *44*, 508–518.
- [3] F. Asinger, *Methanol, Chemie- und Energierohstoff*, Akademie-Verlag, Berlin, **1987**.

- [4] G. A. Olah, A. Goepfert, G. K. S. Prakash, *Beyond Oil and Gas: The Methanol Economy*, Wiley-VCH, Weinheim, Germany, **2006**.
- [5] a) A. Goepfert, M. Czaun, J.-P. Jones, G. K. Surya Prakash, G. A. Olah, *Chem. Soc. Rev.* **2014**, *43*, 7995–8048; b) K. Sordakis, C. Tang, L. K. Vogt, H. Junge, P. J. Dyson, M. Beller, G. Laurency, *Chem. Rev.* **2017**, *118*, 372–433; c) G. A. Olah, G. K. S. Prakash, A. Goepfert, *J. Am. Chem. Soc.* **2011**, *133*, 12881–12898.
- [6] a) M. Behrens, F. Studt, I. Kasatkin, S. Kühn, M. Hävecker, F. Abild-Pedersen, S. Zander, F. Girgsdies, P. Kurr, B.-L. Kniep, M. Tovar, R. W. Fischer, J. K. Nørskov, R. Schlögl, *Science* **2012**, *336*, 893–897; b) K. C. Waugh, *Catal. Today* **1992**, *15*, 51–75; c) M. Behrens, *Angew. Chem. Int. Ed.* **2014**, *53*, 12022–12024.
- [7] a) J. Artz, T. E. Müller, K. Thenert, J. Kleinekorte, R. Meys, A. Sternberg, A. Bardow, W. Leitner, *Chem. Rev.* **2018**, *118*, 434–504; b) G. Fiorani, W. Guo, A. W. Kleij, *Green Chem.* **2015**, *17*, 1375–1389.
- [8] G. A. Olah, *Angew. Chem. Int. Ed.* **2013**, *52*, 104–107.
- [9] A. Álvarez, A. Bansode, A. Urakawa, A. V. Bavykina, T. A. Wezendonk, M. Makkee, J. Gascon, F. Kapteijn, *Chem. Rev.* **2017**, *117*, 9804–9838.
- [10] a) E. Alberico, M. Nielsen, *Chem. Commun.* **2015**, *51*, 6714–6725; b) S. Kar, J. Kothandaraman, A. Goepfert, G. K. Surya Prakash, *J. CO₂ Util.* **2018**, *23*, 212–218.
- [11] J. R. Khusnutdinova, J. A. Garg, D. Milstein, *ACS Catal.* **2015**, *5*, 2416–2422.
- [12] N. M. Rezayee, C. A. Huff, M. S. Sanford, *J. Am. Chem. Soc.* **2015**, *137*, 1028–1031.
- [13] a) S. Kar, A. Goepfert, J. Kothandaraman, G. K. S. Prakash, *ACS Catal.* **2017**, 6347–6351; b) S. Kar, R. Sen, A. Goepfert, G. K. S. Prakash, *J. Am. Chem. Soc.* **2018**, *140*, 1580–1583.
- [14] D. Wass, M. Everett, *Chem. Commun.* **2017**, *53*, 9502–9504.
- [15] A. P. C. Ribeiro, L. M. D. R. S. Martins, A. J. L. Pombeiro, *Green Chem.* **2017**, *19*, 4811–4815.
- [16] C. A. Huff, M. S. Sanford, *J. Am. Chem. Soc.* **2011**, *133*, 18122–18125.
- [17] K. Sordakis, A. Tsurusaki, M. Iguchi, H. Kawanami, Y. Himeda, G. Laurency, *Chem. Eur. J.* **2016**, *22*, 15605–15608.
- [18] a) F. M. A. Geilen, B. Engendahl, M. Hölscher, J. Klankermayer, W. Leitner, *J. Am. Chem. Soc.* **2011**, *133*, 14349–14358; b) T. vom Stein, M. Meuresch, D. Limper, M. Schmitz, M. Hölscher, J. Coetzee, D. J. Cole-Hamilton, J. Klankermayer, W. Leitner, *J. Am. Chem. Soc.* **2014**, *136*, 13217–13225.
- [19] S. Wesselbaum, T. vom Stein, J. Klankermayer, W. Leitner, *Angew. Chem. Int. Ed.* **2012**, *51*, 7499–7502.
- [20] S. Wesselbaum, V. Moha, M. Meuresch, S. Brosinski, K. M. Thenert, J. Kothe, T. v. Stein, U. Englert, M. Holscher, J. Klankermayer, W. Leitner, *Chem. Sci.* **2015**, *6*, 693–704.
- [21] T. J. Korstanje, J. Ivar van der Vlugt, C. J. Elsevier, B. de Bruin, *Science* **2015**, *350*, 298–302.
- [22] a) J. Schneidewind, R. Adam, W. Baumann, R. Jackstell, M. Beller, *Angew. Chem. Int. Ed.* **2017**, *56*, 1890–1893; b) W. Liu, B. Sahoo, K. Junge, M. Beller, *Acc. Chem. Res.* **2018**.
- [23] W. Liu, B. Sahoo, A. Spannenberg, K. Junge, M. Beller, *Angew. Chem. Int. Ed.* **2018**, *57*, 11673–11677.
- [24] A. Muth, O. Walter, G. Huttner, A. Asam, L. Zsolnai, C. Emmerich, *J. Organomet. Chem.* **1994**, *468*, 149–163.
- [25] M. Meuresch, S. Westhues, W. Leitner, J. Klankermayer, *Angew. Chem. Int. Ed.* **2016**, *55*, 1392–1395.
- [26] B. G. Schieweck, J. Klankermayer, *Angew. Chem. Int. Ed.* **2017**, *56*, 10854–10857.
- [27] A. Kütt, T. Rodima, J. Saame, E. Raamat, V. Mäemets, I. Kaljurand, I. A. Koppel, R. Y. Garlyauskayte, Y. L. Yagupolskii, L. M. Yagupolskii, E. Bernhardt, H. Willner, I. Leito, *J. Org. Chem.* **2011**, *76*, 391–395.
- [28] S. Beyreuther, A. Frick, J. Hunger, G. Huttner, B. Antelmann, P. Schober, R. Soltek, *Eur. J. Inorg. Chem.* **2000**, *2000*, 597–615.
- [29] A. D. Chowdhury, R. Jackstell, M. Beller, *ChemCatChem* **2014**, *6*, 3360–3365.
- [30] M. Brookhart, B. Grant, A. F. Volpe, *Organometallics* **1992**, *11*, 3920–3922.

5. Selected Publications

5.5. Additive-free cobalt-catalysed hydrogenation of carbonates to methanol and alcohols

F. Ferretti, F. K. Scharnagl, A. Dall'Anese, R. Jackstell, S. Dastgir, and M. Beller, *Catal. Sci. Technol.* **2019**, *9*, 3548-3553

Reproduced from *Catal. Sci. Technol.* **2019**, *9*, 3548-3553 with permission from the Royal Society of Chemistry.

Contributions: F.K.S. synthesised modified Triphos-ligands and screened cyclic and acyclic carbonates, as well as formates and formaldehyde in the catalytic reaction. In addition, he prepared the manuscript together with M.B. The overall contribution is about 30%.



Cite this: *Catal. Sci. Technol.*, 2019, 9, 3548

Received 16th May 2019,
Accepted 12th June 2019

DOI: 10.1039/c9cy00951e

rsc.li/catalysis

Additive-free cobalt-catalysed hydrogenation of carbonates to methanol and alcohols†

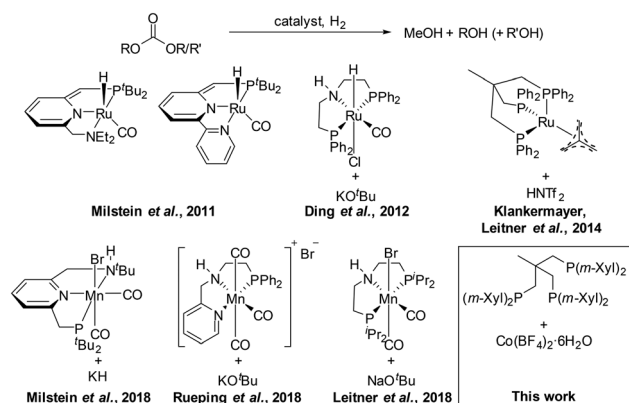
Francesco Ferretti,^{ab} Florian Korbinian Scharnagl,^a Anna Dall'Anese,^{ac} Ralf Jackstell,^a Sarim Dastgir^d and Matthias Beller^{id,*a}

Reduction of various organic carbonates to methanol and alcohols can be achieved in the presence of a molecularly-defined homogeneous cobalt catalyst. Specifically, the use of $\text{Co}(\text{BF}_4)_2$ in combination with either commercial or tailor-made tridentate phosphine ligands allows for additive-free hydrogenations of carbonates. Optimal results are obtained at relatively mild conditions (120 °C, 50 bar hydrogen pressure) in the presence of xylyl-Triphos L4.

Introductions

The catalytic hydrogenation of carbon dioxide to methanol is of general interest in the context of the so-called “Methanol Economy”. This concept comprises the capture of carbon dioxide from the atmosphere and its conversion to methanol or dimethyl ether, using dihydrogen as pointed out originally by Asinger¹ and Olah.^{2,3} Although most efforts focused on heterogeneous catalysts, also the development of suitable molecularly-defined catalysts is interesting due to the potentially higher activity. Thus in recent years, notable contributions in this area have been made by the groups of Milstein,⁴ Klankermayer and Leitner,^{5–7} Olah and Prakash,^{8–13} Sanford,^{14,15} Himeda and Laurency,¹⁶ Wass,¹⁷ Martins and Pombeiro,¹⁸ as well as our group.^{19,20} So far, a ruthenium-based PNP pincer complex constitutes the most productive homogeneous system with a reported turnover number (TON) of 9900, albeit after 10 days.¹² An alternative approach to the direct hydrogenation of carbon dioxide makes use of cyclic and/or acyclic organic carbonates. The former derivatives can be easily synthesised from carbon dioxide and epoxides, as already done on industrial scale in the so-called OMEGA process by Shell. The latter carbonates are mainly obtained from CO_2 by indirect methods (*i.e.* alcoholysis of other carbon dioxide derivatives such as urea or cyclic carbonates) nowadays, but can also be directly prepared from CO_2 and alcohols.^{21–23}

Subsequent hydrogenation leads to methanol and the corresponding alcohols.²⁴ This indirect strategy for CO_2 reduction was first demonstrated by Milstein in 2011, who reported the selective hydrogenation of carbonates, carbamates and formates to methanol using different ruthenium-PNN-pincer complexes.^{25–27} Later on, the use of ruthenium-based NHC-pincer systems has been described.^{28,29} The groups of Leitner and Klankermayer extensively studied $[\text{Ru}(\text{Triphos})(\text{TMM})]$ (Triphos = 1,1,1-tris(diphenylphosphinomethyl)ethane and TMM = trimethylene methane) in hydrogenations of carboxylic and carbonic acid derivatives, including cyclic and acyclic carbonates in the presence or the absence of the additive HNTf_2 .³⁰ So far, the most productive catalyst for this reaction has been reported by the group of Kuiling Ding. By using the commercial ruthenium-MACHO pincer complex, they achieved catalyst TONs up to 87 000 for the hydrogenation of cyclic carbonates, which is about one order of magnitude higher compared to the direct conversion of carbon dioxide



Scheme 1 Overview of selected reported homogeneous systems for the hydrogenation of organic carbonates to the corresponding alcohols.

^a Leibniz-Institut für Katalyse e.V. an der Universität Rostock, Albert-Einstein-Straße 29a, 18059 Rostock, Germany. E-mail: matthias.beller@catalysis.de

^b Dipartimento di Chimica, Università degli Studi di Milano, Via. C. Golgi 19, 20133 Milano, Italy

^c Dipartimento di Scienze Chimiche e Farmaceutiche, Università di Trieste, Via Licio Giorgieri 1, 34127 Trieste, Italy

^d Qatar Environment and Energy Research Institute (QEERI), Hamad bin Khalifa University (HBKU), Qatar Foundation, Doha, Qatar

† Electronic supplementary information (ESI) available. See DOI: 10.1039/c9cy00951e

to methanol, underlining the possible advantage of this indirect CO₂ reduction route.³¹ Apart from expensive precious metal complexes, the first non-noble metal catalysts for this transformation were reported only very recently. In 2018, the groups of Leitner,³² Rueping³³ and Milstein³⁴ at the same time reported manganese pincer complexes for the hydrogenation of organic carbonates under basic conditions (Scheme 1).

Modifying a system based on the combination of cobalt and Triphos, initially reported by Elsevier and de Bruin for the reduction of carboxylic acid,³⁵ our group succeeded in the direct hydrogenation of carbon dioxide with a homogeneous cobalt catalyst.¹⁹ Later on, improved results have been obtained by us,²⁰ as well as by Klankermayer and Schieweck.⁷ To the best of our knowledge, the applicability of such complexes for reduction of organic carbonates has not been reported yet. In this context, herein we describe the efficient hydrogenation of cyclic and acyclic carbonates in 2,2,2-trifluoroethanol (TFE) in the presence of Co(BF₄)₂·6H₂O and a modified Triphos ligand.

Results and discussion

At the beginning of our investigations, different cobalt precursors in the presence of the ligand Triphos were tested for the hydrogenation of the model substrate diethyl carbonate at 120 °C and 50 bar H₂ (see Table 1). Unfortunately, no active catalyst could be generated in the presence of coordinating anions such as halides (entries 1 and 2), acetyl acetonate (entries 3 and 4), carbonate and acetate (entries 6 and 7). Also the use of the cobalt hexafluoroacetylacetonate did not show any appreciable yield of MeOH (entry 5). Finally, we found that Co(NTf₂)₂ and Co(BF₄)₂·6H₂O are both suitable for the hydrogenation of carbonates (entries 8 and 9), even at reduced catalyst loadings of 2 mol% (entries 10 and 11). Co(NTf₂)₂ afforded the highest conversions but a lower selectivity than Co(BF₄)₂. Although the use of Co(NTf₂)₂ gave good

activities for CO₂ reduction,²⁰ here the low yield of alcohols is ascribed to the decomposition of the triflimide-anion which reacted with the substrate. In fact, we observed by GC-MS the formation of several unidentified by-products containing fragments derived both from diethyl carbonate and the NTf₂-anion.

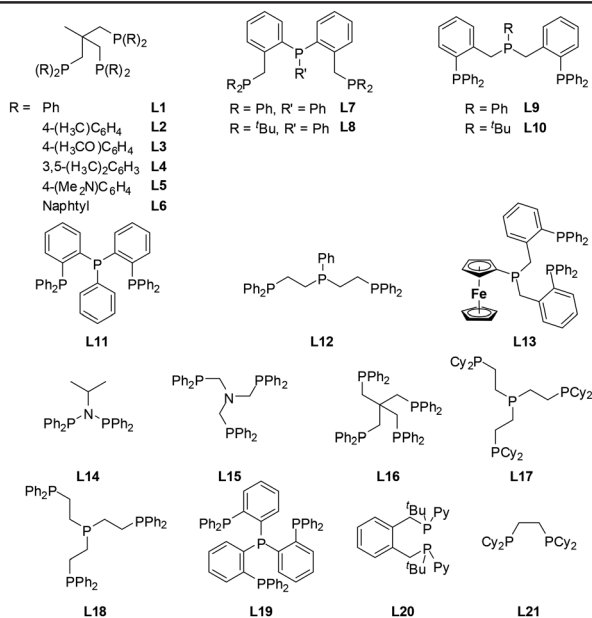
After identifying an active catalyst system, we tried to improve the comparably low activity investigating different ligands in the presence of cobalt tetrafluoroborate hexahydrate. Here, a variety of bidentate (L20 and L21), tridentate (L1–L14) and tetradentate ligands (L15–L19) was tried. Similar to Co-catalysed hydrogenation reactions of carboxylic compounds, also in the case of carbonates solely ligands with the Triphos backbone were suitable. All the other ligands tested gave only traces of methanol and ethanol (Table 2).

Among the Triphos-type ligands, the xylyl-Triphos L4 revealed the highest productivity, followed by anisyl- (L3) and *p*-tolyl-Triphos (L2). The dimethylamino-substituted Triphos L5 showed a slightly better productivity than L1. Thus, the substitution of the phenyl ring of Triphos with electron-donating groups seems to be beneficial for the system activity. However, the results are difficult to rationalize only on the base of the basicity of the phosphorus. The catalytic behaviour can be better explained taking into account the steric properties of the ligands. Indeed, Leitner and Klankermayer recently showed the benefit of using sterically hindered ligands by comparing the activity of L1, L2 and L4 in the ruthenium/Triphos-catalysed hydrogenation of methyl benzoate and lactams. The increased activity in the order L4 > L2 > L1 is ascribed to the suppression of inactive hydride bridged ruthenium dimers formation.³⁶ The same trend was not noticed when cobalt was used instead of ruthenium for either the reduction of CO₂^{7,20} or reductive transformation of carboxylic acids,³⁷ suggesting a negligible role of dimers in catalyst deactivation. On the other hand, [(Triphos)₂Co₂(μ-H₃)]⁺ was found inactive, in the absence of acid co-catalysts, for the synthesis of

Table 1 Testing different cobalt precursors for the hydrogenation of diethyl carbonate

| Entry | Co precursor | Conversion [%] | Yield EtOH [%] | Yield MeOH [%] |
|-----------------|--|----------------|----------------|----------------|
| 1 | CoCl ₂ | 6 | <1 | <1 |
| 2 | CoF ₂ | 2 | <1 | <1 |
| 3 | Co(acac) ₂ | 4 | <1 | <1 |
| 4 | Co(acac) ₃ | 4 | <1 | <1 |
| 5 | Co(acac ^F) ₂ | 2 | <1 | <1 |
| 6 | CoCO ₃ ·0.33H ₂ O | 1 | <1 | <1 |
| 7 | Co(OAc) ₂ | 3 | <1 | <1 |
| 8 | Co(NTf ₂) ₂ | 60 | 37 | 13 |
| 9 | Co(BF ₄) ₂ ·6H ₂ O | 36 | 31 | 25 |
| 10 ^a | Co(NTf ₂) ₂ | 44 | 36 | 8 |
| 11 ^a | Co(BF ₄) ₂ ·6H ₂ O | 24 | 22 | 16 |

Reaction conditions: general conditions: 1.0 mmol diethyl carbonate, 2 mol% cobalt precursor, 2.4 mol% L1, 2 mL THF, 120 °C, 50 bar H₂, 18 h. Conversions and yields were calculated *via* GC using hexadecane as internal standard. acac^F = hexafluoroacetylacetonate. ^a Co precursor = 0.02 mmol (2 mol%), L1 = 0.024 mmol.

Table 2 Hydrogenation of diethyl carbonate: variation of ligands in combination with $\text{Co}(\text{BF}_4)_2 \cdot 6\text{H}_2\text{O}$ 

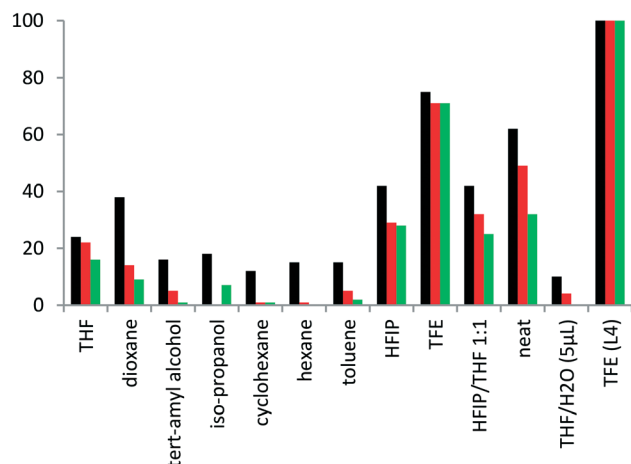
| Entry | Ligand | Conversion [%] | Yield (EtOH) [%] | Yield (MeOH) [%] |
|-------|-----------|----------------|------------------|------------------|
| 1 | L1 | 24 | 22 | 16 |
| 2 | L2 | 37 | 32 | 26 |
| 3 | L3 | 45 | 37 | 32 |
| 4 | L4 | 57 | 48 | 42 |
| 5 | L5 | 30 | 27 | 22 |
| 6 | L6 | 4 | <1 | 0 |
| 7 | L7 | 4 | <1 | <1 |
| 8 | L8 | 19 | <1 | <1 |
| 9 | L9 | 29 | <1 | <1 |
| 10 | L10 | 32 | 1 | <1 |
| 11 | L11 | 17 | <1 | 0 |
| 12 | L12 | 6 | <1 | <1 |
| 13 | L13 | 5 | 1 | <1 |
| 14 | L14 | 4 | <1 | <1 |
| 15 | L15 | 6 | <1 | <1 |
| 16 | L16 | 2 | <1 | <1 |
| 17 | L17 | 4 | <1 | 0 |
| 18 | L18 | 3 | <1 | 0 |
| 19 | L19 | 11 | <1 | 0 |
| 20 | L20 | 6 | <1 | 0 |
| 21 | L21 | 3 | <1 | <1 |
| 22 | No ligand | 4 | <1 | <1 |

General conditions: 1.0 mmol diethyl carbonate, 2 mol% $\text{Co}(\text{BF}_4)_2 \cdot 6\text{H}_2\text{O}$, 2.4 mol% ligand, 2 mL THF, 120 °C, 50 bar H_2 , 18 h. Conversions and yields were calculated *via* GC using hexadecane as internal standard.

dimethoxymethane and methyl formate from CO_2 .⁷ Considering the absence of additives in the present system, the prevention of dimer formation is a possible explanation for the order of activity of the ligands.

Next, the performance of the *in situ*-generated catalyst with commercial ligand L1 has been investigated in different solvents (Scheme 2). By far the best results were obtained with 2,2,2-trifluoroethanol (TFE) leading to 71% yield of both methanol and ethanol (conversion: 75%). Quantitative conversion and GC-yields for both alcohols have been achieved by combining the best solvent with the best ligand, L4. Previously, such beneficial effect of fluorinated solvents has been

observed by Elsevier,³⁸ as well as by Klankermayer.⁷ Interestingly, TFE gave significantly better results compared to the related solvent 1,1,1,3,3,3-hexafluoro isopropanol (HFIP). THF showed the best productivity as a non-fluorinated solvent. The sensitivity of the system towards water was shown by combining THF with 5 μL (0.28 mmol) of distilled water. Adding this small amount dropped the conversion from 24% to 10% and the yield of ethanol from 22% to 4%. Methanol formation could not be observed anymore. All other solvents resulted in low conversions, yields and selectivities. With an optimised system in hand, the hydrogenation of different organic carbonates was investigated in more detail (Table 3).



Scheme 2 Hydrogenation of diethyl carbonate: solvent screening. Reaction conditions: 1.0 mmol diethyl carbonate, 2 mol% $\text{Co}(\text{BF}_4)_2 \cdot 6\text{H}_2\text{O}$, 2.4 mol% **L1** or **L4**, 2 mL solvent, 120 °C, 50 bar H_2 , 18 h. Conversions and yields were calculated *via* GC using hexadecane as internal standard. The ethanol yield could not be determined in the case of isopropanol as solvent.

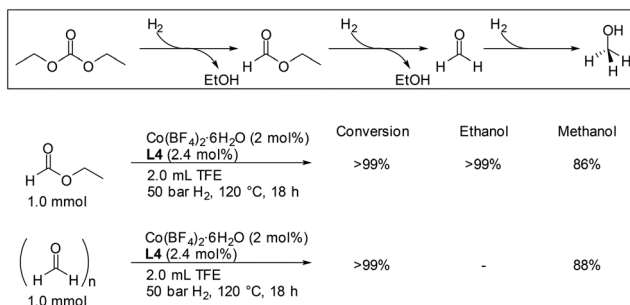
Dimethyl carbonate **1** gave three equivalents of methanol in a yield of 85% at full conversion. Almost quantitative yields of both alcohols have been achieved for di-*n*-butyl carbonate **2**. Also the aromatic carbonate **3** was effectively converted to methanol and phenol. The asymmetric aromatic/aliphatic carbonates **4** and **5** yielded the three corresponding alcohols. For dibenzyl carbonate **6**, a low methanol yield (11%) was observed, even though the conversion and the yield of benzylic alcohol both have been high (>99%/88%). A similar behaviour was found for the perfluorinated carbonate **10**, although at a lower conversion. It is worth noticing that the used cobalt source contains six equivalents of water and both benzyl alcohol and pentafluorophenol are good leaving groups. Thus, for **6** and **10** hydrolysis of the substrates would lead to formation of alcohol and carbon dioxide. This, at least in part, accounts for the discrepancy of methanol and alcohol yields. The asymmetric carbonate **8**, which bears one hexafluorophenol unit yielded in 92% of methanol, along with 97% of 9-fluorenyl methanol and 91% of hexafluorophenol. Also the fluorinated substrate **9** was converted to methanol in high yield. Noteworthy, also the cyclic carbonates **12** and **13** were readily transformed to the diols and methanol. These carbonates are of particular interest *vide supra*, as they are commercially produced from carbon dioxide and epoxides or oxetanes.³⁹

As the hydrogenation of diethyl carbonate potentially occurs stepwise *via* ethyl formate and/or formaldehyde, these compounds have been investigated in separate hydrogenation experiments (Scheme 3). Both, ethyl formate and paraformaldehyde were completely hydrogenated, giving methanol in 86% and 88%, respectively, and ethanol in >99%. Therefore, although only traces of ethyl formate were detected by GC for the model substrate, we cannot exclude that these compounds indeed are intermediates in the hydrogenation of diethyl carbonate.

Table 3 Hydrogenation of carbonates to the corresponding alcohols: substrate scope

| $\text{RO-CO-OR}' \xrightarrow[\text{50 bar H}_2, 120^\circ\text{C}, 18\text{ h}]{\text{Co}(\text{BF}_4)_2 \cdot 6\text{H}_2\text{O} (2\text{ mol}\%), \text{L4} (2.4\text{ mol}\%), 2.0\text{ mL TFE}}$ | | $\text{MeOH} + \text{ROH} + \text{R}'\text{OH}$ | | | |
|--|-----------|---|----------|-------------------|----------|
| Entry | Substrate | Conv. [%] | MeOH [%] | ROH [%] | R'OH [%] |
| 1 | | >99 | 85 | — | — |
| 2 | | >99 | 98 | >99 | — |
| 3 | | 92 | 96 | 73 | — |
| 4 | | >99 | >99 | >99 | — |
| 5 | | 94 | 84 | n.d. ^a | 89 |
| 6 | | >99 | 11 | 88 | — |
| 7 | | >99 | 94 | 54 | — |
| 8 | | >99 | 92 | 97 | 91 |
| 9 | | >99 | 80 | n.d. ^a | — |
| 10 | | 53 | 5 | 43 | — |
| 11 | | >99 | 85 | 75 | — |
| 12 | | >99 | 96 | 90 | — |

Reaction conditions: 1.0 mmol diethyl carbonate, 2 mol% $\text{Co}(\text{BF}_4)_2 \cdot 6\text{H}_2\text{O}$, 2.4 mol% **L4**, 2 mL TFE, 120 °C, 50 bar H_2 , 18 h. Conversions and yields were calculated *via* GC using hexadecane as internal standard. When $\text{R} = \text{R}'$, yields are reported as 2 ROH. ^a The peak of ROH overlaps with the one of TFE in the gas-chromatogram.



Scheme 3 Hydrogenation of the potential intermediates ethyl formate and formaldehyde.

Conclusions

In conclusion, we investigated the homogeneous cobalt-catalysed hydrogenation of organic carbonates for the first time. The combination of $\text{Co}(\text{BF}_4)_2 \cdot 6\text{H}_2\text{O}$ with a Triphos-derived ligand **L4** resulted in an active catalytic system suitable for reduction of both cyclic and acyclic carbonates. At relatively mild conditions, good to very good yields of methanol and the corresponding alcohols have been obtained using the solvent TFE.

Experimental section

Materials

All chemicals were purchased from commercial sources and were used as received without additional purification, if not stated otherwise. Molecular hydrogen was purchased from Linde. All experiments were carried out under argon atmosphere by using standard Schlenk-techniques, unless stated otherwise. Solvents were dried and distilled or directly used from a solvent purification system (MBraun). THF was stored over molecular sieves 3 Å. Diethyl carbonate was distilled prior to use. The ligands **L2**–**L6**,³⁷ **L7**–**L9**,⁴⁰ **L11**,⁴⁰ **L15**,⁴¹ **L16**,⁴² **L17**,⁴³ **L19**,⁴⁴ and **L20**⁴⁵ have been synthesised according to literature-reported procedures.

Catalytic experiments were conducted in 4 mL screw cap vials, closed with a polytetrafluoroethylene (PTFE)/white rubber septum (Wheaton 13 mm Septa) and phenolic cap and connected with atmosphere by a needle, inside a 300 mL Parr autoclave and stirred with a magnetic stirring bar. GC measurements were carried out on a 7890A GC-System with HP-5 column (polydimethylsiloxane with 5% phenyl groups, length 30 m, i.d. 0.32 mm, film 0.25 μm) and with a FID coupled with a 7693 autosampler from Agilent Technologies. Argon was used as carrier gas. GC-analyses for methanol quantification were performed on an Agilent HP-6890 chromatograph with a FID detector and an Agilent HP Ultra 1 column (19091A-105, 50 m, 0.20 mm i.d., 0.33 μm film thickness, 100% dimethylpolysiloxane) using argon as carrier gas.

In a typical catalytic experiment, $\text{Co}(\text{BF}_4)_2 \cdot 6\text{H}_2\text{O}$ (6.81 mg, 2.0 mmol) and ligand (2.4 mmol) were fast weighed in the air and transferred into a 4 mL glass vial. If used, solid substrates were also weighed in the air and added into the vial. The vial was subsequently set under argon. 2.0 mL solvent

were added and the mixture stirred for 5–10 min. Then, liquid substrates were added and the vials were placed in a metal plate inside a 300 mL autoclave. After closing, the reactor was pressurised with hydrogen (about 20 bar), which was released again. This procedure was carried out three times, after which 50 bar H_2 were introduced. The autoclave was then heated inside an aluminium block to 120 °C for 18 h. Afterwards the reaction was quenched with an ice-bath and the reactor vented. Hexadecane (30 μL) was added to the reaction as internal standard for GC, along with 2 mL THF. After proper mixing, GC was measured of the sample.

Conflicts of interest

There are no conflicts to declare.

Acknowledgements

Financial support from Qatar National Research Fund, a member of Qatar foundation, Qatar (Grant numbers NPRP9-212-1-042, & NPRP8-235-1-055), BMWi (project MethaCycle, 03ET6071A) and the State of Mecklenburg-Vorpommern, Germany is gratefully acknowledged. We thank the analytical department of LIKAT for the support and Prof. Uwe Rosenthal for providing **L14**.

References

- 1 F. Asinger, *Methanol, Chemie- und Energierohstoff*, Akademie-Verlag, Berlin, 1987.
- 2 G. A. Olah, A. Goepfert and G. K. S. Prakash, *Beyond Oil and Gas: The Methanol Economy*, Wiley-VCH, Weinheim, 2nd edn, 2009.
- 3 G. A. Olah, *Angew. Chem., Int. Ed.*, 2013, 52, 104–107.
- 4 J. R. Khusnutdinova, J. A. Garg and D. Milstein, *ACS Catal.*, 2015, 5, 2416–2422.
- 5 S. Wesselbaum, T. vom Stein, J. Klankermayer and W. Leitner, *Angew. Chem., Int. Ed.*, 2012, 51, 7499–7502.
- 6 S. Wesselbaum, V. Moha, M. Meuresch, S. Brosinski, K. M. Thenert, J. Kothe, T. vom Stein, U. Englert, M. Hölscher, J. Klankermayer and W. Leitner, *Chem. Sci.*, 2015, 6, 693–704.
- 7 B. G. Schieweck and J. Klankermayer, *Angew. Chem., Int. Ed.*, 2017, 56, 10854–10857.
- 8 J. Kothandaraman, A. Goepfert, M. Czaun, G. A. Olah and G. K. S. Prakash, *J. Am. Chem. Soc.*, 2016, 138, 778–781.
- 9 S. Kar, A. Goepfert, J. Kothandaraman and G. K. S. Prakash, *ACS Catal.*, 2017, 7, 6347–6351.
- 10 S. Kar, R. Sen, A. Goepfert and G. K. S. Prakash, *J. Am. Chem. Soc.*, 2018, 140, 1580–1583.
- 11 S. Kar, A. Goepfert, V. Galvan, R. Chowdhury, J. Olah and G. K. S. Prakash, *J. Am. Chem. Soc.*, 2018, 140, 16873–16876.
- 12 S. Kar, R. Sen, J. Kothandaraman, A. Goepfert, R. Chowdhury, S. B. Munoz, R. Haiges and G. K. S. Prakash, *J. Am. Chem. Soc.*, 2019, 141, 3160–3170.
- 13 S. Kar, A. Goepfert and S. G. Prakash, *ChemSusChem*, 2019, DOI: 10.1002/cssc.201900324.
- 14 C. A. Huff and M. S. Sanford, *J. Am. Chem. Soc.*, 2011, 133, 18122–18125.

- 15 N. M. Rezayee, C. A. Huff and M. S. Sanford, *J. Am. Chem. Soc.*, 2015, **137**, 1028–1031.
- 16 K. Sordakis, A. Tsurusaki, M. Iguchi, H. Kawanami, Y. Himeda and G. Laurenczy, *Chem. – Eur. J.*, 2016, **22**, 15605–15608.
- 17 D. Wass and M. Everett, *Chem. Commun.*, 2017, **53**, 9502–9504.
- 18 A. P. C. Ribeiro, L. M. D. R. S. Martins and A. J. L. Pombeiro, *Green Chem.*, 2017, **19**, 4811–4815.
- 19 J. Schneidewind, R. Adam, W. Baumann, R. Jackstell and M. Beller, *Angew. Chem., Int. Ed.*, 2017, **56**, 1890–1893.
- 20 F. K. Scharnagl, M. F. Hertrich, G. Neitzel, R. Jackstell and M. Beller, *Adv. Synth. Catal.*, 2018, **361**, 374–379.
- 21 S. Dabral and T. Schaub, *Adv. Synth. Catal.*, 2019, **361**, 223–246.
- 22 M. Aresta, A. Dibenedetto and E. Quaranta, *J. Catal.*, 2016, **343**, 2–45.
- 23 H.-Z. Tan, Z.-Q. Wang, Z.-N. Xu, J. Sun, Y.-P. Xu, Q.-S. Chen, Y. Chen and G.-C. Guo, *Catal. Today*, 2018, **316**, 2–12.
- 24 P. H. Dixneuf, *Nat. Chem.*, 2011, **3**, 578.
- 25 E. Balaraman, C. Gunanathan, J. Zhang, L. J. W. Shimon and D. Milstein, *Nat. Chem.*, 2011, **3**, 609–614.
- 26 F. Hasanayn, A. Baroudi, A. A. Bengali and A. S. Goldman, *Organometallics*, 2013, **32**, 6969–6985.
- 27 Y. Li, K. Junge and M. Beller, *ChemCatChem*, 2013, **5**, 1072–1074.
- 28 X. Wu, L. Ji, Y. Ji, E. H. M. Elageed and G. Gao, *Catal. Commun.*, 2016, **85**, 57–60.
- 29 J. Chen, H. Zhu, J. Chen, Z.-G. Le and T. Tu, *Chem. – Asian J.*, 2017, **12**, 2809–2812.
- 30 T. vom Stein, M. Meuresch, D. Limper, M. Schmitz, M. Hölscher, J. Coetzee, D. J. Cole-Hamilton, J. Klankermayer and W. Leitner, *J. Am. Chem. Soc.*, 2014, **136**, 13217–13225.
- 31 Z. Han, L. Rong, J. Wu, L. Zhang, Z. Wang and K. Ding, *Angew. Chem., Int. Ed.*, 2012, **51**, 13041–13045.
- 32 A. Kaithal, M. Hölscher and W. Leitner, *Angew. Chem.*, 2018, **130**, 13637–13641.
- 33 V. Zubar, Y. Lebedev, L. M. Azofra, L. Cavallo, O. El-Sepelgy and M. Rueping, *Angew. Chem., Int. Ed.*, 2018, **57**, 13439–13443.
- 34 A. Kumar, T. Janes, N. A. Espinosa-Jalapa and D. Milstein, *Angew. Chem., Int. Ed.*, 2018, **57**, 12076–12080.
- 35 T. J. Korstanje, J. Ivar van der Vlugt, C. J. Elsevier and B. de Bruin, *Science*, 2015, **350**, 298–302.
- 36 M. Meuresch, S. Westhues, W. Leitner and J. Klankermayer, *Angew. Chem., Int. Ed.*, 2016, **55**, 1392–1395.
- 37 W. Liu, B. Sahoo, A. Spannenberg, K. Junge and M. Beller, *Angew. Chem., Int. Ed.*, 2018, **57**, 11673–11677.
- 38 H. T. Teunissen and C. J. Elsevier, *Chem. Commun.*, 1998, 1367–1368.
- 39 H. Büttner, L. Longwitz, J. Steinbauer, C. Wulf and T. Werner, *Top. Curr. Chem.*, 2017, **375**, 50.
- 40 A. Dutta Chowdhury, R. Jackstell and M. Beller, *ChemCatChem*, 2014, **6**, 3360–3365.
- 41 A. Phanopoulos, N. J. Brown, A. J. P. White, N. J. Long and P. W. Miller, *Inorg. Chem.*, 2014, **53**, 3742–3752.
- 42 J. Ellermann and K. Dorn, *Chem. Ber.*, 1966, **99**, 653–657.
- 43 R. Adam, C. B. Bheeter, J. R. Cabrero-Antonino, K. Junge, R. Jackstell and M. Beller, *ChemSusChem*, 2017, **10**, 842–846.
- 44 C. Ziebart, C. Federsel, P. Anbarasan, R. Jackstell, W. Baumann, A. Spannenberg and M. Beller, *J. Am. Chem. Soc.*, 2012, **134**, 20701–20704.
- 45 K. Dong, X. Fang, S. Gülak, R. Franke, A. Spannenberg, H. Neumann, R. Jackstell and M. Beller, *Nat. Commun.*, 2017, **8**, 14117.

6. Appendix

6.1. List of Publications

- 1 **“Additive-free cobalt-catalysed hydrogenation of carbonates to methanol and alcohols”**
Francesco Ferretti, Florian Korbinian Scharnagl, Anna Dall’Anese, Ralf Jackstell, Sarim Dastgir, Matthias Beller
Catal. Sci. Technol. **2019**, *9*, 3548-3553
- 2 **“Biomolecule-derived supported cobalt nanoparticles for hydrogenation of industrial olefins, natural oils and more in water”**
Anahit Pews-Davtyan, Florian Korbinian Scharnagl, Maximilian Franz Hertrich, Carsten Robert Kreyenschulte, Stefan Bartling, Henrik Lund, Ralf Jackstell, Matthias Beller
Green Chem. **2019**, *21*, 5104-5112
- 3 **“Supported Cobalt Nanoparticles for Hydroformylation Reactions”**
Maximilian Franz Hertrich, Florian Korbinian Scharnagl, Anahit Pews-Davtyan, Carsten Robert Kreyenschulte, Henrik Lund, Stefan Bartling, Ralf Jackstell, Matthias Beller
Chem. Eur. J. **2019**, *25*, 5534-5538
- 4 **“Homogeneous catalytic hydrogenation of CO₂ to methanol – improvements with tailored ligands”**
Florian Korbinian Scharnagl, Maximilian Franz Hertrich, Gordon Neitzel, Ralf Jackstell, Matthias Beller
Adv. Synth. Catal. **2019**, *361*, 374-379
- 5 **“Reduction of Nitro Compounds Using 3d-Non-Noble Metal Catalysts”**
Dario Formenti, Francesco Ferretti, Florian Korbinian Scharnagl, Matthias Beller
Chem. Rev. **2019**, *119*, 2611-2680
- 6 **“Hydrogenation of terminal and internal olefins using a biowaste-derived heterogeneous cobalt catalyst”**
Florian Korbinian Scharnagl, Maximilian Franz Hertrich, Francesco Ferretti, Carsten Robert Kreyenschulte, Henrik Lund, Ralf Jackstell, Matthias Beller
Sci. Adv. **2018**, *4*, eaau1248
- 7 **“Acyloboranes: synthetic strategies and applications”**
Florian Korbinian Scharnagl, Shubankar Kumar Bose, Todd B. Marder
Org. Biomol. Chem. **2017**, *15*, 1738-1752

6.2. Conference Participation

- 1 **“Homogeneous Cobalt-Catalysed Reduction of CO₂ to Methanol”**
Florian Korbinian Scharnagl, Maximilian Franz Hertrich, Gordon Neitzel, Ralf Jackstell, Matthias Beller
23rd Conference on Organometallic Chemistry (EUCOMC XXIII), 16.-20. June 2019, Helsinki, Finland, Oral-Contribution
- 2 **“Homogeneous Cobalt-Catalysed Reduction of CO₂ to Methanol”**
Florian Scharnagl, Maximilian Hertrich, Jacob Schneidewind, Rosa Adam, Wolfgang Baumann, Ralf Jackstell, Matthias Beller
21st International Symposium On Homogeneous Catalysis (ISHC XXI), 8.-13. July 2018, Amsterdam, The Netherlands, Poster-Contribution
- 3 **“Methanol-Kreislauf zur Speicherung erneuerbarer Energien - Projekt „Metha-Cycle“**
Anastasiya Agapova, Florian Scharnagl, Henrik Junge, Ralf Jackstell, Matthias Beller, Marco Haumann, Christian Schwarz, Johannes Gulden, Andreas Sklarow, Douglas Hoffmann, Stefan Laumann, Christian Heßke
CO₂-Statuskonferenz „CO₂Plus“ (BMBF), 17.-18. April 2018, Berlin, Germany, Poster-Contribution
- 4 *Summer School on Catalysis and Organometallic Synthesis*, 24.-28. July 2017, Würzburg, Germany, Attendance

6.3. Curriculum Vitae

Education

- 11.2016 – 10.2019 PhD-student at the Leibniz-Institut für Katalyse e.V. at the Universität Rostock
Supervisor: Prof. Dr. Matthias Beller
- 10.2014 – 08.2016 Master-student of chemistry at the Julius-Maximilians-Universität Würzburg
Supervisor of Master's Thesis: Prof. Dr. Todd B. Marder
- 05.2011 – 02.2014 Bachelor-student of chemistry at the Julius-Maximilians-Universität Würzburg
Supervisor of Bachelor's Thesis: Prof. Dr. Ingo Fischer
- 09.2002 – 05.2011 Gymnasium Waldkraiburg

Experiences Abroad

- 07.2019 – 10.2019 Guest-scientist at the Cardiff University/Cardiff Catalysis Institute (UK) (ERASMUS-supported)
Supervisor: Prof. Dr. Graham Hutchings
- 03.12 – 14.12.2018 Guest-scientist at the Universidade de Lisboa/Instituto Superior Técnico (Portugal)
Supervisor: Prof. Dr. Armando J.L. Pombeiro
- 03.2014 – 08.2014 ERASMUS-student at the Durham University (UK)
Supervisor: Prof. Dr. Kosmas Prassides